SYNTHESIS, STRUCTURE, SPECTRA AND REDOX PROPERTIES OF CERTAIN COPPER(II) COMPLEXES OF THIOETHER CONTAINING LIGANDS AS MODELS FOR BLUE COPPER PROTEINS

Thesis submitted to

BHARATHIDASAN UNIVERSITY

for the award of the Degree of

DOCTOR OF PHILOSOPHY

in

CHEMISTRY

S. USHA

DEPARTMENT OF CHEMISTRY

BHARATHIDASAN UNIVERSITY

TIRUCHIRAPPALLI - 620 024

MAY 1995

BHARATHIDASAN UNIVERSITY

Department of Chemistry, Tiruchirapalli 620 024, India

Dr. M. Palaniandavar
Professor

Declaration

The research work embodied in this thesis entitled "**SYNTHESIS, STRUCTURE, SPECTRA AND REDOX PROPERTIES OF CERTAIN COPPER(II) COMPLEXES OF THIOETHER CONTAINING LIGANDS AS MODELS FOR BLUE COPPER PROTEINS**" is original and was done by Miss S. Usha at the Department of Chemistry, Bharathidasan University, Tiruchirapalli-620 024, India. It has not previously formed the basis for the award of any Degree, Diploma, Associateship, Fellowship or other similar title of Bharathidasan University or any other University.

M. Palaniandavar

Dr. M. Palaniandavar
Supervisor

BHARATHIDASAN UNIVERSITY

Department of Chemistry, Tiruchirapalli 620 024, India

Declaration

The research work embodied in this thesis entitled "**SYNTHESIS, STRUCTURE, SPECTRA AND REDOX PROPERTIES OF CERTAIN COPPER(II) COMPLEXES OF THIOETHER CONTAINING LIGANDS AS MODELS FOR BLUE COPPER PROTEINS**" is original and was done at the Department of Chemistry, Bharathidasan University, Tiruchirapalli-620 024, India. It has not previously formed the basis for the award of any Degree, Diploma, Associateship, Fellowship or other similar title of Bharathidasan University or any other University.

S. Usha

S. Usha

ACKNOWLEDGEMENTS

I wish to place on record my deep sense of gratitude to my guide and supervisor Dr. M. Palaniandavar, Professor, Department of Chemistry for suggesting me this interesting research problem. I am greatly indebted to him for his words of encouragements, unstinted support throughout the period of this investigation and for his involvement with the research work and valuable ideas and critical evaluation at all stages.

I take this opportunity to thank Dr. M. Krishna Pillay, Professor and Head of the Department for his kindness and ready help whenever required and for his interest and constant encouragement shown to me throughout this work.

I am greatly indebted to other faculty members of Chemistry Department for their help and encouragement during my work.

It gives me great pleasure to express my heart-felt thanks to Professor N. Kitajima and Dr. K. Fujisawa, Tokyo Institute of Technology, Japan, for solving the crystal structure presented in this work. I thank Professor S. A. Matlin, Brunel University, London, for elemental analyses and mass spectra. I also thank CDRI, Lucknow and Dr. S. Anandapadmanabhan, Ooty for elemental analyses.

It is a blessing to have good friends around, who take part in our joys and sorrows. I am greatly indebted to my friends Dr. R. Uma, Mr. R. Viswanathan, Mr. S. Mahadevan, Mr. M. Murali, Mr. M. Vaidyanathan and Mr. M. Velusamy for their help and my hostel friends who voluntarily took part in my pains and pleasures. My sincere thanks are due to them.

I thank RSIC, IIT, Madras for help in recording the EPR spectra. The University Grants Commission, New Delhi is acknowledged for awarding me a Fellowship during this investigation. My sincere thanks are also due to IISc, Bangalore for recording ^{1}H-NMR spectra.

I owe my sincere thanks to the non-teaching staff of Chemistry Department for their help and co-operation throughout this work.

I thank my parents, brothers and sisters for their constant support and love shown to me.

S. Usha

CONTENTS

CHAPTER 1

1. INTRODUCTION

1.1 Importance of Copper

Copper is an essential trace element, although nearly all organisms have access to only very minute amounts of it. Notable exceptions are bacteria involved in the leaching of copper from low-grade ore and the "copper flowers" in Central Africa.[1] Copper is the third most abundant trace metal element[2] in human (80-120 mg in a normal human body) and its amount varies from 2 to 15 ppm in other biological materials, depending on the species and on the type of the tissue. The biological role of copper ions involves their mediation and catalysis of redox reactions. It is an integral part of many proteins and enzymes and the unique geometry and electronic structures found in the active sites of these proteins have catalysed research in many areas of coordination chemistry.

An excess of copper has been found to be harmful, especially to lower organisms such as bacilli, fungi and algae.[3] A deficiency of copper in mammals can cause anaemia as it has an essential role in hemoglobin synthesis.[4-6] In human, the highest levels of copper are found in the liver, brain, lung and kidneys. Copper is absorbed in the intestine by the serum protein albumin to which it is loosely bound. It plays a key role in iron transport and metabolism into hemoproteins and some cases of anaemia in infants have been

found to require combined supplements of copper and iron.[7] A genetic defect in copper absorption, the kinky hair syndrome (*Menke's* disease),[8] characterized by defective keratinization of the hair, neurologic degeneration and anomalies of bones and arteries is fatal unless treated immediately with parenteral administration of copper. Although low molecular weight copper complexes are being investigated as possible therapeutic drugs for this disease, no adequate treatment has yet been found.

Wilsons's disease or hepatolenticular degeneration is another fatal inherited disease accompanied by decreased levels of copper in the blood. However, in this syndrome, there is an excessive storage of copper in the liver, probably owing to defective synthesis of ceruloplasmin by the hepatic cells. This disease can be treated with *D*-penicillamine[9] or glycyl-glycyl-*L*-histidine[10] which removes the accumulated copper from the body. Copper and its amino acid complexes are being used as antiinflammatory and antirheumatoid arthritic agents; other drugs against these diseases are believed to function by release of copper from serum albumin.[11]

1.2 Coordination Chemistry of Copper

Complexes of copper in which its oxidation state can range from 0 to +4 are known. The +1 and +2 oxidation states are the most common in both synthetic and biological copper systems.[2] Only a relatively small number of Cu(III) species have been characterised

although more Cu(III) complexes are observed or postulated as intermediates in a variety of reactions.[12] Compounds of the 0 and +4 oxidation states are extremely rare. The preferred or observed coordination numbers and stereochemistry for copper ions vary dramatically with oxidation state. For the spherically symmetric d^{10} Cu(I) ion, coordination numbers range from two to five, with four predominating. The most common stereochemistries are linear two-coordinate and tetrahedral four-coordinate with some distortions of these geometries, particularly in the presence of chelating type of ligands. A few penta-coordinate copper(I) complexes have been characterized.[13]

In an octahedral environment the cupric ion which has nine d electrons, would possess a degenerate ^2E_g electronic ground state. A geometric distortion which removes this degeneracy would produce a more stable electronic structure, in accordance with the Jahn-Teller Theorem. Consequently, Cu(II) is normally found in a tetragonal environment with four strongly bound equatorial ligands and one or two weakly bound axial ligands. Tetragonal coordination geometry induces a splitting in the d orbitals. The $d_{x^2-y^2}$ orbital has the greatest repulsion with the equatorial ligands. Therefore, it is the highest-energy metal-centered orbital which is half occupied, and characterizes the tetragonal Cu(II) ground state as $^2B_{1g}$.[14] However, four-coordinate tetrahedral or planar Cu(II) complexes are also known.[15] The differences in the preferred coordination numbers and geometries of Cu(I) and Cu(II) dictate

the redox reactions of copper between these two oxidation states be accompanied by drastic coordination changes; the energy barrier for this rearrangement profoundly affects both the kinetics and thermodynamics of such reactions.[16]

The copper nucleus (^{63}Cu = 69 %, ^{65}Cu = 31 %) with a nuclear spin (I) of 3/2 couples to the unpaired electron and produces a hyperfine splitting of the transition into 2I+1 = 4 components. This splitting is quite evident in the $g_{\parallel}$ region ($A_{\parallel}$) but is significantly smaller and often unresolved in the $g_{\perp}$ region.[17]

Typical reduction potentials of Cu(II)/Cu(I) couples, and the dramatic variations in such potentials, depend on ligand donor type and coordination geometry. The standard aqueous copper ion reduction potentials are



$$Cu^{+}_{aq} + e^{-} = Cu^{0}_{aq} \quad E = +\,0.52\ V \quad (NHE)$$



$$Cu^{2+}_{aq} + e^{-} = Cu^{+}_{aq} \quad E = +\,0.15\ V \quad (NHE)$$

giving,



$$2\ Cu^{+}_{aq} = Cu^{0} + Cu^{2+} \quad E = +\,0.37\ V.$$

This shows that Cu^{+} is unstable in aqueous solution with respect to disproportionation to metallic copper and Cu^{2+}. Thus, there is essentially no aqueous chemistry of the cuprous ion in the absence of other Cu(I)-stabilising ligands. Copper(I) is a soft acid favouring coordination to soft bases such as S and P ligands and unsaturated N containing ligands. Cu(II) predominantly favours O

and N ligand coordination.[18]

1.3 Copper Proteins - Classification

A number of important proteins and enzymes contain copper ions at their active sites. These copper protein sites are associated with a variety of vital biological functions, including oxygen transport and activation, electron transfer, iron metabolism, and superoxide dismutation. The protein ligand imposes an unusual geometric and electronic structure at the copper site. As a consequence, copper proteins often exhibit unique and characteristic spectral features compared to small molecule copper complexes. Studying these spectral features provides insight into the correlation between active site electronic structure and biological function.

Based on spectroscopic properties (mainly EPR), the active sites of copper proteins have been classified into three groups,[19] I, II and III and this was originally applied to blue oxidases to distinguish the four copper ions contained in these proteins. The new classification based on structural features and spectroscopic properties covering all types of copper sites known to date is as follows:[20]

Type I. Mononuclear copper having a trigonal basal plane with an N_2S ligand donor set (S denotes thiolate sulfur from cysteine); exhibits unusual spectroscopic properties: 1) a strong absorption band at 600 nm, 2) a small $A_{\parallel}$ value of < 70 G, and 3)

a high reduction potential (generally > 250 mV).

Type II. Mononuclear copper site exhibiting a normal EPR spectrum. This type, however, can be divided into the following three classes: **Type IIA**: The ligand donors come from ordinary protein residues, such as histidine imidazole, cysteine thiolate, and water (or hydroxide); **Type IIB**: The ligand donors include unusual protein side chains; **Type IIC**: The copper is bridged to another metal ion, forming a hetero-dinuclear metal site.

Type III. EPR-silent binuclear copper site that binds dioxygen as peroxide and exhibits unusual physicochemical characteristics: 1) diamagnetism, 2) two characteristic absorption bands at 350 and 580 nm, and 3) a low O-O stretching vibration frequency ($\approx 750\ cm^{-1}$).

Type IV. Trinuclear copper site having an isosceles triangle shape; two copper ions are strongly magnetically coupled.

As first predicted by spectroscopy, the geometry of the Type I blue copper site is very different from that of normal copper centers in that it is a distorted tetrahedron with a short cysteine (Cys) thiolate S-Cu bond of 2.13 A. The remaining three ligands are two imidazole N atoms from histidine (His) residues and a thioether S from methionine (Met) with a very long Cu-Met bond length of 2.90 A.[21]

The most striking feature associated with the Type I copper

site is its intense blue colour resulting from an absorption at ≈ 600 nm. The molar absorption coefficients (ϵ) of the band are located in the range of 3000 - 7000 M^{-1} cm^{-1}, much higher than the visible band observed for ordinary copper(II) complexes; for the latter the d-d band appears at 600-800 nm with ϵ < 700 M^{-1} cm^{-1}.[20]

The EPR spectra of oxidized blue copper centers exhibit $g_{\parallel} > g_{\perp} > 2.00$, indicating that the half-occupied ground state orbital is $3d_{x^2-y^2}$. This ground state is found in normal tetragonal copper(II) complexes. However, the EPR spectra of blue copper centers exhibit unusually small parallel hyperfine splitting, the magnitude of which (60×10^{-4} cm^{-1}) is about one-third that of normal copper hyperfine splitting. Since the half-occupied 3d orbital associated with this EPR signal is involved in the electron-transfer reactivity of the blue copper proteins, it is essential to have a clear understanding of the electronic structural origin of the small $A_{\parallel}$ splitting associated with this ground-state wave function.[22] For the blue copper site, both the small hyperfine splitting and intense low-energy absorption band result from a highly covalent Cu-S(Cys) bond that activates the site for directional, efficient, long-range electron transfer.[21]

The blue copper proteins are involved in electron transport and provide one of the best examples of active site design. Electron transfer reactions proceed by a transition state in which the structures are intermediate between the reactant and product states. In many cases, formation of the intermediate involves a

simple adjustment in metal-ligand bond lengths. However, in the case of Cu(I) and Cu(II), it is more complicated because the two states normally have different geometries, tetrahedral and tetragonal (square-planar or octahedral) respectively. In such instances redox interconversions is more demanding in terms of energy. In the case of the blue copper proteins the existence of a compromise geometry acceptable to both oxidation states makes it easier to interconvert the two. From a not very favourable situation, therefore, nature has learnt how to use copper as a redox center.[23]

1.4 The Active Site Structures in Certain Type I Copper Proteins

1.4.1 The Active Site Structure of Plastocyanin

Plastocyanins are the best characterized among the Type I blue copper proteins. The list of completed plastocyanin sequences now includes those from 20 higher plants, 4 green algae and one blue-green alga.[24-26] Plastocyanin is involved in electron transport between photosystems II and I of the chloroplast in higher plants and algae.[27] More specifically, its function is to transfer electrons from cytochrome f (360 mV) to the chlorophyll-containing pigment $P700^{+}$ (520 mV) which is a component of photosystem I. Photosynthesis occurs at the highly convoluted thylakoid membranes inside the chloroplast. Both the Cu(II) and Cu(I) poplar structures (Fig. 1.1) have been refined to resolutions of 1.6 A.[28] The dimensions of the distorted tetrahedral Cu(II) active site do not

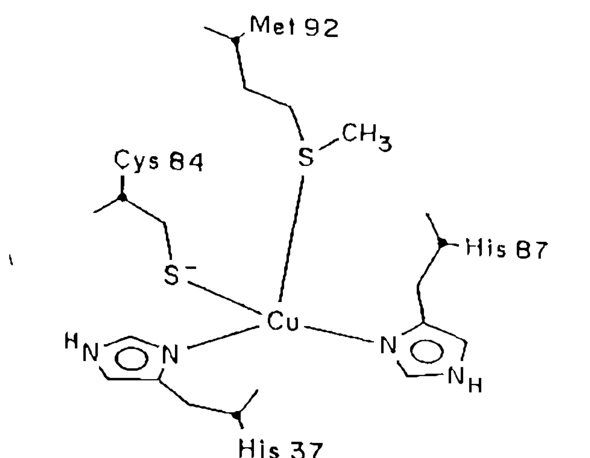


Fig. 1.1 The active site in Plastocyanin

vary for structures determined at pH 6.0 and 4.2, whereas Cu(I) site shows a change in geometry from four to three coordination as the pH is decreased from 7.8 to 3.8 (Fig. 1.2).[26b] The two Cu-N(His) and Cu-S(Cys) bond lengths are normal, as observed in low-molecular weight coordination complexes, but the Cu-S(Met) distance is unusually long at 2.90 Å. This and other features have provoked much interest in the spectroscopic properties of the proteins.

The structure of apoplastocyanin obtained by soaking crystals of poplar PCu(I) in 0.15 M CN^- to remove the metal has been determined to 1.8 Å resolution.[27] The structure closely resembles that of the haloprotein. In particular, the positions of the Cu-binding residues in the apo- and haloproteins differ by only

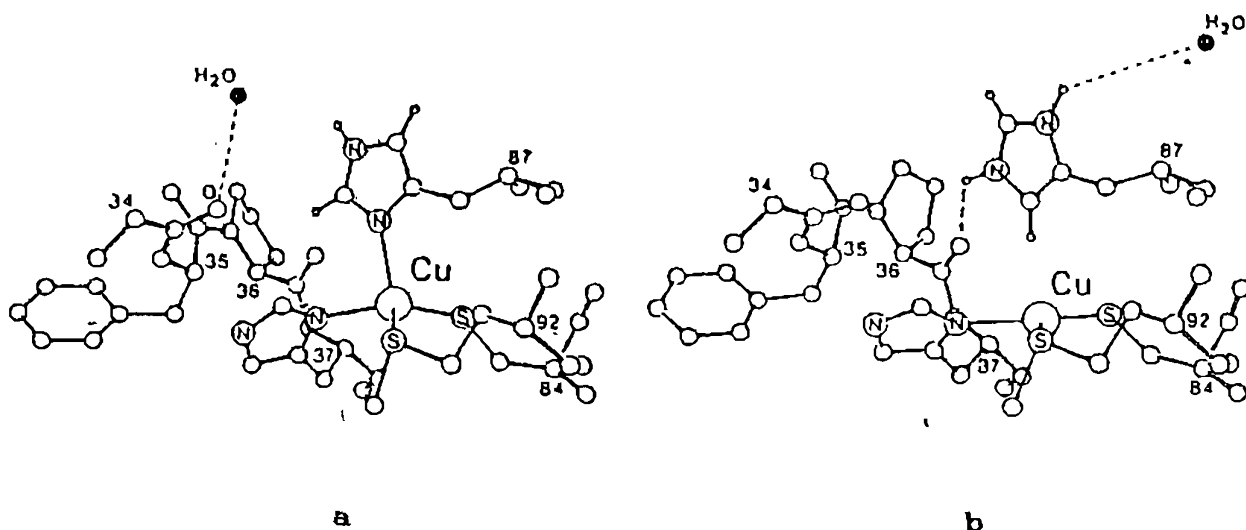


Fig. 1.2 The copper site in Plastocyanin at high (7.8) (a) and low (3.8) pH (b) (Ref. 28b)

0.1 - 0.3 Å; this and the crystal structure of Hg(II) substituted plastocyanin[30] indicate that the irregular geometry of the metal at the active site is imposed by the polypeptide backbone.

1.4.2 The Active Site Structure of Azurin

Azurins are found in the respiratory chains of various denitrifying bacteria, where their role is to transport electrons between cytochrome c_{551} and cytochrome oxidase. The kinetics of the reaction of *P. aeruginosa* azurin and cytochrome c_{551} has been studied.[31] The role of the pseudoazurins is believed to be to transfer electrons to a copper-containing nitrite reductase[32] and their properties appear to be intermediate between those of plastocyanin and azurin.

The refinement of the structure of Cu(II) state of azurin has shown (Fig. 1.3) that the geometry is close to that of a

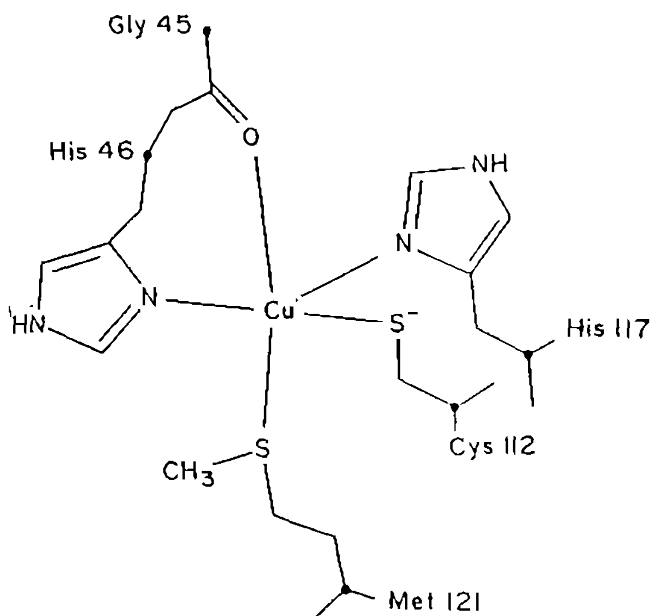


Fig. 1.3 The active site in azurin

distorted trigonal-bipyramid geometry (with axial bonds elongated) rather than the tetrahedral arrangement as in plastocyanin.[33] The two N(His) bonds and the S(Cys) bond are in a trigonal plane, and are supplemented by the much larger S(met) bond (Cu-S of 3.13 A) and the bond to the peptide carbonyl of Gly 45 (Cu-O of 3.11 A), which occupy the two axial positions. The copper ion is 0.10 A from the plane defined by His 46, Cys 112, and His 117. The same geometric arrangement applies in the case of the Cu(I) protein.[23]

1.5 Importance of Sulfur Coordination in Type I Proteins

A very puzzling observation with blue copper proteins is the fact that the energy of the charge-transfer transition responsible for their strong blue colour does not vary much between proteins,[34] whereas the standard chemical reduction potential does. To explain this, Gray and Malmstrom[35] suggested that subtle changes in protein structure between the various blue proteins introduce a variation in M ---> π back bonding causing an increasing stabilization of the Cu(I) state as the π interactions become stronger. This idea has received support from an observed linear correlation of increasing LF splittings with decreasing electron transfer reaction enthalpies.[36] Recently it has been confirmed experimentally that delocalisation of electron density into the thiolate cysteine ligand is the origin of the small parallel hyperfine splitting in the EPR spectrum of blue copper centers.[22]

Resonance Raman spectra of Type I copper proteins (cupredoxins) show a multiplicity of vibrational fundamentals between 250 and 500 cm^{-1}, which is assigned to coupling of the Cu-S(Cys) stretch with deformations of the Cys and His ligand side chains. A similar set of vibrational frequencies is observed for eleven different cupredoxins. These findings suggest that all cupredoxins have a highly conserved $Cu(His)_2Cys$ geometry including i) a trigonal planar array for the three Cu ligands and ii) a coplanar arrangement of the Cu-S-Cβ-Cα-N atoms in the Cu-cysteinate

moiety. A number of cupredoxin-type proteins have a strong absorption band near 460 nm in addition to their characteristic absorption near 600 nm. Excitation within either absorption band yields a similar resonance raman spectrum. Thus, both the electronic transitions are likely to have (Cys)S ---> Cu(II) charge transfer character.

The orientation of the $d_{x^2-y^2}$ orbital is sensitively dependent on the overlap with the Cys S pπ orbital, which in turn depends on the length of Cu-S(Cys) bond.[37] In plastocyanin this bond is so short that the strong π-overlap orients the $d_{x^2-y^2}$ orbital such that its lobes are bisected by the Cu-S bond axis. The shape and orientation of the $d_{x^2-y^2}$ orbital and thus the overlap with orbitals from which optical transitions are observed therefore depend sensitively on the Cu-S(Cys) bond length.[38]

Further, even though there is a possibility that the apical thioether ligand may control the Cu(II)/Cu(I) redox potential, its definite role still remains ambiguous.[39] So the synthesis and study of spectra and redox of low molecular weight coordination compounds containing Cu-S bonds are essential to further address this point.

1.6 Cyclodextrins and their Inclusion Complexes

Cyclodextrins (CDs) are naturally occurring molecular receptors which can alter the physical properties and chemical reactivities of guest molecules.[40] The lower members of this family are toroidally shaped polysaccharides made up of six (α-CD), seven

(β-CD) (Fig. 1.4) and eight (τ-CD) D-glucose monomers, joined by α(1-4) bonds.[41] The cyclodextrin exterior is hydrophilic, due to the hydroxyl groups that surround both rims of the cavity, the interior is hydrophobic with a diameter of 5 Å (α), 6 - 7 Å (β) and 7 - 8 Å (τ) and is capable of binding appropriately sized

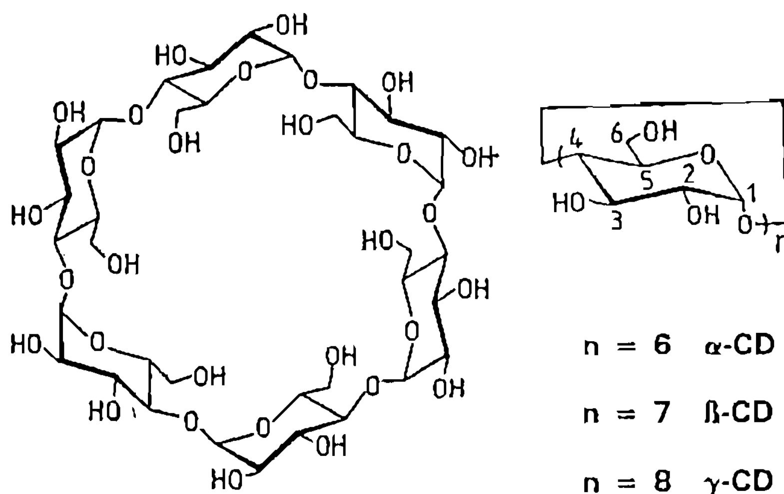


Fig. 1.4 Structure of β-cyclodextrin

molecules.[42-46] These CDs are the most important and widely studied examples of host molecules.

The rate and stereochemistry of organic reactions are significantly changed by the inclusion complexation of cyclodextrin with a substrate. The mode of action in these reactions are very similar to those in enzymes or biological receptors, so that cyclodextrins have been regarded as a good model compound for such

biopolymers. Since the structures of cyclodextrins are well defined, one can observe what is really happening at the action site more unequivocally than in the cases of biopolymers. The CDs have very interesting catalytic properties and have been used as models of hydrolytic enzymes. Many enzyme models have been reported[47] based on CDs or chemically modified CDs.[48] The first artificial metalloenzyme (Fig. 1.5) having a substrate binding

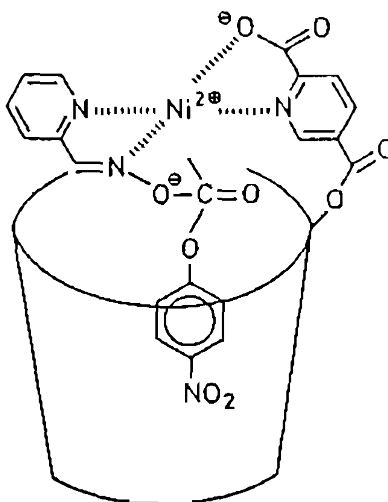


Fig. 1.5 Structure of a inclusion complex formed by a Ni(II) complex with β-CD, which has been reported as a model for a metalloenzyme (Ref. 49)

cyclodextrin cavity and a Ni(II) complex, has been reported by Breslow *et al.*[49]

Metal complexes of modified cyclodextrins or metallo-cyclodextrins have been studied as metalloprotein models[50] and it has been reported by Brown *et al.* that enantioselectivity of a Ni(II) complex is increased by complexation with modified β-CD (Fig. 1.6).[51]

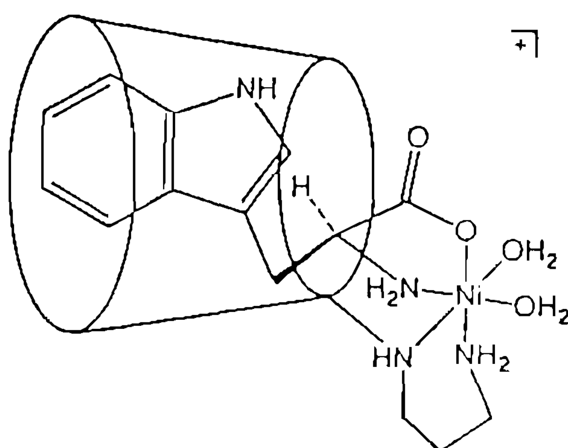


Fig. 1.6 A possible structure of [Ni(β-CDpn)(S)-trp]$^+$, which exhibits increased enantioselectivity due to complexation with β-CD (Ref. 51)

CDs may be involved in the second-coordination sphere of metal complexes by including hydrophobic organic inner-sphere ligands and so there is a growing interest in the use of CDs as second-sphere ligands for transition metal complexes.[45b,52] For the first time, a transition metal complex-CD adduct, trialkyl-phosphaneplatinum complex with β-CD has been charaterised by X-ray crystallography (Fig. 1.7).[53] Such reports have implications for

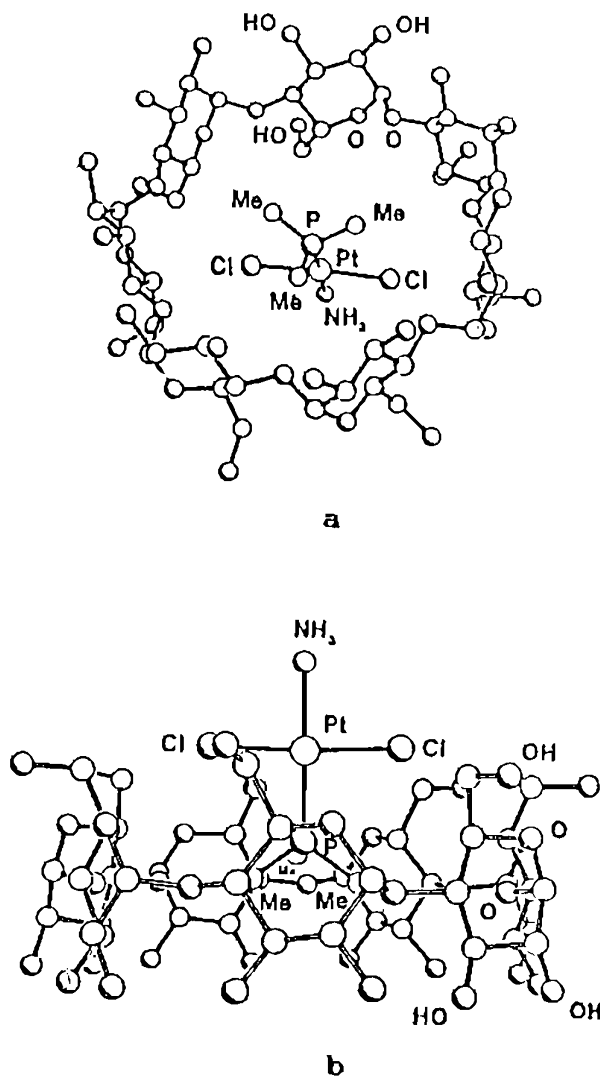


Fig. 1.7 Structure of the adduct formed between β-CD and *trans*-[Pt(PMe_3)Cl_2(NH_3)]; a) crystal viewed looking into the β-CD face carrying the secondary hydroxyl groups b) side on view of the adduct (Ref. 53)

the design of drug delivery systems and water-soluble catalysis. Cyclodextrins may also form metal rotaxane complexes by including bridging ligands such as α,ω-diaminoalkanes and α,ω-bis(4,4'-

dipyridinium)alkanes coordinated to chlorobis(ethylenediamine)-cobalt(III)[54] and pentacyanoferrate(II) centers.[55]

In the present investigation the redox and spectral behaviour of certain selected copper(II) complexes in the presence of different CDs will be undertaken.

1.7 Surfactants and their Interaction with Metal Complexes

The self-assembly of amphiphilic species in water giving rise to the formation of 'molecular clusters' called micelles (Fig. 1.8) is one of the central research topics in colloid science.[56] Micelles in water are described as spherical aggregates of a

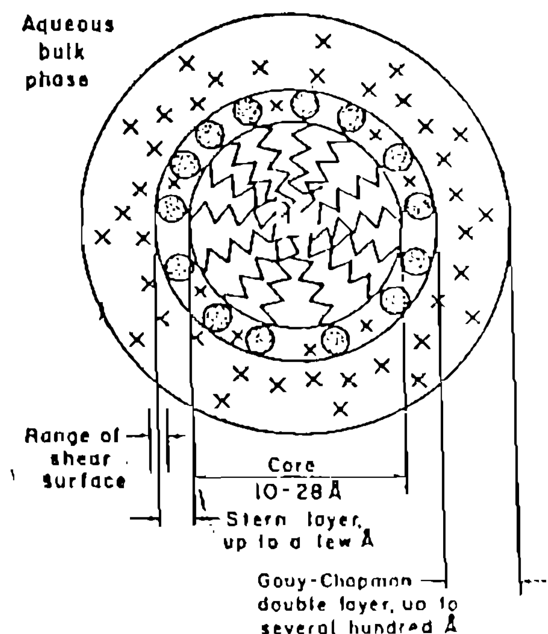


Fig. 1.8 A two dimensional schematic representation of the regions of a spherical ionic micelle. The counterions (X), the head groups (⊛) and the hydrocarbon chain (⋀⋀⋀) are shematically indicated

surfactant monomer and catalysis of reactions within micelles has been studied extensively. They resemble enzymes in structure and functions since both micelles and enzymes bind substrates in a noncovalent manner. There are numerous studies of micellar models of enzymes. For carboxypeptidase enzyme a successful micellar model has been reported by Tagaki *et al.*[39]

Aqueous solutions of ionic micelles composed of surfactants with hydrocarbon tails of 8-18 carbons attached to cationic or anionic head groups are attractive model systems for the ion binding properties of the much more complex systems of natural and synthetic liposomes and vesicles and biological membranes.[40]

Micelles and reversed micelles are able to solubilize substances which are insoluble in the bulk phase of the system considered. This solubilization is due to solvation by the amphiphile and concomitantly a change in the order of the solubilized molecules may occur as a consequence of its modified solvation shell. The results obtained by interaction with micelles are generally interpreted in terms of pseudophase model in which the totality of the aggregates in solution is assumed to act as a separate phase. A two-site model has been successfully applied to the distributions of counter ions; they are assumed to be either "bound" to the micellar pseudophase or "free" in the aqueous phase.[41]

The electrochemical characteristics of ferrocene derivatives

solubilised and immobilised in anionic, cationic and nonionic micelles and the effect of electrical double layer on electron transfer through the interface have been reported by Fujihira *et al.*[62]

Divalent metal ions having positive charges are highly hydrophilic and cannot be incorporated into cationic micelles. Anionic micelles tend to form water insoluble salts with divalent metal ions. Interactions of non-ionic micelles with divalent metal ions appear to be small. Thus incorporation of a divalent metal ion into a micelle to form a catalytic center is not a straightforward process without some devices. A simple device is to use a mixed micellar system which is composed of chemically inert surfactant moleculees and lipophilic ligands having a strong chelating ability towards metal ions together with a nucleophilic group for catalysis, such as illustrated in Fig. 1.8a

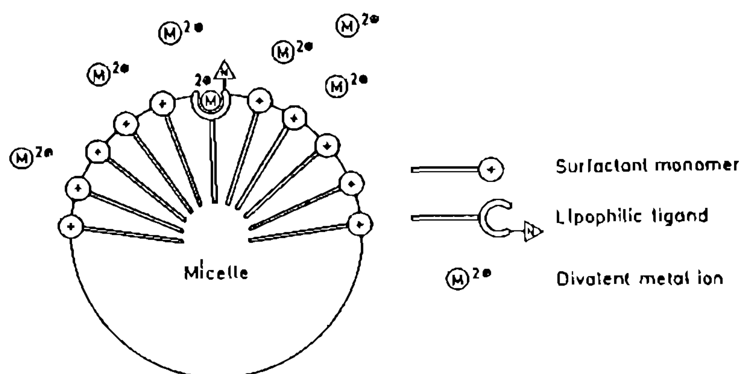


Fig. 1.8a Schematic illustration of a micellar model of a metalloenzyme

Redox behaviour of cobalt phenanthroline and terpyridine complexes in micellar solutions has been reported by Davies *et al.*;[63] by incorporating different substituents in the ligands of the complexes and studying the changes in redox potentials in different micelles, the importance of hydrophobic interactions in addition to the electrostatic interactions has been demonstrated. Kirchhoff *et al.*[64] have studied the electrochemistry of technetium complexes in the presence of cationic, anionic and non-ionic micelles.

The kinetics of the quinoline-promoted incorporation of copper(II) ion by tetraphenylporphine have been examined in a mineral oil in water microemulsion stabilized by the anionic surfactant sodium cetyl sulfate and 1-pentanol as cosurfactant.[65]

In the present study, the spectral and redox behaviour of certain copper(II) complexes in different micelles has been investigated.

1.8 Model Compounds for Copper Proteins

It is generally believed that an enzyme provides not only the particular structure that constitutes the active site but that it also provides the environment necessary for catalysis. Thus within an aqueous solution, it seems that only a large molecule can supply the hydrophobic exterior contributing to the solubility. Because of this it may be assumed that the active site is not situated on the outer surface of the protein molecule. Also it is

unlikely that a small molecule, with a structure similar to that of the active site, would have any pronounced enzymatic properties in dilute aqueous solution. Even though a small molecule may have a low catalytic activity, it is in the study of the low molecular weight model system that it is possible to obtain highly accurate data rather than in the study of the protein itself. The interpretation of the data obtained for a small molecule is less ambiguous than those obtained for a large protein. Thus a detailed investigation of a low molecular weight complex may yield important information regarding the geometry of the metal binding site for such metal ion-protein molecule. On the other hand, when the metal ion is bound very specifically to a site having a hydrophobic environment, then it might be possible, at least in a few cases, to describe the geometry *via* a solid model compound, or *via* a complex formed in a solvent of less polar properties than those of water. These models are structural models, and they quite generally indicate how proteins interact with copper ions; they should not be considered as dynamic models supposed to have an "enzymatic" function in an aqueous solution.[44]

The copper centers in proteins catalyze a variety of substrate oxidation or oxygenation reactions or bind and transport dioxygen leading to extensive efforts by bioinorganic chemists to learn about the structures and mechanism of action of the protein active sites. This approach involves the synthesis and characterization of low molecular weight compounds that can duplicate either the physicochemical properties of the protein

active sites and/or mimic their functional attributes. The role of such model systems is to establish firmly the relevant coordination chemistry as a basis upon which reasonable and meaningful conclusions can be drawn from investigations carried out on the proteins.

Significant parallel advances have been made both in our knowledge of the protein active sites and in O_2 reactivities with synthetic copper coordination complexes in the last few years.[18]

Rorabacher's group has isolated many Cu(II) complexes of the cyclic polythioether ligands and found that these complexes have high Cu(II)/Cu(I) redox potentials.[67-69] Some of these complexes exhibit a strong band at 600 nm with very high intensity as in blue proteins.[67,68] However, the X-ray crystal structures of Cu(II) complexes of [14]ane-S_4 and Et_2-2,3,2-S_4 are planar and not tetrahedral (Fig. 1.9).[70]

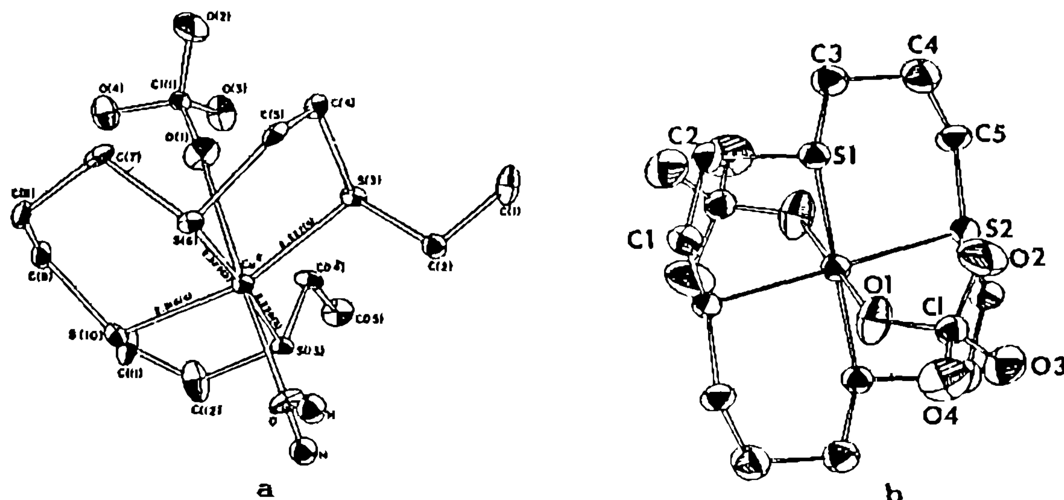


Fig. 1.9 X-ray crystal structures of a) [Cu(Et_2-2,3,2-S_4)(OH_2)(ClO_4)](ClO_4) (Ref. 70a) and b) Cu(14-ane-S_4)(ClO_4)$_2$ (Ref. 70b)

X-ray crystal structures of both Cu(II) and Cu(I) forms (square pyramidal and tetrahedral respectively) of a chelating N_2S_2 ligand (1,8-bis(prid-2-yl)-3,6-dithiaoctane) (Fig. 1.10) have been

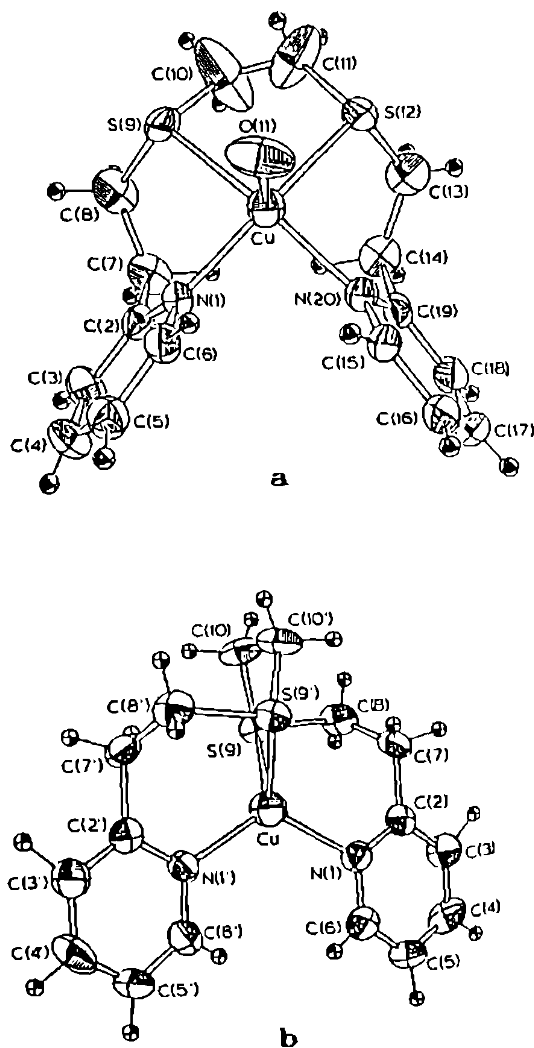


Fig. 1.10 X-ray crystal structures of a) perchlorato[1,8-bis-(pyrid-2-yl)-3,6-dithiaoctane]copper(II) cation and b) (1,8-bis(pyrid-2-yl)-3,6-dithiaoctane)copper(I) cation (Ref. 71)

reported by Brubaker *et al.*[71] This complex resembles only the high

redox potential of the blue proteins but not the spectral properties.[71]

Spectral and electrochemical investigations for Cu(II) complexes of N_2S_3 ligands (S, thioether; N, pyridyl, pyrazolyl, benzimidazolyl) were carried out by Kanters,[72] Haanstra[73] and Lucas *et al.*[74] These complexes mimic only the redox potentials of the blue proteins but not the spectral properties. The X-ray crystal structures of Cu(II) complexes of pyridyl and pyrazolyl ligands[74] are square based ones (Fig. 1.11).

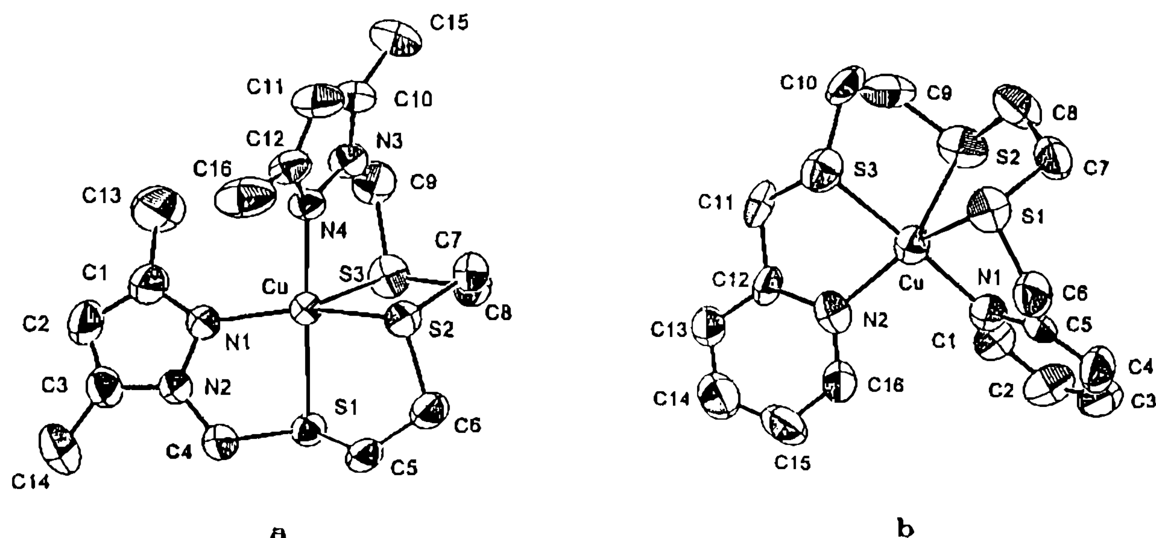


Fig. 1.11 X-ray crystal structures of a) $[Cu(1,9\text{-bis}(3,5\text{-dimethyl-}1\text{-pyrazolyl})\text{-}2,5,8\text{-trithianonane})]^{2+}$ b) $[Cu(1,9\text{-bis-}(\text{pyrid-}2\text{-yl})\text{-}2,5,8\text{-trithianonane})]^{2+}$ (Ref. 74a)

Using a hindered tripodal pyrazolyl ligand Thompson *et al.*

reported a copper complex as blue protein model which was expected to have a tetrahedral coordination geometry. The compound exhibits an intense 600 nm band but not the EPR spectral properties of blue proteins.[75]

Reedijk *et al.* isolated a series of Cu(II) complexes with N_2S_2 ligands (S, thioether; N, pyrazolyl, imidazolyl, benz-imidazolyl) as Type I models.[73,76] In these complexes, they have attained only the high redox potentials but not the spectral properties. Most of the X-ray crystal structures of these Cu(II) complexes are either distorted octahedral or trigonal bipyramidal but not tetrahedral (Fig. 1.12).[77]

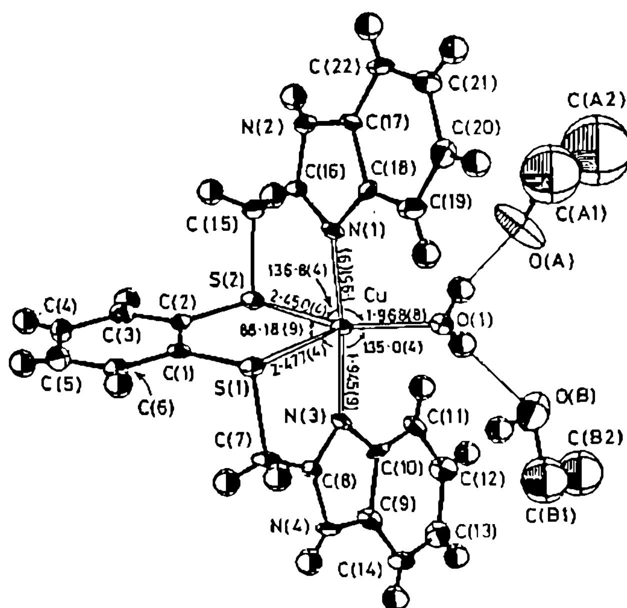
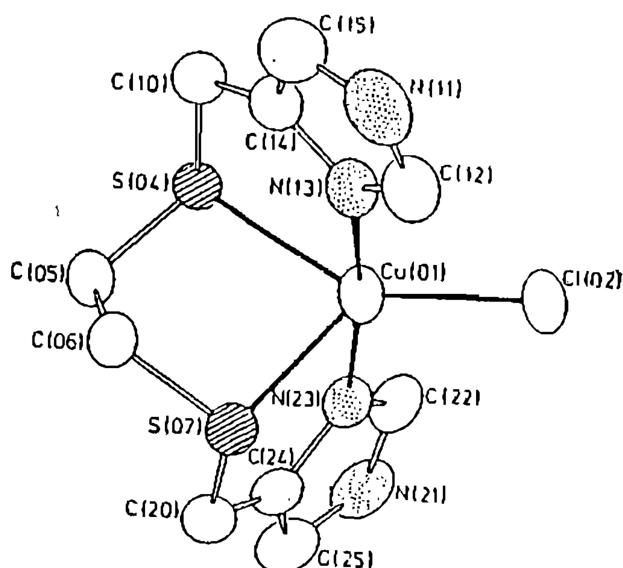
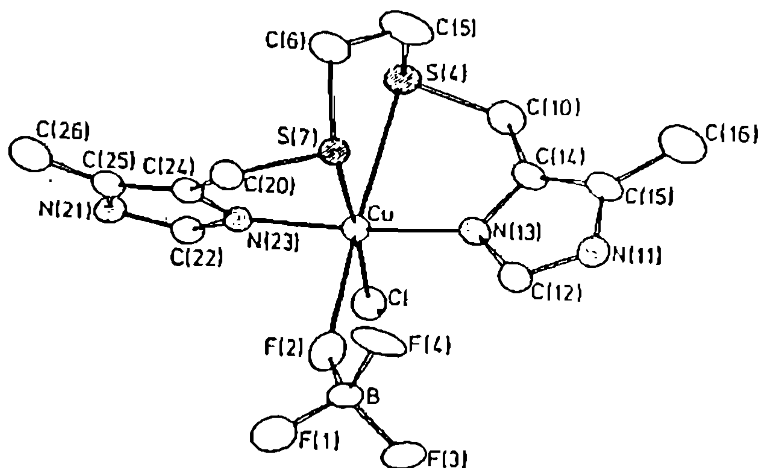


Fig. 1.12a X-ray crystal structure of a) $[Cu(bbtb)(H_2O)]^{2+}$ (Ref. 77b)



a



b

Fig. 1.12b X-ray crystal structures of a) $[Cu(bbdhx)Cl]^{+}$ and b) $[Cu(bidhx)Cl(BF_4)]$ (Ref. 77c)

Cu(II)-thiolate complexes are usually unstable with respect to intramolecular redox reorganization and form copper(I) and disulfide and other thiol-derived oxidation products;[21] however,

they can be stabilised by adding bulkiness to the ligand. Kitajima *et al.*[78] reported a group of Cu(II)-thiolate complexes of hindered pyrazolyl ligands. One of the Cu(II) complexes, Cu(Cl)(HB(3,5-$iPr_2pz)_3$) (Fig. 1.13) with tetrahedral geometry exactly mimics only the spectral properties of the blue site but in CH_2Cl_2 solution.[79]

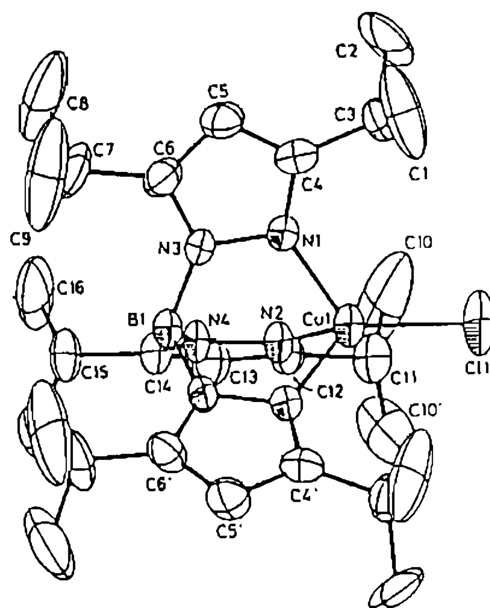


Fig. 1.13 ORTEP view of Cu(Cl)(HB(3,5-$iPr_2pz)_3$) (Ref. 78a)

All known active sites in copper proteins are "intrinsic"; that is they are formed only through the intimate interaction of the copper ions with the ligating protein residues. This generates a copper site which is quite different, both in geometry and ligation, from small molecule copper complexes. It is unrealistic

to expect to synthesize a copper complex which is a detailed model for an intrinsic protein site. It is possible, however, to generate small, X-ray crystallographically defined, electronic structural analogues which duplicate specific protein features and which can be studied in detail. Our understanding of the electronic and geometric structure of protein active sites has clearly benefited from such model studies. As our knowledge of active sites in copper proteins increases, electronic structure analogues will become of even great importance.[17]

1.9 Modelling Strategy

One of the major goals of research in bioinorganic chemistry has been to understand the origin of the spectral features and to use this information to generate a working model of the geometric structure of the active site in the absence of X-ray crystallographic information.

Extensive synthetic work has been undertaken in order to clarify the active site structures and the origins of the unusual spectroscopic characteristics of copper proteins. These studies are based on the premise that the chemistry of copper proteins is mostly dependent on the coordination structure of the copper sites. The high kinetic lability of copper and its tendency to adopt different coordination numbers and geometries in the +1 and +2 oxidation states pose formidable obstacles in the design and synthesis of appropriate small-molecule systems.

The first step in modelling is choosing a suitable ligand. Chelating ligands with N (imidazole, pyrazole, pyridine or benzimidazole) and S (thiolate, thioether or disulfide) donors with suitable chelate ring structures are good choices. Sulfur-containing groups, like thioether or thiolate are important when modelling Type I proteins. Usually in model complexes the thiolate group is substituted by a thioether donor due to the low stability of the former. In proteins the peptide backbone sometimes imposes an unusual geometry upon the active site, which makes it suitable for a specific function. Hence, equally important for the stereochemistry is the presence of large substituents like the benzo-ring in the benzimidazole. Besides direct steric effects of such bulky groups on the coordination geometry, they may also prevent the metal ion to be approached by compounds that would give side reactions. In the proteins an analogous feature is encountered; the active site is immersed in the bulk of the protein and is only accessible to specific substrates. By deliberately varying the steric constraints in model compounds it is possible to investigate the relation between the structure and activity in the model compound.[79] The copper complexes are characterized using various spectral and electrochemical techniques and finally their properties are correlated with the features of natural proteins.

1.10 Scope of the Present Investigation

The present thesis describes the synthesis and physical and

chemical properties of low-molecular weight compounds containing thioether sulfur donors, as models for Type I copper proteins. Also the spectral and redox properties of certain of these model complexes in aqueous solutions of various cyclodextrins and micelles have been studied.

One of the special properties of the blue copper proteins is fast electron transfer and high redox potential, which are responsible for their electron transfer function and it is believed that both steric hindrance and presence of thioether sulfur are necessary for this.[17] Rorabacher *et al.* have systematically carried out spectral and electrochemical studies on Cu(II) complexes of various macrocyclic polythiaether ligands[67,68] and concluded that the presence of π-donor atoms is more essential to the high redox potential of the blue proteins than is the tetrahedral geometry imposed by the protein superstructure. By contrast, several others suggested[80] that the relatively high redox potentials of blue proteins is due to sometimes unusual copper coordination geometry in them. Thus the definite role of thioether coordination to copper(II) has not been unambiguously established. Very recently Solomon *et al.* have ascribed[37b,81] the unique spectral features of blue copper proteins to a high anisotropic covalency of the ground state wavefunction involving the thiolate ligand which provides a very efficient superexchange pathway for long range electron transfer. The present thesis aims at studying the importance of

copper-thioether coordination in affecting the spectral and redox properties and this constitutes the scope of Chapters 3 to 5. It is proposed to synthesise several multidentate thioether-containing ligands and their copper(II) complexes, investigate their spectral and redox properties and evaluate the effect of varying geometric constraints upon the spectral and electrochemical properties of copper. By increasing the number of sulfur donors and changing the chelate ring size in a systematic manner geometric constraints around copper may be varied. A series of open chain tetra- and pentathioether carboxylic acid ligands and their Cu(II) complexes, with varying chelate ring sizes will be isolated. In Chapter 3 the spectral and electrochemical properties of these complexes will be discussed in comparison with those of the corresponding cyclic thiaether ligands.[92]

A number of reports on Cu(II) complexes of tetradentate ligands[76,93] with N_2S_2 donor set have appeared and the changes in spectral and redox properties[94,95] on varying the chelate ring sizes have been evaluated. So it is of great interest to probe the consequences of enlarging the ligand by varying the chelate ring sizes and number of sulfur donor atoms from two to three to four to five, on structure and properties of copper(II) complexes. So in Chapter 4 the consequences of incorporating two methylene groups between sulfur and benzimidazole (bzim) in a $Cu^{II}N_2S_2$ complex and between sulfur and pyridine (py) donors in a $Cu^{II}N_2S_3$ complex on

structure and spectral and redox properties of copper(II) complexes are probed. It is also planned to isolate and study the copper(II) complexes of bis(benzimidazolyl) ligands with four and five thioether donor atoms, incorporating various anions. The effect of different chelate ring systems around copper(II), on the spectral and redox behaviour of these complexes will be analysed in Chapter 5. It is proposed to derive the possible co-ordination geometries of these complexes from their ligand-field and EPR spectra, in comparison with those of related complexes. This study is expected to throw light on the effect of increasing number of thioether donors on the redox and spectral properties.

Though useful, most of the previous studies of Type I model compounds were restricted to non-aqueous solvents and are not directly relevant to the biological environment encountered by copper proteins. In an effort to understand the redox fate of biomimetic copper(II) complexes in more biologically relevant media, a study of their electrochemical properties in aqueous surfactant solution has been initiated. In Chapter 6 is probed the behaviour in micellar solutions of a few copper(II) complexes containing biomimetic donors like thioether and py or bzim nitrogen, which have been investigated as models for the blue sites (Chapter 4).[71,74] The influence of anionic (SDS), cationic (CTAB), and nonionic (Triton X-100) surfactants on the redox behaviour will be discussed.

The irreversible MV^{+}/MV^{0} redox couple in aqueous solution becomes reversible by specific inclusion complex formation with β-CD.[84] Also CDs have been studied extensively as models for enzyme active sites.[48,87] So it is proposed to investigate the electrochemical behaviour of certain Cu(II) complexes designed as models for blue proteins, in the presence of CDs. Such a study is expected to throw light on their redox behaviour and the results of the study are presented in Chapter 7.

At the outset of Chapters 3 to 7 a brief introduction and a review of the relevant previous work are provided. The study of the importance of copper-thioether coordination starts with the synthesis of ligands which contain the desired functional groups. The ligands will be complexed mostly with $Cu(ClO_4)_2.6H_2O$ and in some cases with various copper(II) salts to highlight the effect of anions. The general experimental materials, methods and techniques are described in Chapter 2 and the procedures for the synthesis of ligands and the preparations of their copper(II) complexes are included in the respective chapters.

In order to determine the coordination geometry of the copper complexes, physical methods like UV-Vis and EPR techniques will be used. The X-ray crystal structure analyses of suitable single crystals will be undertaken. Since it is generally accepted that a change in valence state involving Cu(II) and Cu(I) species must be involved in the reactions of many copper proteins, the

electrochemistry of well characterised copper(II) complexes will be investigated using cyclic and differential pulse voltammetric techniques. Further, the techniques employed so far for studying micelle metal complex interactions have been almost confined to spectroscopic ones eventhough the electrochemical techniques are more informative than the former. Finally, the relationship between redox and structure of the complexes will be analysed in the light of those of the active sites of copper proteins.

Parts of this thesis have been published before[88,89] or have been submitted for publication.[90,91]

References

(1) Lontie, R. In *Copper Proteins and Copper Enzymes*; Vol. I; Lontie, R., Ed.; CRC Press: Florida, 1984.

(2) Hathaway, B. J. In *Comprehensive Coordination Chemistry*; Vol. 5; Wilkinson, G.; Gillard, R. G.; McCleverty, J. A., Eds.; Pergamon Press: Oxford, 1987.

(3) Steward, F. C. Ed.; In *Plant Physiology*; Vol. 3; Academic Press: New York, 1963.

(4) Stiles, W. In *Trace Elements in Plants*; 3rd Ed., University Press: Cambridge, 1961.

(5) Fox, H. M.; Vevers, G. In *The Nature of Animal Colours*; Sidgwick and Jactoson: London, 1961.

(6) Marston, H. R.; Allen, S. H. *Nature (London)* **1967**, *215*, 645.

(7) McMurray, W. C. In *A Synopsis of Human Biochemistry, with Medical Applications*; Harper and Row Publishers: Philadelphia, 1982; p 108.

(8) Danks, D. M.; Campbell, P. E.; Stevens, B. J.; Mayne, V.; Cartwright, E. *Pediatrics* **1972**, *50*, 188.

(9) Walshe, M. In *The Biochemistry of Copper*; Peisach, J.; Aisen, P.; Blumberg, W. E., Eds.; Academic Press: New York, 1966; p 475.

(10) Lau, S. -J.; Kruck, T. P. A.; Sarkar, B. *J. Biol. Chem.* **1974**, *249*, 5878.

(11) Jackson, G. E.; May, P. M.; Williams, D. R. *J. Inorg. Nucl. Chem.* **1978**, *40*, 1189.

(12) Margerum, D. W.; Owens, G. D. *Metal Ions Biol. Syst.* **1981**, *12*, 75.

(13) Drew, M. G. B.; Cairns, C.; McFall, S. G.; Nelson, S. M. *J. Chem. Soc., Dalton Trans.* **1980**, 2020; Gagne, R. R.; Allison, J. L.; Ingle, D. M. *Inorg. Chem.* **1979**, *18*, 2767; Gagne, R. R.; Koval, C. A.; Smith, T. J.; Cimolino, M. C. *J. Am. Chem. Soc.* **1979**, *101*, 4571.

(14) Solomon, E. I.; Hare, J. W.; Dooley, D. M.; Dawson, J. H.; Stephens, P. J.; Gray, H. B. *J. Am. Chem. Soc.* **1980**, *102*, 168.

(15) Addison, A. W. In *Copper Coordination Chemistry: Biochemical and Inorganic Perspectives*; Karlin, K. D.; Zubieta, J., Eds.; Adenine: Guilderland, New York, 1983; pp 109-128.

(16) a) Rorabacher, D. B.; Martin, M. J.; Koenigbauer, M. J.; Malik, M.; Schroeder, R. R.; Endicott, J. F.; Ochrymowycz, L. A. In *Copper Coordination Chemistry: Biochemical and Inorganic Perspectives*; Karlin, K. D.; Zubieta, J., Eds.; Adenine: Guilderland, New York, 1983; pp 167-202; b) J. Zubeita, Hayes, J. C.; Karlin, K. D. *ibid.* pp 97-108.

(17) Solomon, E. I.; Penfield, K. W.; Wilcox, D. E. In *Structure and Bonding*; Hemmerich, P., *et al.*, Eds.; Springer-Verlag: New York, 1983; p 4.

(18) Karlin, K. D.; Gultneh, Y. *Bioinorganic Chemistry of Copper*; Karlin, K. D.; Tyeklar, Z., Eds.; Chapman & Hall: New York, 1993; pp 219-327.

(19) Malkin, R.; Malmstrom, B. G. *Adv. Enzym.* **1970**, *33*, 177.

(20) Kitajima, N. *Adv. Inorg. Chem.* 1992, *39*, 1.

(21) Solomon, E. I.; Lowery, M. D. *Science* **1993**, *259*, 1575.

(22) Shadle, S. E.; Penner-Hahn, J. E.; Schugar, H. J.; Hedman, B.; Hodgson, K. O.; Solomon, E. I. *J. Am. Chem. Soc.* **1993**, *115*, 767.

(23) Sykes, A. G. *Adv. Inorg. Chem.* **1991**, *36*, 377.

(24) Sykes, A. G. *Chem. Soc. Rev.* **1985**, *14*, 283; Sykes, A. G. *Struct. Bonding* **1990**, *73*, 1.

(25) Aitken, A. *Biochem. J.* **1975**, *149*, 675; Katoh, S.; Takamiya, A. *Nature (London)* **1961**, *189*, 665.

(26) Colman, P. M.; Freeman, H. C.; Guss, J. M.; Murata, M.; Norris, V. A.; Ramshaw, J. A. M.; Venkatappa, M. P. *Nature (London)* **1978**, *160*, 309; Guss, J. M.; Freeman, H. C. *J. Mol. Biol.* **1983**, *169*, 521.

(27) Haehnel, W. *Annu. Rev. Plant Physiol.* **1984**, *35*, 659; Hauska, G.; Nitschke, W.; Herrmann, R. G. *J. Bioenerg. Biomembr.* **1988**, *20*, 211.

(28) a) Guss, J. M.; Freeman, H. C. *J. Mol. Biol.* **1983**, *169*, 521; b) Guss, J. M.; Harrowell, P. R.; Murata, M.; Norris, V. A.; Freeman, H. C. *J. Mol. Biol.* **1986**, *192*, 361.

(29) Garrett, T. P. J.; Clingeletter, D. J.; Guss, J. M.; Rogers, S. J.; Freeman, H. C. *J. Biol. Chem.* **1984**, *259*, 2822.

(30) Church, W. B.; Guss, J. M.; Potter, J. J.; Freeman, H. C. *J. Biol. Chem.* **1986**, *261*, 234.

(31) Farver, O.; Blatt, Y.; Pecht, I. *Biochemistry* **1982**, *21*, 3556; Corin, A. F.; Bersohn, R.; Cole, P. E. *Biochemistry* **1983**, *22*, 2032.

(32) Liu, M. -Y.; Liu, M. -C.; Payne, W.J. Legall, J. *J. Bacteriol.* **1986**, *166*, 604.

(33) Norris, G. E.; Anderson, B. F.; Baker, E. N. *J. Mol. Biol.* **1983**, *165*, 504; *J. Am. Chem. Soc.* **1986**, *108*, 2784; Baker, E. N. *J. Mol. Biol.* **1988**, *203*, 1071.

(34) Malmstrom, B. G. *Biol. Metals* **1990**, *3*, 64.

(35) Gray H. B.; Malmstrom, B. G. *Comments Inorg. Chem.* **1983**, *2*, 203.

(36) Gray, H. B.; Solomon, E. I. In *Copper Proteins*; Spiro, T. G., Ed.; John Wiley & Sons: New York, 1981; p 1.

(37) a) Solomon, E. I.; Baldwin, M. J.; Lowery, M. D. *Chem. Rev.* **1992**, *218*, 427; b) Penfield, W. P.; Gewirth, A. A.; Solomon, E. I. *J. Am. Chem. Soc.* **1985**, *107*, 4519.

(38) den Blaauwen, T.; Canters, G. W. *J. Am. Chem. Soc.* **1993**, *115*, 1121.

(39) Karlsson, B. G.; Aasa, R.; Malmstrom, B. G.; Lundberg, L. G. *FEBS Lett.* **1989**, *253*, 99.

(40) Bender, M. L.; Komiyama, M. *Cyclodextrin Chemistry*; Springer-Verlog: New York, 1978, pp 14-16; Pagington, J. S. *Chem. Br.* **1987**, 455; Bergeron, R. J. In *Inclusion Compounds*; Vol. 3; Atwood, J. L.; Davies, J. E. D.; MacNicol, D. D., Eds.; Academic Press: London, 1984; p 391.

(41) Ohashi, M.; Kasatani, K.; Shinohara H.; Sato, H. *J. Am. Chem. Soc.* **1990**, *112*, 5824.

(42) Munoz de La Pena, A.; Ndou, T. T.; Zung, J. B.; Greene, K. L.; Live, D. H.; Warner, I. M. *J. Am. Chem. Soc.* **1991**, *114*, 1572.

(43) Komiyama, M.; Bender, M. L. *J. Am. Chem. Soc.* **1978**, *100*, 2259; Eftink, M. R.; Andy, M. L.; Bystrom, K.; Perlmutter, H. D.; Kristol, D. *J. Am. Chem. Soc.* **1989**, *111*, 6765; Paleper, R.; Reinsborough, V. C. *Aust. J. Chem.* **1990**, *43*, 2119.

(44) Sanemasa, I.; Fujiki M.; Deguchi, T. *Bull. Chem. Soc. Jpn.* **1988**, *61*, 2663; Goledzinowski, M. *J. Electroanal. Chem.* **1989**, *267*, 171.

(45) a) Yokoi, H.; Satoh, M.; Iwaizumi, M. *J. Am. Chem. Soc.* **1991**, *113*, 1530 b) Alston, D. R.; Ashton, P. R.; Lilley, T. H.; Stoddart, J. F.; Zarzycki, R. *Carbohydrate Res.* **1989**, *192*, 259; c) Trainor, G. L.; Breslow, R. *J. Am. Chem. Soc.* **1981**, *103*, 154.

(46) Harada, A.; Takahashi, S. *J. Chem. Soc., Chem. Commun.* **1986**, 1229; Wylie, R. S.; Macartney, D. H. *Inorg. Chem.* **1993**, *32*, 1830; Shortreed, M. E.; Wylie, R. S.; Macartney, D. H. *Inorg. Chem.* **1993**, *32*, 1824.

(47) Krechl, J.; Castulik, P. *Chemica Scripta* **1989**, *29*, 173 and refs cited therein.

(48) Tabushi, I. *Acc. Chem. Res.* **1982**, *15*, 66; Breslow, R. In *Inclusion Compounds*; Atwood, J. L.; Davies, J. E. D.; MacNicol, D. D., Eds.; Academic Press: London, 1984; Vol. 3, p 473.

(49) Breslow, R.; Overman, L. E. *J. Am. Chem. Soc.* **1970**, *92*, 1075.

(50) Tabushi, I. *Coord. Chem. Rev.* **1988**, *86*, 1; Cucinotta, V.; D'Alessandro, F.; Impellizzeri, G.; Maccarrone, G.; Vecchio, G. *J. Chem. Soc., Chem. Commun.* **1992**, 1743.

(51) Brown, S. E.; Coates, J. H.; Easton, C. J.; van Eyk, S. J.; Lincoln, S. F.; May, B. L.; Stile, M. A.; Whalland, C. B.; Williams, M. L. *J. Chem. Soc., Chem. Commun.* **1994**, 47.

(52) Colquhoun, H. M.; Stoddart, J. F.; Williams, D. J. *Angew. Chem. Int. Ed. Engl.* **1986**, *25*, 487.

(53) Alston, D. R.; Slawin, A. M. Z.; Stoddart, J. F.; Williams, D. J.; Zarzycki, R. *Angew. Chem. Int. Ed. Engl.* **1988**, *27*, 1184.

(54) Ogino, H.; Ohata, K. *Inorg. Chem.* **1984**, *23*, 3312.

(55) Wylie, R. S.; Macartney, D. H. *J. Am. Chem. Soc.* **1992**, *114*, 3136.

(56) Breslow, R.; Hunt, J. T.; Smiley, R.; Tarnowski, T. *J. Am. Chem. Soc.* **1983**, *105*, 5337.

(57) Matsui, Y.; Nishioka, T.; Fujita, T. In *Topics in Current Chemistry*; Vol. 128; Boschke, F. L., Ed.; Springer-Verlag: New York, 1985.

(58) Gehlen, M. H.; De Schryver, F. C. *Chem. Rev.* **1993**, *93*, 199.

(59) Eiki, T.; Mori, M.; Kawada, S.; Matsushima, K.; Tagaki, W. *Chem. Lett.* **1980**, 1431; Ogino, K.; Tomita, I.; Machiya, K.; Tagaki, W. *ibid.* **1982**, 1875.

(60) Fendler, J. H. *Membrane Mimetic Chemistry*; Wiley-Interscience: New York, 1982; Israelachvili, J. *Intermolecular and Surface Forces*, 2nd ed.; Academic Press: London, 1991; Jain, M. K. *Introduction to Biological Membranes;* 2nd ed.; John Wiley & Sons: New York, 1988; p 423.

(61) Bunton, C. A.; Nome, F.; Quina, F. H.; Romsted, L. S. *Acc. Chem. Res.* **1991**, *24*, 357; Lindman, B.; Wennerstrom, H. *Top. Curr. Chem.* **1980**, *87*, 32; Gustavsson, H.; Lindman, B. *J. Am. Chem. Soc.* **1978**, *100*, 4647.

(62) Fujihira, M.; Yanagisawa, M.; Kondo, T. *Bull. Chem. Soc. Jpn.* **1993**, *66*, 3600.

(63) Davies, K. M.; Hussam, A. *Langmuir* **1993**, *9*, 3270; Davies, K. M.; Hussam, A.; Rector, B. R., Jr.; Owen, I. M.; King, P. *Inorg. Chem.* **1994**, *33*, 1741.

(64) Kirchhoff, J. R.; Heineman, W. R.; Deutsch, E. *Inorg. Chem.* **1988**, *27*, 3608.

(65) Mackay, R. A.; Dixit, N. S.; Agarwal, R. In *Inorganic Reactions in Organized Media*; Holt, S. L., Ed.; ACS symposium series 177; American Chemical Society: Washington, D. C., 1982; p 179.

(66) Osterberg, R. *Coord. Chem. Rev.* **1974**, *12*, 309.

(67) a) Dockal, E. R.; Jones, T. E.; Sokol, W. F.; Engerer, R. J.; Rorabacher, D. B.; Ochrymowycz, L. A. *J. Am. Chem. Soc.* **1976**, *98*, 4322; Bernardo, M. M.; Heeg, M. J.; Schroeder, R. R.; Ochrymowycz, L. A.; Rorabacher, D. B. *Inorg. Chem.* **1992**, *31*, 191.

(68) Young, I. R.; Ochrymowycz, L. A.; Rorabacher, D. B. *Inorg. Chem.* **1986**, *25*, 2576; Martin, M. J.; Endicott, J. F.; Ochrymowycz, L. A.; Rorabacher, D. B. *Inorg. Chem.* **1987**, *26*, 3012; Corfield, P. W. R.; Ceccarelli, C.; Glick, M. D.; Moy, I. W-Y.; Ochrymowycz L. A.; Rorabacher, D. B. *J. Am. Chem. Soc.* **1985**, *107*, 2399.

(69) Meagher, N, E.; Juntunen, K. L.; Heeg, M. J.; Salhi, C. A.; Dunn, B. C.; Ochrymowycz, L. A.; Rorabacher, D. B. *Inorg. Chem.* **1994**, *33*, 670; b) Aronne, L.; Yu, Q.; Ochrymowycz, L. A.; Rorabacher, D. B. *Inorg. Chem.* **1995**, *34*, 1844; c) Dunn, B. C.; Ochrymowycz, L. A.; Rorabacher, D. B. *Inorg. Chem.* **1995**, *34*, 1954.

(70) a) Diaddario Jr., L. L.; Dockal, , E. R.; Glick, M. D.; Ochrymowycz, L. A.; Rorabacher, D. B. *Inorg. Chem.* **1985**, *24* 356; b) Glick, M. D.; Gavel, D. P.; Diaddario, L. L.; Rorabacher, D. B. *Inorg. Chem.* **1976**, *15*, 1976.

(71) Brubaker, G. R.; Brown, J. N.; Yoo, M. K.; Kinsey, R. A.; Kutchan, T. M.; Mottel, E. A. *Inorg. Chem.* **1979**, *18*, 299.

(72) Kanters, R. P. F.; Yu, R.; Addison, A. W.; *Inorg. Chim. Acta* **1992**, *196*, 97.

(73) Haanstra, W. G.; Cabral, M. F.; Cabral, J. de. O.; Driessen, W. L.; Reedijk, J. *Inorg. Chem.* **1992**, *31*, 3150.

(74) a) Adhikary, B.; Lucas, C. R. *Inorg. Chem.* **1994**, *33*, 1376; b) Liu, S.; Lucas, C. R.; Hynes, R. C.; Charland, J. P.; *Can. J. Chem.* **1992**, *70*, 1773.

(75) Thompson, J. S.; Marks, T. J.; Ibers, J. A. *J. Am. Chem. Soc.* **1979**, *101*, 4180; Thompson, J. S.; Zitzmann, J. L.; Marks, T. J.; Ibers, J. A. *Inorg. Chim. Acta* 1980, *46*, L101.

(76) van Rijn, J.; Driessen, W. L.; Reedijk, J.; Lehn, J. -M. *Inorg. Chem.* **1984**, *23*, 3584; Bouwman, E.; Burik, A.; Ten Hove, J. C.; Driessen, W. L.; Reedijk, J. *Inorg. Chim. Acta* **1988**, *150*, 125; Tullemans, A. H. J.; Bouwman, E.; de Graaff, R. A. G.; Driessen, W. L.; Reedijk, J. *Recl. Trav. Chem. Pays-Bas.* **1990**, *109*, 70; Lockhart, J. C.; Clegg, W.; Hill, M. N. S.; Rushton, D. J. *J. Chem. Soc., Dalton Trans.* **1990**, 3541; Schilstra, M. J.; Birker, P. J. M. W. L.; Verschoor, G. C.; Reedijk, J. *Inorg. Chem.* **1982**, *21*, 2637.

(77) a) Birker, P. J. M. W. L.; Helder, J.; Hankel, G.; Krabs, B.; Reedijk, J. *Inorg. Chem.* **1982**, *21*, 357; b) Rietmeijer, F. J.; Birker, P. J. M. W. L.; Gorter, S.; Reedijk, J. *J. Chem. Soc., Dalton Trans.* **1982**, 1191; c) Bouwman, E.; Day, R.; Driessen, W. L.; Tremel, W.; Krebs, B.; Wood, J. S.; Reedijk, J. *Inorg. Chem.* **1988**, *27*, 4618.

(78) a) Kitajima, N.; Fujisawa, K. Moro-oka, Y. *J. Am. Chem. Soc.* **1990**, *112*, 3210; b) Kitajima, N.; Fujisawa, K.; Tanaka, M.; Moro-oka, Y. *J. Am. Chem. Soc.* **1992**, *114*, 9232.

(79) Uma, R. '*Synthesis, Structure, Spectra and Redox Interconversions in Certain Copper(II) Complexes as Models for Copper Proteins*', Ph.D. thesis, Bharathidasan University, Tiruchirappalli, 1993.

(80) Addison, A. W.; Rao, T. N.; Reedijk, J.; van Rijn, J.; Verschoor, G. C. *J. Chem. Soc., Dalton Trans.* **1984**, 1349.

(81) Gewirth, A. A.; Solomon, E. I. *J. Am. Chem. Soc.* **1988**, *110*, 3811.

(82) Bernardo, M. M.; Schroeder, R. R.; Rorabacher, D. B. *Inorg. Chem.* **1991**, *30*, 1241; Jones, T. E.; Rorabacher, D. B.; Ochrymowycz, L. A. *J. Am. Chem. Soc.* **1975**, *97*, 7485.

(83) Bouwman, E.; Driessen, W. L.; Reedijk, J. *Coord. Chem. Rev.* **1990**, *104*, 143; Bouwman, E.; ten Hove, J. C.; Driessen, W. L.; Reedijk, J. *Polyhedron* **1988**, *7*, 2591.

(84) Bouwman, E. Ph. D. 'Modelling the Blue Copper Site with Imidazole-Thioether Ligands' thesis, Leiden University, The Netherlands.

(85) a) Addison, A. W.; Palaniandavar, M.; Reedijk, J.; van Rijn, J., Rao, T. N. to be communicated. b) Addison, A. W.; Palaniandavar, M. *Abstracts, American Chemical Society 188th National Meeting*, Washington DC, **1984**, INOR-068.

(86) Sivagnanam, U.; Palaniandavar, M. *J. Electroanal. Chem.* **1992**, *341*, 197.

(87) Tabushi, I.; Shimizu, N.; Sugimoto, T.; Shiozuka, M.; Yamamura, K. *J. Am. Chem. Soc.* **1977**, *99*, 7100.

(88) Sivagnanam. U.; Pandiyan, T.; Palaniandavar, M. *Indian J. Chem.* **1993**, *32B*, 572

(89) Sivagnanam, U.; Palaniandavar, M. *J. Chem. Soc., Dalton Trans.* **1994**, 2277.

(90) Usha, S.; Palaniandavar, M.; Fujisawa, K. communicated.

(91) Usha, S.; Palaniandavar, M. Communicated.

CHAPTER 2

2. GENERAL EXPERIMENTAL MATERIALS, METHODS AND TECHNIQUES

2.1 Materials

2.1.1 Chemicals

The following chemicals were used as received. Sodium borohydride, copper tetrafluoroborate hexahydrate, 2-vinylpyridine, 3-chloropropionic acid, tetra-*N*-ethylammonium bromide, sodium perchlorate, sodiumdodecyl sulfate and cetyltrimethylammonium bromide (**Fluka**); iodine, thiourea and copper(II) chloride dihydrate (**s.d's Fine chem pvt ltd**, India); bis(2-mercaptoethyl)sulfide, 1,2-ethanedithiol, 2-chloromethylpyridine hydrochloride, 1,3-propanedithiol, α-cyclodextrin, β-cyclodextrin and γ-cyclodextrin (**Aldrich**); $Cu(NO_3)_2.3H_2O$ (**BDH, India**); 1,2-diaminobenzene, magnesium sulfate and sodium perchlorate (**Sisco, India**); chloroethanol, magnesium turnings, potassium hydroxide, sodium bicarbonate, 2-chloroacetic acid and hydrobromic acid (**E. Merck**); Triton X-100 (Ubichem); copper perchlorate hexahydrate and tetra-*N*-hexylammonium perchlorate (**G. F. Smith, USA**).

2.1.2 Solvents

Methanol (Analar), ethanol, acetonitrile, dichloromethane (Analar) (**Merck**, India and **Qualigens**, India) and dimethylformamide (Analar) (**Qualigens**, India).

2.1.3 Preparation and Purification of Supporting Electrolytes

Tetra-N-hexylammonium perchlorate (THAP)

This electrolyte purchased from G. F. Smith was recrystallised twice from aqueous ethanol and dried under vacuum over P_4O_{10}.

Sodium perchlorate

Sodium perchlorate was recrystallised from methanol and then used.

Tetra-*N*-ethylammonium bromide (TEABr)

The tetra-*N*-ethylammonium bromide obtained from Fluka was recrystallised twice from aqueous ethanol and dried under vacuum over P_4O_{10}.

2.1.4 Purification of Solvents

The commercial solvents were distilled and then used for the preparation of the complexes. For spectroscopic and electrochemical studies methanol was purified by refluxing it with Mg turnings and iodine and then distilled. Dimethylformamide was distilled (40 - 50 °C) under reduced pressure, after drying it over P_4O_{10} and neutralising the resulting phosphoric acid generated by the addition of crystalline NaOH pellets. Acetonitrile was dried over P_4O_{10} and then distilled. Commercial ethanol was distilled and used.

Acetonitrile (100 % purity) was obatined by refluxing it with P_4O_{10} for 2 hours and then distilling it.

2.2 Physical Methods

The **elemental analyses** were performed at the Central Drug Research Institute (CDRI), Lucknow, India, Hindustan Photofilms, Ootacamund, India and City University, London.

The **^{1}H NMR spectra** were obtained at room temperature using Bruker 100 MHz and 270 MHz spectrometers and the chemical shift values are reported with respect to tetramethylsilane as internal standard and the values are reported as: δ-values (multiplicity, coupling constant, assignment). The **mass spectra** were obtained from Finnigan 4000 GC-MS instrument with data for the lower mass fragments truncated below m/e = 50 and 10% intensity and if the parent ion peak could not be observed, the molecular ion peak with highest mass is reported. Melting points reported are uncorrected. The **infrared spectra** were recorded as Nujol mulls or KBr discs using Shimadzu IR-435 instrument and the frequencies are reported in cm^{-1}. The **diffuse reflectance** and the **solution spectra** were measured on a HITACHI U-3400 double beam UV-Vis-NIR spectrophotometer.

The **EPR spectra** were obtained on a Varian E-12 X-band spectrometer, the field being calibrated with diphenylpicryl-hydrazyl (DPPH). The g_o and A_o values were estimated at ambient

temperature and $g_{\parallel}$ and $A_{\parallel}$ at 77 K. The values of $A_{\perp}$ and $g_{\perp}$ were computed as $1/2(3A_o-A_{\parallel})$ and $1/2(3g_o-g_{\parallel})$ respectively. Second order corrections[1,2] were applied to the resonance fields of the transitions, from which g_o and A_o were obtained.

2.3 Electrochemical Techniques

Cyclic Voltammetry and Differential Pulse Voltammetry on glassy carbon electrode and platinum sphere electrode were performed at 25.0 ± 0.2 °C. The temperature of the electrochemical cell was maintained by a cryocirculator (HAAKE D8-G). Voltammograms were generated with the use of EG&G PAR Model 273 potentiostat. An IBM PS-2 computer along with EG&G M-270 software was employed to control the experiments and to acquire the data. An EPSON FX-850 printer and HP plotter (DMP-40) were used to print and plot out the cyclic voltammograms respectively. A three electrode system consisting of a platinum sphere (0.2328 cm^2) or glassy carbon working electrode (0.3778 cm^2), a platinum plate auxiliary electrode and a reference electrode was used. The reference electrode for non-aqueous solutions was $Ag(s)/Ag^+$ which consists of a Ag wire immersed in a solution of $AgNO_3$ (0.01 M) and tetra-*N*-hexylammonium perchlorate (0.1 M) in acetonitrile placed in a tube fitted with a vycor plug using a sleeve.[3] The $E_{1/2}$ observed under identical conditions for Fc/Fc^+ couple in acetonitrile was 0.100 V with respect to Ag/Ag^+ reference electrode. A saturated calomel electrode (EG&G Princeton Applied Research) was used in the case

of aqueous solutions. The $E_{1/2}$ value observed under identical conditions for Fe(II)/Fe(III) couple for hydroxymethylferrocene in aqueous 0.1 M $NaClO_4$ solution is 0.194 V *vs* SCE and ΔE_p° (ΔE_p at zero scan rate) is 59 mV. The experimental solutions were deoxygenated by bubbling research grade nitrogen and an atmosphere of nitrogen was maintained over the solution during measurement. The solvents for the electrochemical experiments were purified and distilled as described earlier.

The redox potential $E_{1/2}$ was calculated from the anodic (E_{pa}) and cathodic (E_{pc}) peak potentials of CV traces as (E_{pa} + E_{pc})/2. The redox potentials were also estimated from the DPV (Differential Pulse Voltammetry) peak potential E_p using the relation[4]

$$E_{1/2} = E_p + \Delta E/2$$

where $E_{1/2}$ is the equivalent of the average of E_{pc} and E_{pa} in CV experiments and ΔE is the pulse amplitude.

References

(1) Ingram, D. J. E. In *Spectroscopy at Radio and Microwave Frequencies*; Butterworths: London, 1966; p 305.

(2) Kosmau, D.; Bereman, R. D. In *Spectroscopy in Biochemistry*; Vol. 2; Bell, J. E. CRC press, Boca Raton: FL, 1981.

(3) Parker, V. D. In *Electroanalytical Chemistry*; Vol 14; Bard, A. J., Ed.; Marcel Dekker: New York, 1986; p 18.

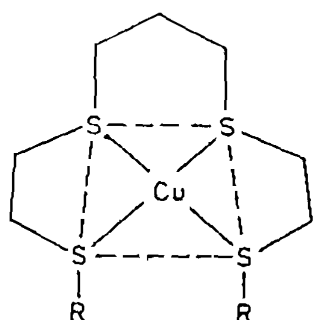
(4) Bard, A. J.; Faulkner, L. R. *Electrochemical Methods: Fundamental Applications*, Wiley: New York, 1980; p 194.

CHAPTER 3

3. HIGH POTENTIAL COPPER(II) COMPLEXES OF OPEN CHAIN TETRA- AND PENTATHIAETHER LIGANDS

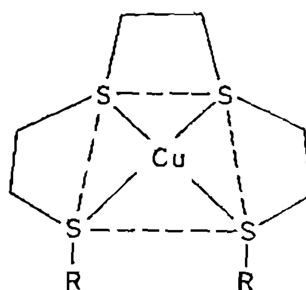
3.1 Introduction

There is continuing interest in the coordination complexes of copper(II) with thioether donors, in view of the methionin sulfur coordination to copper in the active sites of the blue copper proteins plastocyanin and azurin.[1-3] It has not yet been clearly resolved whether the unusual thermodynamic and spectral properties of these proteins are due to sulfur coordination or the unique tetrahedrally distorted coordination geometry of the active site.[4] Through extensive studies on copper complexes of thioether ligands Rorabacher *et al.* have made it apparent that thioether sulfur donor atoms, though weak, tend to be selective for copper in the so-called copper triangle.[5,6] Based on the successful X-ray crystal structure and electrochemical study of Cu(II) and Cu(I) complexes (Fig. 3.1) of exactly the same open-chain [R_2-2,3,2-S_4, R = Me (L1), Et (L2)][7] and the cyclic polythiaether[8,9] ([14]ane-S_4 (L8), [15]ane-S_5 (L9)) ligands (Fig. 3.1), they have concluded that the presence of π-donor atoms is more essential to the high



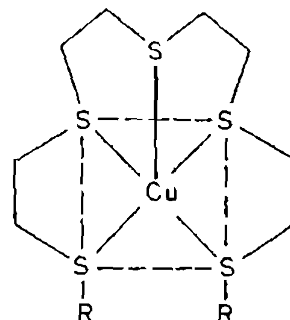
a

R = Me (L1), Et (L2)
CH_2COOH (L3)
CH_2CH_2COOH (L4)



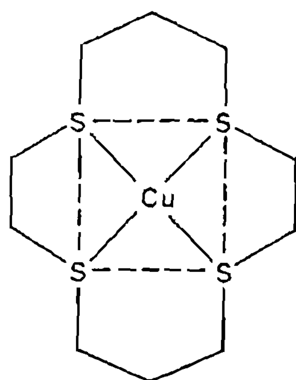
b

R = CH_2COOH (L5)
CH_2CH_2COOH (L6)



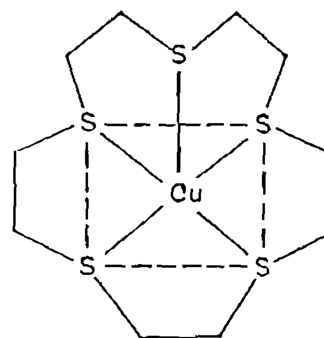
c

R = CH_2COOH (L7)



d

$[Cu(L8)]^{2+}$



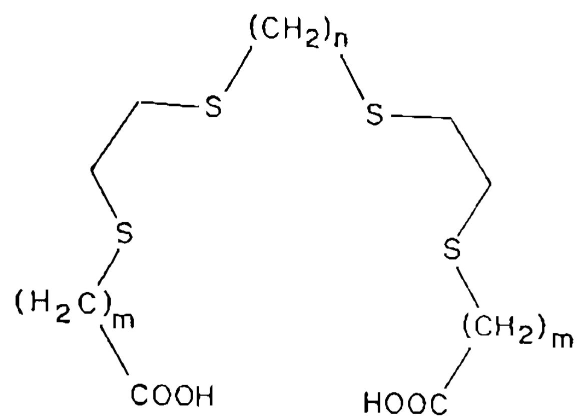
e

$[Cu(L9)]^{2+}$

Fig. 3.1 Proposed geometries for the copper(II) complexes. Axial ligation is present in structures 1a, 1b and 1d

potential of the blue proteins than is the tetrahedral geometry imposed by the protein superstructure.[6] Both the resonance Raman[10] and recent thermodynamic measurements[2a,11] on perchlorate adduct formation imply that all the sulfurs in these complexes remain coordinated to Cu(II) in aqueous solution also.

However, several electrochemical studies on low molecular weight coordination compounds involving varying donor atoms have concluded that the unusual copper coordination geometry in blue proteins is directly responsible for their relatively high redox potentials.[12] In order to probe the effect of varying geometric constraints upon the electrochemical properties of copper in a systematic manner, it is essential to acquire electrochemical data on a series of copper(II) complexes of single multidentate ligands while maintaining a constant donor set. In this chapter are described the synthesis of open-chain tetra- and pentathiaether ligands (L3, L4, L5, L6 and L7, Scheme 3.1), spectral and electrochemical properties of copper(II) complexes of these ligands, ostensibily involving the same S_4 and S_5 donor sets respectively. The effect of varying geometry by systematically changing the chelate ring size and number of sulfur donor atoms on the spectral and electrochemical behaviour is discussed in comparison with the corresponding cyclic thiaether complexes reported[3,13] already.

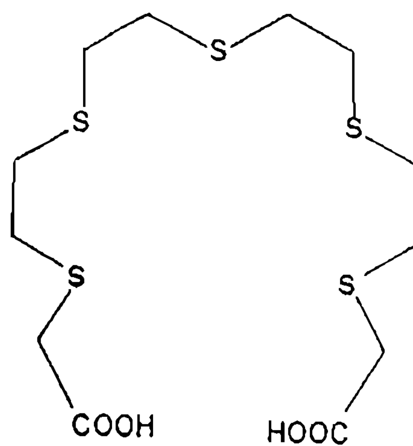


L5 $n = 2$, $m = 1$

L6 $n = 2$, $m = 2$

L3 $n = 3$, $m = 1$

L4 $n = 3$, $m = 2$



L7

Scheme 3.1

3.2 Experimental

3.2.1 Synthesis of Ligands

2,5,8,11-Tetrathiadodecane-1,12-dicarboxylic Acid (L5)

Stirred (0.5 h) was 1,2-ethanedithiol (9.3 g, 98 mmol) with sodium borohydride (0.5 g, 13 mmol) in 95 % ethanol (100 mL) under dinitrogen. Then 87 % potassium hydroxide (18.8 g, 281 mmol) was added followed by water (30 mL). After the dissolution of the alkali, 2-chloroethanol (16.12 g, 200 mmol) in ethanol (30 mL) was added over a period of 1 hour, stirred overnight, refluxed (0.5 h) and then the solvent was removed (rotary evaporator). The solid was refluxed (0.5 h) with thiourea (14.9 g, 196 mmol) and 48 % hydrobromic acid (43.2 g, 250 mmol). After cooling, sodium hydroxide (25.2 g, 630 mmol) in water (50 mL) was added slowly in a fast stream of nitrogen. During the alkali addition the mercaptan layer separated initially but dissolved off completely at the end of the addition. Then the mixture was heated to nearly 80 °C and 2-chloroacetic acid (17.6 g, 186 mmol) which was already neutralised with sodium bicarbonate (15.7 g, 186 mmol) in water (50 mL), was added slowly with constant stirring. The mixture was stirred overnight and then refluxed (5 h). The pH of the solution was reduced to one using 6N hydrochloric acid during which a voluminous mass separated. The precipitate was recrystallised from aqueous ethanol. Yield, 66 %, m.p. 88 °C; (Found: C, 35.9; H, 5.48. $C_{10}H_{18}S_4O_4$ requires C, 36.3; H, 5.49 %); MS: m/z 330 (M^+) (0.7%); IR : 1680, 1420; ^1H NMR (DMSO-d_6): δ 2.48 (s, 4H, $-S-CH_2-CH_2-S-$),

2.78 (s, 4H, $-S-CH_2-$), 2.86 (s, 4H, $-CH_2-S-$), 3.2 (s, 4H, $-S-CH_2-COOH$).

3,6,9,12-Tetrathiatetradecane-1,14-dicarboxylic Acid (L6)

Stirred (0.5 h) was 1,2-ethanedithiol (9.5 g, 101 mmol) with sodium borohydride (0.5 g, 13 mmol) in 95 % ethanol (100 mL) under dinitrogen. Then 87 % potassium hydroxide (18.9 g, 282 mmol) was added followed by water (30 mL). After the dissolution of the alkali, 2-chloroethanol (16.22 g, 201 mmol) in ethanol (20 mL) was added over a period of 1 hour, stirred overnight, refluxed (0.5 h) and then the solvent was removed (rotary evaporator). The solid was refluxed (0.5 h) with thiourea (14.9 g, 196 mmol) and 48 % hydrobromic acid (43.1 g, 250 mmol). After cooling, sodium hydroxide (25.4 g, 635 mmol) in water (50 mL) was added slowly in a fast stream of nitrogen. During the alkali addition the mercaptan layer separated initially but dissolved off completely at the end of the addition. Then the mixture was heated to nearly 80 °C and 3-chloropropionic acid (20.8 g, 186 mmol) which was already neutralised with sodium bicarbonate (15.7 g, 186 mmol) in water (50 mL), was added slowly with constant stirring. The mixture was stirred overnight and then refluxed (5 h). The pH of the solution was reduced to one using 6N hydrochloric acid during which a voluminous mass separated. The voluminous precipitate obtained was recrystallised from aqueous ethanol. Yield, 68 %, m.p. 162 °C; (Found: C, 39.9; H, 6.01. $C_{12}H_{22}S_4O_4$ requires C, 40.2; H, 6.18 %);

MS: m/z 133 (18%); IR: 1680, 1420; [1]H NMR (DMSO-d_6): δ 2.09 (s, 4H, $-S-CH_2-CH_2-S-$), 2.51 (t, 8H, J = 7.0, $-S-CH_2-CH_2-S-$), 3.57 (t, 4H, $-S-CH_2-$), 4.10 (t, 4H, $-CH_2-COOH$).

2,5,9,12-Tetrathiatridecane-1,13-dicarboxylic Acid (L3)

Stirred (0.5 h) was 1,3-ethanedithiol (10.8 g, 99 mmol) with sodium borohydride (0.5 g, 13 mmol) in 95 % ethanol (100 mL) under dinitrogen. Then 87 % potassium hydroxide (18.7 g, 280 mmol) was added followed by water (30 mL). After the dissolution of the alkali, 2-chloroethanol (16.2 g, 201 mmol) in ethanol (30 mL) was added over a period of 1 hour, stirred overnight, refluxed (0.5 h) and then the solvent was removed (rotary evaporator). The solid was refluxed (0.5 h) with thiourea (14.9 g, 196 mmol) and 48 % hydrobromic acid (43.1 g, 250 mmol). After cooling, sodium hydroxide (25.2 g, 630 mmol) in water (50 mL) was added slowly in a fast stream of nitrogen. During the alkali addition the mercaptan layer separated initially but dissolved off completely at the end of the addition. Then the mixture was heated to nearly 80 °C and 2-chloroacetic acid (17.6 g, 186 mmol) which was already neutralised with sodium bicarbonate (15.7 g, 186 mmol) in water (50 mL), was added slowly with constant stirring. The mixture was stirred overnight and then refluxed (5 h). The pH of the solution was reduced to one using 6N hydrochloric acid during which a voluminous mass separated. The precipitate was recrystallised from aqueous ethanol. Yield, 69 %, m.p. 84 °C; (Found: C, 38.5; H,

5.87. $C_{11}H_{20}S_4O_4$ requires C, 38.4; H, 5.85 %); MS: m/z 344 (M^+) (3%); IR: 1690, 1420; ^1H NMR (DMSO-d_6): δ 1.86 (t, 2H, J = 7.1, $-CH_2-$), 2.67 (t, 4H, J = 7.1, $-CH_2-S-$), 2.78 (s, 8H, $-S-CH_2-CH_2-S-$), 3.20 (s, 4H, $S-CH_2-COOH$).

2,6,10,13-Tetrathiatridecane-1,15-dicarboxylic Acid (L4)

This ligand was prepared from the reported procedure[14] as follows. Stirred (0.5 h) was 1,3-propanedithiol (11.0 g, 102 mmol) with sodium borohydride (0.5 g, 13 mmol) in 95 % ethanol (100 mL) under dinitrogen. Then 87 % potassium hydroxide (19.1 g, 286 mmol) was added followed by water (30 mL). After the dissolution of the alkali, 2-chloroethanol (16.75 g, 208 mmol) in ethanol (20 mL) was added over a period of 1 hour, stirred overnight, refluxed (0.5 h) and then the solvent was removed (rotary evaporator). The solid was refluxed (0.5 h) with thiourea (15.1 g, 198 mmol) and 48 % hydrobromic acid (43.5 g, 253 mmol). After cooling, sodium hydroxide (25.5 g, 636 mmol) in water (50 mL) was added slowly in a fast stream of nitrogen. During the alkali addition the mercaptan layer separated initially but dissolved off completely at the end of the addition. Then the mixture was heated to nearly 80 °C and 3-chloropropionic acid (21.0 g, 188 mmol) which was already neutralised with sodium bicarbonate (15.7 g, 186 mmol) in water (50 mL), was added slowly with constant stirring. The mixture was stirred overnight and then refluxed (5 h). The pH of the solution was reduced to one using 6N hydrochloric acid during which a

voluminous mass separated. The voluminous precipitate obtained was recrystallised from aqueous ethanol. Yield, 70 %, m.p. 142 °C.

2,5,8,11,14-Pentathiapentadecane-1,15-dicarboxylic Acid (L7)

Stirred (0.5 h) was 2-mercaptoethylsulfide (3.1 g, 20 mmol) with sodium borohydride (0.5 g, 13 mmol) in 95 % ethanol (75 mL) under dinitrogen. Then 87 % potassium hydroxide (3.9 g, 58 mmol) was added followed by water (20 mL). After the dissolution of the alkali, 2-chloroethanol (3.26 g, 40.5 mmol) in ethanol (20 mL) was added over a period of 1 hour, stirred overnight, refluxed (0.5 h) and then the solvent was removed (rotary evaporator). The solid was refluxed (0.5 h) with thiourea (3.24 g, 42.6 mmol) and 48 % hydrobromic acid (9.45 g, 54.9 mmol). After cooling, sodium hydroxide (5.04 g, 126 mmol) in water (50 mL) was added slowly in a fast stream of nitrogen. During the alkali addition the mercaptan layer separated initially but dissolved off completely at the end of the addition. Then the mixture was heated to nearly 80 °C and 2-chloroacetic acid (3.52 g, 37.2 mmol) in water (30 mL), was added slowly with constant stirring. The mixture was stirred overnight and then refluxed (5 h). The pH of the solution was reduced to one using 6N hydrochloric acid during which a voluminous mass separated. The solid formed was separated and recrystallised from aqueous methanol. Yield, 72 %, m.p. 99 °C; (Found: C, 37.3; H, 5.81. $C_{12}H_{22}S_5O_4$ requires C, 36.9; H, 5.68 %); MS: m/z 391 (M^+) (10%); IR: 1685, 1420; ^{1}H NMR (DMSO-d_6): δ 2.09 (s, 4H, $-S-CH_2-$),

2.50 (s, 4H, $-CH_2-S-$), 2.60 (t, 4H, J = 6.7, $-S-CH_2-$), 3.53 (t, 4H, J = 6.6, $-CH_2-S-$), 3.65 (s, 4H, $-CH_2-COOH$).

3.3 Results and Discussion

3.3.1 Synthesis

Almost all the present ligands have limited solubility in water and methanol. However, the addition of a solution of $Cu(ClO_4)_2.6H_2O$ in methanol to a suspension of the ligands in methanol in 1:1 stoichiometry, with stirring led to the formation of dark green solutions which on standing became eventually reductively bleached by solvent, either thermally or photochemically[13] like many other chelates involving thioether donors.[14] Our attempts to isolate solid complexes by slow evaporation of these solutions were thwarted and so we made spectral and electrochemical studies on these dark green solutions immediately after preparation. On adding excess ligands, they were found insoluble. The copper(II) complexes isolated at higher pH (7.0 - 10.0) were insoluble in most of the solvents and were not investigated.

3.3.2 Spectra

All the five Cu(II) complexes in frozen methanol solution exhibit X-band EPR spectra with g and A values that match with those of free Cu(II).[14] This is obviously due to the low stability of Cu(II)-thiaether complexes[13] and the displacement of coordinated

thioether by methanol[2] at low temperature.

All the present complex species display only one ligand field band in the range 14.3 - 16.3 kK, both in methanol (Fig. 3.2) and acetonitrile (Fig. 3.3) solutions (Table 3.1). The entries in this Table suggest that acetonitrile a strong donicity solvent does not displace any coordinated thioether from copper. The band positions are generally in the same range as those observed for $[Cu(L2)]^{2+}$ (16.3 kK) in which the ethyl groups displace one of the sulfur atoms by 0.78 A from the CuS_3 plane[7] and so we suggest a similar non-planar S_4 coordination for the present open-chain tetrathiaether complexes. The lower $\bar{\nu}_{max}$ values of $[Cu(L4)]^{2+}$ compared to $[Cu(L3)]^{2+}$ and $[Cu(L2)]^{2+}$, and of $[Cu(L6)]^{2+}$ compared to $[Cu(L5)]^{2+}$ imply that the steric demand of CH_2CH_2COOH group distorts the coordination of the fourth sulfur atom more significantly than do CH_2CH_3 and CH_2COOH groups. However, the possibility of preferential axial interaction by unionised CH_2CH_2COOH group contributing to this lowering in $\bar{\nu}_{max}$ cannot be ruled out. Further, $[Cu(L5)]^{2+}$ possesses a ligand field stronger than that $[Cu[12]ane\text{-}S_4]^{2+}$ does (14.8 kK).[13] Obviously, the open chain ligand L5 provides an optimal fit for the nearly square planar coordination, better than the corresponding macrocyclic ligand, as expected. Thus they appear to be fit for S_4 rather than S_3D (D = donor solvent) coordination.[16] The latter requires 'folding' of such ligands[17] to generate adjacent five-membered chelate ring systems joined at thioether sulfur. We suggest that

Table 3.1 Electronic spectral data[a] ($\bar{\nu}_{max}$ in kK and ϵ in M^{-1} cm^{-1} in parentheses) for $[CuL]^{2+}$ systems in methanol and acetonitrile at 25 °C

Complex	Solvent	$\bar{\nu}_{max}$ (ϵ)	
		Ligand Field	Charge Transfer
$[Cu(L3)]^{2+}$	MeOH	16.3 (58)	25.5 (560)
	MeCN	16.5 (61)	24.9 (320)
$[Cu(L4)]^{2+}$	MeOH	14.5 (29)	23.9 (60)
	MeCN	14.6 (69)	24.2 (500)
$[Cu(L5)]^{2+}$	MeOH	15.6 (88)	24.9 (640)
	MeCN	15.1 (82)	25.8 (350)
$[Cu(L6)]^{2+}$	MeOH	13.6 (49)	27.1 (130)
	MeCN	14.3 (121)	25.6 (640)
$[Cu(L7)]^{2+}$	MeOH	14.7 (86)	25.8 (550)
	MeCN	14.9 (113)	25.7 (660)

[a] [Cu] = 0.01 M; [L] = 0.011 M; $[NaClO_4]$ = 0.1 M

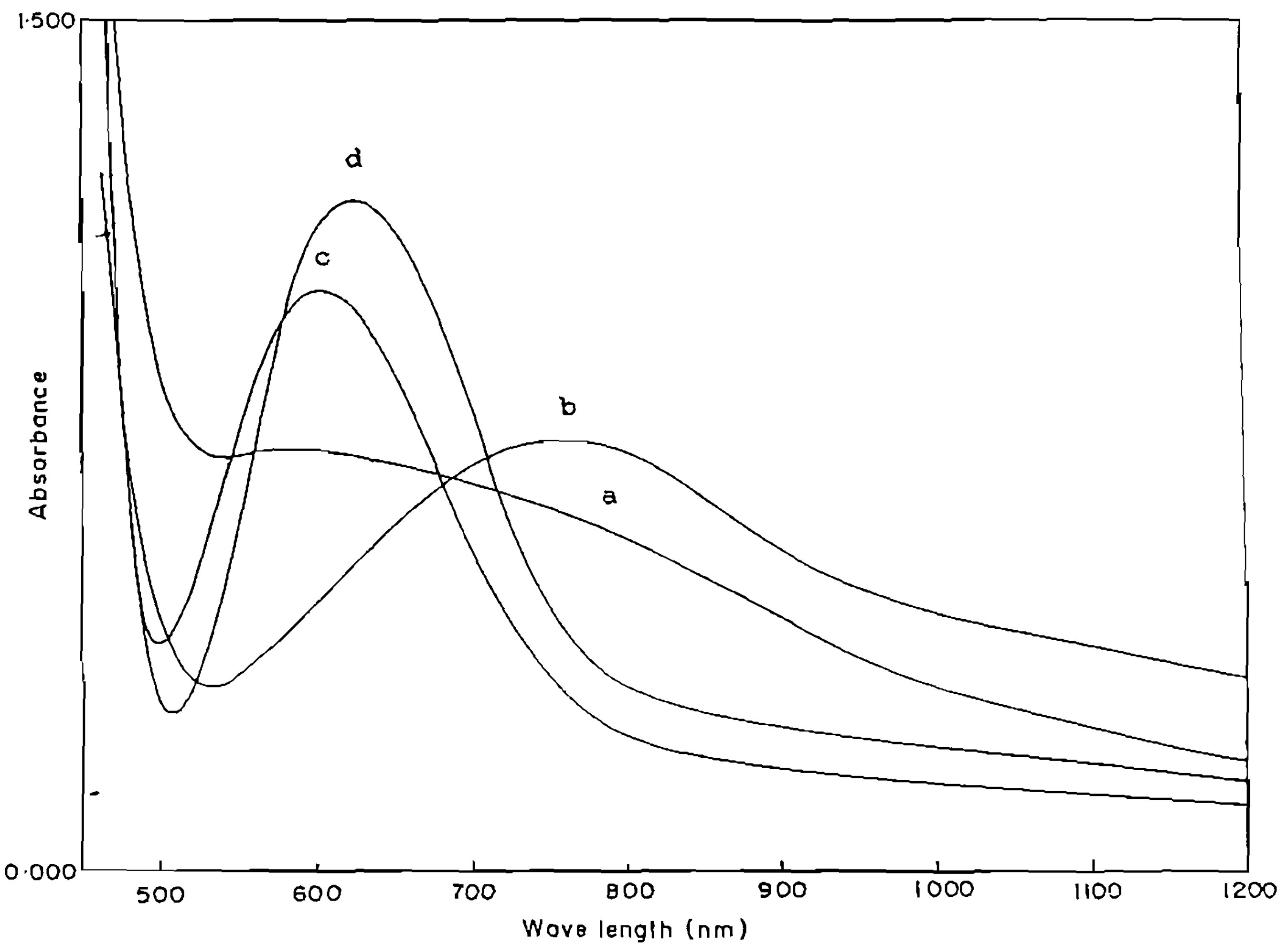


Fig. 3.2 Ligand field spectra of $[Cu(L4)]^{2+}$ (a), $[Cu(L6)]^{2+}$ (b), $[Cu(L3)]^{2+}$ (c) and $[Cu(L5)]^{2+}$ (d), all generated in situ in methanol

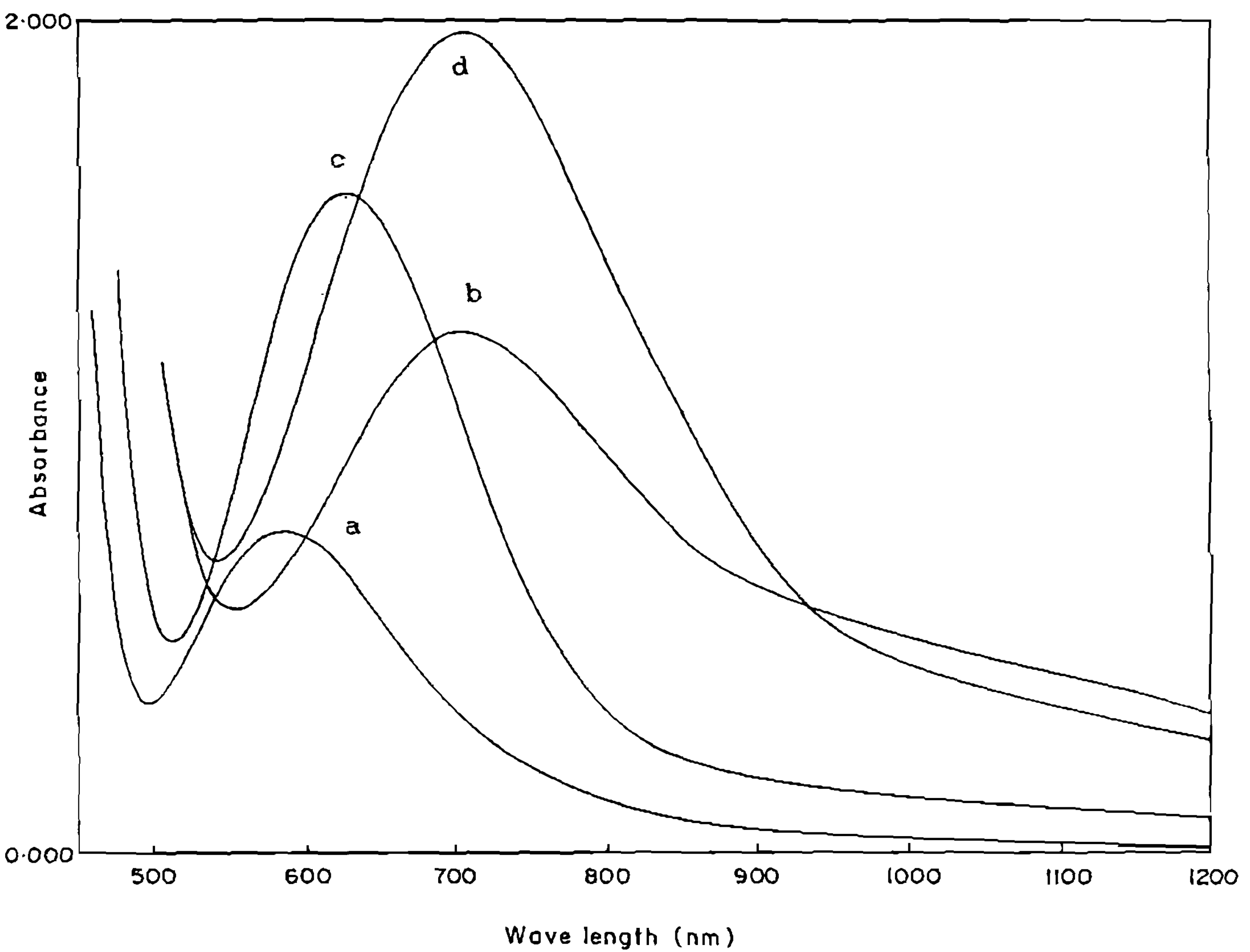


Fig. 3.3 Ligand field spectra of $[Cu(L3)]^{2+}$ (a), $[Cu(L5)]^{2+}$ (b), $[Cu(L4)]^{2+}$ (c) and $[Cu(L6)]^{2+}$ (d), all generated in situ in acetonitrile

such a folding occurs only when strong donors are available within the multidentate ligand to default to equatorial positions, as observed in $[Cu(L10)]^{2+}$ [L10 = 1,9-bis(2-pyridyl)-2,5,8-trithianonane],[17] $[Cu(L11)_2]^{2+}$ [L11 = bis(benz)imidazolyl-methylsulfide],[18] [Cu(L12)] [L12 = $^{-}OOC-CH_2-S-(CH_2CH_2-S)_2-CH_2COO^{-}$],[19] and $[Cu(L13)(L14)]^{+}$ [L13 = bis(benzimidazolyl)-methylsulfide, L14 = acetylacetone].[20] So the present complexes are interesting candidates for molecular dynamics calculations. Their X-ray crystal structures are obviously essential for establishing our suggestions but our attempts to even isolate them were not so far fruitful.

The increase in ligand field strength caused by bonding the fifth sulfur donor in $[Cu(L7)]^{2+}$, is offset by the probable axial coordination of one of the sulfurs (Fig. 3.1c) as in its corresponding cyclic analogue $[Cu(L9)]^{2+}$.[13] Further, the lower band position for $[Cu(L7)]^{2+}$ compared to that for $[Cu(L9)]^{2+}$ (17.7 kK), illustrates the fitness of the cyclic ligand L9 to provide a square planar S_4 core to copper(II); this is similar to that of L8[a] compared to L2.

The intense band observed around 26.0 kK (Fig. 3.4) for all the present $[Cu(L)]^{2+}$ systems is assigned to $S(\sigma)$ ---> Cu(II) charge transfer transition.[21-23] In methanol solution the trend in ϵ_{max} value of this CT band is $[Cu(L5)]^{2+}$ > $[Cu(L3)]^{2+}$ > $[Cu(L6)]^{2+}$ > $[Cu(L4)]^{2+}$ and is the same as that in ϵ_{max} of LF band.

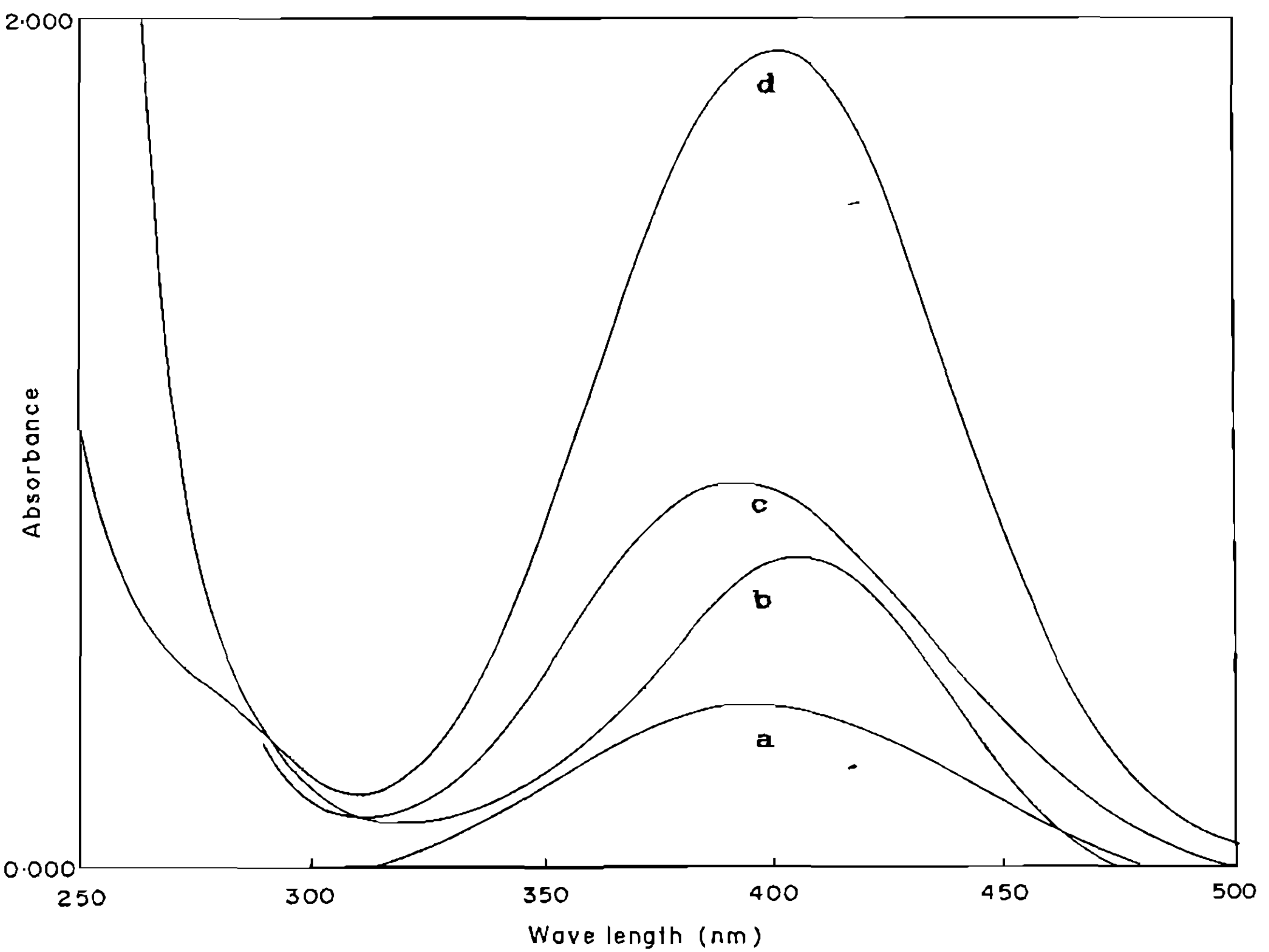


Fig. 3.4 Charge transfer bands of $[Cu(L3)]^{2+}$ (a), $[Cu(L5)]^{2+}$ (b), $[Cu(L4)]^{2+}$ (c) and $[Cu(L6)]^{2+}$ (d), all generated in situ in acetonitrile

This trend is consistent with the fast bleaching of $[Cu(L6)]^{2+}$ and reflects the poor Cu-S overlap caused by the enhanced distortion due to CH_2CH_2COOH groups. Interestingly the ϵ_{max} value shows a distinct decrease upon going from methanol to acetonitrile (Fig. 3.4), for both $[Cu(L3)]^{2+}$ and $[Cu(L5)]^{2+}$ systems while a sharp increase for both $[Cu(L4)]^{2+}$ and $[Cu(L6)]^{2+}$ systems, suggesting the susceptibility of the distorted geometries of $[Cu(L4)]^{2+}$ and $[Cu(L6)]^{2+}$ to solvent coordination.

3.3.3 Electrochemistry

All the present Cu(II) complexes exhibit a well defined cathodic wave (0.230 - 0.280 V) and a corresponding anodic wave (0.400 - 0.600 V). The values of the diffusion coefficients (Table 3.2) calculated from the slope of the straight line obtained in the plot of i_{pc} *vs* $\nu^{1/2}$ using Randles Sevcik's equation[26] are in the range 1.4 - 2.4 X 10^{6} cm^2/s and are typical of Cu(II) complexes involving one electron redox process.[27]

The ΔE_p values of $[Cu(L)]^{2+}$ systems are in the range 114 to 310 mV at 50 mV/s scan rate. The limiting peak-to-peak potential separations ($\Delta E_p°$) for all the complexes are greater than the Nernstian ΔE_p value ($\approx$ 60 mV) for one electron transfer. For $[Cu(L3)]^{2+}$ and $[Cu(L6)]^{2+}$ systems this value is 66 and 70 mV respectively (Table 3.2) and the peak current ratio is nearer to unity. These characteristics suggest that these complexes tend to

Table 3.2 Redox properties[a] of $[CuL](ClO_4)_2$ systems in methanol at 25 °C

Complex (0.001 M)	E_{pc} mV	E_{pa} mV	ΔE_p mV	ΔE_p° [b] mV	$E_{1/2}$[c] (mV) CV	DPV[d]	i_{pa}/i_{pc}	$D \times 10^6$ cm^2/s
$[Cu(L3)]^{2+}$	272	386	114	71	329	331	1.1	1.3
	[a] 82	218	136	92	150	149	1.2	1.8
$[Cu(L4)]^{2+}$	284	594	310	129	439	447	0.7	1.5
$[Cu(L5)]^{2+}$	232	414	182	112	323	305	1.0	2.4
$[Cu(L6)]^{2+}$	376	538	162	66	457	479	0.9	2.4
$[Cu(L7)]^{2+}$	276	468	192	113	372	374	1.1	2.1

[a] supporting electrolyte : 0.1 M THAP; Ref : $Ag/AgNO_3$ (0.01 M/THAP 0.1 M in acetonitrile); scan rate : 50 mV/s; [b] ΔE_p° is the peak potential separation extrapolated to zero scan rate; [c] Measured $E_{1/2}$ of Fc/Fc^+ couple in acetonitrile is 100 mV *vs* Ag/Ag^+; add 544 mV to convert the potentials to NHE; [d] scan rate 1 mV/s; pulse height 50 mV; [e] in 80 % methanol (v/v)

exhibit Nernstian electrochemical behaviour. The $[Cu(L4)]^{2+}$, $[Cu(L5)]^{2+}$ and $[Cu(L7)]^{2+}$ systems (Fig. 3.5) exhibit relatively less reversible redox behaviour. The origin of this difference in behaviour is not apparent.

The redox potentials obtained from CV are consistent with those from DPV (Fig. 3.6, Table 3.2). It has been already shown that when π-bonding is important the incorporation of six-membered rings would facilitate the stabilisation of Cu(I) by favouring tetrahedral distortion and raise the redox potential.[28] But this is not apparent in the present systems. One significant consequence of the very high redox potential of $[Cu(L6)]^{2+}$ system is the comparatively fast bleaching, immediately after its generation. The redox potentials of $[Cu(L3)]^{2+}$ and $[Cu(L4)]^{2+}$, and of $[Cu(L5)]^{2+}$ and $[Cu(L6)]^{2+}$ systems, eventhough they have the same chelate ring structures of 555 and 565 respectively, are interestingly different and this is consistent with the electronic spectral results. This trend reveals that the geometric distortion by and/or axial interaction of propionic acid moiety destabilises Cu(II) state and elevates $E_{1/2}$.

Further, the $E_{1/2}$ values observed for tetrathiaether complexes are much higher than those calculated[29] using Addison's ΔE_L values, probably due to the higher contribution from the sterically induced destabilisation of Cu(II) state, as explained above. The addition of the fifth sulfur donor and its attendant

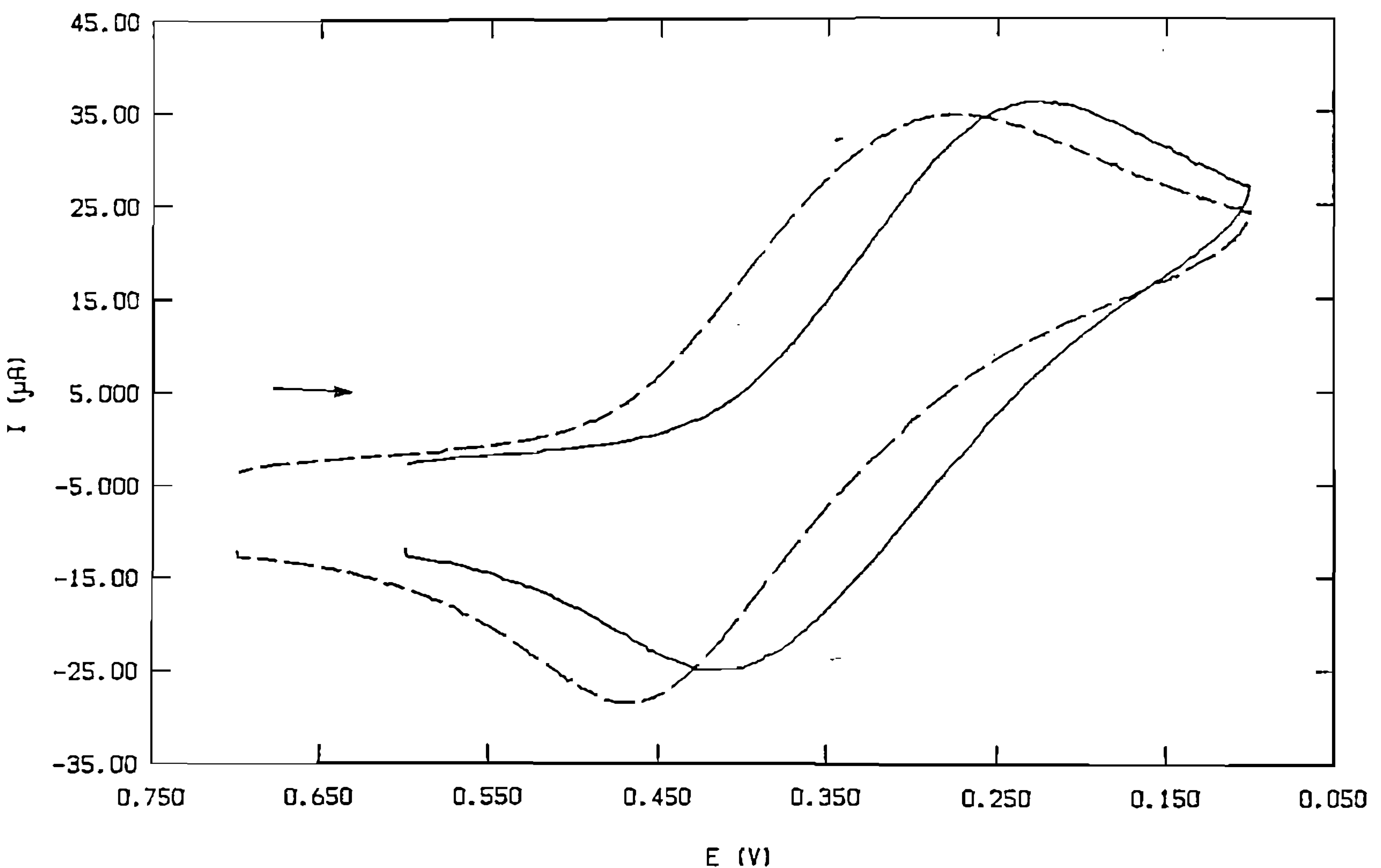


Fig. 3.5 Cyclic voltammograms of $[Cu(L5)]^{2+}$ (——) and $[Cu(L7)]^{2+}$ (---) at 50 mV/s scan rate, all generated in situ in methanol (0.1 M THAP) *vs* Ag/Ag^{+} electrode at 25 °C

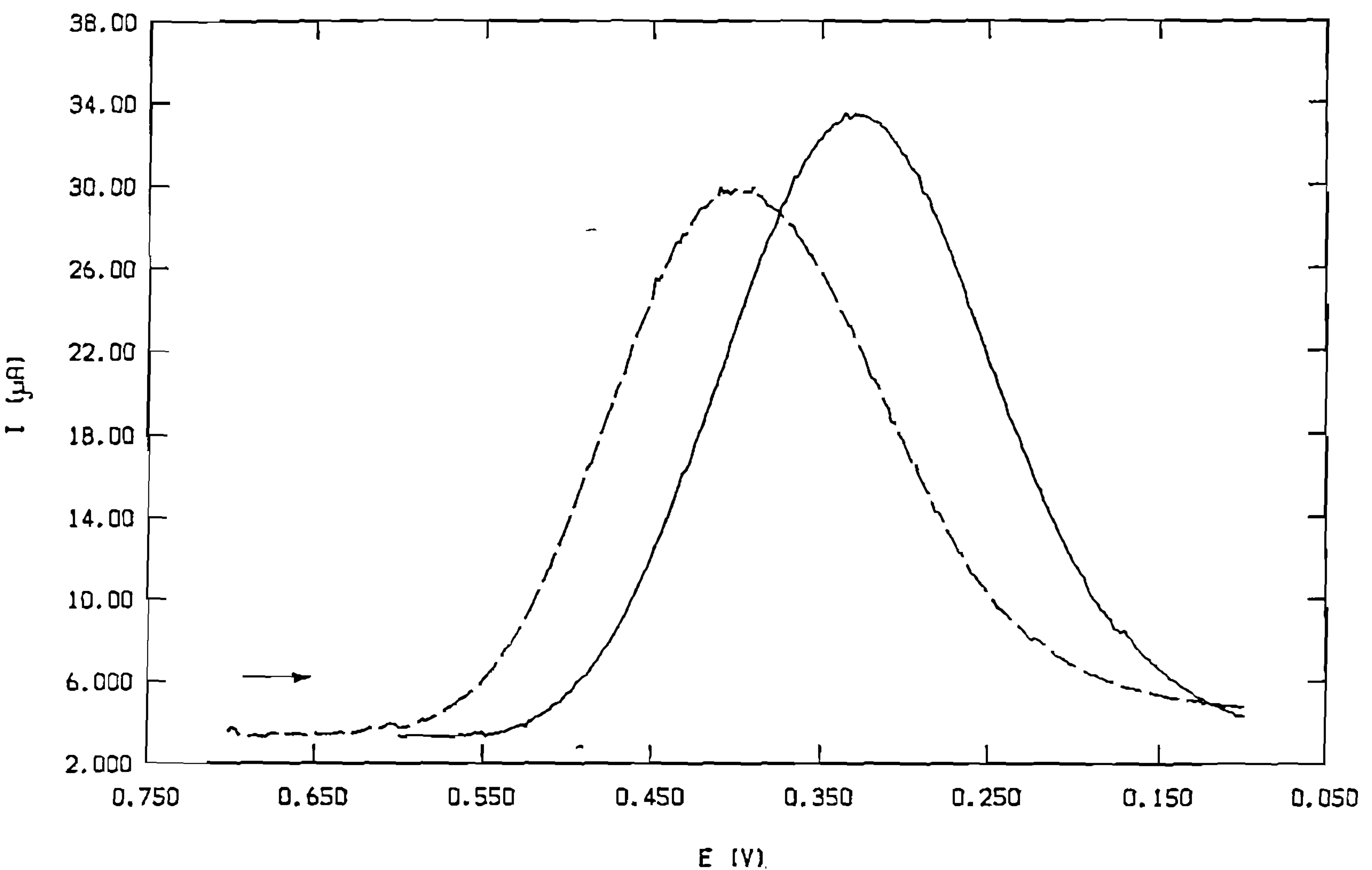


Fig. 3.6 Differential pulse voltammograms of $[Cu(L5)]^{2+}$ (——) and $[Cu(L7)]^{2+}$ (---) at 1 mV/s scan rate, all generated in situ in methanol (0.1 M THAP) *vs* Ag/Ag^{+} electrode at 25 °C

five-membered chelate ring, as in $[Cu(L7)]^{2+}$ is expected to raise the $E_{1/2}$ by about 95 mV[29] which is higher than the experimental $E_{1/2}$ difference between $[Cu(L5)]^{2+}$ and $[Cu(L7)]^{2+}$ of about 60 mV. The structural origin of this elevation is evident from the lower position of the visible band and hence the CFSE, of $[Cu(L7)]^{2+}$ compared to $[Cu(L5)]^{2+}$. A similar enhancement of ≈ 100 mV in $E_{1/2}$ of $[Cu(L8)]^{2+}$, by the incorporation of axial sulfur donor as in $[Cu(L9)]^{2+}$ complex has been observed.[3] In 80 % methanol $[Cu(L3)]^{2+}$ possesses a redox potential (Table 3.2) higher (≈ 45 mV) than that $[Cu(L8)]^{2+}$ does.[3,6] The greater flexibility of the open chain ligand L3, compared to the cyclic ligand L8, facilitates the formation of tetrahedral coordination geometry around Cu(I) formed on electron transfer.

3.4 Conclusions

When the terminal groups in the present open chain tetrathiaether ligands are changed from CH_2COOH to CH_2CH_2COOH, there is a significant increase in redox potential of their Cu(II) complexes. An increase in the number of sulfur atoms from four to five increases the redox potential appreciably as expected.[3,29] On the other hand, no significant change in the potential is observed upon replacing a five-membered chelate ring by a six-membered chelate ring. This is in contrast to the results observed for Cu(II) complexes of bis(benzimidazol-2-yl) tetrathioether compounds (Chapter 5).[30]

References

(1) Pett, V. B.; Diaddario, Jr. L. L.; Dockal, E. R.; Corfield, P. W. R.; Ceccarelli, C.; Glick, M. D.; Ochrymowycz, L. A.; Rorabacher, D. B. *Inorg. Chem.* **1983**, *22*, 3661.

(2) a) Nazarenko, A. Y.; Izatt, R. M.; Lamb, J. D.; Desper, J. M.; Matysik, B. E.; Gellman, S. H. *Inorg. Chem.* **1992**, *31*, 3990; b) Desper, J. M.; Gellman, S. H.; Wolf, R. E., Jr.; Cooper, S. R. *J. Am. Chem. Soc.* **1991**, *113*, 8663.

(3) Bernardo, M. M.; Schroeder, R. R.; Rorabacher, D. B. *Inorg. Chem.* **1991**, *30*, 1241.

(4) Solomon, E. I.; Lowery, M. D. *Science* **1993**, *259*, 1575 and references cited therein.

(5) Martin, M. J.; Endicott, J. F.; Ochrymowycz, L. A.; Rorabacher, D. B. *Inorg. Chem.* **1987**, *26*, 3012.

(6) Bernardo, M. M.; Heeg, M. J.; Schroeder, R. R.; Ochrymowycz, L. A.; Rorabacher, D. B. *Inorg. Chem.* **1992**, *31*, 191.

(7) Diaddario, L. L., Jr.; Dockal, E. R.; Glick, M. D.; Ochrymowycz, L. A.; Rorabacher, D. B. *Inorg. Chem.* **1985**, *24*, 356.

(8) Glick, M. D.; Gavel, D. P.; Diaddario, L. L.; Rorabacher, D. B. *Inorg. Chem.* **1976**, *15*, 1190.

(9) Corfield, P. W. R.; Ceccarelli, C.; Glick, M. D.; Moy, I. W-Y.; Ochrymowycz, L. A.; Rorabacher, D. B. *J. Am. Chem. Soc.* **1985**, *107*, 2399.

(10) Ferris, N. S.; Woodruff, W. H.; Rorabacher, D. B.; Jones, T. E.; Ochrymowycz, L. A. *J. Am. Chem. Soc.* **1978**, *100*, 5930.

(11) a) Diaddario, L. L., Jr.; Ochrymowycz, L. A.; Rorabacher, D. B. *Inorg. Chem.* **1992**, *31*, 2347; b) Sokol, L. S. W. L.; Ochrymowycz, L. A.; Rorabacher, D. B. *Inorg. Chem.* **1981**, *20*, 3189; c) Young, I. R.; Ochrymowycz, L. A.; Rorabacher, D. B. *Inorg. Chem.* **1986**, *25*, 2576.

(12) Yokoi, H.; Addison, A. W. *Inorg. Chem.* **1977**, *16*, 1341.

(13) Jones, T. E.; Rorabacher, D. B.; Ochrymowycz, L. A. *J. Am. Chem. Soc.* **1975**, *97*, 7485.

(14) Palaniandavar, M.; Addison, A. W.; Sinn, E. to be published.

(15) Addison, A. W.; Stenhouse, J. H. *Inorg. Chem.* **1978**, *17*, 2161.

(16) Kanters, R. P. F.; Yu, R.; Addison, A. W. *Inorg. Chim. Acta* **1992**, *196*, 97.

(17) Liu, S.; Lucas, C. R.; Hynes, R. C.; Charland, J-P. *Can. J. Chem.* **1992**, *70*, 1773.

(18) a) van Steenbergen, A. C.; Bouwman, E.; de Graaff, G.; Driessen, W. L.; Reedijk, J.; Zanello, P. *J. Chem. Soc., Dalton Trans.* **1990**, 3175; b) Prochaska, H. J.; Schwindinger, W. F.; Schwartz, M.; Burk, M. J.; Bernarducci, E.; Lalancette, R. A.; Potenza, J. A.; Schugar, H. J. *J. Am. Chem. Soc.* **1981**, *103*, 3446.

(19) Palaniandavar, M.; Addison A. W.; Sinn, E. unpublished results.

(20) Addison, A. W.; Burke, P. J.; Henrick, K. *Inorg. Chem.* **1982**, *21*, 60.

(21) Addison, A. W.; Nageswara Rao, T. *J. Chem. Soc., Dalton Trans.* **1984**, 1349.

(22) Addison, A. W.; Burke, P. J.; Henrick, K.; Nageswara Rao, T.; Sinn, E. *Inorg. Chem.* **1983**, *22*, 3645.

(23) Sakurai, T.; Suzuki, S.; Nakahara, A. *Bull. Chem. Soc. Jpn.* **1981**, *54*, 2313.

(24) Dagdigian, J. V.; McKee, V.; Reed, C. A. *Inorg. Chem.* **1982**, *21*, 1332.

(25) Miskowski, V. M.; Thich, J. A.; Solomon, R.; Schugar, H. J. *J. Am. Chem. Soc.* **1976**, *98*, 8344.

(26) Bard, A. J.; Faulkner, L. R. *Electrochemical methods: Fundamental applications*; John Wiley & Sons: New York, 1980; p 218.

(27) Sakaguchi, U.; Addison, A. W. *J. Chem. Soc., Dalton Trans.* **1979**, 600.

(28) Pandiyan, T.; Palaniandavar, M.; Lakshminarayanan, M.; Manohar, H. *J. Chem. Soc., Dalton Trans.* **1992**, 3377.

(29) a) Augustin, M. A.; Yandell, J. K.; Addison, A. W.; Karlin, K. D. *Inorg. Chim. Acta* **1981**, *55*, L35; b) Addison, A. W. *Inorg. Chim. Acta* **1989**, *162*, 217.

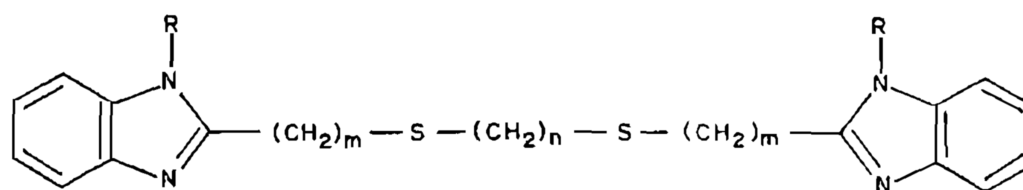
(30) Sivagnanam. U.; Palaniandavar, M. *J. Chem. Soc., Dalton Trans.* **1994**, 2277.

CHAPTER 4

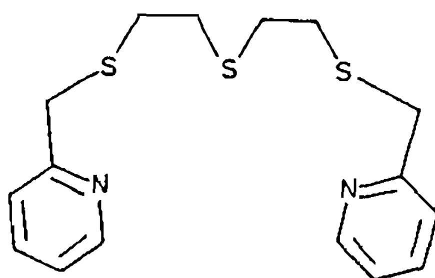
4. SYNTHESIS, CRYSTAL STRUCTURE, SPECTRA AND REDOX OF COPPER(II) COMPLEXES OF LIGANDS WITH TWO AND THREE THIOETHER DONORS.

4.1 Introduction

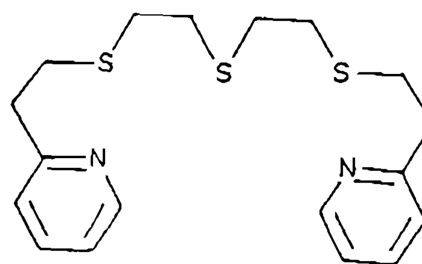
The active site in blue copper proteins contains two histidine imidazoles, a methionine thioether and a cysteine thiolate coordinated to Cu(II), with a geometry closer to trigonal (bi)pyramidal.[1-3] Even though there is a possibility that the apical thioether ligand may control the Cu(II)/Cu(I) redox potential, its definite role still remains ambiguous.[4] So there is a growing interest in the Cu(II) complexes of tetradentate bis((benz)imidazol-2-yl)-dithioether ligands;[5-10] the thiolate group being substituted by an extra thioether donor, they offer a CuN_2S_2 chromophore as in blue proteins. A remarkable feature of this class of complexes is that many of them often possess trigonal bipyramidal geometry. By contrast, the complexes of 4-imidazolyl ligands form a surprising number of 'compressed' octahedral structures.[9,10] Thus in the N_2S_2 complex [Cu(bbdh)Cl]Cl [bbdh = 1,6-bis(2-benzimidazolyl)-2,5-dithiahexane] with 555 chelate ring system (**Scheme 4.1**) a trigonal bipyramidal geometry is observed.[5] On adding a methylene group between the thioether sulfurs (bmdhp,



R = H	m = 1	n = 2	bbdh
R = CH_3	m = 1	n = 3	bmdhp
R = H	m = 2	n = 2	bbdo



pttn



pttu

Scheme 4.1

Scheme 4.1) [bmdhp = 1,7-bis-(N-methylbenzimidazol-2′-yl)-2,6-dithiaheptane] in this complex, the geometry becomes trigonally distorted tetragonal pyramidal[8] and significant changes in spectral and redox properties[11] are observed. So it is of great interest to probe the consequences of enlarging the ligand by varying the chelate ring sizes on structure and properties of CuN_2S_2 complexes. In the present chapter the consequences of incorporating two methylene groups between sulfur and benzimidazole (bzim) donors (bbdo, **Scheme 4.1**) [bbdo = 1,8-bis(benzimidazol-2-yl)-3,6-dithiaoctane] on structure and spectral and redox properties of copper(II) complexes are discussed. The present work also provides an opportunity to gain insight into the relative importance of the contributions from the coordination of thioethers[12-14] and the bulky bzim,[11,14,15] both of which are known to contribute to the positive redox potential, by comparison with related compounds.

Though the coordination chemistry of Cu(II) complexes of linear N_2S_2 ligands have been well studied, those of pentadentate N_2S_3 ligands have been less thoroughly studied. Addison *et al.* studied such Cu(II) complexes containing pyridyl,[16] quinolyl[16] and benzimidazolyl[11] moieties. Very recently, Liu *et al.* and Adhikary *et al.* have described the structure and properties of Cu(II) complexes of trithioether ligands containing substituted pyrazolyl and pyridyl $[Cu(pttn)^{2+}]$ moieties (Fig. 1.11).[17] To understand the effect of ligand enlargement the spectral and redox properties of

the Cu(II) complex of pttu [1,11-bis(pyrid-2-yl)-3,6,9-trithia-undecane], obtained by adding one more methylene group between pyridine and sulfur in pttn (Scheme 4.1), have been investigated.

4.2 Experimental

4.2.1 Synthesis of Ligands

1,8-bis(benzimidazol-2-yl)-3,6-dithiaoctane (bbdo)

The diacid 3,6-dithiaoctane-1,8-dicarboxylic acid was prepared as follows. Stirred (0.5 h) was 1,2-ethanedithiol (4.8 g, 50.1 mmol) with sodium borohydride (0.5 g, 13 mmol) in 95 % ethanol (75 mL) under dinitrogen. Then 87 % potassium hydroxide (11.7 g, 175.4 mmol) was added, followed by water (20 mL). After the dissolution of alkali, 2-chloropropionic acid (10.9 g, 100 mmol) in water (15 mL) was added slowly with constant stirring. The mixture was stirred overnight at 50 °C. Then the pH of the solution was lowered to one using 6N hydrochloric acid during which a voluminous mass separated. The precipitate was recrystallised from aqueous ethanol. Yield, 82 %, m.p. 121 - 123 °C; (Found: C, 40.1; H, 5.87. $C_8H_{14}O_4S_2$ requires C, 40.3; H, 5.92 %); ^{1}H-NMR (DMSO-d_6): δ 2.13 (s, $-S-CH_2-CH_2-S-$), 3.24 (t, $-S-CH_2-$), 3.98 (t, $-CH_2-COOH$).

The above diacid (4.8 g, 20.0 mmol) was refluxed with *o*-phenylenediamine (4.4 g, 40.7 mmol) in 4N hydrochloric acid (100 mL) for 48 hours and then cooled. The hydrochloride obtained was dissolved in water and neutralised with aqueous ammonia under cold

conditions. The free base thus obtained was collected, recrystallised from aqueous ethanol and then dried over P_4O_{10}. Yield, 60 %, m.p. 98 °C; (Found: C, 62.6; H, 5.81; N, 14.9. $C_{20}H_{22}S_2N_4$ requires C, 62.8; H, 5.80; N, 14.7 %); ^{1}H-NMR (DMSO-d_6): δ 2.01 (s, -S-CH_2-CH_2-S-), 3.01 (m, -CH_2-CH_2-bzim) 7.21 - 7.18 (m, bzim-5,6 protons), 7.54 - 7.50 (m, bzim-4,7 protons).

1,11-bis(pyrid-2-yl)-3,6,9-trithiaundecane (pttu)

The ligand pttu was prepared by adding 2-vinylpyridine (2.1 g, 20 mmol) slowly with stirring to bis(2-mercaptoethyl)sulfide (1.5 g, 10 mmol) and the stirring continued for two hours. To the resulting solution was added water with stirring and the precipitate obtained was collected, recrystallised from aqueous ethanol and dried over P_4O_{10}. Yield, 67 %, m.p. 63 - 65 °C; (Found: C, 59.5; H, 6.73; N, 7.53. $C_{18}H_{24}N_2S_3$ requires C, 59.3; H, 6.63; N, 7.68 %); ^{1}H-NMR (DMSO-d_6): δ 2.45 (s, 2 x -S-CH_2-CH_2-S-), 3.40 (t, -S-CH_2-), 3.48 (t, -CH_2-py), 7.54 - 7.69 (m, py-3,5 protons), 8.02 (m, py-4 protons), 8.95 (d, py-6 protons).

4.2.2 Preparation of Complexes

The complexes [Cu(bbdo)]$(ClO_4)_2$ (I),[11] [Cu(bbdo)]$(NO_3)_2$ (II), [Cu(pttu)]$(ClO_4)_2$ (III) and [Cu(pttu)]Cl_2 (IV) were obtained by adding the corresponding Cu(II) salt in methanol to a methanolic solution of bbdo or pttu in 1:1 molar ratio and then cooling the solutions. The product formed was filtered, washed with small amounts of cold methanol and then dried over P_4O_{10}. Anal. Calcd.

for $C_{20}H_{22}S_2N_4O_8Cl_2Cu$ (I): C, 37.2; H, 3.44; N, 8.69. Found: C, 37.5; H, 3.72; N, 8.75. Calcd. for $C_{20}H_{22}S_2N_6O_6Cu$ (II): C, 42.1; H, 3.89; N, 14.7. Found: C, 41.8; H, 3.96; N, 14.4. Calcd. for $C_{18}H_{24}S_3N_2O_8Cl_2Cu$ (III): C, 34.5; H, 3.86; N, 4.47. Found: C, 34.3; H, 3.91; N, 4.28. Calcd. for $C_{18}H_{24}S_3N_2Cl_2Cu$ (IV): C, 43.3; H, 4.85; N, 5.61. Found: C, 43.1; H, 4.91; N, 5.42%.

Single crystals of [Cu(bbdo)]$(NO_3)_2$ suitable for X-ray structure analysis were obtained on slow evaporation of the methanolic solution obtained on mixing the Cu(II) nitrate salt and the ligand bbdo in 1:1 ratio.

Single crystals of [Cu(pttu)]$(ClO_4)_2$ suitable for X-ray structure analysis were obtained as follows: Cu(II) perchlorate salt in methanol was added to the ligand pttu in methanol/ acetonitrile mixture (1:1 v/v) and the solution obtained on slow evaporation gave both Cu(II) and Cu(I) crystals.

Caution. During handling of the perchlorate salts care should be taken because of the possibility of explosion. [Cu(pttu)]$(ClO_4)_2$ caused explosion during transfer of sample in our laboratory.

4.2.3 Crystallographic Data Collection and Structure Analysis

Preliminary cell dimensions and space group of [Cu(bbdo)(NO_3)](NO_3) were determined and refined on a Rigaku AFC-5 diffractometer. The intensities were collected on the same

diffractometer with graphite-monochromated Mo-Kα radiation. The data were collected at a temperature of 23 ± 1 °C using ω-2θ scan technique to a maximum 2θ value of 42.0°. Scans of (1.30 + 0.10 tanθ)° were made at a speed of 6.0°/min (in ω). The weak reflections [$I < 0.1\ \sigma(I)$] were rescanned (maximum of 3 scans) and the counts were accumulated to ensure good counting statistics. Stationary background counts were recorded on each side of the reflection. Other details regarding the data collection and processing are collected in Table 4.1. Of the 2885 reflections, 2771 were unique (R_{int} = 0.092). The intensities of three representative reflections were measured after every 100 reflections. No decay correction was applied. Azimuthal scans of several reflections indicated no need for absorption correction. The data were corrected for Lorentz and polarisation effects.

The structure was solved by heavy-atom Patterson methods[18] and expanded using Fourier techniques.[19] Some non-hydrogen atoms were refined anisotropically, while the rest were refined isotropically. Hydrogen atoms were included but not refined. The final cycle of full-matrix least squares refinement[20] was based on 1138 observed reflections [$I > 2.0\sigma(I)$] and 216 variable parameters and converged with unweighted and weighted agreement factors of R = 0.079 and R_w = 0.051 respectively.

All calculations were carried out with TEXSAN[21] crystallographic software package of Molecular Structure

Table 4.1 Crystallographic and data collection parameters for $[Cu(bbdo)(NO_3)]NO_3$

Empirical Formula	$C_{20}N_6H_{22}CuS_2O_6$
Formula Weight	570.1
Crystal System	Monoclinic
Lattice Type	Primitive
Lattice Parameters	a = 15.990(7) Å b = 13.706(4) Å c = 10.972(4) Å β = 93.90(3)°
Volume	2399(2) $Å^3$
Space Group	$P2_1/a$ (#14)
Z value	4
Crystal Dimensions	0.40 x 0.20 x 0.05 mm
Density (calc)	1.578 g/cm^3
Diffractometer used	Rigaku AFC-5
Radiation	MoK_α (λ = 0.71069 Å) graphite monochromated
Temperature	296 K
F(000)	1172.00
Scan Type	ω-2θ
Scan Rate	6.0°/min(in ω) - up to 3 scans
No. of Reflections Measured	Total: 2885 Unique: 2711 (R_{int} = 0.092)
Residuals: R; R_w	0.079; 0.051

Corporation. Final atomic coordinates are collected in Tables 4.2, bond lengths and angles in Table 4.3 and 4.4 respectively and mean plane data in Table 4.5.

4.3 Results and Discussion

4.3.1 Description of the Structure of [Cu(bbdo)(NO_3)](NO_3) and Comparison with Related Structures

In Figure 4.1 is depicted the projection as well as the atomic numbering scheme of the complex cation. The compound crystallizes in the monoclinic space group $P2_1/a$ with four molecules in the unit cell. The coordination geometry around copper(II) is best described as severely distorted and elongated octahedral, with both the bzim nitrogens [Cu-N(11), 1.93(1); Cu-N(21), 1.99(1) A], one of the oxygen atoms of the nitrate ion [Cu-O(11), 2.06(1) A] and one of the thioether sulfurs [Cu-S(2), 2.443(6) A] forming the distorted equatorial plane. The other sulfur donor [Cu-S(1), 2.533(6) A] and the second oxygen atom from the coordinated nitrate anion occupy the axial positions, with the latter at a longer distance of 2.727(6) A. The bulky bzim groups on the ligand apparently prevent the other nitrate ion from coordinating.

The copper, S(2) and the two bzim nitrogens N(11) and N(21) are coplanar within ± 0.03 A while O(11) of the nitrate ion is displaced from this equatorial plane by 1.04 A away from S(1). The

Table 4.2 Atomic coordinates ($x10^4$) involving non-hydrogen atoms and equivalent isotropic displacement coefficients

atom	x	y	z	B_{eq}
Cu	0.0747(2)	0.1820(2)	0.1162(2)	3.17(6)
S(1)	0.1954(3)	0.0773(4)	0.2018(5)	4.1(2)
S(2)	0.1485(4)	0.3267(5)	0.1967(5)	4.5(2)
O(11)	-0.0270(9)	0.124(1)	0.016(1)	5.5(5)
O(12)	-0.079(1)	0.265(1)	0.068(2)	6.7(6)
O(13)	-0.1549(9)	0.158(1)	-0.031(2)	7.7(6)
O(21)	0.8274(9)	0.414(1)	0.694(1)	5.6(5)
O(22)	0.835(1)	0.282(1)	0.594(2)	7.3(6)
O(23)	0.8905(10)	0.411(1)	0.532(1)	7.0(6)
N(1)	-0.090(1)	0.186(2)	0.015(2)	4.7(8)
N(2)	0.850(1)	0.370(2)	0.606(2)	5.1(7)
N(11)	0.1271(9)	0.2057(10)	-0.034(1)	2.7(4)
N(12)	0.2156(9)	0.202(1)	-0.184(1)	3.2(5)
N(21)	0.0179(9)	0.161(1)	0.270(1)	2.9(4)
N(22)	-0.0575(10)	0.191(1)	0.424(1)	4.2(5)
C(1)	0.220(1)	0.062(1)	-0.047(2)	4.3(5)
C(2)	0.263(1)	0.057(1)	0.080(2)	3.7(5)
C(3)	0.249(1)	0.172(2)	0.290(2)	5.7(6)
C(4)	0.250(1)	0.274(2)	0.227(2)	6.2(6)
C(5)	0.113(1)	0.348(1)	0.347(2)	4.0(5)

C(6)	0.020(1)	0.332(2)	0.347(2)	4.4(5)
C(11)	0.188(1)	0.160(1)	-0.084(2)	3.1(5)
C(12)	0.114(1)	0.287(1)	-0.112(2)	2.9(5)
C(13)	0.169(1)	0.284(1)	-0.206(2)	2.8(5)
C(14)	0.166(1)	0.353(1)	-0.303(2)	3.9(5)
C(15)	0.105(1)	0.420(2)	-0.289(2)	4.7(5)
C(16)	0.049(1)	0.424(1)	-0.210(2)	4.2(5)
C(17)	0.052(1)	0.358(1)	-0.111(2)	3.6(5)
C(21)	-0.007(1)	0.226(1)	0.343(2)	3.0(5)
C(22)	-0.019(1)	0.075(1)	-0.304(1)	2.2(4)
C(23)	-0.070(1)	0.096(1)	0.400(2)	3.2(4)
C(24)	-0.115(1)	0.021(1)	0.454(2)	3.7(5)
C(25)	-0.105(1)	-0.071(2)	0.408(2)	4.2(5)
C(26)	-0.055(1)	-0.091(1)	0.319(2)	4.1(5)
C(27)	-0.012(1)	-0.022(1)	0.262(2)	3.7(5)

Table 4.3 Interatomic distances (Å) involving non-hydrogen atoms of $[Cu(bbdo)(NO_3)]NO_3$ (E.S.D.s are given in parentheses)

Atoms	Distances	Atoms	Distances
Cu - S(1)	2.533(6)	Cu - S(2)	2.443(6)
Cu - O(11)	2.06(1)	Cu - O(12)	2.727(8)
Cu - N(11)	1.93(1)	Cu - N(21)	1.99(1)
S(1) - C(2)	1.79(2)	S(1) - C(3)	1.80(2)
S(2) - C(4)	1.79(2)	S(2) - C(5)	1.80(2)
O(11) - N(1)	1.31(2)	O(12) - N(1)	1.24(2)
O(13) - N(1)	1.19(2)	N(11) - C(11)	1.30(2)
N(11) - C(12)	1.41(2)	O(21) - N(2)	1.21(2)
O(22) - N(2)	1.24(2)	O(23) - N(2)	1.21(2)
N(12) - C(11)	1.34(2)	N(12) - C(13)	1.37(2)
N(21) - C(21)	1.28(2)	N(21) - C(22)	1.39(2)
N(22) - C(21)	1.33(2)	N(22) - C(23)	1.35(2)
C(1) - C(2)	1.51(2)	C(1) - C(11)	1.49(2)
C(3) - C(4)	1.55(3)	C(5) - C(6)	1.51(2)
C(6) - C(21)	1.51(3)	C(12) - C(13)	1.40(2)
C(12) - C(17)	1.40(2)	C(13) - C(14)	1.42(2)
C(14) - C(15)	1.34(2)	C(15) - C(16)	1.37(2)
C(16) - C(17)	1.40(2)	C(22) - C(23)	1.40(2)
C(22) - C(27)	1.41(2)	C(23) - C(24)	1.40(2)
C(24) - C(25)	1.38(2)	C(25) - C(26)	1.33(2)
C(26) - C(27)	1.35(2)		

Table 4.4 Bond angles (deg) involving the non-hydrogen atoms of $[Cu(bbdo)(NO_3)]NO_3$ (E.S.D.s are given in parentheses)

Atoms	Angles	Atoms	Angles
S(1)-Cu-S(2)	89.4(2)	S(1)-Cu-O(11)	122.4(5)
S(1)-Cu-N(11)	92.8(5)	S(1)-Cu-N(21)	89.2(4)
S(2)-Cu-O(11)	148.1(5)	S(2)-Cu-N(11)	86.8(4)
S(1)-Cu-O(12)	164.1(6)	S(2)-Cu-N(21)	92.7(5)
O(11)-Cu-N(11)	88.8(6)	O(11)-Cu-N(21)	90.5(6)
N(11)-Cu-N(21)	178.0(7)	Cu-S(1)-C(2)	107.0(7)
Cu-S(1)-C(3)	96.4(7)	Cu-S(2)-C(4)	98.4(8)
Cu-S(2)-C(5)	106.8(7)	Cu-O(11)-N(1)	109(1)
Cu-N(11)-C(11)	131(1)	Cu-N(11)-C(12)	126(1)
Cu-N(21)-C(21)	127(1)	Cu-N(21)-C(22)	125(1)
C(2)-S(1)-C(3)	103.2(9)	C(4)-S(2)-C(5)	103.8(9)
O(11)-N(1)-O(12)	118(2)	O(11)-N(1)-O(13)	116(2)
O(12)-N(1)-O(13)	124(2)	O(21)-N(2)-O(22)	120(2)
O(21)-N(2)-O(23)	120(2)	O(22)-N(2)-O(23)	119(2)
C(11)-N(12)-C(13)	106(1)	C(21)-N(22)-C(23)	108(1)
N(12)-C(11)-C(1)	118(1)	C(11)-N(11)-C(12)	101(1)
C(21)-N(21)-C(22)	105(1)	C(2)-C(1)-C(11)	114(1)
S(1)-C(2)-C(1)	114(1)	S(1)-C(3)-C(4)	115(1)
S(2)-C(4)-C(3)	113(1)	S(2)-C(5)-C(6)	110(1)
C(5)-C(6)-C(21)	114(1)	N(11)-C(11)-N(12)	116(1)
N(11)-C(11)-C(1)	124(1)	N(11)-C(12)-C(13)	110(1)
N(11)-C(12)-C(17)	128(1)	N(21)-C(21)-N(22)	113(1)
C(13)-C(12)-C(17)	120(1)	N(12)-C(13)-C(12)	104(1)
N(12)-C(13)-C(14)	132(1)	C(12)-C(13)-C(14)	123(1)
C(13)-C(14)-C(15)	114(1)	C(14)-C(15)-C(16)	124(2)
C(15)-C(16)-C(17)	122(2)	C(12)-C(17)-C(16)	114(1)
N(21)-C(21)-C(6)	126(1)	N(22)-C(21)-C(6)	120(1)
N(21)-C(22)-C(23)	108(1)	N(21)-C(22)-C(27)	131(1)
C(23)-C(22)-C(27)	119(1)	N(22)-C(23)-C(22)	104(1)
N(22)-C(23)-C(24)	134(2)	C(22)-C(23)-C(24)	120(1)
C(23)-C(24)-C(25)	116(1)	C(24)-C(25)-C(26)	122(2)
C(25)-C(26)-C(27)	122(2)	C(22)-C(27)-C(26)	117(1)

Table 4.5 Least-Squares planes data for $[Cu(bbdo)(NO_3)]NO_3$

Plane Number 1

Atoms defining plane	Distance	esd
N(11)	-0.0103	0.0134
N(12)	-0.0145	0.0139
C(11)	-0.0517	0.0183
C(12)	0.0607	0.0173
C(13)	0.0452	0.0169
C(14)	0.0173	0.0185
C(15)	-0.0308	0.0198
C(16)	-0.0499	0.0194
C(17)	0.0176	0.0178
Cu	0.1325	

Mean deviation from plane is 0.0331 A

Chi-square: 43.3

Plane Number 2

Atoms defining plane	Distance	esd
N(21)	-0.0174	0.0137
N(22)	0.0380	0.0142
C(21)	0.0146	0.0186
C(22)	-0.0208	0.0165
C(23)	-0.0323	0.0192
C(24)	-0.0335	0.0189
C(25)	-0.0045	0.0194
C(26)	0.0431	0.0189
C(27)	0.0131	0.0183
Cu	-0.4083	

Mean deviation from plane is 0.0241 A

Chi-square: 23.4

Dihedral angles between least-squares planes

plane	plane	angle
2	1	44.61

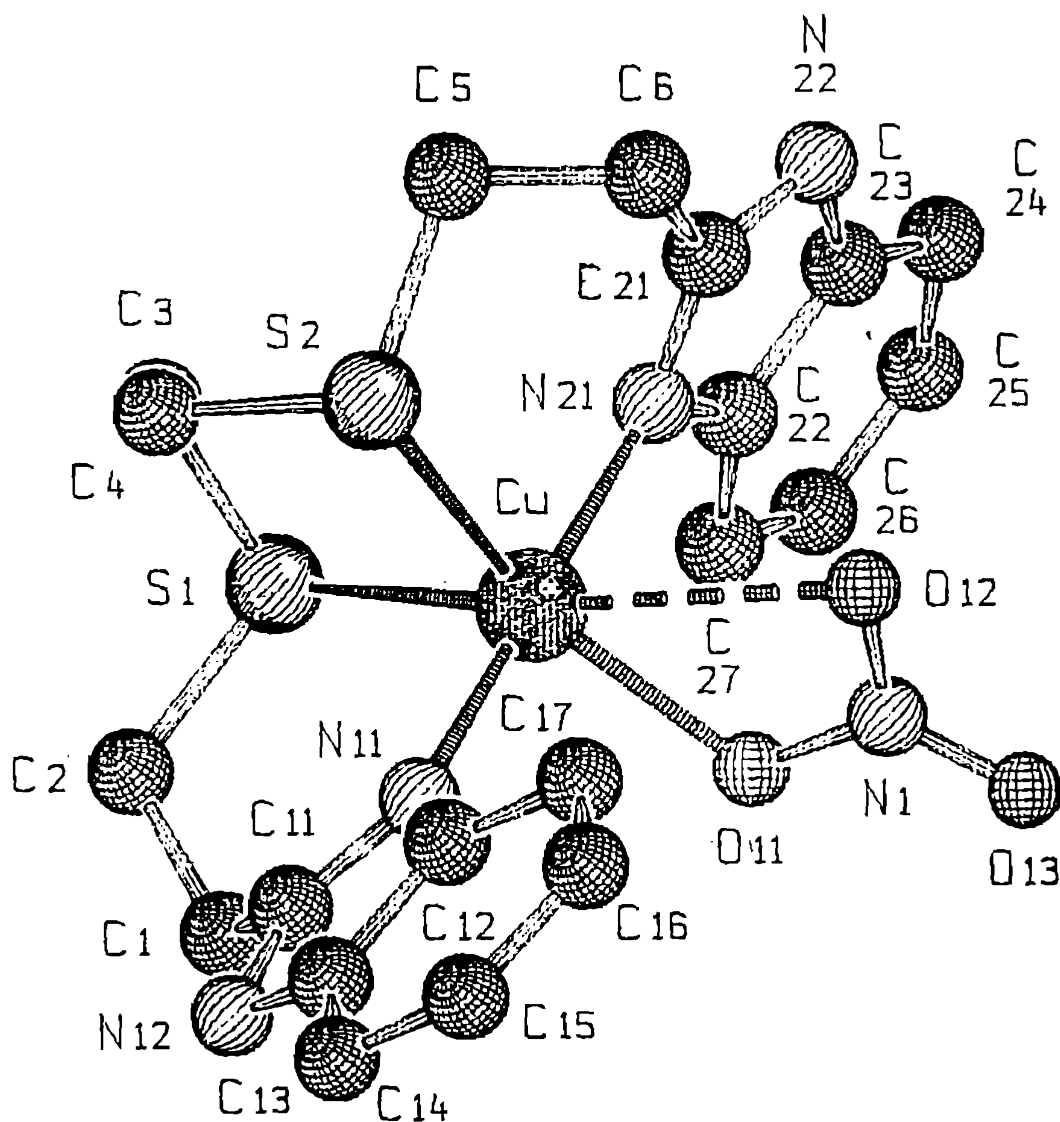


Fig. 4.1 Atomic labelling scheme* of the cation $[Cu(bbdo)(NO_3)]^+$. For clarity the hydrogen atoms and the NO_3 anion are omitted

* *SCHAKAL, A Fortran program for plotting crystal structures*, Germany, 1992.

least squares plane containing the NO_3^- ion makes a dihedral angle of 76.1° with the N(11)N(21)S(2)Cu least squares plane and is displaced towards bzim with N(11) nitrogen because of steric hindrance from the other bulky bzim. Thus though N(21)-Cu-O(11) [90.5(6)°] and N(11)-Cu-O(11) [88.8(6)°] bond angles are almost 90° ideal, the O(12) atom is off-the-axis and the S(1)-Cu-O(12) bond angle [164.1(6)°] is less than 180° ideal. The S(1)-Cu-O(11) bond angle of 122.4(5)° and the S(2)-Cu-O(11) bond angle of 148.1(5)° deviate very much from 90° and 180° ideal respectively. So it appears that it is the two bulky bzim groups assisted by the flexibility of Cu-S bonds, which lead to the folding of the N_2S_2 ligand.

On the other hand, while S(2) is coordinated at a short distance, S(1) at a rather long distance as a consequence of Jahn-Teller distortion; this reveals that the very symmetric ligand is coordinated in an assymmetric fashion. The Cu-S distances are similar to those in $[Cu(bbdh)Cl]^+$ [5] but longer than those in $[Cu(bmdhp)(H_2O)]^{2+}$,[8] suggesting that the addition of a methylene group between the thioethers as in the latter, rather than that between thioether and bzim groups as in the present complex, leads to stronger coordination of thioethers. The $Cu-N_{bzim}$ bond distances are in good agreement with those in similar compounds.[5,8] Further, the N(11)-Cu-N(21) bond angle of 178.0(7)° and the S(1)-Cu-S(2) angle of 89.4(2)° are close to the `ideal' angles of 180° and 90°

respectively. On the other hand, the corresponding N-Cu-N bond angles in $[Cu(bbdh)Cl]^+$ [165.9(2)°][6] and $[Cu(bbtb)(H_2O)]^{2+}$ [bbtb = 1,2-bis(benzimidazol-2′-ylmethylthio)benzene, Fig. 1.12a][7] [175.2(3)°] are much less than 180° ideal. It appears that the incorporation of two methylene groups between -S- and bzim ring as in the present compound relieves the strain in the molecule and thus the dihedral angle between the bzim rings in the present complex is only 44.6° while it is higher [76.5(2)°] in $[Cu(bbtb)(H_2O)]^{2+}$.

The equatorial $Cu-O(NO_2)$ bond length is remarkably shorter than that in square planar $[Cu(L)(NO_3)_2]$ [L = 1,3-bis(5-methylimidazol- 4-yl)-2-thiapropane][22] as well as in $[Cu(bidhx)(NCS)(NO_3)]$ [bidhx = 1,6-bis(5-methylimidazol-4-yl)-2,5-dithiahexane].[23] The O(12) of the coordinated nitrate group is potentially at a bonding distance of 2.727(6) A. In $[Cu(bipy)_2(ONO_2)]^+$ a $Cu-O(NO_2)$ bond length as long as 2.818 A is considered to be bonding.[24] The difference between the two Cu-O bonds is 0.667 A which is only very slightly less than the difference, 0.7 A previously suggested[25,24] for an unsymmetrically coordinated bidentate nitrate group. So the nitrate group in the present structure is considered unsymmetrically coordinated and the mean Cu-O distance is 2.394 A, a distance which is less than the Cu-S bond distances. The long $Cu-O(NO_2)$ bond distance is also partly a consequence of Jahn-Teller distortion. The coordinated nitrate has an internal O-N-O bond

angle of 118° which is almost the same as that (120°) for the uncoordinated nitrate. This illustrates that the coordinated nitrate does not undergo any distortion due to bulky bzim groups. Thus it appears that the ligand folding is brought about by the bzim rather than nitrate coordination. The bzim rings are planar, with negligible deviation (0.033 and 0.024 A) from the least squares plane.

The coordination geometry of the present complex is different from the trigonal bipyramidal geometry generally expected for the analogous CuN_2S_2 complexes like [Cu(bbdh)Cl]Cl,[6] [Cu(bbtb)(H_2O)](ClO_4)$_2$ (Fig. 1.12a),[7] [Cu(bidhx)Cl]Cl.2H_2O (Fig. 1.12b)[26] and [Cu(bmdhp)(H_2O)](ClO_4)$_2$;[8] the last one possesses a trigonally distorted rectangular pyramidal geometry.

The coordination geometry around Cu(II) in the present complex may be alternatively described as distorted trigonal bipyramidal, if the nitrate ion is considered to be monodentate i.e. Cu-O(12) interaction is non-bonding or at least very weak (Fig. 4.1a). Such a coordination geometry is expected of CuN_2S_2 complexes and is very similar to that of $[Cu(bbdh)Cl]^+$ in which S(1)-Cu-S(2) and N(21)-Cu-N(11) bond angles are very close to 90° and 180° ideal respectively; S(1)-Cu-O(11) and S(2)-Cu-O(11) bond angles are also close to 120°. For such geometries Addison *et al.* have proposed the structural index τ which has been defined as $\tau = (\beta-\alpha)/60$, with α and β being the two largest coordination

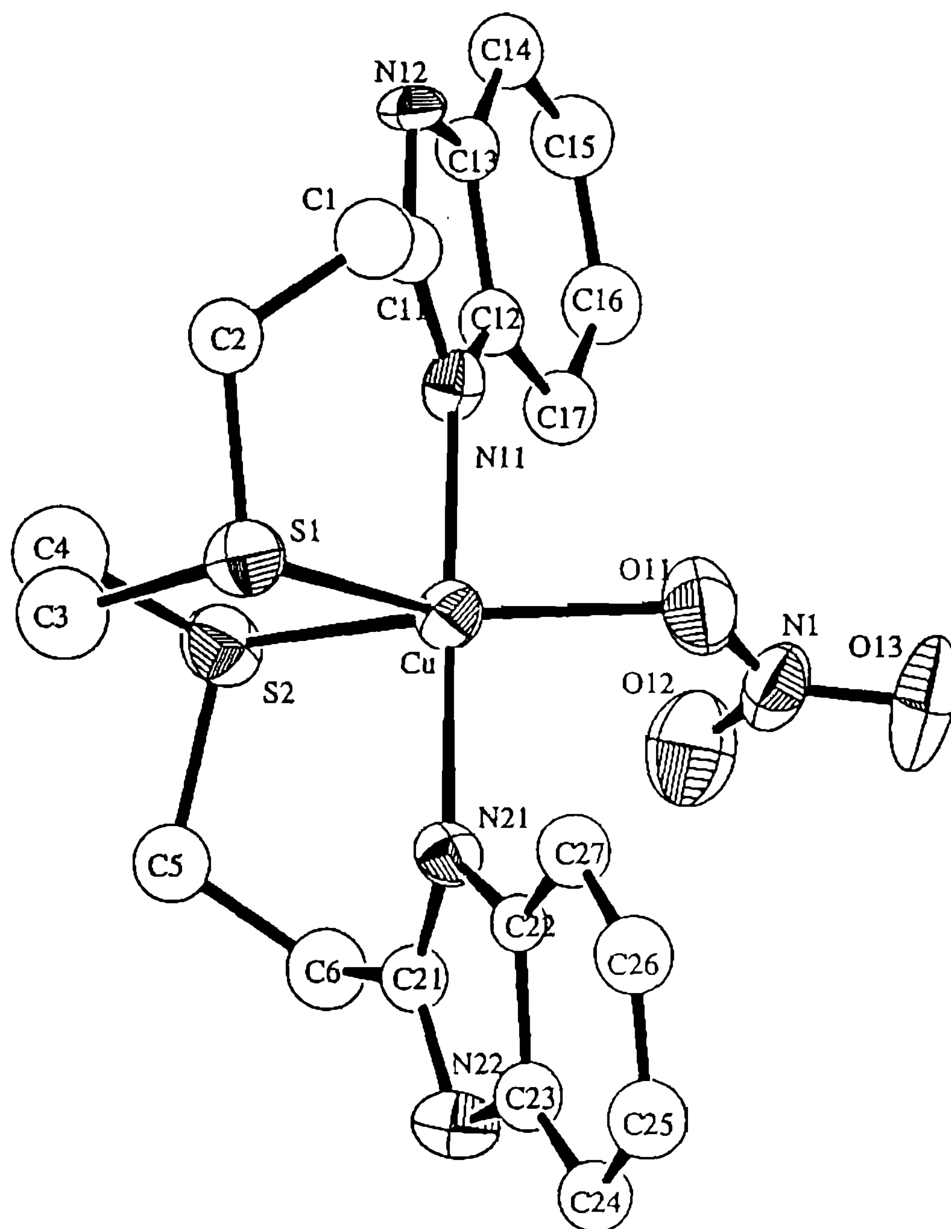


Fig. 4.1a ORTEP projection and atomic labelling of the cation $[Cu(bbdo)(NO_3)]^+$ showing nitrate anion as monodentate. For clarity the hydrogen atoms and the NO_3 anion are omitted

angles.[8] This geometric parameter is applicable to five-coordinate structures as an index of the degree of trigonality, within the structural continuum between trigonal bipyramidal and rectangular pyramidal. For a perfect square-pyramidal geometry, τ is equal to zero, while it is unity in a perfect trigonal-bipyramidal geometry. The trigonality index τ for the present structure is 0.50 while it is 0.38 for $[Cu(bbdh)Cl]^{+}$.[5] The increase in trigonality is obviously because of the incorporation of two methylene groups between thioether and bzim moieties; this is also evident from the N(11)-Cu-N(21) bond angle of almost 180° ideal and the decreased dihedral angle between the two bzim groups (44.6°) compared to $[Cu(bbtb)(H_2O)]^{2+}$ (76.1°).[7]

Further, the replacement of five-membered chelate ring(s) in $[Cu(bbdh)Cl]^{+}$ by six-membered one(s) and the fusion of a benzene ring between the thioether donors, as in $[Cu(bbtb)(H_2O)]^{2+}$ (τ = 0.64)[7] lead to enhanced distortion towards trigonality. Interestingly, the addition of a CH_2 group in between sulfur and bzim lead to almost the same constraint at copper as that in between two sulfur atoms as in $[Cu(bmdhp)(H_2O)]^{2+}$ (τ = 0.48).[8] But the thioethers in the present compounds are located in the trigonal plane while only one of the thioethers in the trigonal plane in the latter. However, it is cautioned that the possible differences in ligating properties may be overruled by the influence of coordinating solvent or anion; however, in the present complex the

nitrate ion does not appear to influence. The steric hindrance from bzim N(11) appears to move down O(21) from the plane containing S(2)S(1)CuO(11).

The S(1)-Cu-S(2) bond angle of 89.4(2)° which is less than 120° ideal, is due to the constraints from ethylene bridge between the sulfur atoms and is similar to that in $[Cu(bbdh)Cl]^{+}$ [90.39(6)°][5] and $[Cu(bmdhp)(H_2O)]^{2+}$ [88.69(5)°],[6] suggesting that the bond angle is not affected very much by the number of methylene groups linking the thioether sulfurs illustrating the flexibility of the bigger thioether atom.

A comparison of the present structure with that of its diaza analogue[27] $[Cu(bbda)]^{2+}$ [bbda = N,N′-bis(benzimidazol-2-ylethyl)ethane-1,2-diamine] which possesses a square planar CuN_4 chromophore suggests that the presence of flexible Cu-S bond(s) is essential for ligand folding and formation of trigonal bipyramidal geometry. This is in conformity with the earlier observation that π-bonding atoms confer on Cu(II) with the ability to distort its coordination sphere from planarity even in the absence of steric forces.[28] On the other hand, the pyridine analogue[29] of the present complex, *viz.* $[Cu(pdto)(ClO_4)]^{+}$, (Fig. 1.10a) possesses a square pyramidal structure ($\tau = 0.12$). So it is evident that in addition to coordinated thioethers, sterically hindered bzim groups may also lead to the adoption of trigonal bipyramidal geometry.

If one assumes that NO_3^- is coordinated in a bidentate fashion, then the present geometry can be regarded either as distorted monocapped trigonal bipyramidal or as heavily distorted octahedral.

4.3.2 Infrared Spectra

The infrared spectrum of $[Cu(bbdo)(NO_3)](NO_3)$ shows two medium intensity bands around 1460 and 1280 cm^{-1} and a strong band around 1390 cm^{-1}, which are expected of the coordinated nitrate anion;[30] however, it is difficult to diagnose whether the NO_3^- anion is monodentate or bidentate. For $[Cu(bbdo)](ClO_4)_2$ the infrared spectrum shows a split band around 1100 cm^{-1}, typical of ClO_4^- anion, coordinated to copper and/or hydrogen-bonded possibly to bzim hydrogens.[31]

4.3.3 Electronic Spectra

The $[Cu(bbdo)]^{2+}$ complexes show a broad band centered around 16.0 kK with a more intense band on its low energy side, compatible with a trigonal bipyramidal geometry;[32] however, on dissolution in methanol or acetonitrile two well separated (> 3 kK) (Table 4.6) bands of almost equal intensity (Fig. 4.2) were observed suggesting a change in geometry from trigonal bipyramidal to a square-derived one by additional solvation of copper with a $d_{x^2-y^2}$ rather than d_{z^2} ground state.[33,34] In the solid state $[Cu(pttu)]^{2+}$, like its homologue $[Cu(pttn)]^{2+}$ exhibits two bands,[16,35] suggesting a

Table 4.6 Electronic spectral data for Cu(II) complexes

Complex	Medium	LF*	CT*
$[Cu(bbdo)](ClO_4)_2$	Solid	16.0 (w) 11.1 (s)	
	MeOH	16.6 (216) 11.2 (258)	29.1 (2843)
	MeCN	16.9 (220) 11.6 (210)	28.7 (2810)
	H_2O	16.7 (170) 11.4 (190)	29.3 (3760) 24.7 (1420)
$[Cu(bbdo)(NO_3)]NO_3$	Solid	15.7 (w) 11.5 (s)	
	MeOH	16.5 (221) 11.3 (216)	29.0 (2305)
	MeCN	16.3 (157) 11.2 (112)	29.3 (3018)
$[Cu(pttu)](ClO_4)_2$	Solid	16.7 (s) 11.1 (w)	
	H_2O	16.7 (300)	26.4 (1910)
	MeOH	16.5 (430)	26.3 (2540)
	MeCN	16.3 (490) 11.1 (100)	26.1 (3280)
$[Cu(pttu)]Cl_2$	Solid	11.2	
	MeOH	14.8 (256)	27.4 (2160)

* $\bar{\nu}_{max}$ values reported in kK and ϵ in M^{-1} cm^{-1} within parentheses; concentration of the complex in solution = 0.002 M

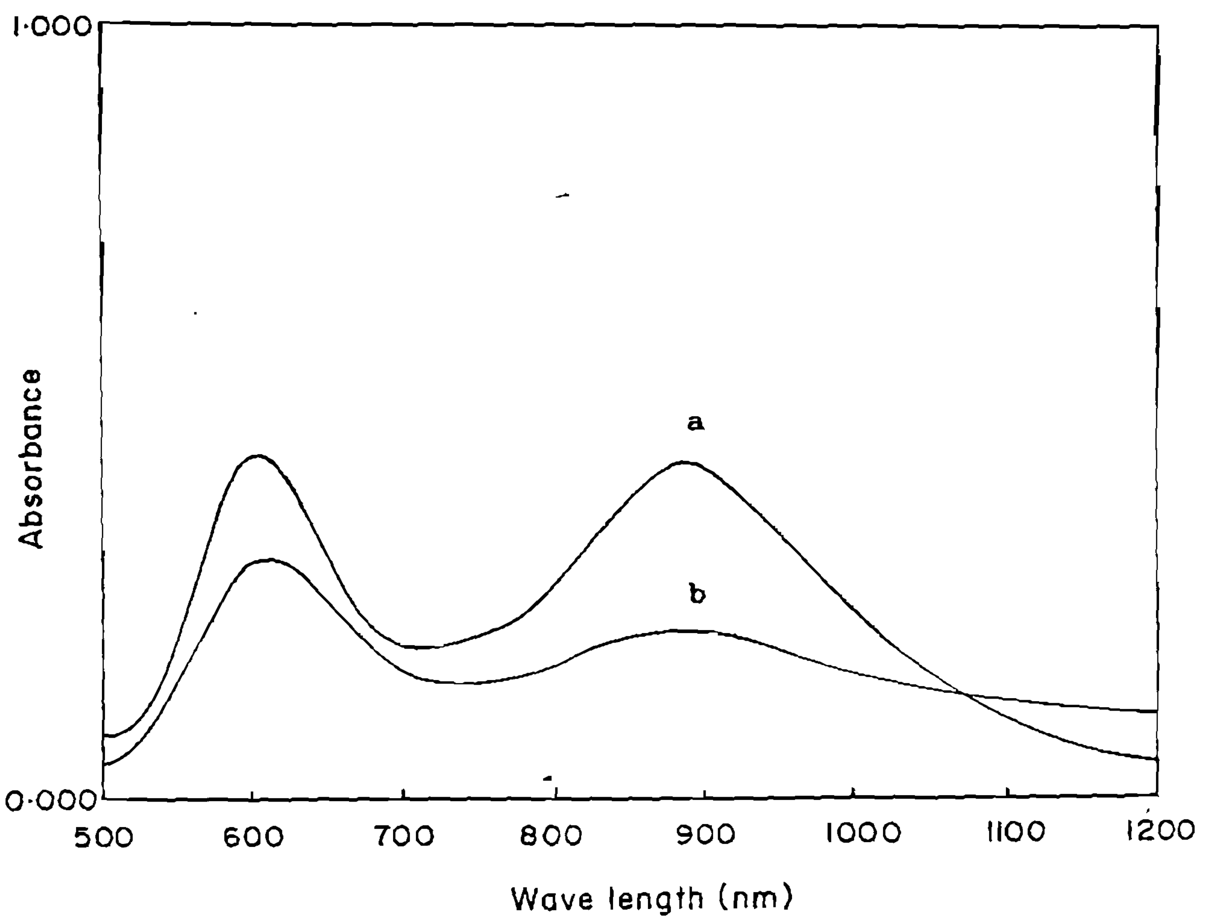


Fig. 4.2 Electronic spectra of $[Cu(bbdo)(NO)_3](NO_3)$ (0.002 M) in methanol (a) and acetonitrile (b)

trigonal bipyramidal geometry as found for the latter (Fig. 1.11b). In solution also the observed spectral features are similar to $[Cu(pttn)]^{2+}$ and are consistent with a square-based geometry. In contrast, the chloride complex shows a very broad ligand field feature centered around 11.2 kK, which is different entirely from that for the perchlorate.

An intense S(σ) ---> Cu(II) CT band around 29.0 kK was observed for both $[Cu(bbdo)]^{2+}$ and $[Cu(pttu)]^{2+}$ complexes. There is no appreciable change in position of LF and CT bands of $[Cu(bbdo)]^{2+}$, when the anion is changed from perchlorate to nitrate, irrespective of the solvent used.

4.3.4 EPR Spectra

The polycrystalline EPR spectra of both nitrate (Fig. 4.3) and perchlorate complexes of bbdo are rhombic with three g values [lowest $g \le 2.03$; $R = (g_2-g_1)/(g_3-g_2) = 2.1$ and 1.5 respectively] (Table 4.7). The low values for g_1 and $R > 1$ obey Hathaway's criterion[31] for distorted trigonal bipyramidal geometry and so the geometry of the nitrate discussed above[33,36] should be described as a distorted trigonal bipyramidal or at least as monocapped trigonal bipyramidal rather than as a square-based one; however, the polycrystalline EPR spectra of the analogous $[Cu(bbdh)Cl]^{+}$, $[Cu(bmdhp)H_2O]^{2+}$ and $[Cu(bbtb)H_2O]^{2+}$, all with trigonal bipyramidal or trigonally distorted tetragonal pyramidal

Table 4.7 EPR spectral data for Cu(II) complexes

Complex	Medium	$g_{\parallel}$	$A_{\parallel}$*	$g_{\perp}$
$[Cu(bbdo)](ClO_4)_2$	Solid	2.207 2.124 2.009	-	-
	MeOH	2.227	146	2.071
$[Cu(bbdo)(NO_3)]NO_3$	Solid	2.185 2.134 2.029	-	-
	MeOH	2.241 2.026	157	-
	DMF	2.210 2.215	145 131	-
$[Cu(pttu)](ClO_4)_2$	Solid	2.174	-	2.031
	MeOH	2.427	-	-
$[Cu(pttu)]Cl_2$	Solid	2.1951 2.0911 2.0331	-	-

* A in units of 10^{-4} cm^{-1}

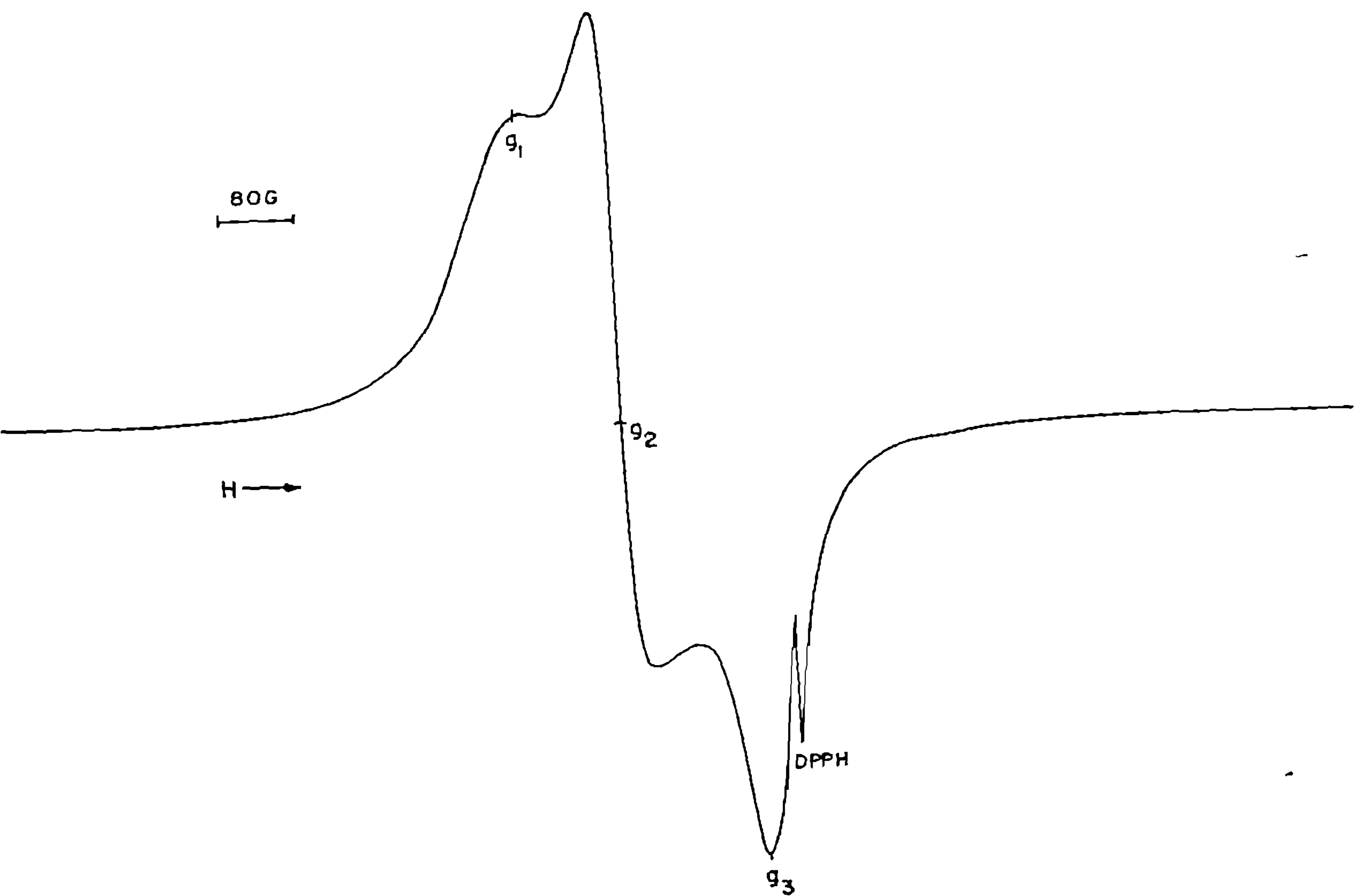


Fig. 4.3 Polycrystalline EPR spectrum of $[Cu(bbdo)(NO)_3](NO_3)$ at room temperature

geometry as expected above are not rhombic.

The frozen DMF solution spectrum of the nitrate (Fig. 4.4) shows clearly resolved peaks in the $g_{\parallel}$ region, consistent with the presence of three species. As the solution is diluted, the signals corresponding to cupric nitrate grew relative to those of other species. On the addition of excess $NaNO_3$, the signals corresponding to the less abundant species with high $g_{\parallel}$ value decreased in intensity and a well-defined axial spectrum with a weak rhombic component for the other species, possibly $[Cu(bbdo)(NO_3)]^+$, tend to appear; however, the signals for cupric nitrate remained (Fig. 4.4). A similar dissociative equilibrium involving ligand and solvent was observed also in frozen methanol solution of the nitrate and similar difficulty in illustrating the spectra has been observed previously for other $[CuN_2S_2]^{2+}$ complexes.[6,17] The $g_{\parallel}$ values for the different species in solution are in the same range as that observed for Cu(II) thioether complexes.[8,16,57] The less abundant species, as it has a high $g_{\parallel}$ value, are likely to arise from a square-based geometry, with at least one of the weakly coordinated thioethers replaced by solvent. The spectrum of the perchlorate complex in frozen methanol solution is axial with g and A values close to those observed for the more abundant species of the nitrate (Table 4.7); however, no dissociative equilibrium could be discerned.

The polycrystalline EPR spectrum of $[Cu(pttu)](ClO_4)_2$ is

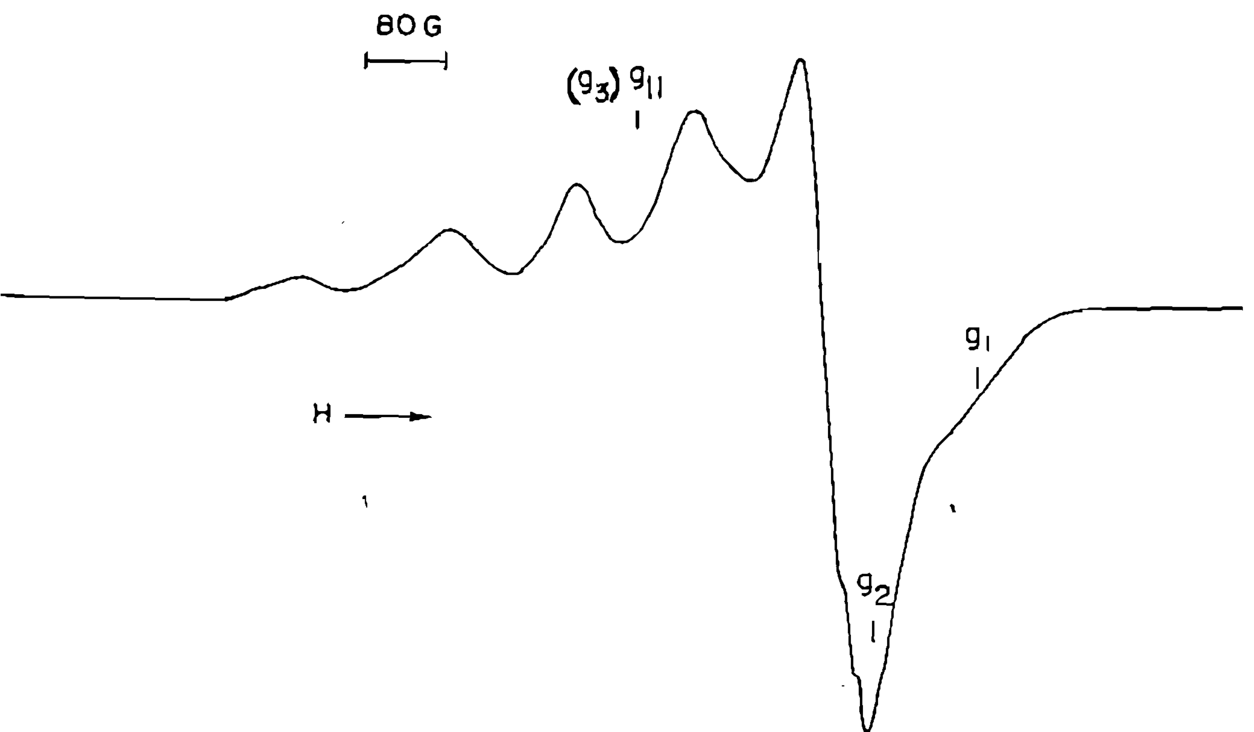


Fig. 4.4 EPR spectrum of $[Cu(bbdo)(NO)_3](NO_3)$ at 77 K in DMF in the presence of excess $NaNO_3$

axial (Fig. 4.5) suggesting that the ground state is predominantly $d_{x^2-y^2}$;[33,34] however, the chloride complex (Fig. 4.6), exhibits a rhombic spectrum with three g values and $g_{min} \leq 2.03$ and R = 0.6, suggesting a trigonal bipyramidal geometry with a half-filled d_{z^2} orbital. The $g_{||}$ values are in the same range as that observed for other Cu(II)-thioether complexes.[8,16,37] In aqueous solution (Fig. 4.7) the perchlorate complex shows $g_{||}$ and $A_{||}$ values (2.172 and 170.4 x 10^{-4} cm^{-1} respectively) similar to other Cu(II) complexes of di- and tetrathioether ligands.[15] The frozen methanol solution, interestingly, shows clearly resolved peaks (Fig. 4.7a) but with g values same as those observed for free copper. Such dissociation in solution is common for Cu(II) complexes of thioether ligands and macrocyclic tetrathioether complexes.[38]

4.3.5 Electrochemistry

The Cu(II)/Cu(I) redox couple of $[Cu(bbdo)]^{2+}$ is quasireversible in both methanol (Fig. 4.8) and acetonitrile solutions as evident from values of $\triangle E_p^{\circ}$ (Table 4.8) and i_{pa}/i_{pc}, the latter being nearly equal to unity up to 0.2 V/s scan rate. The values of diffusion coefficient calculated ($\approx$ 2.5 x 10^{-6} cm^2/s) from the slope of the linear plot of i_{pc} *vs* $\nu^{1/2}$ using Randles Sevciks' equation,[39] are within the range (Table 4.8) observed for similar CuN_2S_2 complexes undergoing Cu(II)/Cu(I) redox.[8,40]

The Cu(I) product formed on electrochemical reduction of

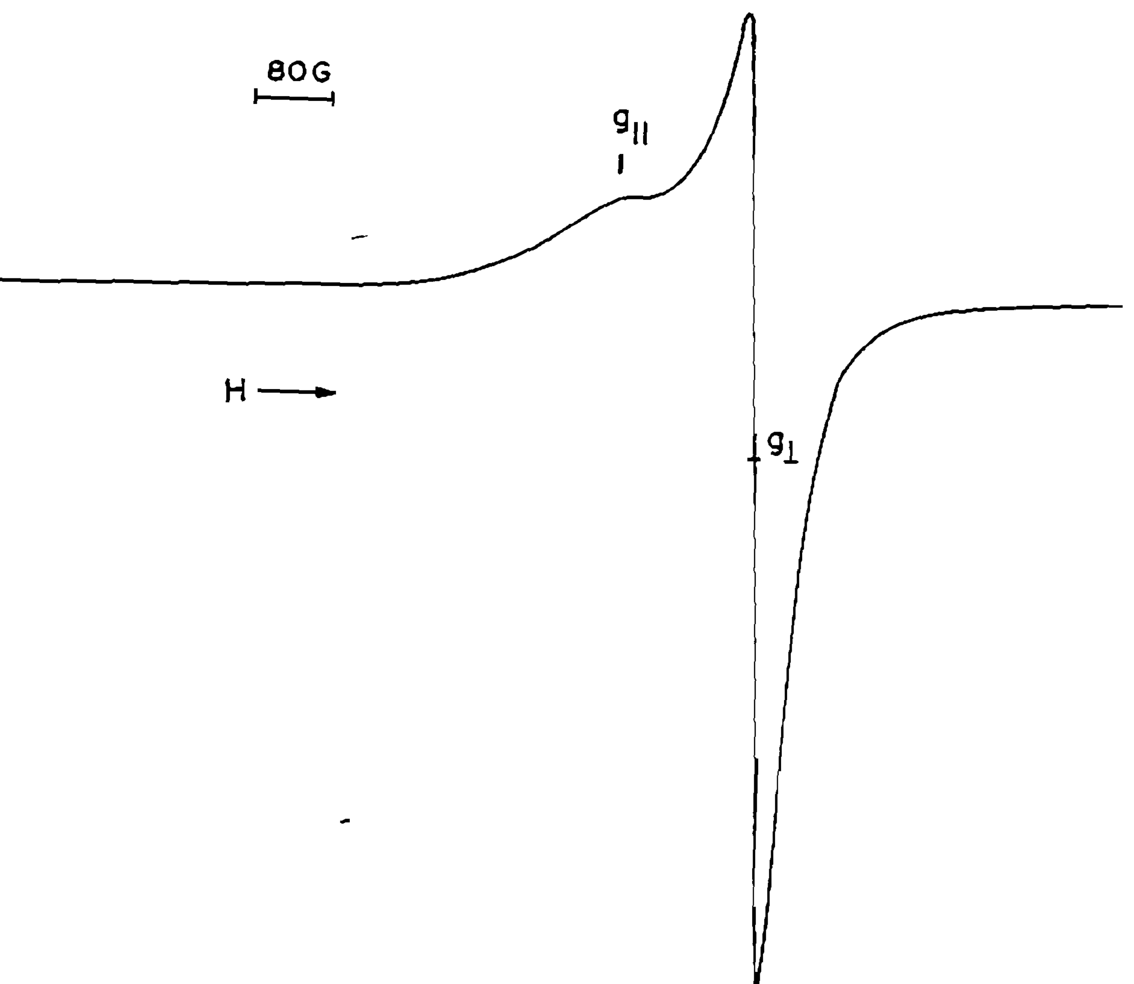


Fig. 4.5 Polycrystalline EPR spectrum of $[Cu(pttu)](ClO_4)_2$ at room temperature

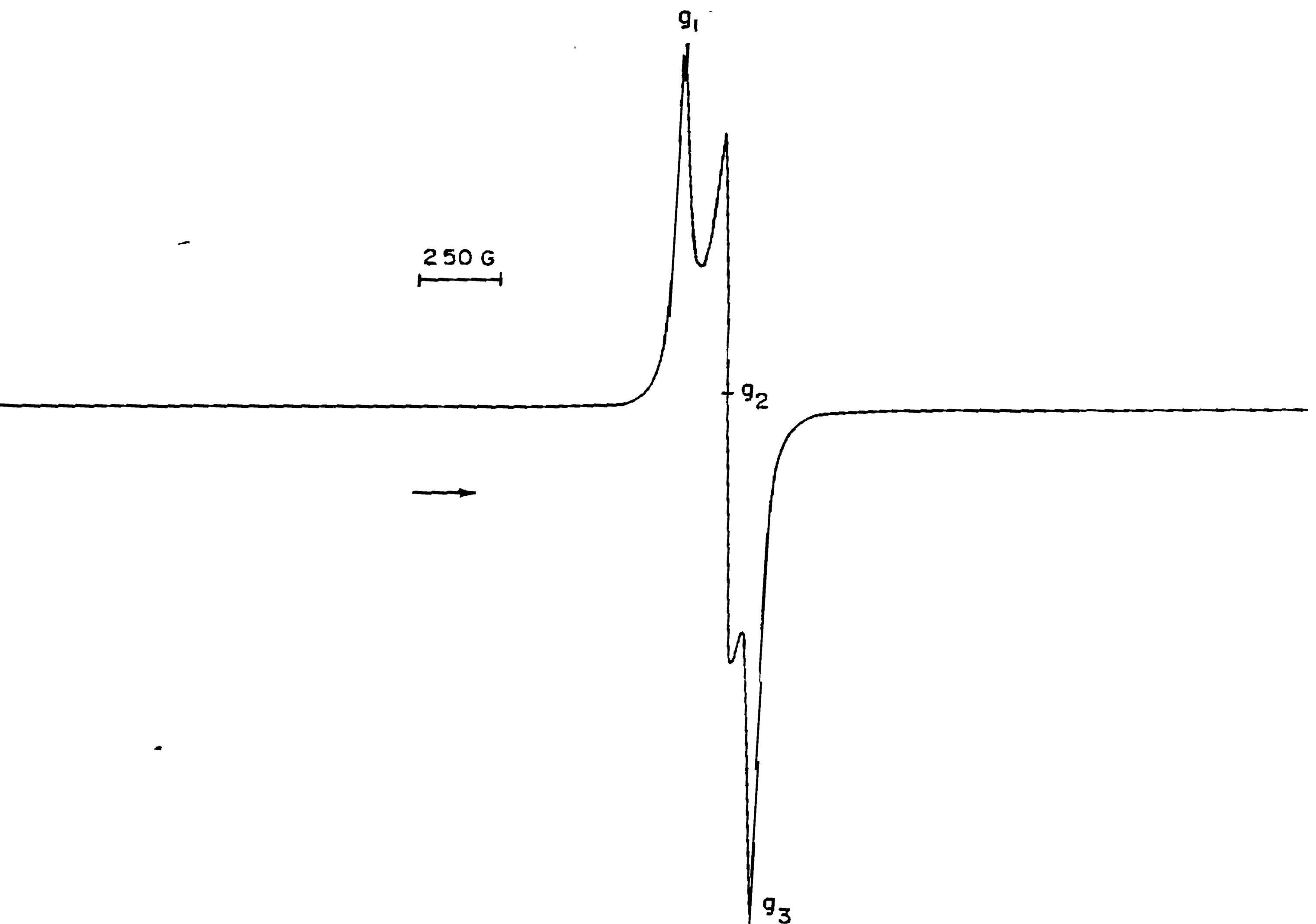


Fig. 4.6 Polycrystalline EPR spectrum of $[Cu(pttu)]Cl_2$ at room temperature

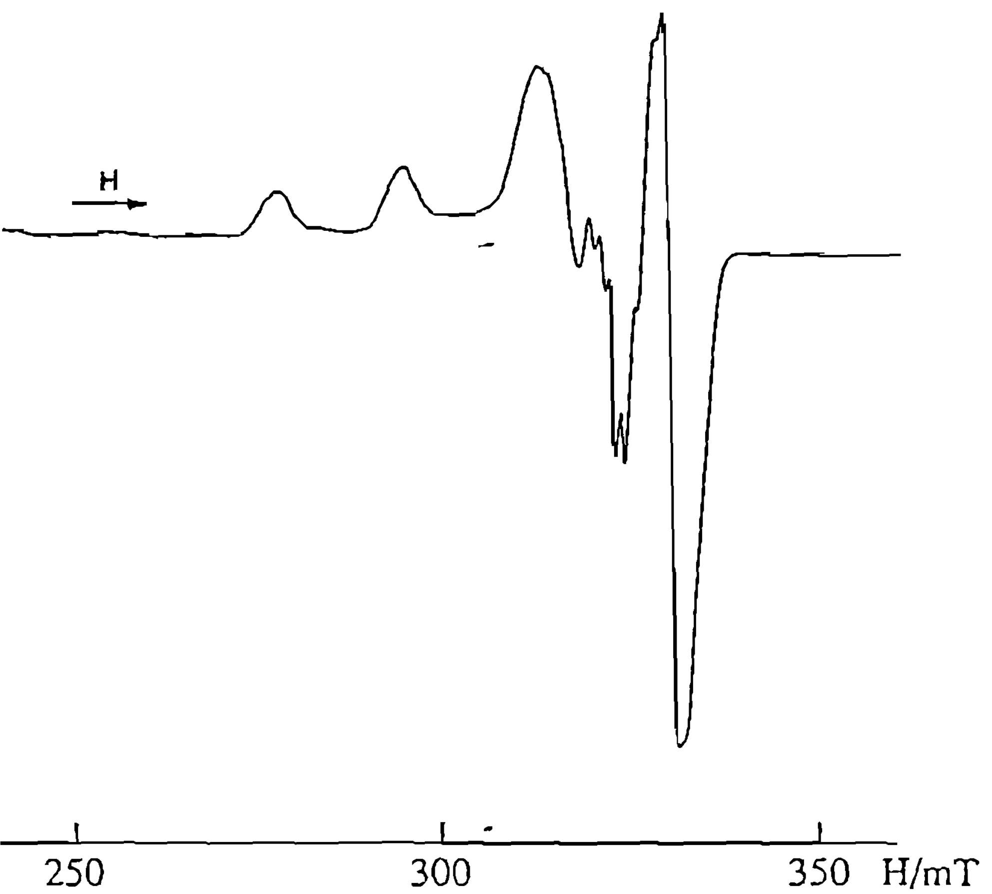


Fig. 4.7 EPR spectrum of $[Cu(pttu)](ClO_4)_2$ at 77 K in aqueous solution

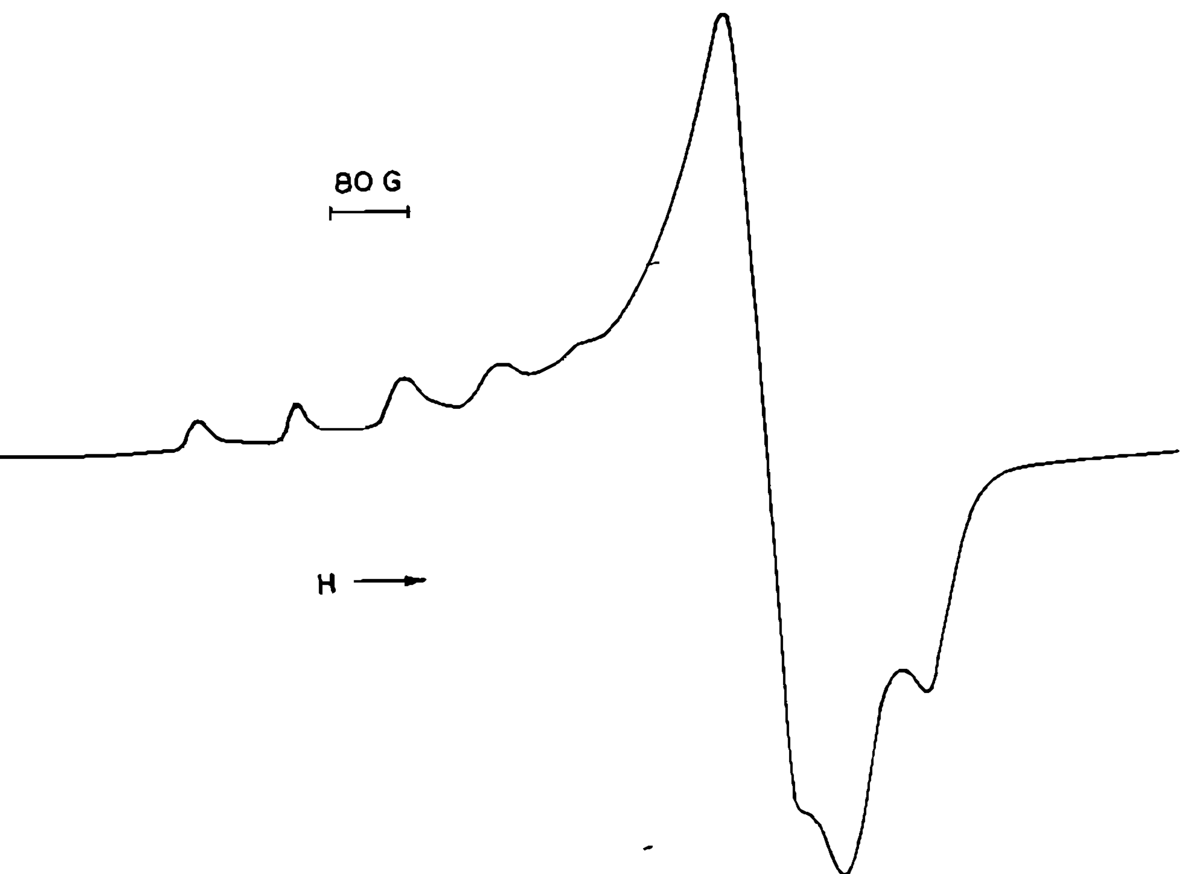


Fig. 4.7a EPR spectrum of $[Cu(pttu)](ClO_4)_2$ at 77 K in methanol/ethanol mixture (1:1 v/v)

Table 4.8 Electrochemical data[a] for the Cu(II) complexes at 25 °C on a glassy carbon electrode

Complex	Medium	E_{pc} V	E_{pa} V	ΔE_p mV	ΔE_p^0 mV	$E_{1/2}$(V) CV	DPV[b]	i_{pa}/i_{pc}	$Dx10^6$ cm^2/s
$[Cu(bbdo)](ClO_4)_2$	MeOH/ THAP	0.258	0.340	82	63	0.299	0.298	1.1	2.5
	H_2O/ $NaClO_4$	0.419	0.546	127	100	0.483	0.450	2.8	1.2
$[Cu(bbdo)(NO_3)]NO_3$	MeOH/ THAP	0.218	0.308	90	66	0.263	0.253	1.1	2.5
	MeOH/ $NaNO_3$	0.182	0.272	90	62	0.227	0.211	1.0	2.8
	MeCN/ THAP	0.198	0.296	98	75	0.247	0.245	1.2	2.6
$[Cu(pttu)](ClO_4)_2$	MeOH/ THAP	0.322	0.406	84	78	0.364	0.355	1.0	3.7
	H_2O/ $NaClO_4$	0.430	0.510	80	67	0.470	0.474	1.1	4.9

[a] Measured *vs* non-aqueous silver reference electrode for methanol and acetonitrile (add 544 mV to convert into NHE) and *vs* SCE for aqueous solutions; scan rate 50 mV/s; complex concentration, 0.001 M; concentration of supporting electrolye, 0.100 M. [b] scan rate 1 mV/s

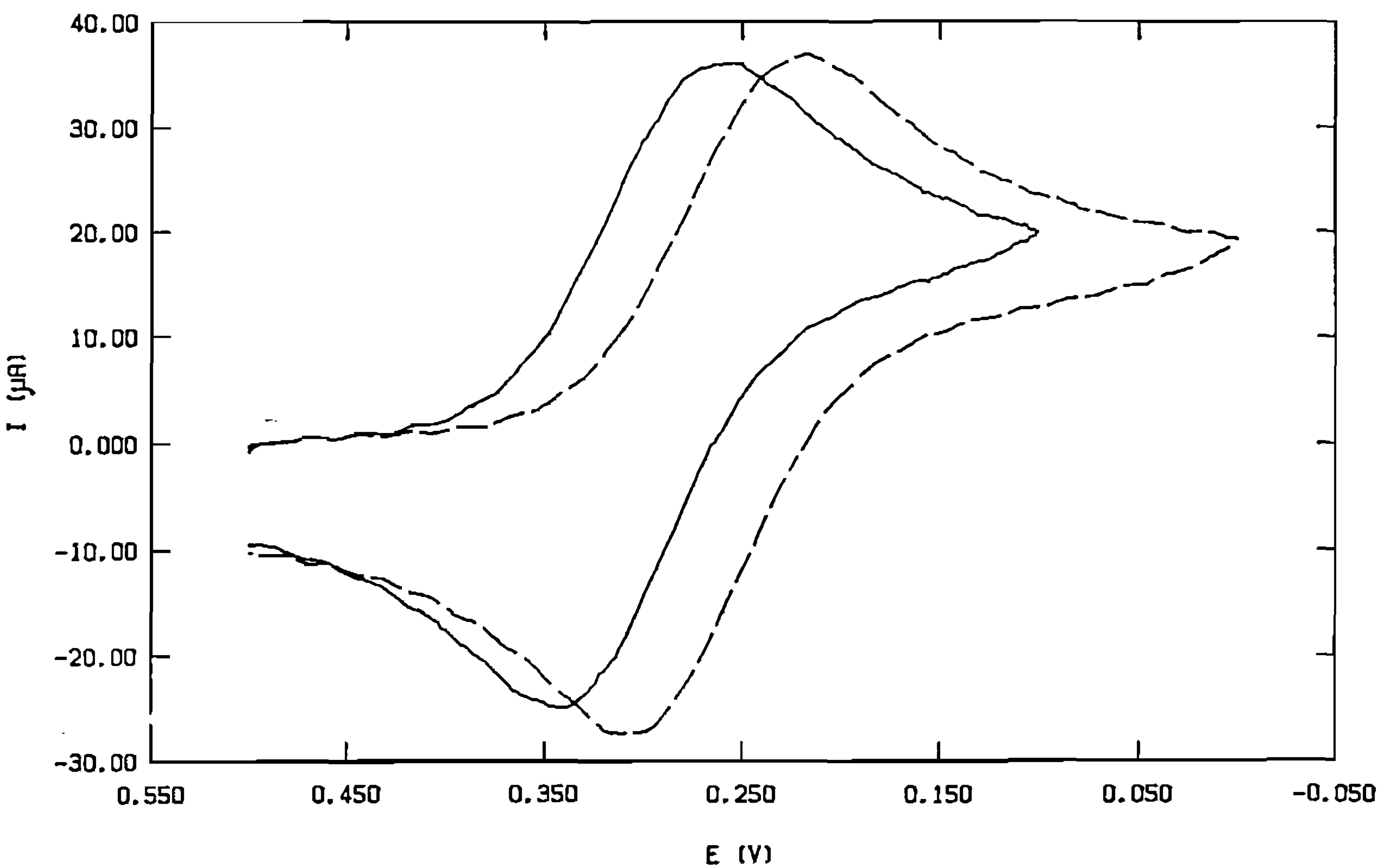


Fig. 4.8 Cyclic voltammograms (at 50 mV/s scan rate) of $[Cu(bbdo)(NO_3)](NO_3)$ (0.001 M) (----) and $Cu(bbdo)(ClO_4)_2$ (0.001 M) (——) on a glassy carbon electrode in methanol (0.1 M THAP) at 25 °C

$[Cu(bbdo)]^{2+}$ may possess a tetrahedral CuN_2S_2 core as in the X-ray crystal structure of its py analogue[29] $[Cu(pdto)]^{+}$ or contain copper linearly coordinated by the two bzim nitrogen atoms with the sulfur atoms having moved out of range for strong bonding as found for its homologue[4] $[Cu(bbdhp)]^{+}$ {bbdhp = 1,7-bis(benzimidazolyl)-2,6-dithiaheptane}. So the significant differences expected in the structures of Cu(II) and Cu(I) forms of the present complexes would mean greater structural rearrangement occurring during electron transfer,[41] following dissociation of coordinated anion. This is reflected in the higher ΔE_p and ΔE_p° values ($\approx$ 60 mV for reversible electron transfer); however, it is difficult to exclude the contribution of other factors like solvent coordination etc. in determining the peak potential separation. Thus the cyclic voltammogram of $[Cu(bbdo)]^{2+}$ obtained on glassy carbon electrode in aqueous solution suggests, however, that the redox is irreversible with i_{pa}/i_{pc} = 2.9; this is possibly due to stronger coordination of water and adsorption of Cu(I) species on the electrode.[42] The adsorption is evident from the decrease in i_{pa}/i_{pc} when the scan rate is increased.[43] We have observed in aqueous solution similar adsorption of copper(I) species of $[Cu(pdto)]^{2+}$ containing aromatic ligand moieties, on glassy carbon electrode.[44]

Even though the colour and spectral patterns for the perchlorate and nitrate complexes are the same, the redox potential

of the nitrate is lower and ΔE_p higher than the perchlorate suggesting that nitrate anions interact with copper even in solution. Further, Cu-O(NO_2) bond breaking may be involved during electron transfer, as a greater structural rearrangement during redox reaction will always lead to higher ΔE_p value. In fact, when $NaNO_3$ is used as the supporting electrolyte, a significant lowering of $E_{1/2}$ is observed for the nitrate (Table 4.8); this is consistent with the results from EPR studies. Among the bis(benzimidazolyl)-dithioether complexes the $E_{1/2}$ value varies as $[Cu(bbdh)]^{2+}$ [11] < $[Cu(bmdhp)]^{2+}$ [11] < $[Cu(bbdo)]^{2+}$ in methanol, suggesting that six-membered chelate rings in the presence of π-donors stabilise Cu(I) state as expected.[41,35,45]

Both the present nitrate and perchlorate complexes exhibit $E_{1/2}$ and ΔE_p values, higher and lower respectively than its pyridine analogue $[Cu(pdto)]^{2+}$; this may be due to the bulky bzim group which confers a geometry much more distorted than the square-based one for the latter. In fact, the $E_{1/2}$ values calculated for the present complexes using Addison's ΔE_L parameters[46] are lower than the adjusted values [$E_{adj} = E_{expt1} - 0.215$ V (in methanol)].[46] This implies that the contribution by the bulky bzim to $E_{1/2}$ is much higher than that by pyridine and imidazole and in fact, a better agreement with the observed values was seen when a ΔE_{bzim} value of +165 mV was used[15] for calculating the $E_{1/2}$ of $[Cu(bbdh)]^{2+}$. The value of $E_{1/2}$ calculated for the

present complex, however, is still lower (60 mV) than the observed one, illustrating that the present Cu(II) structure in solution is not completely square-based, a geometry required for the additivity of $E_{1/2}$ to be valid and may possess[40] some trigonal bipyramidal structural component. In this regard it is to be noted that the $E_{1/2}$ may be influenced by the stability of not only Cu(II) but Cu(I) structure also.

The Cu(II)/Cu(I) couple of $[Cu(pttu)]^{2+}$ exhibits nearly reversible redox behaviour both in aqueous and methanol (Fig. 4.9) solutions, as understood from the ΔE_p° and i_{pa}/i_{pc} values. The ΔE_p° values of Cu(II) complexes of pdto, pttn and pttu in aqueous solution are 74, 64 and 67 mV respectively. This is very interesting because $[Cu(pdto)]^{2+}$ on reduction apparently does not undergo any bond-breaking as understood from their Cu(II) and Cu(I) structures; $[Cu(pttu)]^{+}$ also possesses a tetrahedral structure but with a Cu-N_{py} bond dissociated as revealed in its preliminary crystal structure (Fig. 4.10). Thus the reversibility of a Cu(II)/Cu(I) couple depends not only on bond-breaking of chelating ligands but also of coordinated anions.

On the incorporation of a third sulfur donor in the N_2S_2 chelate $[Cu(pdto)]^{2+}$ to obtain $Cu(pttu)^{2+}$ a raise in the $E_{1/2}$ by 95 mV is expected.[46] In fact, in aqueous solution the observed difference in $E_{1/2}$ between $[Cu(pdto)]^{2+}$ and $[Cu(pttu)]^{2+}$ is 108 mV which is in fair agreement with this value. On the other hand, the

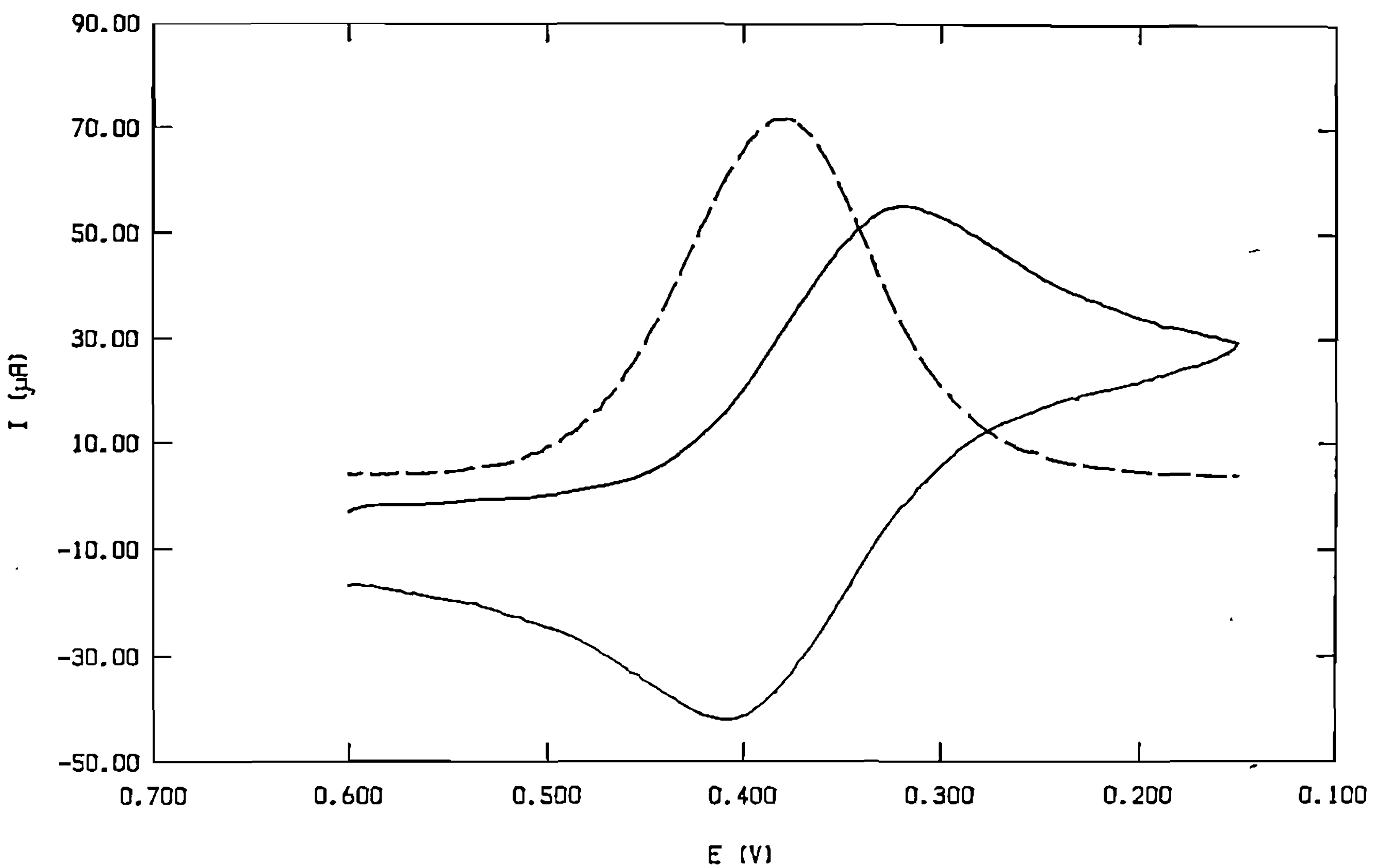


Fig. 4.9 Cyclic voltammogram (——) (at 50 mV/s scan rate) and differential pulse voltammogram (----) (at 1 mV/s scan rate) of $Cu(pttu)(ClO_4)_2$ (0.001 M) on a glassy carbon electrode in methanol (0.1 M THAP) at 25 °C

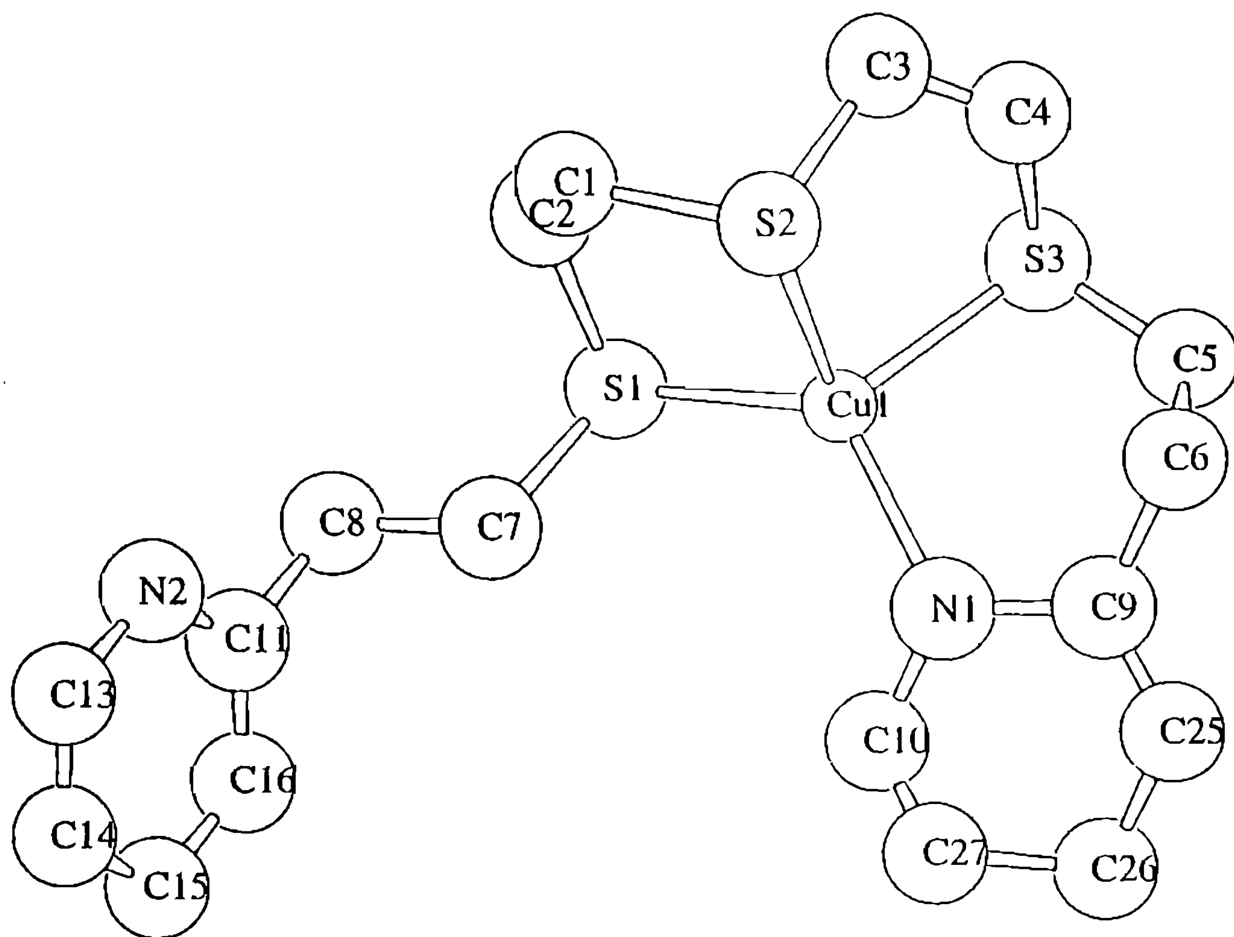


Fig. 4.10 Preliminary ORTEP projection of $[Cu(pttu)]^+$ cation

experimental difference between $[Cu(pdto)]^{2+}$ and $[Cu(pttn)]^{2+}$ (Scheme 4.2, Chapter 6) in aqueous solution is -25 mV, suggesting that not only the addition of sulfur but also the attendant five-membered chelate rings dictate the change in the $E_{1/2}$ value. The present complex $[Cu(pttu)]^{2+}$ exhibits an $E_{1/2}$ value higher than its homologue $[Cu(pttn)]^{2+}$, suggesting that six-membered chelate rings increase the $E_{1/2}$ of Cu(II)/Cu(I) couple, as observed previously.[18] Thus the complex $[Cu(pttu)]^{2+}$ exhibits a redox potential higher than $[Cu(pdto)]^{2+}$ and $[Cu(pttn)]^{2+}$ (Scheme 4.2)[44] suggesting that the increase in number of coordinated sulfur atoms from two to three increases while five-membered chelate rings decrease the redox potential of Cu(II)/Cu(I) redox couple.

4.4 Conclusions

The present complex exhibits a distorted monocapped trigonal bipyramidal geometry. The geometry can also be best described as a severely distorted octahedral, in spite of the presence of two ethylene bridges in between the thioether and bzim donors. This is interesting because the bis(pyridyl)-dithioether and bis(benzimidazolyl)-diamine analogues, which contain such bridges between -S- and py and -NH- and bzim respectively, possess only square-based geometries. This is obviously because of geometric distortion induced by steric effects of the bulky bzim groups, facilitated by coordinated thioethers. Such differences in structures are reflected in their spectral and electrochemical

behaviour. Thus the present structure gives a further demonstration of the flexibility (plasticity) of copper(II) ion.[23]

Further, the present study leads to the conclusion that Cu(II) complexes of all tetradentate bis(benzimidazol-2-yl) dithioether ligands, irrespective of the length of the ligand backbone, consistently possess a trigonal bipyramidal-based coordination geometry in the solid state.[5,7] Similar to other members of its class, the present complex is sensitive to interactions with solvents and anions, tend to adopt a square-based geometry in solution and display an enhanced redox potential expected of ligand enlargement. A water molecule or a halogenide or a relatively strongly coordinating anion like nitrate ion can be bound to copper(II) as the fifth ligand.

References

(1) Colman, P. M.; Freeman, H. C.; Guss, J. M.; Murata, M.; Norris, V. A.; Ramshaw, J. A. M.; Venkatappa, M. P. *Nature* **1978**, *272*, 319.

(2) Guss, J. M.; Harrowell, P. R.; Murata, M.; Norris, V. A.; Freeman, H. C. *J. Mol. Biol.* **1986**, *192*, 361.

(3) a) Adman, E. T.; Stenkamp, R. E.; Sieker, L. C.; Jensen, L. H. *J. Mol. Biol.* **1978**, *123*, 35.
b) Baker, E. N. *ibid.* **1988**, *203*, 1071.

(4) Karlsson, B. D.; Aasa, R.; Malmstrom, B. G.; Lundberg, L. G. *FEBS Lett.* **1989**, *253*, 99

(5) Birker, P. J. M. W. L.; Helder, J.; Hankel, G.; Krabs, B.; Reedijk, J. *Inorg. Chem.* **1982**, *21*, 357.

(6) Schilstra, M. J.; Birker, P. J. M. W. L.; Verschoor, G. C.; Reedijk, J. *Inorg. Chem.* **1982**, *21*, 2637.

(7) Rietmeijer, F. J.; Birker, P. J. M. W. L.; Gorter, S.; Reedijk, J. *J. Chem. Soc., Dalton Trans.* **1982**, 1191.

(8) Addison, A. W.; Rao, T. N.; Reedijk, J.; van Rijn, J.; Verschoor, G. C. *J. Chem. Soc., Dalton Trans.* **1984**, 1349.

(9) Bouwman, E.; Driessen, W. L.; Reedijk, J. *Coord. Chem. Rev.* **1990**, *104*, 143.

(10) Bouwman, E.; ten Hove, J. C.; Driessen, W. L.; Reedijk, J. *Polyhedron* **1988**, *7*, 2591.

(11) a) Addison, A. W.; Palaniandavar, M.; Reedijk, J.; van Rijn, J., Rao, T. N. to be communicated. b) Addison, A. W.; Palaniandavar, M. *Abstracts, American Chemical Society 188th National Meeting*, Washington DC, **1984**, INOR-068.

(12) a) Dockal, E. R.; Jones, T. E.; Sokol, W. F.; Engerer, R. J.; Rorabacher, D. B.; Ochrymowycz, L. A. *J. Am. Chem. Soc.* **1976**, *98*, 4322. b) Bernardo, M. M.; Heeg, M. J.; Schroeder, R. R.; Ochrymowycz, L. A.; Rorabacher, D. B. *Inorg. Chem.* **1992**, *31*, 191.

(13) Haanstra, W. G.; Cabral, M. F.; Cabral, J. de. O.; Driessen, W. L.; Reedijk, J. *Inorg. Chem.* **1992**, *31*, 3150.

(14) Casella, L.; Gullotti, M.; Pintar, A.; Pinciroli, F.; Vigano, R.; Zanello, P. *J. Chem. Soc., Dalton Trans.* **1989**, 1161.

(15) Usha, S.; Palaniandavar, M. *J. Chem. Soc., Dalton Trans.* **1994**, 2277.

(16) Kanters, R. P. F.; Yu, R.; Addison, A. W. *Inorg. Chim. Acta* **1992**, *196*, 97.

(17) Adhikary, B.; Lucas, C. R. *Inorg. Chem.* **1994**, *33*, 1376 and references cited therein.

(18) PATTY: Beurskens, P. T.; Admiraal, G.; Beurskens, G.; Bosman, W. P.; Garcia-Granda, S.; Gould, R. O.; Smits, J. M. M.; Smykalla, C. (1992). The DIRDIF program system, Technical Report of the Crystallography Laboratory, University of Nijmegen, The Netherlands.

(19) DIRDIF92: Beurskens, P. T.; Admiraal, G.; Beurskens, G.; Bosman, W. P.; Garcia-Granda, S.; Gould, R. O.; Smits, J. M. M.; Smykalla, C. (1992). The DIRDIF program system, Technical Report of the Crystallography Laboratory, University of Nijmegen, The Netherlands.

(20) Function minimized: $\Sigma w(|F_o| - |F_c|)^2$, where $w = 1/\sigma^2(F_o) = 4F_o^2/\sigma^2(F_o^2)$, $\sigma^2(F_o^2) = [S^2(C+R^2B) + (pF_o^2)^2]/L_p^2$, S = Scan rate, C = Total Integrated Peak Count, R = Ratio of Scan Time to background counting time, B = Total Background Count and L_p = Lorentz-polarization factor.

(21) *TEXSAN* - Crystal Structure Analysis Package, Molecular Structure Corporation, Woodlands, TX 1985 and 1992.

(22) van Steenbergen, A. C.; Bouwman, E.; de Graaff, R. A. G.; Driessen, W. L.; Reedijk, J.; Zanello, P. *J. Chem. Soc., Dalton Trans.* **1990**, 3175.

(23) Bouwman, E.; Day, R.; Driessen, W. L.; Tremel, W.; Krebs, B.; Wood, J. S.; Reedijk, J. *Inorg. Chem.* **1988**, *27*, 4614.

(24) Fereday, R. J.; Hodgson, P.; Tyagi, S.; Hathaway, B. J. *Inorg. Nucl. Chem. Lett.* **1981**, *17*, 243.

(25) Addison, C. C.; Loga n, N.; Wallwork, S. C.; Carner, C. D. *Quart. Rec.* **1971**, *25*, 289.

(26) Bouwman, E.; Burik, A.; Ten Hove, J. C.; Driessen, W. L.; Reedijk, J. *Inorg. Chim. Acta* **1988**, *150*, 125.

(27) Pandiyan, T.; Palaniandavar, M.; Lakshminarayanan, M.; Manohar, H. *J. Chem. Soc., Dalton Trans.* **1992**, 3377.

(28) Dorfman, J. R.; Bereman, R. D.; Whangbo, M. -H. in 'Copper Coordination Chemistry: Biochemical and Inorganic Perspectives', Karlin, K.D.; Zubieta, J. (eds), Adenine Press: New York, 1983.

(29) Brubaker, G. R.; Brown, J. N.; Yoo, M. K.; Kinsey, R. A.; Kutchan, T. M.; Mottel, E. A. *Inorg. Chem.* **1979**, *18*, 299.

(30) Nakamoto, K. *Infrared Spectra of Inorganic and Coordination Compounds*, 2nd Ed.; John Wiley & Sons: New York, 1970; p 171.

(31) Foley, J.; Kennefick, D.; Phelan, D.; Tyagi, S.; Hathaway, B. J. *J. Chem. Soc., Dalton Trans.* 1983, 2333; Bailey, N. A.; Bastida, R.; Fenton, D. E.; Lockwood, S. J.; McLean, C. H. *J. Chem. Soc., Dalton Trans.* **1988**, 839.

(32) Hathaway, B. J.; Billing, D. E. *Coord. Chem. Rev.* **1970**, *5*, 143.

(33) a) Procter, I. M.; Hathaway, B. J.; Billing, D. E.; Dudley, R.; Nicholls, P. *J. Chem. Soc. (A)* **1969**, 1192.
b) Billing, D. E.; Dudley, R. J.; Hathaway, B. J.; Tomlinson, A. A. G. *J. Chem. Soc. (A)* **1971**, 691.

(34) Fitzgerald, W.; Hathaway, B. J. *J. Chem. Soc., Dalton Trans.* **1981**, 567.

(35) Liu, S.; Lucas, C. R.; Hynes, R. C.; Charland, J.- P. *Can. J. Chem.* **1992**, *70*, 1773.

(36) Addison, A. W.; Sinn, E. *Inorg. Chem.* **1983**, *22*, 1225.

(37) a) Dagdigian, J. V.; McKee, V.; Reed, C. A. *Inorg. Chem.* **1982**, *21*, 1332. b) Miskowski, V. M.; Thich, J. A.; Solomon, R.; Schugar, H. J. *J. Am. Chem. Soc.* **1976**, *98*, 8344.

(38) Jones, T. E.; Rorabacher, D. B.; Ochrymowycz, L. A. *J. Am. Chem. Soc.* **1975**, *97*, 7485.

(39) Bard, A. J.; Faulkner, L. R. *Electrochemical methods: Fundamental applications*; John Wiley & Sons: New York, 1980; P 218.

(40) Sakaguchi, U.; Addison, A. W. *J. Chem. Soc., Dalton Trans.* **1979**, 600.

(41) Zanello, P. *Comments Inorg. Chem.* **1988**, *8*, 45.

(42) Anson, F. C.; Lee, C. W. *Inorg. Chem.* **1984**, *23*, 837.

(43) Wopschall, R. H.; Shain, I. *Anal. Chem.* **1967** *39*, 1514.

(44) Usha, S.; Palaniandavar, M. communicated.

(45) Nikles, D. E.; Powers M. J.; Urbach, F. L. *Inorg. Chem.* **1983**, *22*, 3210.

(46) Addison, A. W. *Inorg. Chim. Acta* **1989**, *162*, 217.

CHAPTER 5

5. INFLUENCE OF CHELATE RING SIZE AND NUMBER OF SULFUR DONOR ATOMS ON SPECTRA AND REDOX BEHAVIOUR OF COPPER(II) BIS(BENZIMIDAZOLYL)TETRA- AND PENTATHIOETHER COMPLEXES

5.1 Introduction

The crystal structures of the electron-transfer blue proteins plastocyanin[1] and azurin[2] reveal that copper in the active sites is coordinated to two histidine nitrogen atoms, a methionine thioether and a cysteine thiolate. As the novel spectroscopic and redox properties[3,4] of these proteins are often associated with their unusual active geometry and copper-sulfur coordination, there has been continuing interest in copper(II) complexes of ligands containing biologically relevant thioether and (benz)-imidazole nitrogen donors. A family of copper(II) complexes of bis(benzimidazolyl)-di-[5-8] and -trithia[7] ligands have been investigated. Among complexes with CuN_2S_2 chromophores, those involving the 555 chelate ring system possess trigonal-bipyramidal geometry[5,7] while with the 565 chelate ring system[8] a geometry intermediate between trigonal-bipyramidal and square-pyramidal is found. Recently the spectral and electrochemical behaviour of these complexes have been studied[9] in detail. It is now well known that thioether donors destabilise[10] the copper(II) state, elevating,

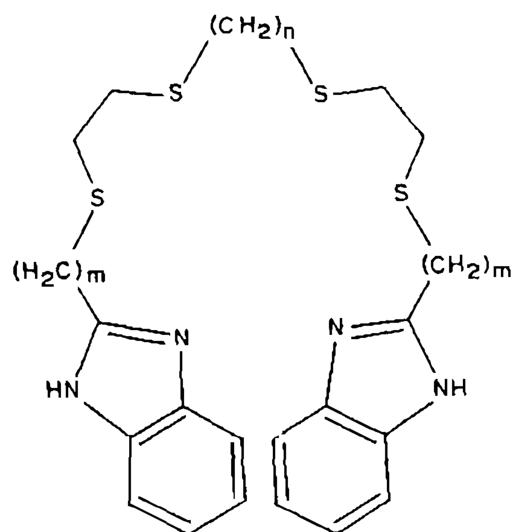
while the incorporation of five-membered chelate rings depresses,[9] the Cu(II)/Cu(I) redox potentials. Studies on copper(II/I) complexes of bis(imidazolyl)dithia[11,12] and bis(benzimidazolyl)-diaza[13] ligands illustrate the effect of bulky benzimidazole moieties on structures and spectra.

These observations prompted us to investigate systematically the effect of incorporating increasing numbers of sulfur donor atoms, entailing different chelate ring systems around copper(II), on the spectral and redox behaviour. In this chapter we describe the isolation and study of copper(II) complexes of bis(benz-imidazolyl) ligands, with four (L1 - L4) and five (L5) thioether donor atoms (Scheme 5.1) and address the effect of the increasing number of thioether donors among complexes with all-five-membered chelate rings. Attempts are also made to infer the coordination geometries of these complexes from their ligand field and EPR spectra in comparison with related complexes.

5.2 Experimental

5.2.1 Synthesis of Certain Multidentate Benzimidazole-Derived Ligands

Benzimidazoles are readily prepared by the ring-closure reaction of 1,2-diaminobenzenes with a carboxylic acid[14]. The tetra- and pentathioether benzimidazoles (Scheme 5.1) have been synthesised[15] by this method, from their corresponding dicarboxylic acid precursors described in Chapter 3, as follows.

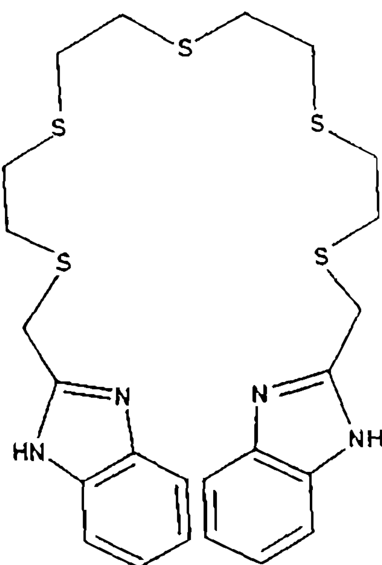


L1 $n = 2, m = 1$ N_2S_4(55555)

L2 $n = 3, m = 1$ N_2S_4(55655)

L3 $n = 2, m = 2$ N_2S_4(65556)

L4 $n = 3, m = 2$ N_2S_4(65656)



L5 N_2S_5(555555)

Scheme 5.1

1,12-Bis(benzimidazol-2-yl)-2,5,8,11-tetrathiadodecane (L1)

The diacid 2,5,8,11-tetrathiadodecane-1,12-dicarboxylic acid (Chapter 3) (6.4 g, 19 mmol) was ground with *o*-phenylenediamine (4.2 g, 39 mmol), fused and stirred for one hour at 160 °C. The blue colour solid obtained was recrystallised from aqueous ethanol using decolourising charcoal. Yield, 51 %, m.p. 118 °C; (Found: C, 55.4; H, 5.80; N, 11.6. $C_{22}H_{24}S_4N_4$ requires C, 55.7; H, 5.52; N, 11.8 %); MS: m/z 205 (11 %); ^{1}H NMR (DMSO-d_6): δ 2.50 (s, 4H, $-S-CH_2-CH_2-S-$), 2.73 (d, 8H, J = 6.8, $-S-CH_2-CH_2-S-$), 3.96 (s, 4H, $-S-CH_2$-BzIm), 7.17 - 7.13 (m, 4H, J = 3.2, BzIm-5,6), 7.53 - 7.49 (m, 4H, J = 3.1, BzIm-4,7); UV (methanol): nm (log ε) 285 (3.72), 277 (3.78), 247 (3.67), 204 (4.48).

1,14-Bis(benzimidazol-2-yl)-3,6,9,12-tetrathiatetradecane (L2)

The diacid 3,6,9,12-tetrathiatetradecane-1,14-dicarboxylic acid (Chapter 3) (10.2 g, 28 mmol) was ground with *o*-phenylenediamine (6.0 g, 56 mmol) and kept (1 h) at 160 °C with stirring. The blue product separated on cooling was recrystallised from aqueous tetrahydrofuran (charcoal). Yield, 49 %, m.p. 122 °C; (Found: C, 56.9; H, 6.32; N, 10.7. $C_{24}H_{30}S_4N_4$ requires C, 57.3; H, 6.01; N, 11.1 %); MS: m/z 343 (12 %), ^{1}H NMR (DMSO-d_6): δ 1.36 (s, 4H, $-S-CH_2-CH_2-S$), 2.60 (t, 8H, J = 6.9, $-S-CH_2-CH_2-S-$), 3.03 (d, 4H, J = 6.1, $-S-CH_2-$), 3.09 (d, 4H, J = 6.2, $-CH_2$-BzIm), 7.16 - 7.13 (m, 4H, J = 3.1, BzIm-5,6), 7.51 - 7.48 (m, 4H, J = 2.9,

BzIm-4,7); UV (methanol): nm (log ∊) 281 (3.56), 275 (3.56), 243 (3.51), 208 (4.33).

1,13-Bis(benzimidazol-2-yl)-2,5,9,12-tetrathiatridecane (L3)

The diacid 2,5,9,12-tetrathiatridecane-1,13-dicarboxylic acid (Chapter 3) (11.1 g, 32 mmol) was refluxed (32 h) with *o*-phenylenediamine (6.9 g, 64 mmol) in 6N hydrochloric acid (100 mL). The solid separated on cooling was suspended in water, neutralised with aqueous ammonia and recrystallised from aqueous ethanol. Yield, 53 %, m.p. 200 °C (d); (Found: C, 56.9; H, 5.56; N, 11.7. $C_{23}H_{28}S_4N_4$ requires C, 56.5; H, 5.77; N, 11.5 %); MS: m/z 223 (21%); ^{1}H NMR (DMSO-d_6): δ 2.01 (s, 2H, $-CH_2-$), 2.51 (t, 4H, $-CH_2-S-$), 2.79 (s, 8H, $-S-CH_2-CH_2-S-$), 3.98 (s, 4H, $-CH_2-$BzIm), 7.15 - 7.18 (m, 4H, J = 3.1, BzIm-5,6), 7.49 - 7.52 (m, 4H, J = 3.1, BzIm-4,7); UV (methanol): nm (log ∊) 285 (4.17), 277 (4.23), 248 (4.09).

1,15-Bis(benzimidazol-2-yl)-3,6,10,13-tetrathiapentadecane (L4)

The corresponding thiocarboxylic acid, 3,6,10,13-tetrathiapentadecane-1,15-dicarboxylic acid was prepared as reported in Chapter 3. This diacid (14.9 g, 40 mmol) was treated with *o*-phenylenediamine (8.7 g, 81 mmol) in 6N hydrochloric acid (75 mL) and refluxed (24 h). The hydrochloride separated on cooling was neutralised with aqueous ammonia and the product was recrystallised from aqueous ethanol. Yield, 52 %, m.p. 182 °C;

(Found: C, 58.5; H, 5.93; N, 11.1. $C_{28}H_{32}S_4N_4$ requires C, 58.1; H, 6.24; N, 10.8 %); MS: m/z 205 (15 %), ^{1}H NMR (DMSO-d_6): δ 2.15 (s, 2H, -CH_2-), 2.51 (t, 4H, -CH_2-S-), 2.75 (s, 8H, -S-CH_2-CH_2-S-), 3.02 (d, 4H, J = 6.5, -S-CH_2-), 3.10 (d, 4H, J = 6.4, -CH_2-BzIm), 7.14 - 7.17 (m, 4H, J = 3.0, BzIm-5,6), 7.48 - 7.52 (m, 4H, J = 3.0, BzIm-4,7); UV (methanol): nm (log ε) 281 (4.10), 275 (4.15), 244 (4.07), 216 (4.29).

1,15-Bis(benzimidazol-2-yl)-2,5,8,11,14-pentathiapentadecane (L5)

The diacid 2,5,8,11,14-pentathiapentadecane-1,15-dicarboxylic acid (Chapter 3) (3.5 g, 9 mmol) was refluxed (24 h) with *o*-phenylenediamine (2.0 g, 18 mmol) in 6N hydrochloric acid (100 mL), the hydrochloride separated on cooling was neutralised with aqueous ammonia and then the solid obtained was recrystallised from aqueous ethanol. Yield, 55 %, m.p. 210 °C (d); (Found: C, 53.7; H, 5.73; N, 10.7. $C_{24}H_{30}S_5N_4$ requires C, 53.9; H, 5.65; N, 10.5 %); MS: m/z 253 (25 %); ^{1}H NMR (DMSO-d_6): δ 2.1 (s, 4H, -S-CH_2-), 2.55 (s, 4H, -CH_2-S-), 2.79 (s, 4H, -S-CH_2-), 3.32 (s, 4H, -CH_2-S-), 3.99 (s, 4H, -CH_2-BzIm), 7.19 (m, 4H, BzIm-5,6), 7.52 (m, 4H, BzIm-4,7).

5.2.2 Preparation of the Complexes

The corresponding copper(II) perchlorate complexes were isolated as follows.

$[Cu(L1)](ClO_4)_2$. A solution of $Cu(ClO_4)_2.6H_2O$ (0.37 g, 1 mmol) in methanol (1 mL) was added with stirring to a methanolic solution (20 mL) of L1, (0.47 g, 1 mmol) and then cooled. The complex obtained was filtered off, washed with cold methanol and dried over P_4O_{10} under vacuum.

$[Cu(L2)](ClO_4)_2$, $[Cu(L4)](ClO_4)_2$ and $[Cu(L5)](ClO_4)_2$ were prepared following the procedure used for $[Cu(L1)](ClO_4)_2$. Copper(II) complexes of some of the ligands were isolated as chlorides, nitrates and tetrafluoroborates by adopting the same procedure used to synthesise the perchlorate complexes, and starting from the respective copper(II) salt. The results of elemental analysis (Table 5.1) correspond to 1:1 complex formation.

5.3 Results and Discussion

5.3.1 Synthesis

All the copper(II) perchlorate complexes except $[Cu(L3)]^{2+}$ were isolated as crystalline solids and are stable. The analytical data for these 1:1 complexes are collected in Table 5.1. As $[Cu(L3)]^{2+}$ is very unstable possibly due to facile reduction[4] of Cu(II) in the presence of ligand, physical measurements were therefore carried out on a freshly prepared solution containing $Cu(ClO_4)_2$ and L3 in 1:1.1 ratio. Attempts to isolate single crystals of the complexes were unsuccessful.

Table 5.1 Analytical data[a] for $[CuL]^{2+}$ complexes

Complex	% C	% H	% N	% Cu
$[Cu(L1)](ClO_4)_2.2H_2O$	33.8 (34.2)	3.63 (3.91)	6.99 (7.25)	7.93 (8.22)
$[Cu(L1)](BF_4)_2.3/2H_2O$	35.5 (35.8)	3.84 (3.95)	7.12 (7.58)	8.31 (8.60)
$[Cu(L1)](NO_3)_2.1/2H_2O$	39.0 (39.4)	3.94 (4.05)	12.1 (12.5)	9.18 (9.47)
$[Cu(L1)]Cl_2.H_2O$	42.0 (42.1)	4.11 (4.49)	9.19 (8.93)	10.3 (10.1)
$[Cu(L2)](ClO_4)_2.2H_2O$	34.8 (35.1)	3.76 (4.10)	7.54 (7.12)	8.32 (8.07)
$[Cu(L2)]Cl_2.2H_2O$	41.7 (41.9)	4.62 (4.89)	8.91 (8.50)	9.41 (9.64)
$[Cu(L4)](ClO_4)_2$	38.9 (38.5)	3.92 (4.14)	7.55 (7.19)	8.37 (8.16)
$[Cu(L4)](BF_4)_2.H_2O$	38.7 (38.9)	4.23 (4.44)	7.67 (7.28)	8.46 (8.23)
$[Cu(L4)](NO_3)_2.1/2H_2O$	41.8 (42.1)	4.28 (4.66)	11.4 (11.8)	8.64 (8.91)
$[Cu(L4)]Cl_2$	46.4 (46.1)	4.91 (4.95)	8.24 (8.60)	9.48 (9.76)
$[Cu(L5)](ClO_4)_2.H_2O$	35.0 (35.4)	3.62 (3.96)	6.43 (6.87)	7.55 (7.79)
$[Cu(L5)]Cl_2.H_2O$	41.9 (41.9)	4.25 (4.69)	7.73 (8.15)	8.97 (9.25)

[a] Calculated values are within parentheses

5.3.2 Infrared Spectra

The infrared spectra (Fig. 5.1) of all the perchlorates show a strong band (ν_3) split into three components (1070, 1100 and 1140 cm^{-1}) suggesting[14] coordination of ClO_4^-. However, the forbidden ν_1 band which is allowed and appears around 900 cm^{-1} in lower symmetry is absent and a single sharp unsplit band is observed at 620 cm^{-1} (ν_4). This suggests that the uncoordinated perchlorate is in an ionic form and that the splitting of ν_3 band may be due to ClO_4^- hydrogen bonded[17] to NH of the benzimidazole moiety. The tetrafluoroborate complexes also show a split ν_3 band around 1070 cm^{-1}, suggesting such hydrogen bonding rather than coordination of the anion.

5.3.3 Electronic Spectra

The reflectance spectra of all the present complexes show either one broad or two well separated (> 3.0 kK) ligand field bands in the visible region (Fig. 5.2). In methanol solution noticeable differences in ligand field features are observed (Table 5.2), implying structural changes, such as displacement of axially coordinated thioether, by solvent or anion. Thus in methanol solution both the ClO_4^- and BF_4^- salts of $[Cu(L1)]^{2+}$ exhibit (Fig. 5.3) only one ligand field band, although they show different spectral features in the solid state. These spectral data suggest that the geometry[18,19] of the complexes is likely to be distorted octahedral rather than trigonal bipyramidal, both in solution and

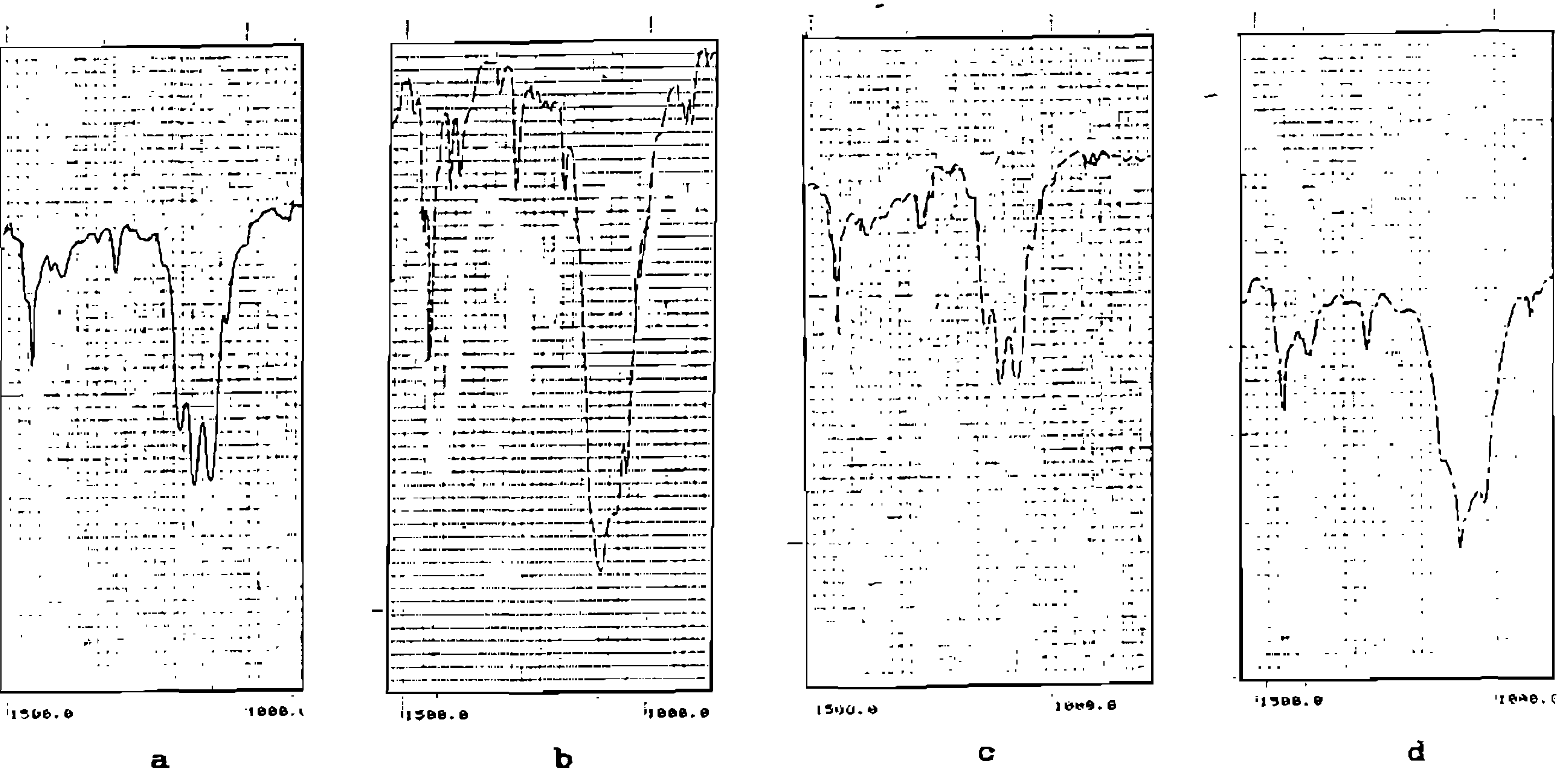


Fig. 5.1 Infrared spectra (900 - 1500 cm^{-1}) of $[Cu(L2)](ClO_4)_2$ (a), $[Cu(L4)](ClO_4)_2$ (b), $[Cu(L5)](ClO_4)_2$ (c) and $[Cu(L1)](BF_4)_2$ (d)

Table 5.2 Electronic spectral data of $[CuL]^{2+}$ complexes in methanol[a]; $\bar{\nu}_{max}$ in kK and ϵ (M^{-1} cm^{-1}) in parentheses

Complex	Medium	Ligand Field	Charge Transfer
$[Cu(L1)](ClO_4)_2$	Solid	15.0	26.3
	MeOH	14.8 (175)[b]	28.4 (4230)
$[Cu(L1)](BF_4)_2$	Solid	14.4 16.0	24.9
	MeOH	14.9 (177)[b]	28.5 (3690)
$[Cu(L1)](NO_3)_2$	Solid	15.5	26.5
	MeOH	11.4 (177) 15.2 (234)	30.7 (2420)
$[Cu(L1)]Cl_2$	Solid	12.0 14.6	26.5
	MeOH	11.4 (231) 15.2 (301)	30.8 (2040)
$[Cu(L2)](ClO_4)_2$	Solid	14.1	24.9
	MeOH	11.4 (200) 15.3 (190)	30.7 (2850)
$[Cu(L2)]Cl_2$	Solid	14.8	24.8
	MeOH	12.1 (483) 15.2 (380)	30.4 (3910)
$[Cu(L3)](ClO_4)_2$[c]	MeOH	12.3 (143) 15.3 (286)	26.8 (1360)

......continued

$[Cu(L4)](ClO_4)_2$	Solid	12.0 16.3	24.5
	MeOH	11.2 (256) 16.6 (271)	28.9 (3330)
$[Cu(L4)](BF_4)_2$	Solid	16.5	24.2
	MeOH	12.1 (269) 16.7 (244)	28.9 (2520)
$[Cu(L4)](NO_3)_2$	Solid	11.9 15.9	24.2
	MeOH	11.2 (267) 16.6 (247)	29.1 (3340)
$[Cu(L4)]Cl_2$	Solid	11.9 16.3	23.9
	MeOH	11.1 (289) 16.6 (279)	29.2 (2820)
$[Cu(L5)](ClO_4)_2$	Solid	14.1	24.6
	MeOH	11.5 (270) 15.4 (258)	30.7 (2560)

[a] concentration : ≈ 0.002 M

[b] unsymmetrical band

[c] 1:1 solution of $Cu(ClO_4)_2$ and the ligand in methanol

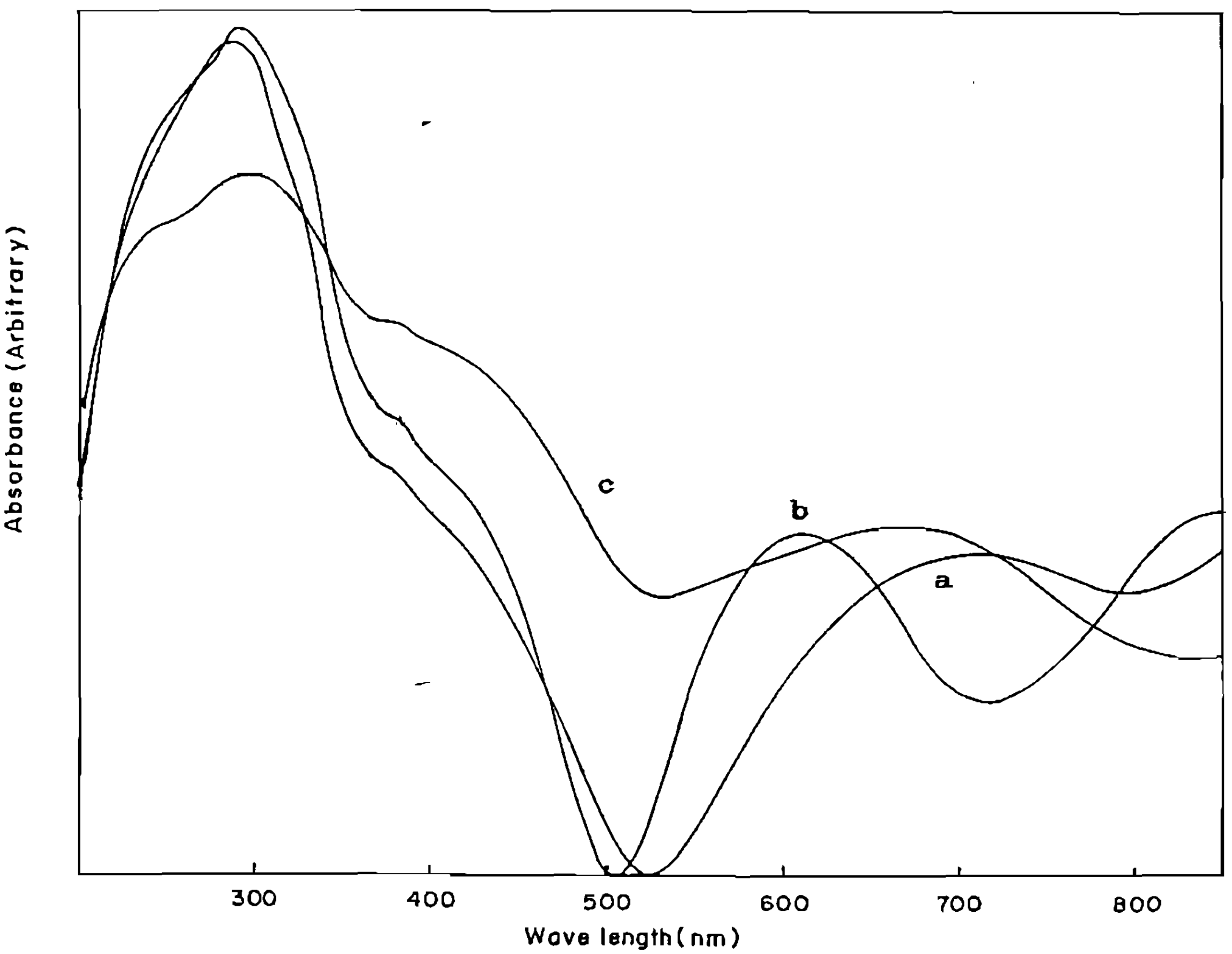
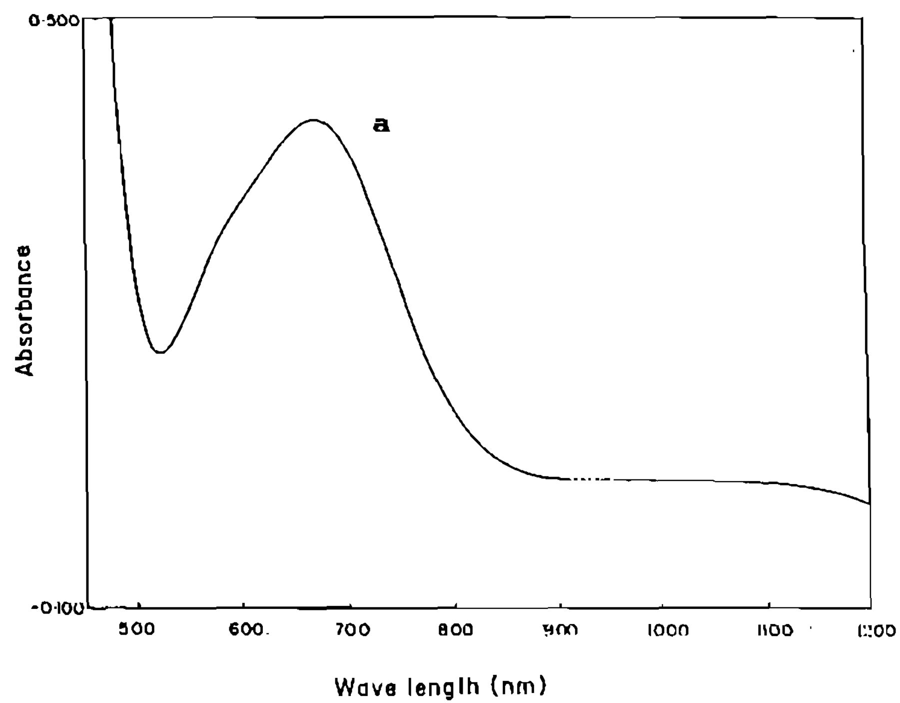


Fig. 5.2 Solid state reflectance spectra of $[Cu(L2)](ClO_4)_2$ (a), $[Cu(L4)](ClO_4)_2$ (b) and $[Cu(L1)](ClO_4)_2$ (c)



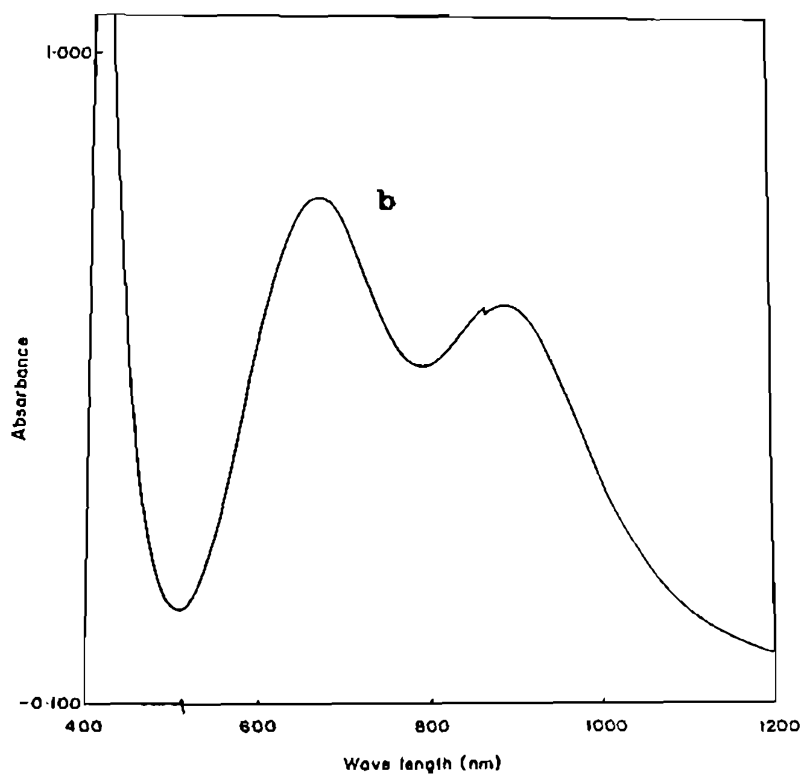


Fig. 5.3 Ligand field spectra of $[Cu(L1)](ClO_4)_2$ (a) and $[Cu(L1)](NO_3)_2$ (b)

the solid state.

The $\bar{\nu}_{max}$ values of all the complexes (Fig. 5.4) are in the same range as for the bis(benzimidazolyl)-dithia and -trithia complexes[9,20] of copper(II), suggesting the presence of an equatorial CuN_2S_2 chromophore.[20,21] The ligand field bands for $[Cu(L1)]^{2+}$ and $[Cu(L4)]^{2+}$ perchlorates are higher in energy than those for other perchlorates, suggesting that the all-five-membered chelate rings as in the former and the alternate six and five membered chelate rings in the latter provide the strongest ligand field environment for Cu(II).

The intense band observed in the region 26.8 - 30.7 kK for all the complexes is assigned to a S(σ) ---> Cu(II) charge transfer (CT) transition.[20,22-25] Among the bis(benzimidazolyl) thioether complexes with all-five-membered chelate rings the ϵ_{max} values[9] of this band steadily increases with increase in the number of sulfur donor atoms up to four but for five it decreases (Fig. 5.5). It appears that this variation originates from structural changes imposed by the disposition or non-coordination of the thioether donors.

The modest enhancement of intensities for the visible band may be attributed to intensity borrowing[26] from the S(σ) ---> Cu(II) CT band. Among the bis(benzimidazolyl) thioether copper(II) complexes with all-five-membered chelate ring systems the relative

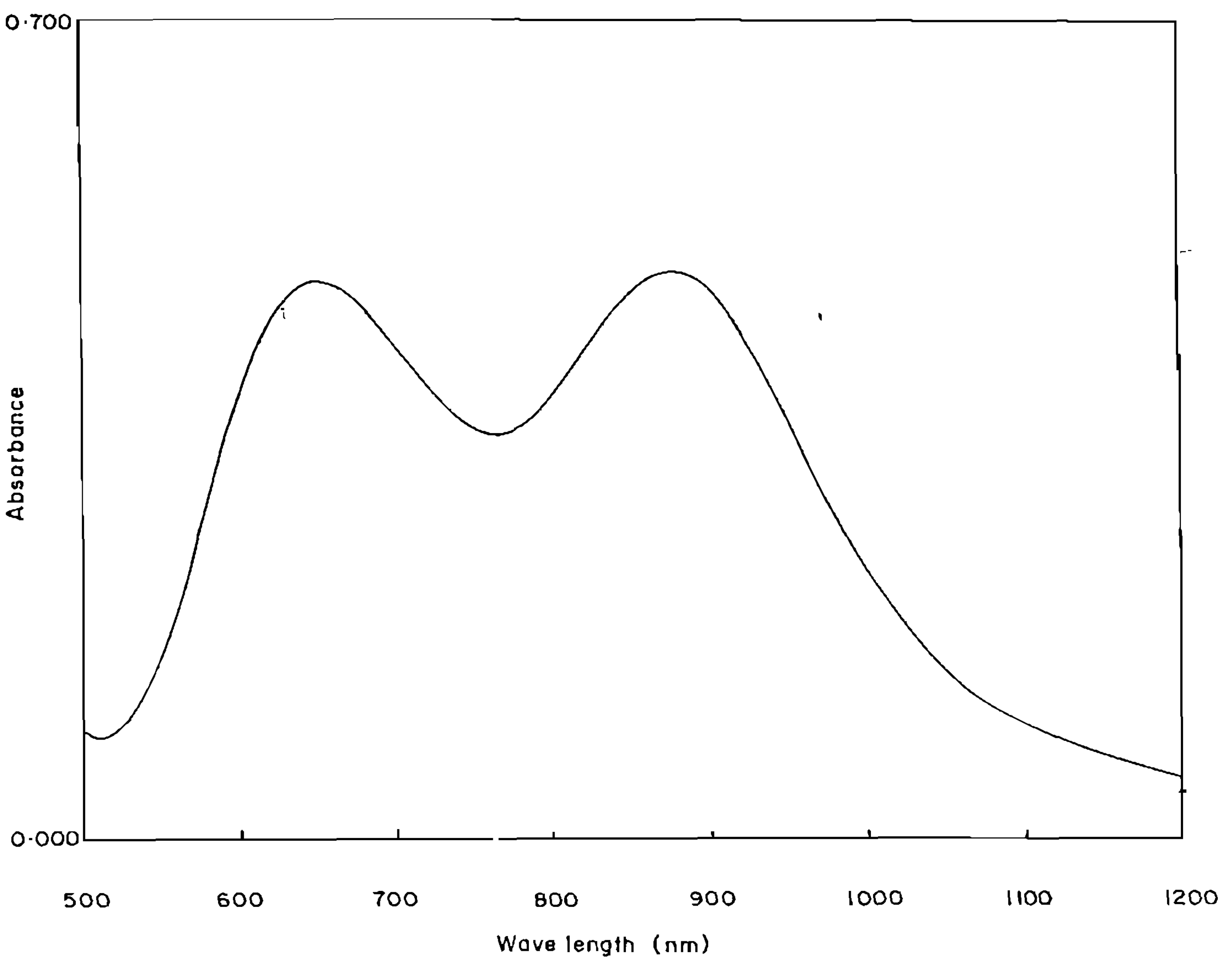


Fig. 5.4 Ligand field spectrum of $[Cu(L5)](ClO_4)_2$

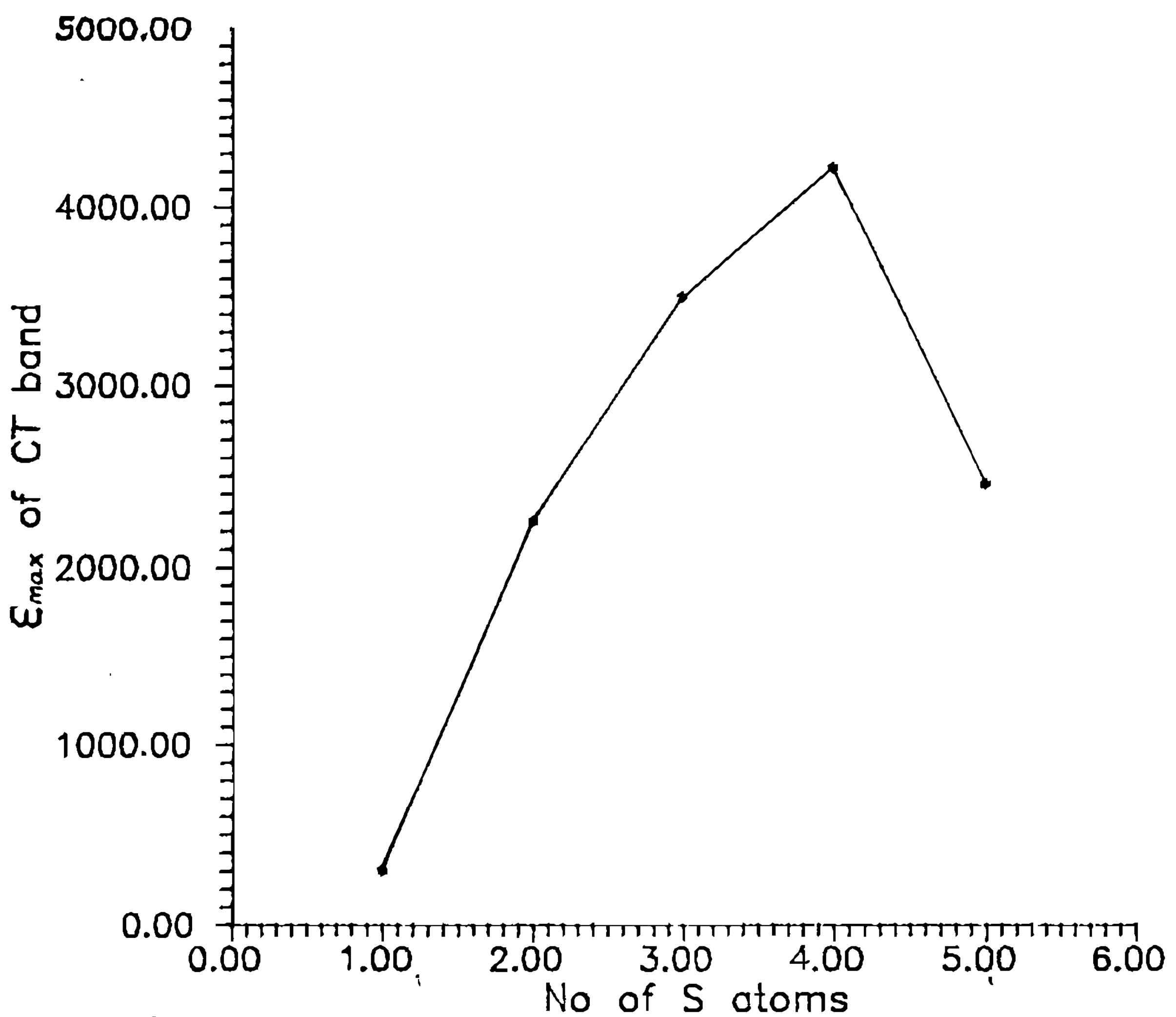


Fig. 5.5 Plot of ϵ_{max} values of the S(σ)--->Cu(II) CT band *vs* the number of sulfur donor atoms in bis(benzimidazol-2-yl) complexes with all five-membered chelate ring systems

intensities of the visible band, calculated using Jorgensen's equation[27] parallel the observed variation in ϵ_{max} of the CT band (Fig. 5.5) and this variation is in agreement with that observed for CuN_2S and CuN_2S_2 complexes[9] (Fig. 5.6). The lower value observed for CuN_2S_3 illustrates that the overlap of an axial thioether with the copper $d_{x^2-y^2}$ orbital is poor and confirms that its higher CT intensity is only structural in origin. Further, the ϵ_{max} value of $[Cu(L1)](ClO_4)_2$ is much lower compared to those of the three other tetrathioether complexes, even though it has the highest ϵ_{max} value for the CT band. This may correspond to a structure (discussed below) and hence a W term[27] less favourable for intensity borrowing. Within the CuN_2S_4 perchlorates the significant variation in intensity of the ligand field bands implies distortion and/or axial interaction affected by the chelate ring size.

5.3.4 EPR Spectra

The polycrystalline spectra of $[Cu(L1)](ClO_4)_2$ and $[Cu(L1)](BF_4)_2$ are axial while those of the other complexes are rhombic (Fig. 5.7). For the latter systems $g_{min} > 2.03$ (Table 5.3) and the R values $[= (g_2-g_1)/(g_3-g_2)]$ are < 1 indicating a predominantly $d_{x^2-y^2}$ ground state.[19,28] This is in contrast to copper(II) complexes of bis(benzimidazolyl) thioether ligands with CuN_2S_2 chromophores with d_{z^2} ground state in trigonal bipyramidal geometry.[29,30] However, the frozen-solution spectra of all the complexes are axial (Fig. 5.8) ($g_{\parallel} > g_{\perp} > 2.0$), illustrating

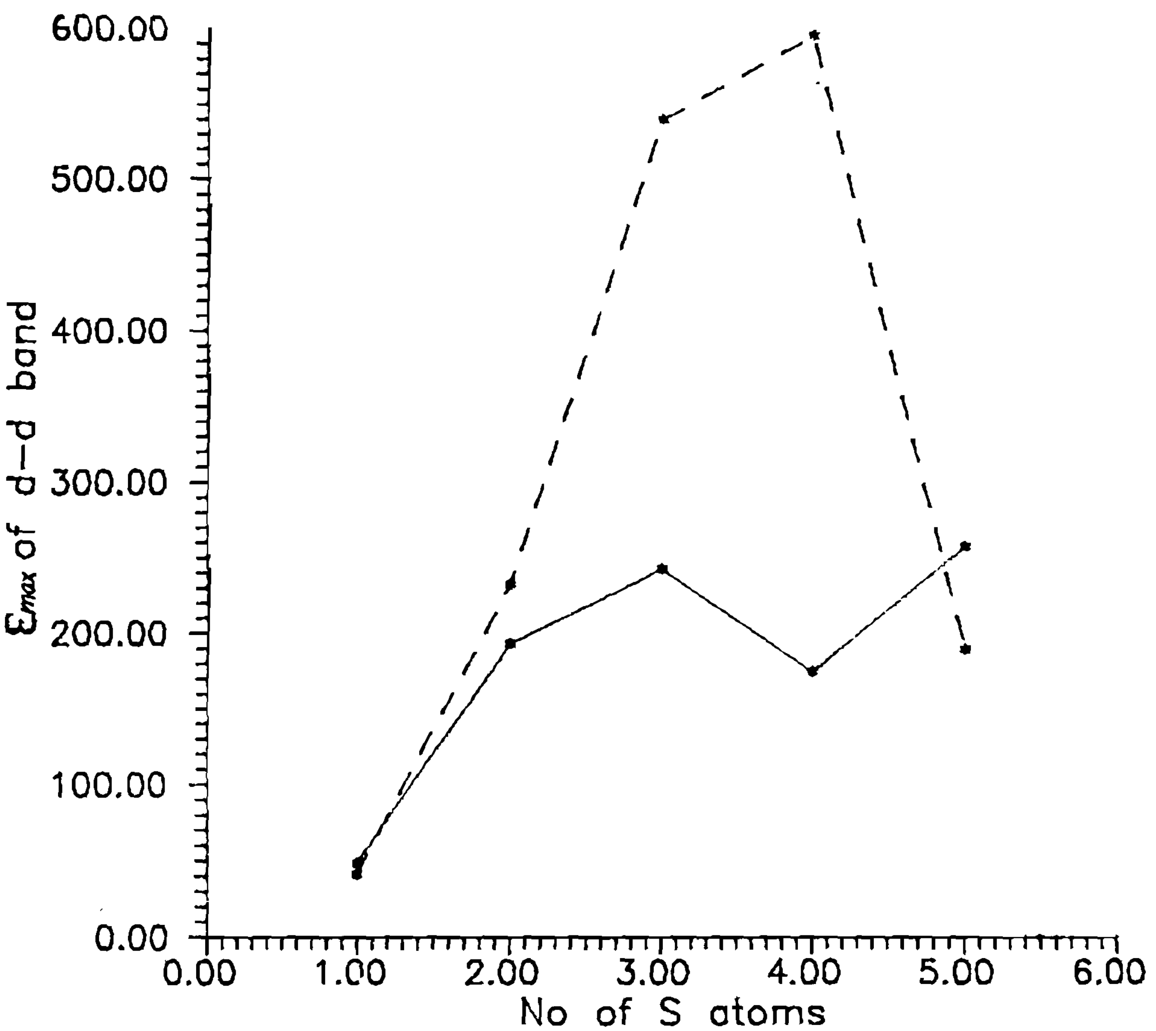


Fig. 5.6 Calculated (——) and observed (----) ϵ_{max} values of the ligand field bands *vs* the number of sulfur donor atoms in bis(benzimidazol-2-yl) complexes with all five-membered chelate ring systems

Table 5.3 EPR spectral data of $[CuL]^{2+}$ complexes

Compound	Medium	g_0	A_0[a]	$g_{\|\|}$	$A_{\|\|}$[a]	$g_\perp$
$[Cu(L1)](ClO_4)_2$[b]	Powder	–	–	2.150	–	2.045
	MeOH/ Me_2CO	2.099	66	2.184	167	2.057
$[Cu(L1)](BF_4)_2$	Powder	–	–	2.155	–	2.043
	MeOH/ Me_2CO	2.095	68	2.186	167	2.050
$[Cu(L1)](NO_3)_2$	Powder	2.164 2.099 2.032	–	–	–	–
	MeOH/ Me_2CO	2.096	49	2.208	124	2.040
$[Cu(L1)]Cl_2$	Powder	2.156 2.075 2.031	–	–	–	–
	MeOH/ Me_2CO	2.118	59	2.198	135	2.078
$[Cu(L2)](ClO_4)_2$	Powder	2.209 2.131 2.014	–	–	–	–
	MeOH/ Me_2CO	2.150	50	2.242	134	2.104
$[Cu(L2)]Cl_2$	Powder	2.028 2.065 2.155	–	–	–	–
	MeOH/ Me_2CO	2.120	61	2.197	131	2.082
$[Cu(L3)](ClO_4)_2$[c]	MeOH/ Me_2CO	2.079	68	2.412	122	1.913

$[Cu(L4)]ClO_4)_2$	Powder	2.202 2.116 2.004	–	–	–	–
	MeOH/ Me_2CO	2.112	64	2.198	138	2.069
$[Cu(L4)](BF_4)_2$	Powder	2.204 2.115 2.006	–	–	–	–
	MeOH/ Me_2CO	2.112	30	2.213	128	2.062
$[Cu(L4)](NO_3)_2$	Powder	2.198 2.120 2.023	–	–	–	–
	MeOH/ Me_2CO	2.113	30	2.288	140	2.026
$[Cu(L4)]Cl_2$	Powder	2.110	–	–	–	–
	MeOH/ Me_2CO	2.112	59	2.195	135	2.071
$[Cu(L5)](ClO_4)_2$	Powder	2.198 2.120 2.011	–	–	–	–
	MeOH/ Me_2CO	2.110	28	2.242	143	2.044
$[Cu(L5)]Cl_2$	Powder	2.094	–	–	–	–
	MeOH/ Me_2CO	2.110	61	2.276	169	2.027

[a] A x 10^4 cm^{-1}

[b] Simulated values: $g_{||}$, 2.250; $A_{||}$, 154; $A_{\perp([illegible])}$, 15; $g_{\perp}$, 2.085

[c] complex prepared in situ

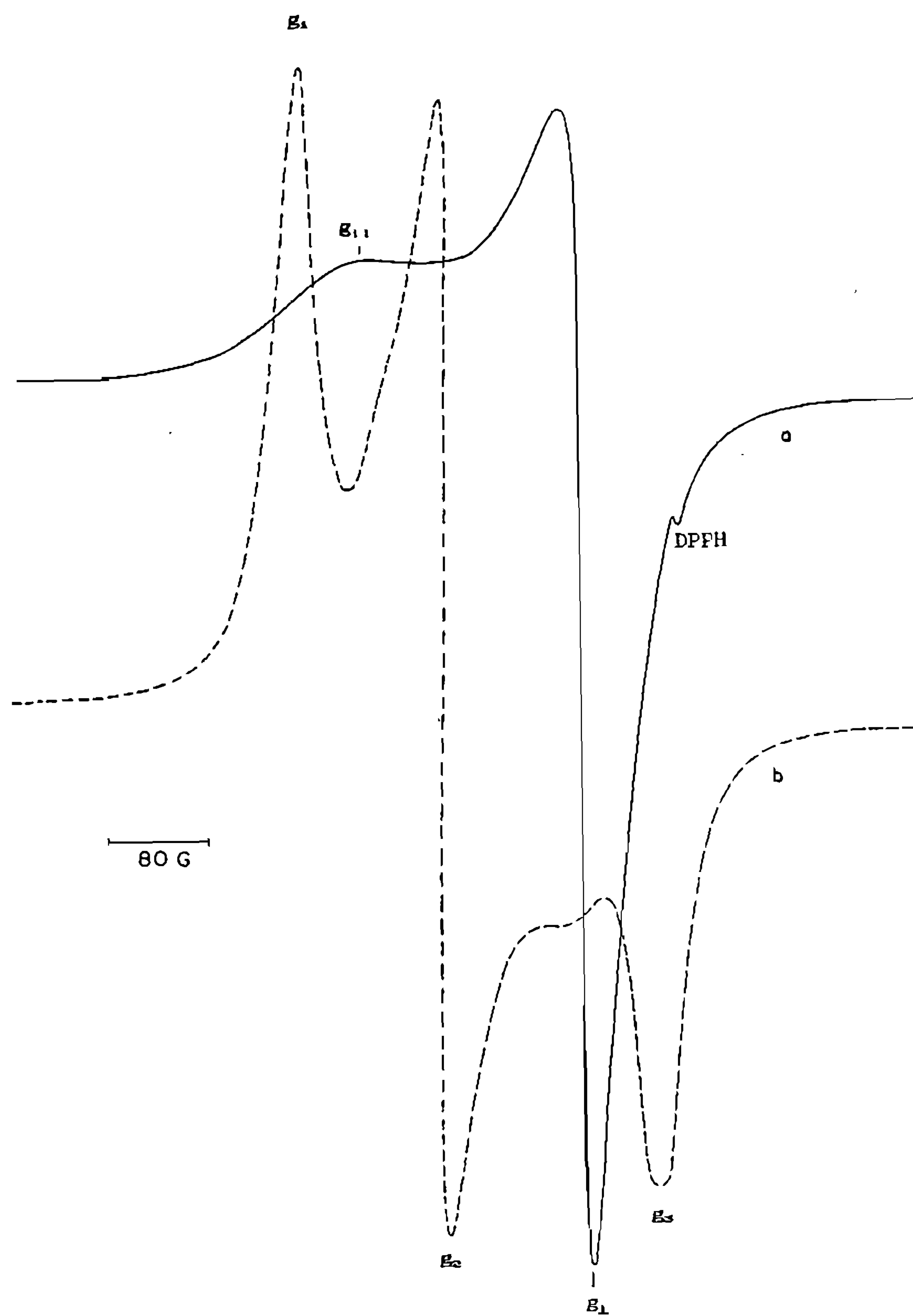


Fig. 5.7 Polycrystalline EPR spectra of $[Cu(L1)](ClO_4)_2$ (——) and $[Cu(L4)](ClO_4)_2$ (----)

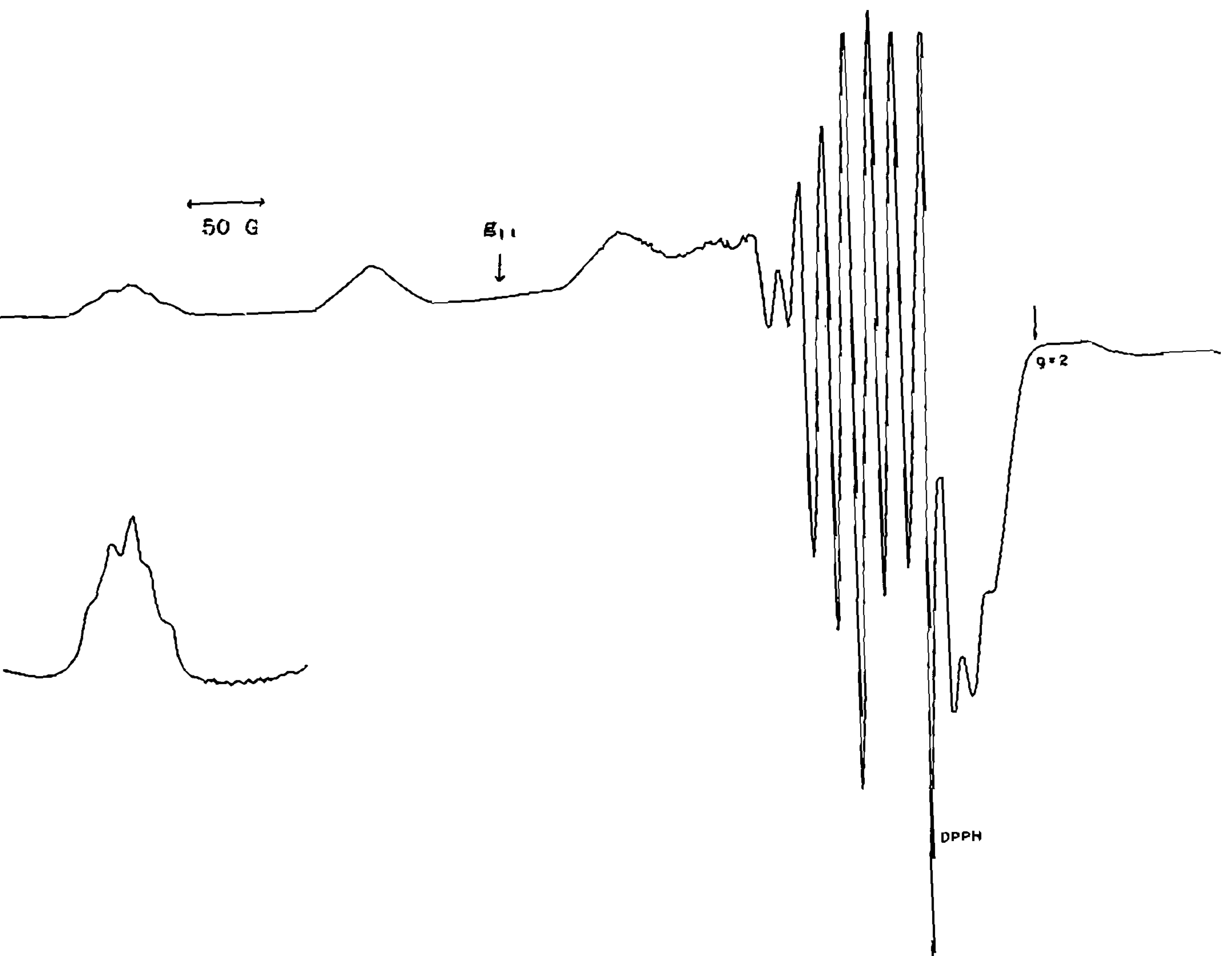


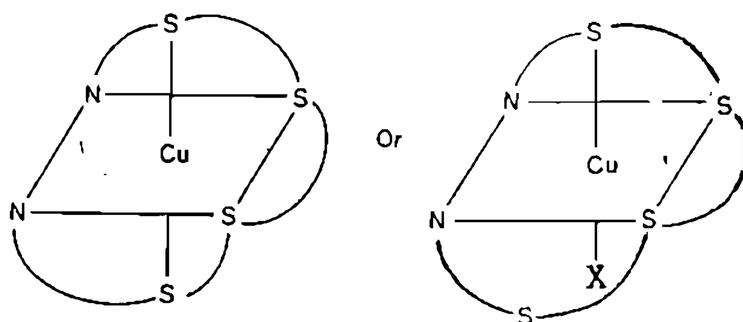
Fig. 5.8 EPR spectrum of $[Cu(L1)](ClO_4)_2$ in methanol at 77 K; inset is expanded spectra in the $g_{\parallel}$ region

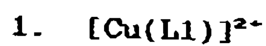
changes in structure on dissolution. The $g_{\parallel}$ (2.29 - 2.20), $g_{\perp}$ (2.09 - 2.04) and $A_{\parallel}$ [(140 - 130) x 10^{-4} cm^{-1}] values of these complexes, except $[Cu(L3)]^{2+}$ are consistent with those reported for bis(benzimidazolyl)[5-9] and other thioether[24,31] complexes with CuN_2S_2 and CuN_2S_3 chromophores and lie in between the N_4 and S_4 delineators in the $g_{\parallel}:A_{\parallel}$ map,[32] supporting an equatorial N_2S_2 donor set as suggested by the electronic spectral data. The high $g_{\parallel}$ value observed for $[Cu(L3)]^{2+}$ illustrates that one or more thioether donors remain uncoordinated[33] at 77 K. The $g_{\parallel}$ value is expected[32] to decrease and the $A_{\parallel}$ value to increase on increasing the number of coordinated sulfur atoms, but interestingly the reverse trend is observed on increasing the number of sulfurs from three to four to five, among all-five-membered chelate rings. This trend is similar to that in the ϵ_{max} values of S(σ) ---> Cu(II) CT band, illustrating the influence of the axial interaction by sulfur. The values of the $g_{\parallel}/A_{\parallel}$ quotient (130 - 170 cm) of all the copper(II) complexes, except $[Cu(L1)]^{2+}$, are higher than the range (105 - 135 cm) expected for square planar complexes.[32] This represents a highly distorted octahedral geometry caused by axial interaction, which is well known to raise[34] $g_{\parallel}$ and lower $A_{\parallel}$ values.

The nitrogen superhyperfine structure ($A_{\perp(N)}$ ≈ 16 G) in the perpendicular region is better resolved in $[Cu(L1)](ClO_4)_2$ (Fig. 5.8) than for the $[Cu(L2)]^{2+}$ and $[Cu(L5)]^{2+}$ perchlorate complexes. The nine lines for the former may originate from the presence of

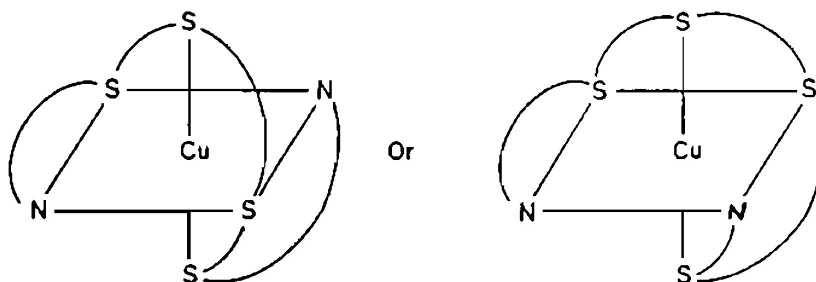
two non-equivalent nitrogens or two equivalent nitrogens in the equatorial plane with the hyperfine structure complicated by the perpendicular features of copper.[35] We favour the latter explanation because in the parallel region only five lines corresponding to two equivalent nitrogens are observed (Fig. 5.8 inset). Further, the spectrum simulated assuming two equivalent nitrogens is identical with the observed one.

The above spectral discussion leads us to propose tentative structures (Fig. 5.9) for the present complexes. All of them contain the inferred CuN_2S_2 equatorial plane. The strong $Cu-N_{bzim}$ bonds[36] would prefer to lie in the equatorial plane and the thioether donors would then be forced to occupy the other equatorial and axial sites or remain unbonded. One of the five thioether donors in $[Cu(L5)]^{2+}$ will not be permitted to form a bond to copper. Further, the observed $g_{||}$ values are nearer to 2.28 rather than 2.31, which is characteristic of a *trans* rather than *cis* disposition of sulfur atoms in the CuN_2S_2 plane;[37] this is also supported by the symmetrical nature of the band at 30.0 kK. Extensive studies[38] on cobalt(III) complexes of open chain thioether ligands have established that a thioether donor linking two five-membered aliphatic chelate rings adopt a non-planar arrangement about the metal. In fact, a folded geometry has been observed for $[Cu(L6).2H_2O]$ (H_2L6 = 2,5,8-trithianonane-1,9-dicarboxylic acid)[39] and $[Cu(L_27)]^{2+}$ [L7 = bis(imidazol-2-ylmethyl)-




1. $[Cu(L1)]^{2+}$

X = anion




2. $[Cu(L2)]^{2+}$, $[Cu(L3)]^{2+}$, $[Cu(L4)]^{2+}$, $[Cu(L5)]^{2+}$

Fig. 5.9 Proposed geometries of the Cu(II) complexes of bis(benzimidazol-2-yl)tetra- and pentathioether ligands

sulfide].[40] So $[Cu(L1)]^{2+}$ with all-five-membered chelate rings would be expected to display a 'folded' geometry which is entirely different from those proposed for other complexes with one or more six-membered chelate rings. During the course of this work the crystal structures of nickel(II) complexes of pyridine analogues of N_2S_3 and N_2S_4 (L1) ligands have been published. All contain the proposed 'folded' geometry with a *cis* disposition of the thioether donors in the equatorial plane. Increasing the number of thioether donors increases the positive character of $E_{1/2}$ of the Ni(II)/Ni(I) couple.[41] The present unique and compact geometry for $[Cu(L1)]^{2+}$ reflects its distinct spectral features:

(i) the position and intensity of the ligand field band which are the highest and lowest respectively, compared to all other complexes

(ii) the $g_{||}/A_{||}$ quotient value of 130 cm and

(iii) the well resolved nitrogen superhyperfine structure.

It is unfortunate that the present complexes do not yield single crystals suitable for X-ray diffraction, since such data would have helped considerably in clarifying much of the interpretation.

5.3.5 Redox properties

All the perchlorate complexes exhibit a well defined cathodic wave (0.250 - -0.050 V) and a corresponding anodic wave (0.180 - 0.560 V) (Fig. 5.10). The diffusion coefficients

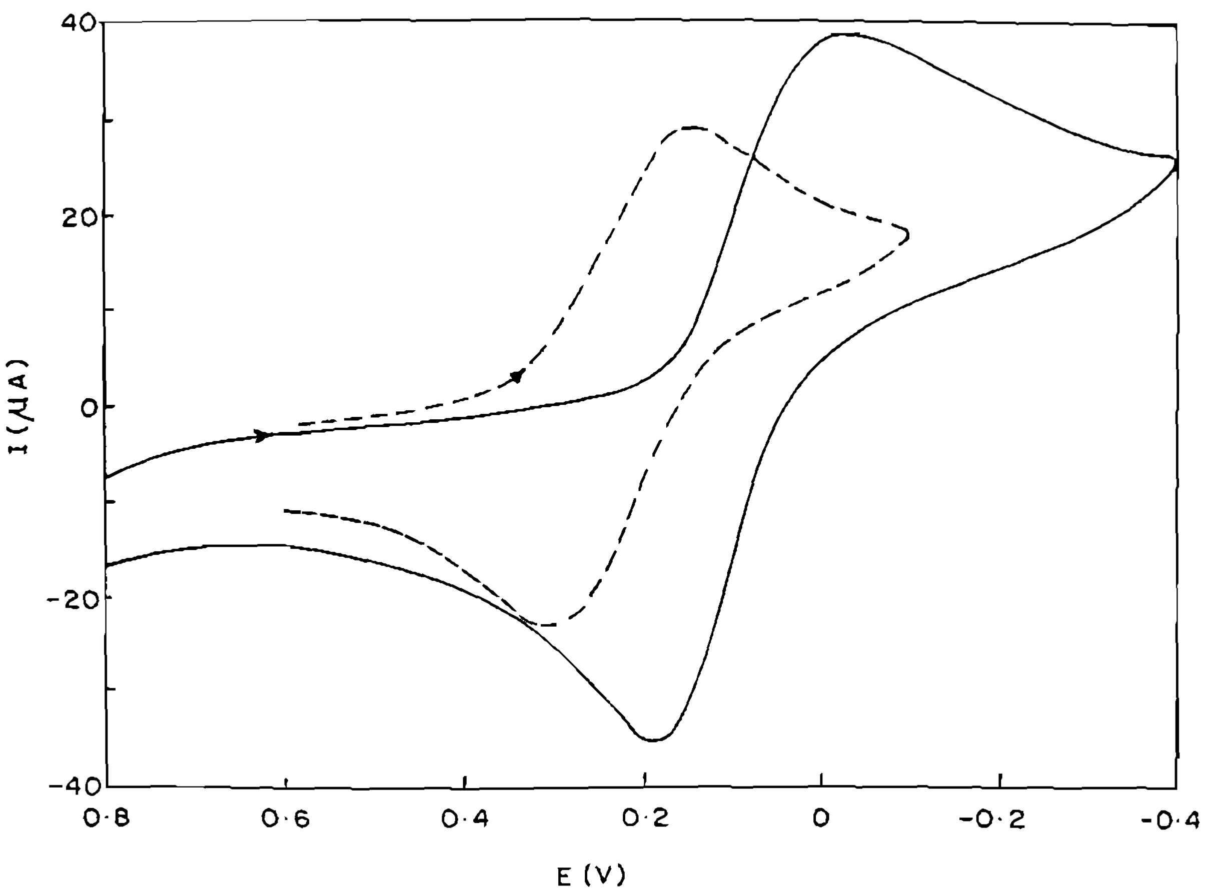


Fig. 5.10 Cyclic voltammograms of $[Cu(L1)](ClO_4)_2$ (----) and $[Cu(L5)](ClO_4)_2$ (——) recorded in methanol (0.1 M THAP) at a scan rate of 50 mV/s

(Table 5.4) calculated from the slope of plots of i_{pc} *vs* $\nu^{1/2}$ using the Randles Sevciks' equation[42] are typical of the Cu(II)/Cu(I) couple.[32] For all the present complexes the peak current ratio (i_{pa}/i_{pc}) is nearer to unity, implying quasi-reversible electron transfer; but the $\Delta E_p°$ values are greater than the Nernstian value ($\Delta E_p \approx 60$ mV) for a one electron redox system. This clearly indicates considerable reorganisation of the coordination spheres during electron transfer, regardless of the precise mechanism. The $[Cu(L1)]^{2+}$ and $[Cu(L4)]^{2+}$ perchlorates exhibit much lower $\Delta E_p°$ values than those of the other complexes, illustrating that the 'folded' geometry in $[Cu(L1)]^{2+}$ and six-membered chelate rings in $[Cu(L4)]^{2+}$ provide low reorganisational energy barriers during electron transfer.

Significant variation in Cu(II)/Cu(I) redox potentials (Table 5.4) is observed among the CuN_2S_4 perchlorates: $[Cu(L2)]^{2+}$ (55655) < $[Cu(L1)]^{2+}$ (55555) < $[Cu(L4)]^{2+}$ (65656) < $[Cu(L3)]^{2+}$ (65556). Six-membered rings present near the bzim moiety (in the CuN_2S_2 equator) elevate $E_{1/2}$ (240 - 176 mV), whereas that present at the middle of the ligands depresses $E_{1/2}$: $[Cu(L2)]^{2+}$ < $[Cu(L1)]^{2+}$ (168 mV) and $[Cu(L4)]^{2+}$ < $[Cu(L3)]^{2+}$ (103 mV). A similar increase in redox potential ($\approx$ 120 mV) representing progressive destabilisation of Cu(II), with increase in length of the bridging carbon chain, has been observed for copper(II) complexes of cyclic tetrathia[43] and open chain N_2S_2 ligands.[44] Further, six-membered

Table 5.4 Electrochemical data[a] for the $[CuL](ClO_4)_2$ complexes at 25 °C

Complex	Temp (°C)	E_{pc} (V)	E_{pa} (V)	ΔE_p (mV)	E_p^{o} [b] (mV)	$E_{1/2}$ (V) CV	$E_{1/2}$ (V) DPV[c]	(i_{pa}/ i_{pc})	Dx10[6] cm²/s	Dnx10[8] gcm/s²
$[Cu(L1)]^{2+}$	25	0.146	0.308	162	120	0.227	0.215	1.0	1.2	0.8
	35	0.144	0.294	150		0.219	0.223	1.0		
	45	0.136	0.306	170		0.221	0.219	0.8		
$[Cu(L2)]^{2+}$	25	-0.110	0.228	338	268	0.059	0.081	1.1	2.7	1.9
	35	-0.042	0.218	260		0.088	0.095	1.1		
	45	0.010	0.198	188		0.104	0.105	1.0		
$[Cu(L3)]^{2+}$	25	0.236	0.570	334	210	0.403	0.435	1.1	1.0	0.7
	35	0.274	0.560	286		0.417	0.443	1.1		
	45	0.308	0.552	244		0.430	0.453	1.1		
$[Cu(L4)]^{2+}$	25	0.230	0.370	140	88	0.300	0.309	1.3	2.4	1.5
	35	0.226	0.386	160		0.306	0.311	1.3		
	45	0.234	0.388	154		0.311	0.325	1.2		
$[Cu(L5)]^{2+}$	25	-0.032	0.186	218	179	0.077	0.087	1.2	2.5	1.6
	35	-0.038	0.200	238		0.081	0.099	1.1		
	45	-0.016	0.214	230		0.099	0.109	0.8		

[a] Measured *vs* non-aqueous silver reference electrode; add 544 mV to convert into NHE; Scan rate 50 mV/s; Supporting electrolyte tetra-*N*-hexylammonium perchlorate (0.1 M); Concentration 0.001 M in complex. [b] ΔE_p^{o} is ΔE_p at zero scan rate. [c] Differential Pulse Voltammetry (DPV), scan rate 1 mV/s, pulse height 50 mV.

rings elevate or five-membered rings depress $E_{1/2}$, if π interaction[13] as in the present thioether chelates is important. This indicates that the redox potentials are affected both by the number and disposition of sulfur donor atoms present. The redox potential of $[Cu(L1)](ClO_4)_2$ decreases (25 mV) on the addition of an excess of Cl^- ions as tetraethylammonium chloride, illustrating that Cl^- ion may coordinate in solution by replacing possibly an axial thioether.

A plot (Fig. 5.11) of the redox potentials of compounds containing only five-membered chelate ring systems *vs* the number of thioether donors reveals that the potential increases up to three, remains the same for four and then decreases for five thioether donors. The observed regular increase is consistent with the empirical suggestion that each thioether donor elevates the potential by +141 mV. However, the values calculated for the present complexes using Addison's $\triangle E_L$ parameters[45] (Fig. 5.11) are lower than the adjusted values ($E_{adj} = E_{1/2} - E^{\circ}$; $E^{\circ} = 215$ mV in methanol[45]). This implies that the contribution by bulky bzim to $E_{1/2}$ is much higher[13] than that by pyridine or imidazole ($\triangle E_{het}$ +52 mV [45]) and in fact a better agreement with the observed values is seen when a $\triangle E_{bzim}$ value of +165 mV is used for the calculation. The values of $E_{1/2}$ calculated for $[Cu(L5)]^{2+}$ are higher than that observed, illustrating that one of the five thioethers is not coordinated. So it is obvious that the additivity in $E_{1/2}$ is

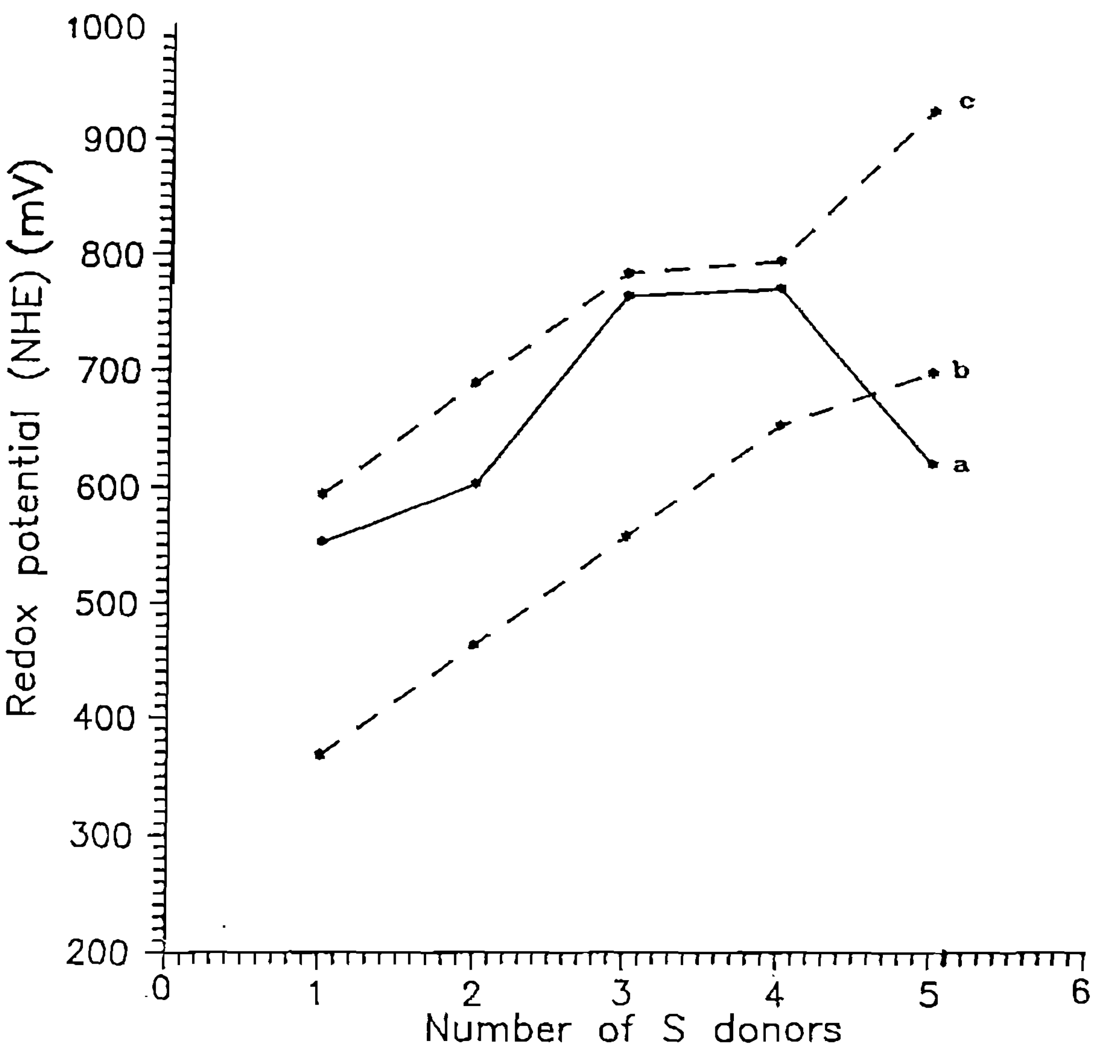


Fig. 5.11 Plot of $E_{1/2}$ values *vs* the number of sulfur donor atoms in bis(benzimidazol-2-yl) complexes with all five-membered chelate ring systems. (a) observed $E_{1/2}$ values (b) empirically calculated $E_{1/2}$ values using Addison's and (c) modified ΔE_L values

applicable only to planar four coordinated copper(II) complexes which on reduction form necessarily four coordinated, probably tetrahedral copper(I) species.

5.4 Conclusions

The novel and distinct spectral and electrochemical behaviour of the CuN_2S_4 perchlorates with all-five-membered chelate rings is suggestive of a unique 'folded' geometry. The Cu(II)/Cu(I) redox potentials increase with decrease in energy of the S(σ) ---> Cu(II) transitions.[26] An increase in the length of the bridging carbon chain among N_2S_4 complexes induces increased tetrahedral distortion and/or axial interaction and makes it easier to access[46] Cu(I). So $E_{1/2}$ is expected to increase with increase[34,47] in $g_{||}$. However, a reverse trend is observed in the $g_{||}$ *vs* $E_{1/2}$ plot for all the present complexes and for complexes of bis(benzimidazolyl) polythioether ligands with all five-membered chelate rings (Fig. 5.12). This leads us to conclude that the spectral properties and the high Cu(II)/Cu(I) redox potentials of all the present complexes are determined not only by distortion and/or axial interaction caused by both the chelate ring structure and number of sulfur donors, but also by the axial/equatorial disposition of the sulfur donors. This is in contrast to planar copper(II) complexes of macrocyclic polythiaether ligands, for which the effect of chelate ring size is more important[48,49] than the number of sulfur donor atoms in governing the redox potentials.

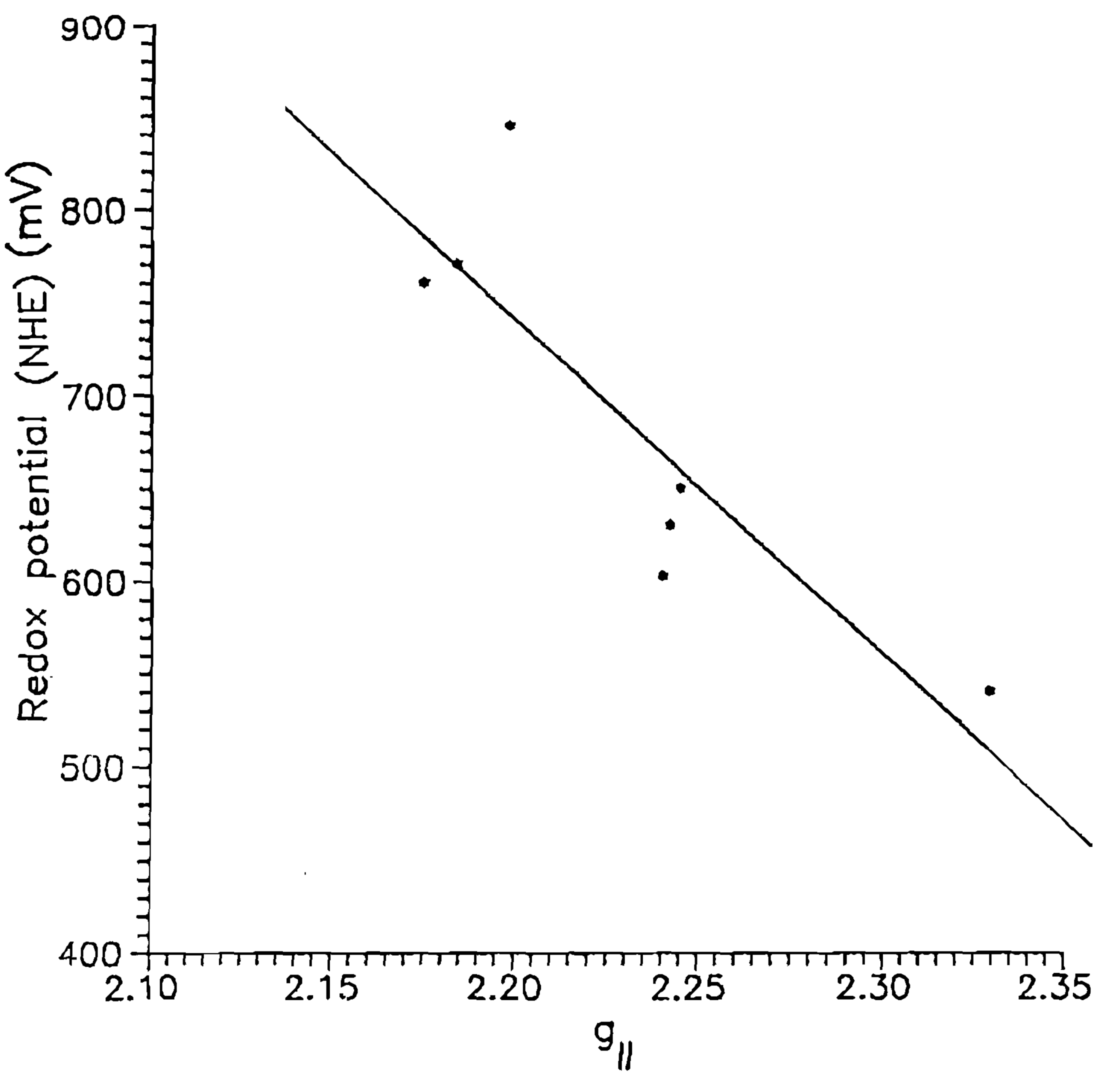


Fig. 5.12 Plot of $E_{1/2}$ (NHE) *vs* $g_{\parallel}$ of Cu(II) complexes of bis(benzimidazol-2-yl) thioether ligands

References

(1) a) Colman, P. M.; Freeman, H. C.; Guss, J. M.; Murata, M.; Norris, V. A.; Ramshaw J. A. M.; Venkatappa, M. P. *Nature (London)* **1978**, *272*, 319; b) Guss J. M.; Freeman H. C. *J. Mol. Biol.* **1983**, *169*, 521.

(2) a) Adman, E. T.; Stenkamp, R. E.; Sieker L. C.; Jensen, L. H. *J. Mol. Biol.* **1978**, *123*, 35; b) Baker, E. N. *ibid.* **1988**, *203*, 1071.

(3) Penfield, K. W.; Gay, R. R.; Himmelwright, R. S.; Eickman, N. C.; Norris, V. A.; Freeman, H. C.; Solomon, E. I. *J. Am. Chem. Soc.* **1981**, *103*, 4382.

(4) a) Birker, P. J. M. W. L.; Godefroi, E. F.; Helder, J.; Reedijk, J. *J. Am. Chem. Soc.* 1982, *104*, 7556; b) Augustin, M. A.; Yandell, J. K.; Addison, A. W.; Karlin, K. D. *Inorg. Chim. Acta* **1981**, *55*, L35.

(5) Birker, P. J. M. W. L.; Helder, J.; Hankel, G.; Krabs, B.; Reedijk, J. *Inorg. Chem.* **1982**, *21*, 357.

(6) Schilstra, M. J.; Birker, P. J. M. W. L.; Verschoor, G. C.; Reedijk, J. *Inorg. Chem.* **1982**, *21*, 2637.

(7) Rietmeijer, F. J.; Birker, P. J. M. W. L.; Gorter, S.; Reedijk, J. *J. Chem. Soc., Dalton Trans.* **1982**, 1191.

(8) Addison, A. W.; Nageswara Rao, T.; Reedijk, J.; van Rijn, J.; Verschoor, G. C. *J. Chem. Soc., Dalton Trans.* **1984, 1349.**

(9) a) Addison, A. W.; Palaniandavar, M. *Abstracts, American Chemical Society 188th National Meeting*, Washington DC, **1984**, INOR-068; b) Addison, A. W.; Palaniandavar, M.; Reedijk, J.; van Rijn, J.; Rao, T. N. to be communicated.

(10) Westerby, B. C.; Juntunen, K. L.; Leggett, G. H.; Pett, V. B.; Koenigbauer, M. J.; Purgett, M. D.; Taschner, M. J.; Ochrymowycz, L. A.; Rorabacher, D. B. *Inorg. Chem.* **1991**, *30*, 2109.

(11) a) van Rijn, J.; Driessen, W. L.; Reedijk, J.; Lehn, J. -M. *Inorg. Chem.* **1984**, *23*, 3584; b) Bouwman, E.; Burik, A.; Hove, J. C. T.; Driessen, W. L.; Reedijk, J. *Inorg. Chim. Acta* **1988**, *150*, 125.

(12) a) Tullemans, A. H. J.; Bouwman, E.; de Graaff, R. A. G.; Driessen, W. L.; Reedijk, J. *Recl. Trav. Chem. Pays-Bas.* **1990**, *109*, 70; b) Bouwman, E.; Driessen, W. L.; Reedijk, J. *Coord. Chem. Rev.* **1990**, *104*, 143; c) Lockhart, J. C.; Clegg, W.; Hill, M. N. S.; Rushton, D. J. *J. Chem. Soc., Dalton Trans.* **1990**, 3541.

(13) Pandiyan, T.; Palaniandavar, M.; Lakshminarayanan, M.; Manohar, H. *J. Chem. Soc., Dalton Trans.* **1992**, 3377.

(14) Addison, A. W.; Burke, P. J. *J. Heterocycl. Chem.* **1981**, *18*, 803; Hendriks, H. M. J.; Birker, P. J. M. L.; van Rijn, J.; Verschoor, G. C.; Reedijk, J. *J. Am. Chem. Soc.* **1982**, *104*, 3607.

(15) Sivagnanam, U.; Pandiyan, T.; Palaniandavar, M. *Indian J. Chem.* **1993**, *32B*, 572.

(16) Foley, J.; Kennefick, D.; Phelan, D.; Tyagi S.; Hathaway, B. J. *J. Chem. Soc., Dalton Trans.* **1983**, 2333.

(17) Bailey, N. A.; Bastida, R.; Fenton, D. E.; Lockwood, S. J.; McLean, C. H. *J. Chem. Soc., Dalton Trans.* **1988**, 839.

(18) Procter, I. M.; Hathaway, B. J.; Billing, D. E.; Dudley, R.; Nicholls, P. *J. Chem. Soc. (A)* **1969**, 1192.

(19) Fitzgerald, W.; Hathaway, B. J. *J. Chem. Soc., Dalton Trans.* **1981**, 567.

(20) Addison, A. W.; Nageswara Rao, T.; Reedijk, J.; van Rijn, J.; Verschoor, G. C. *J. Chem. Soc., Dalton Trans.* **1984**, 1349.

(21) Brubaker, G.; Brown, R.; Yoo, M. K.; Kinsey, R. A.; Kutchan, T. M.; Mottel, E. A. *Inorg. Chem.* **1979**, *18*, 299.

(22) Addison, A. W.; Burke, P. J.; Henrick, K.; Rao, T. N.; Sinn, E. *Inorg. Chem.* **1983**, *22*, 3645.

(23) Sakurai, T.; Suzuki, S.; Nakahara, A. *Bull. Chem. Soc. Jpn.* **1981**, *54*, 2313.

(24) Dagdigian, J. V.; McKee, V.; Reed, C. A. *Inorg. Chem.* **1982**, *21*, 1332.

(25) Miskowski, V. M.; Thich, J. A.; Solomon, R.; Schugar, H. J. *J. Am. Chem. Soc.* **1976**, *98*, 8344.

(26) Nikles, D. E.; Powers, M. J.; Urbach, F. L. *Inorg. Chem.* **1983**, *22*, 3210.

(27) Jorgensen, C. K. *Oxidation Numbers and Oxidation States*; Springer-Verlag: New York, 1969; p 144.

(28) Billing, D. E.; Dudley, R. J.; Hathaway, B. J.; Tomlinson, A. A. G. *J. Chem. Soc. (A)* **1971**, 691.

(29) Addison, A. W.; Sinn, E. *Inorg. Chem.* **1983**, *22*, 1225.

(30) Anderson, O. P.; Perkins, C. M.; Britto, K. K. *Inorg. Chem.* **1983**, *22*, 1267.

(31) Addison, A. W.; Rao, T. N.; Sinn, E. *Inorg. Chem.* **1984**, *23*, 1957.

(32) Sakaguchi, U.; Addison, A. W. *J. Chem. Soc., Dalton Trans.* **1979**, 600.

(33) Martin, M. J.; Endicott, J. F.; Ochrymowycz, L. A.; Rorabacher, D. B. *Inorg. Chem.* **1987**, *26*, 3012.

(34) Nonaka, Y.; Tokh, T.; Kida, S. *Bull. Chem. Soc. Jpn.* **1974**, *17(2)*, 312.

(35) Batra, P.; Mathur, P. *Inorg. Chem.* **1992**, *31*, 1575; Siddiqui, S.; Shepherd, E. *Inorg. Chem.* **1986**, *25*, 3869.

(36) Bernardo, M. M.; Heeg, M. J.; Schroeder, R. R.; Ochrymowycz, L. A.; Rorabacher, D. B. *Inorg. Chem.* **1992**, *31*, 191.

(37) Aoi. N.; Matsubayashi, G.; Tanaka, T. *J. Chem. Soc., Dalton Trans.* **1983**, 1059.

(38) Amundsen, A. R.; Whelan, J.; Bosnich, B. *J. Am. Chem. Soc.* **1977**, *99*, 6730.

(39) Palaniandavar, M.; Addison, A. W.; Sinn, E. to be communicated.

(40) Palaniandavar, M.; Pandiyan, T.; Lakshminarayanan, M.; Manohar, H. *J. Chem. Soc., Dalton Trans.* **1995**, 455.

(41) Adhikary, B.; Liu, S.; Lucas, C. R. *Inorg. Chem.* **1993**, *32*, 5957.

(42) Bard, A. J.; Faulkner, L. R. *Electrochemical methods: Fundamental applications*; John Wiley & Sons: New York, 1980; p 218.

(43) Dockal, E. R.; Jones, T. E.; Sokol, W. F.; Engerer, R. J.; Rorabacher, D. B. *J. Am. Chem. Soc.* **1976**, *98*, 4322.

(44) Zanello, P. *Comments Inorg. Chem.* **1988**, *8*, 45.

(45) Addison, A. W. *Inorg. Chim. Acta* **1989**, *162*, 217.

(46) Gullotti, M.; Casella, L.; Pintar, A.; Suardi, E.; Zanello, P.; Mangani, S. *J. Chem. Soc., Dalton Trans.* **1989**, 1979.

(47) Yokoi, H.; Addison, A. W. *Inorg. Chem.* **1977**, *16*, 1341.

(48) Glick, M. D.; Gavel, D. P.; Diaddario, L. L.; Rorabacher, D. B. *Inorg. Chem.* **1976**, *15*, 1190.

(49) Pett, V. B.; Diaddario, L. L.; Dockal, E. R., Jr.; Corfield, P. W. R.; Ceccarelli, C.; Glick, M. D.; Ochrymowycz, L. A.; Rorabacher, D. B. *Inorg. Chem.* **1983**, *22*, 3661.

CHAPTER 6

6. ELECTROCHEMICAL BEHAVIOUR OF CERTAIN BIOMIMETIC COPPER(II) COMPLEXES IN AQUEOUS AND AQUEOUS MICELLAR SOLUTIONS

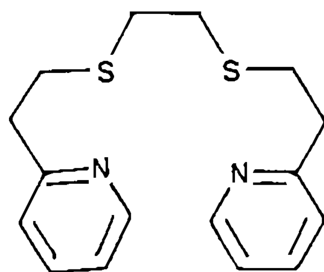
6.1 Introduction

Blue copper proteins exhibit facile electron transfer properties and novel catalytic functions, which are associated with the Cu(II)/Cu(I) redox cycle. Several electrochemical investigations on copper chelates with varying donor atoms and geometries have led to the conclusion that both the coordinated methionine and the approximately tetrahedral structure of active site of these proteins contribute to their unusually high redox potentials (0.18 to 0.68 V *vs* SCE).[1,2] Though useful, most of these previous studies were restricted to non-aqueous solvents and are not directly relevant to the biological environment encountered by copper proteins. Thus, though Cu(II) models which closely mimic their unusual spectral and electrochemical properties have been successfully isolated, they have been studied only in non-aqueous solvents like dichloromethane.[3] In an effort to examine the redox fate of biomimetic copper(II) complexes in more biologically relevant medium, we have initiated a study of their electrochemical

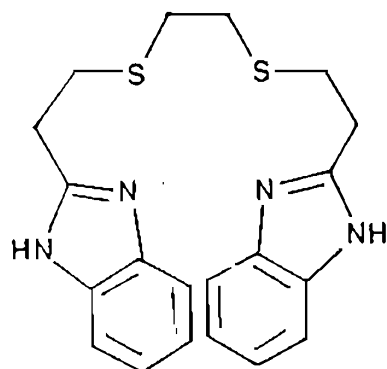
properties in aqueous surfactant solutions.

Micelles are dynamic surfactant aggregates capable of combining with solute molecules *via* hydrophobic and Coulombic interactions. Organized micellar aggregates have been used in a variety of chemical and industrial applications.[4] They are well known to solubilize poorly soluble organic[5,6] as well as coordination compounds[7,8] and are often considered to be biomimetic in that reactions on and within the micelles may mimic reactions at biomembrane interfaces.[9] Thus micelle solubilized ferrocene has been used as a mediator titrant for cytochrome *c* oxidase.[10] Further, such solutions often provide practical enhancement of reaction rates and exhibit catalytic properties.[11] Thus the electrochemically generated Co(I)-bipyridyl complexes bound to SDS micelles reduce allyl chloride in water.[12]

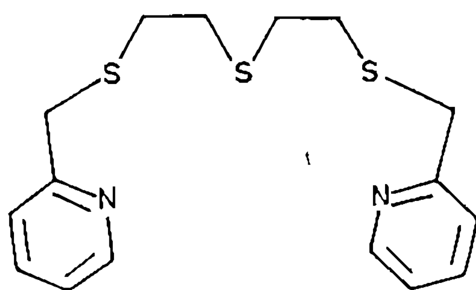
Electrochemical investigations on the interaction of metal complexes with micelles are scarce and reactions involving inorganic compounds in micelles are less well understood. The electrochemistry of ferrocene[13] and cobalt[12] and rhenium[14] complexes in micellar solutions have been studied very recently. In the present study we have chosen a few copper(II) coordination complexes containing biomimetic thioether and pyridine (py) or benzimidazole (bzim) nitrogen donors [Scheme 6.1], which have been investigated as models for blue sites.[15-17] The advantages of choosing these systems are i) their solubility in water, which



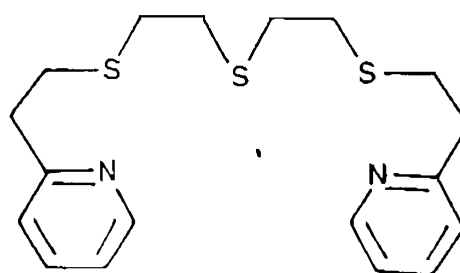
pdto



bbdo



pttn



pttu

Scheme 6.1

enables comparison of redox properties in micellar solution to that in aqueous solution, ii) structures of Cu(I) and Cu(II) forms (Fig. 6.1) of most of these systems are known,[15a,16,17] (Figs. 1.10, 1.11, 4.1) iii) they are known to exhibit simple Cu(II)/Cu(I) redox process and iv) the difference in hydrophobicity of the ligands. In the present work we focus our attention on the influence of anionic (SDS), cationic (CTAB), and nonionic (Triton X-100) surfactants on the redox behaviour - reversibility and redox potential - of Cu(II)/Cu(I) couple and hence the nature of micellar interaction with the copper complexes.

6.2 Experimental

6.2.1 Synthesis of Ligands and their Cu(II) Complexes

1,8-Bis(pyrid-2-yl)-3,6-dithiaoctane (pdto)

The ligand pdto was prepared[18] as follows. To 1,2-ethanedithiol (2.31 g, 24.4 mmol) 2-vinylpyridine (5.2 g, 49.5 mmol) was added while stirring. The mixture was kept aside for 24 hours. The solid formed was recrystallised from petroleum ether (60 - 80) and dried over P_4O_{10} under vacuum. Yield, 78 %; m.p. 48 °C; Lit. m.p. 50 - 51 °C.

The corresponding Cu(II) complex was prepared[19] by adding $Cu(ClO_4)_2.6H_2O$ (0.37 g, 1.0 mmol) in methanol (1 mL) to a methanolic solution (10 mL) of pdto (0.31 g, 1.0 mmol); the solid formed was collected and recrystallised from water. Yield, 80 %.

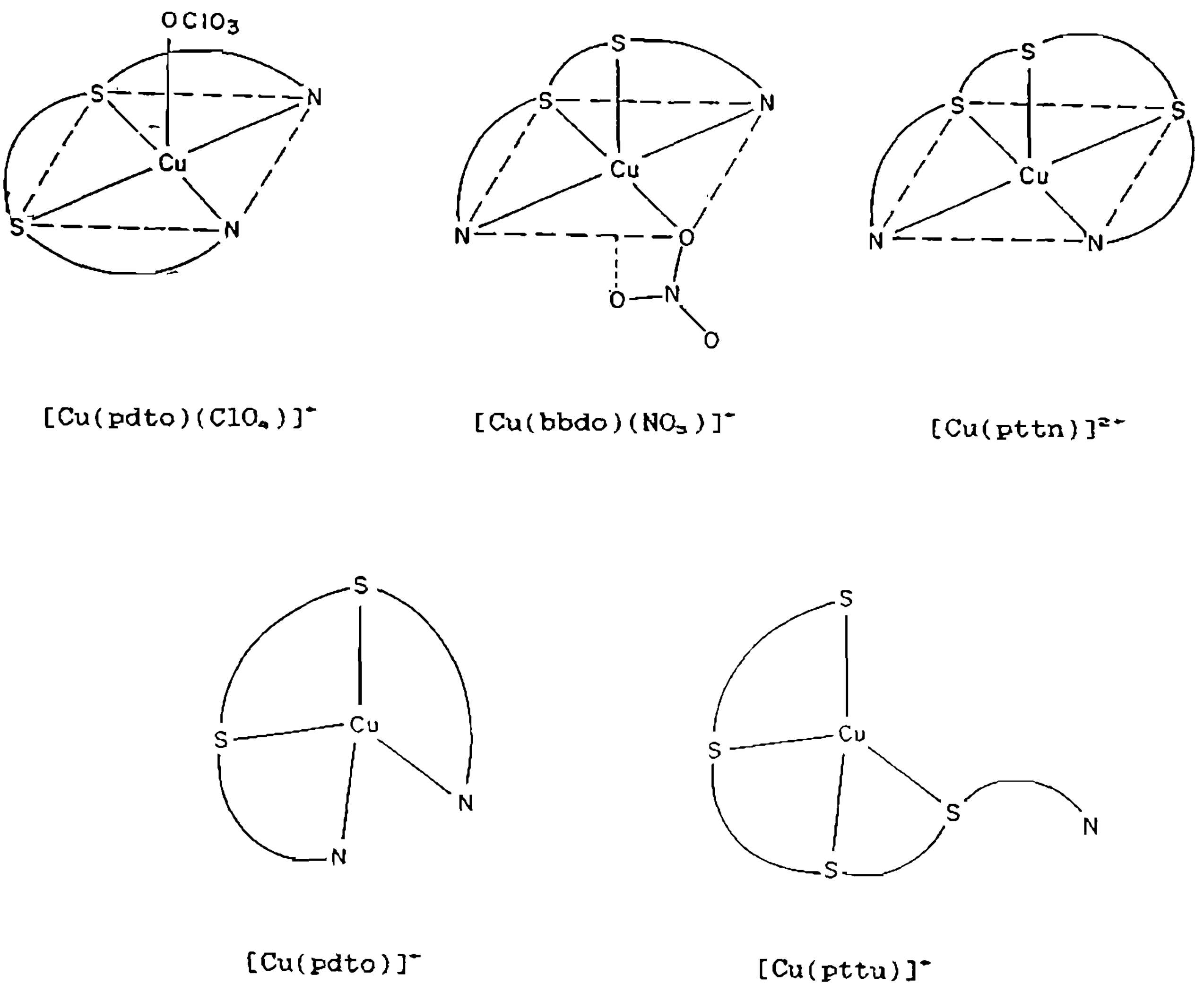


Fig. 6.1 Known structures of Cu(II) and Cu(I) complexes of N_2S_2 and N_2S_3 ligands

1,9-Bis(pyrid-2-yl)-2,5,8-trithianonane (pttn)

This ligand was prepared by following the procedure reported in the literature.[16a] Added was 2-chloromethylpyridine hydrochloride (2.12 g, 13 mmol) in ethanol (25 mL) under nitrogen with stirring to a solution of KOH (1.46 g, 26 mmol) and bis(2-mercaptoethyl)-sulfide (1.0 g, 6.5 mmol) in ethanol (25 mL). A white precipitate of KCl formed immediately. The reaction mixture was stirred (30 min) and refluxed (1 h), cooled to room temperature and then the solvent was removed (rotary evaporator). Water was added, followed by enough KOH to bring the pH to 13 and the product was extracted with dichloromethane. The extract was dried with magnesium sulfate and then the solvent was removed (rotary evaporator) to get the yellow oily product. Yield, 85 %.

The Cu(II) complex was prepared by adding $Cu(ClO_4)_2.6H_2O$ (0.37 g, 1.0 mmol) in methanol (1 mL) to a methanolic solution (10 mL) of pttn (0.34 g, 1.0 mmol); the complex formed was collected and dried over P_4O_{10} under vacuum. Yield, 60 %.

The ligands bbdo [1,8-bis(benzimidazol-2-yl)-3,6-dithia-octane],[17] and pttu [1,11-bis(pyrid-2-yl)-3,6,9-trithiaundecane][17] and their $Cu(ClO_4)_2$ complexes were prepared as described in Chapter 4.

6.2.2 Data Treatment

Nonlinear parameter estimation was performed with a Basica

program. In this program initial estimates of the parameters within their physical limits were entered and the peak current values are calculated from the D_{obs} in each step. Then a simplex search was performed for improving the estimates. The improved estimates were indicated by the lowering of the differences between the computed and the experimental peak current values. After each fitting, plots of observed and calculated peak currents *vs* SDS concentrations were done for visual inspection. If initial estimates are not within reasonable limits, the visual inspection of the plot shows a complete lack of correlation between observed and calculated values. In that case the initial estimates must be chosen carefully. Once the plot appeared satisfactory, the fitting parameters were fine tuned by minimizing the step size of the parameters.

6.3 Results and Discussion

6.3.1 Electronic Spectra and Solution Properties

The hydrophobic tails and polar head groups of monomeric units of ionic surfactant moleculee align in such a way to form micellar assemblies with non-polar interior and a polar interface with the bulk aqueous solution.[19] The solute molecules can be accommodated in the hydrophobic interior, radially at various depths or adsorbed at the micelle surface.[4] Their solubilities are affected mainly by Coulombic and hydrophobic interactions. The

present dipositively charged copper(II) complexes are expected to exhibit Coulombic interactions while the py and bzim moieties of the coordinated ligands hydrophobic interactions with micelles. Thus ^{1}H NMR studies of $[Co(bipy)_3]^{2+}$ complexes have revealed that py rings extend a few C-C bond lengths into the hydrophobic region of SDS micelles.[12b] So in cationic CTAB micelles such interactions may help offset the Coulombic repulsions of the cationic complex with the micellar surface potential.

To understand the mode of micellar solubilization of the present complexes, their electronic spectra in aqueous and aqueous micellar solutions have been measured and the data are collected in Table 6.1. For all the present complexes in water the ligand field (Fig. 6.2) and S(σ) ---> Cu(II) LMCT (Fig. 6.3) bands[15-17] were observed around 16.4 and 28.1 kK respectively. The absorptivity rather than position (Figs. 6.2 and 6.3) of these bands change significantly in micellar solutions, in contrast to the red shifts observed for ferrocene,[13] $[Co(bipy)_3]^{2+}$ [12] and certain $[ML_2X_2]^{2+}$ [20] complexes [M = Re, Tc; L = depe = 1,2-bis-(diethylphosphino)ethane, dmpe = 1,2-(dimethylphosphino)ethane; X = Br, Cl]. This suggests that micellar effect, rather than any major structural change in the coordination sphere, leads to greater allowedness of the bands for the present complexes. All the Cu(II) complexes possesses higher absorptivity for LF bands in more polar acetonitrile (Fig. 6.4) than in water illustrating the

Table 6.1 Electronic spectral data* for the Cu(II) complexes in various solvents in the presence and absence of surfactants

complex	Solvent	Surfactant	LF band	CT band
$[Cu(pdto)]^{2+}$	water	–	16.7 (490)	28.6 (3140)
		SDS	16.7 (550)	28.3 (3220)
		CTAB	16.8 (800)	28.6 (3430)
		Triton X-100	16.7 (310)	28.6 (2230)
	CH_3CN	–	16.9 (740)	27.9 (4660)
		SDS	16.4 (670)	28.1 (4470)
		CTAB	13.6 (400) 15.3 (390)	28.0 (3460)
		Triton X-100	16.8 (550)	28.3 (3790)
	DMF	–	12.7 (32) 16.1 (20)	–
		SDS	13.0 (43)	–
		CTAB	17.0 (310)	–
		Triton X-100	12.6 (35) 16.8 (27)	–
$[Cu(bbdo)]^{2+}$	water	–	11.4 (190) 16.7 (170)	24.7 (1420) 29.3 (3760)
	CH_3CN	–	11.6 (210) 16.9 (220)	28.7 (2810)
	water	SDS	11.8 (100) 15.6 (170)	–
	water	CTAB	11.4 (250) 16.7 (240)	29.3 (2300) 24.7 (905)
	water	Triton X-100	11.3 (180) 16.7 (240)	29.4 (1990) 24.7 (640)

$[Cu(pttn)]^{2+}$	water	–	11.2 (180) 16.7 (410)	28.1 (3590)
	CH_3CN	–	11.2 (190) 16.7 (450)	27.7 (4760)
	water	SDS	11.2 (150) 16.8 (380)	28.0 (3640)
	water	Triton X-100	11.2 (150) 16.7 (350)	28.2 (3160)
$[Cu(pttu)]^{2+}$	water	–	16.7 (300)	26.4 (1910)
	CH_3CN	–	11.1 (100) 16.3 (490)	26.1 (3280)
	water	SDS	16.5 (370)	26.4 (1960)
	water	Triton X-100	16.8 (100)	28.5 (777)

[a] Complex concentration = 0.002 M; surfactant concentration = 0.010 M; $\bar{\nu}_{max}$ values in kK and ϵ in M^{-1} cm^{-1} in parentheses

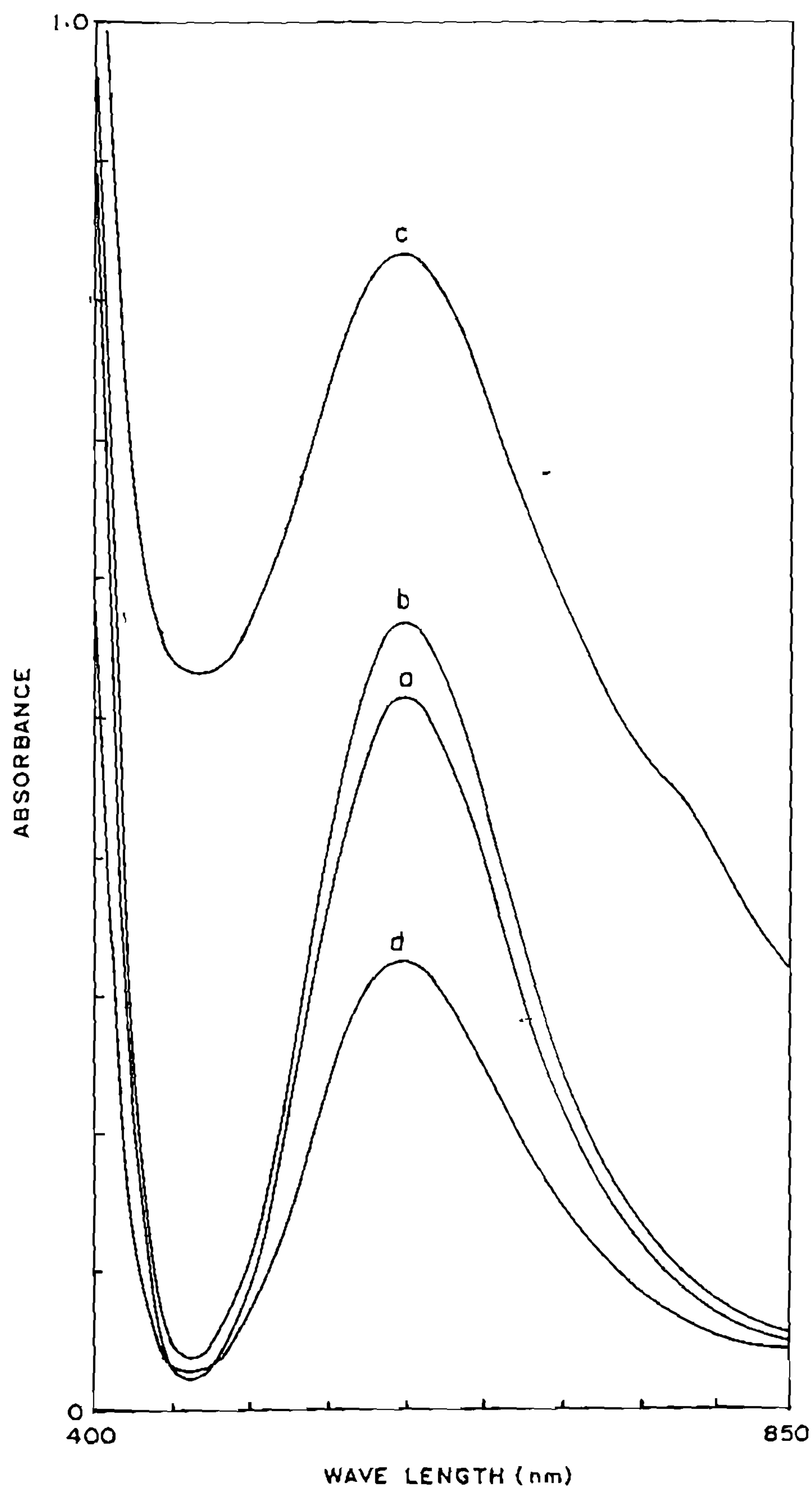


Fig. 6.2 Ligand field spectra of $[Cu(pdto)]^{2+}$ in aqueous (a) and aqueous SDS (0.010 M) (b), CTAB (0.010 M) (c) and Triton X-100 (5 %) (d) solutions

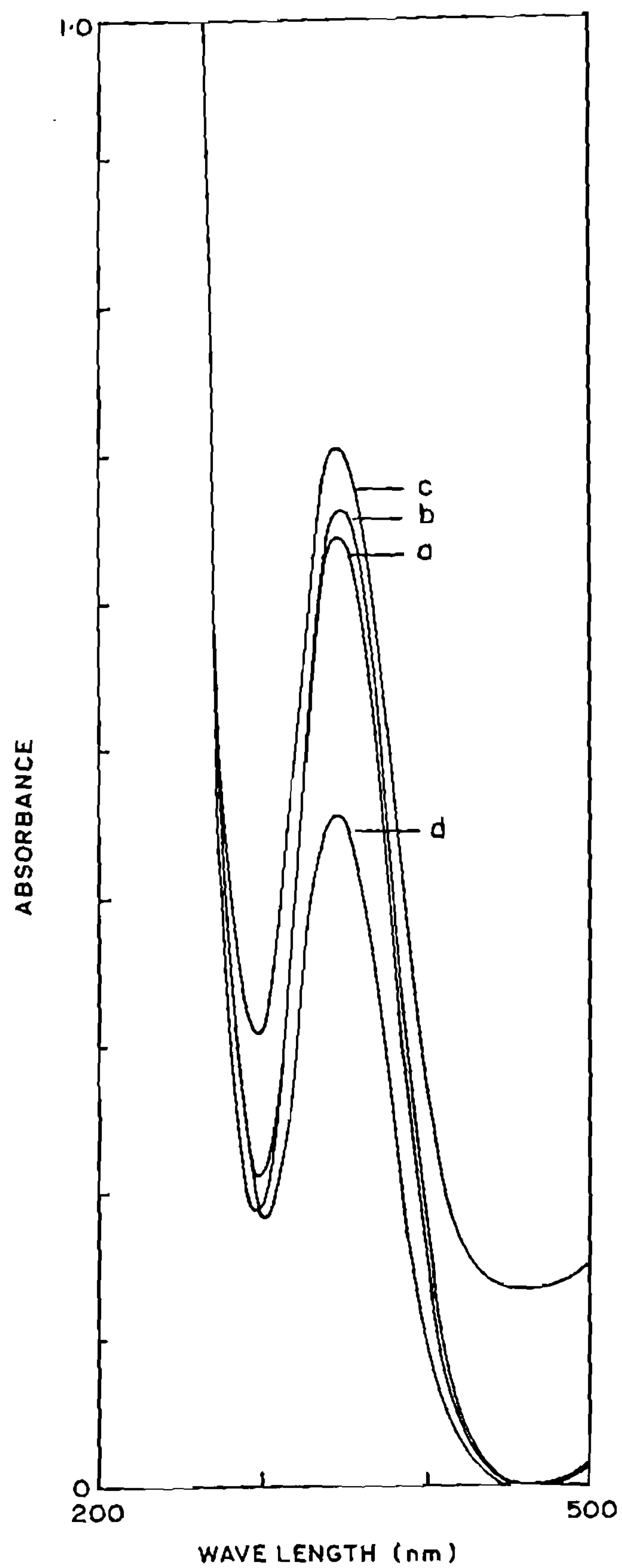


Fig. 6.3 Charge transfer spectra of $[Cu(pdto)]^{2+}$ in aqueous (a) and aqueous SDS (0.010 M) (b), CTAB (0.010 M) (c) and Triton X-100 (5 %) (d) solutions

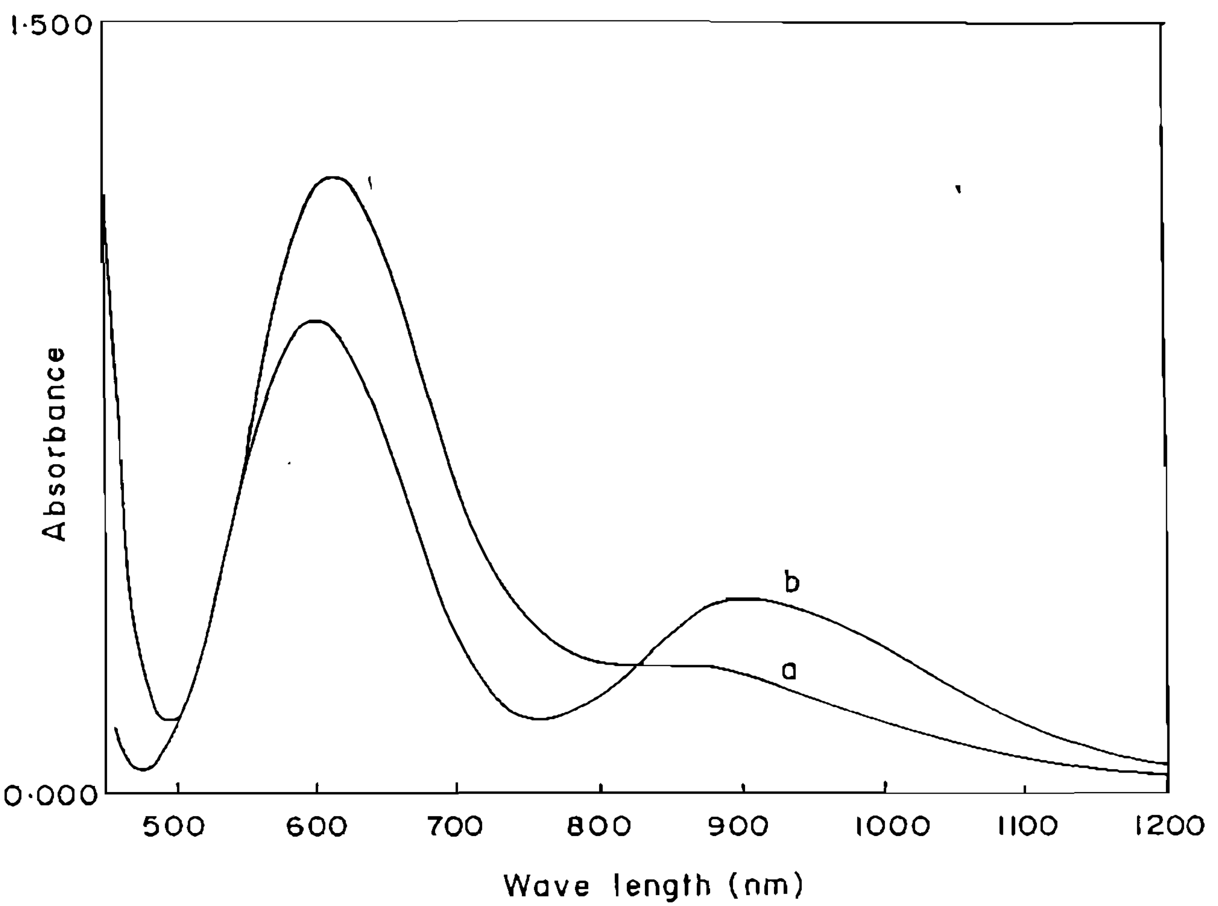


Fig. 6.4 Ligand field spectra of $[Cu(pttn)]^{2+}$ (a) and $[Cu(pttu)]^{2+}$ (b) in acetonitrile

importance of ionic interactions. A similar increase in absorptivity in SDS micellar solution for $[Cu(pdto)]^{2+}$ (Fig. 6.2) and $[Cu(pttu)]^{2+}$ suggests strong Coulombic interaction of complex cations with anionic SDS micelles close to the charged Stern layer, leading to probably a slight distortion in the coordination geometry. It is also possible that hydrophobic interaction of py or bzim ring would enhance the absorptivity of the LMCT and hence the LF band by intensity stealing.[15c] In fact, the ability of $[Cu(pdto)]^{2+}$ and $[Cu(bbdo)]^{2+}$ containing weakly coordinated thioether donors to coordinate to anions like ClO_4^- and NO_3^- (Chapter 4) respectively, is evident from their crystal structures (Fig. 6.1).[15a,17] However, for $[Cu(pttn)]^{2+}$ and $[Cu(bbdo)]^{2+}$ (Fig. 6.5) the absorptivity of the LF band decreases but slightly.

A Coulombic repulsion of cationic CTAB micelles with cationic $[Cu(pdto)]^{2+}$ (Fig. 6.2) complex species is expected to lead to weaker interaction and hence no change in absorptivity of both the LF and LMCT bands compared to water. But, interestingly, an increase in absorptivity is observed; this suggests a stronger interaction of py moiety with the less polar sites present in the hydrophobic region of the micelles, in spite of the electrostatic disadvantage; however, $[Cu(bbdo)]^{2+}$ with a chromophore[17] same as that for $[Cu(pdto)]^{2+}$ but with more hydrophobic bzim ligand moieties, show lower ϵ_{max} values as in SDS micelles. For all the complexes the hypochromic shift of both the bands in Triton X-100

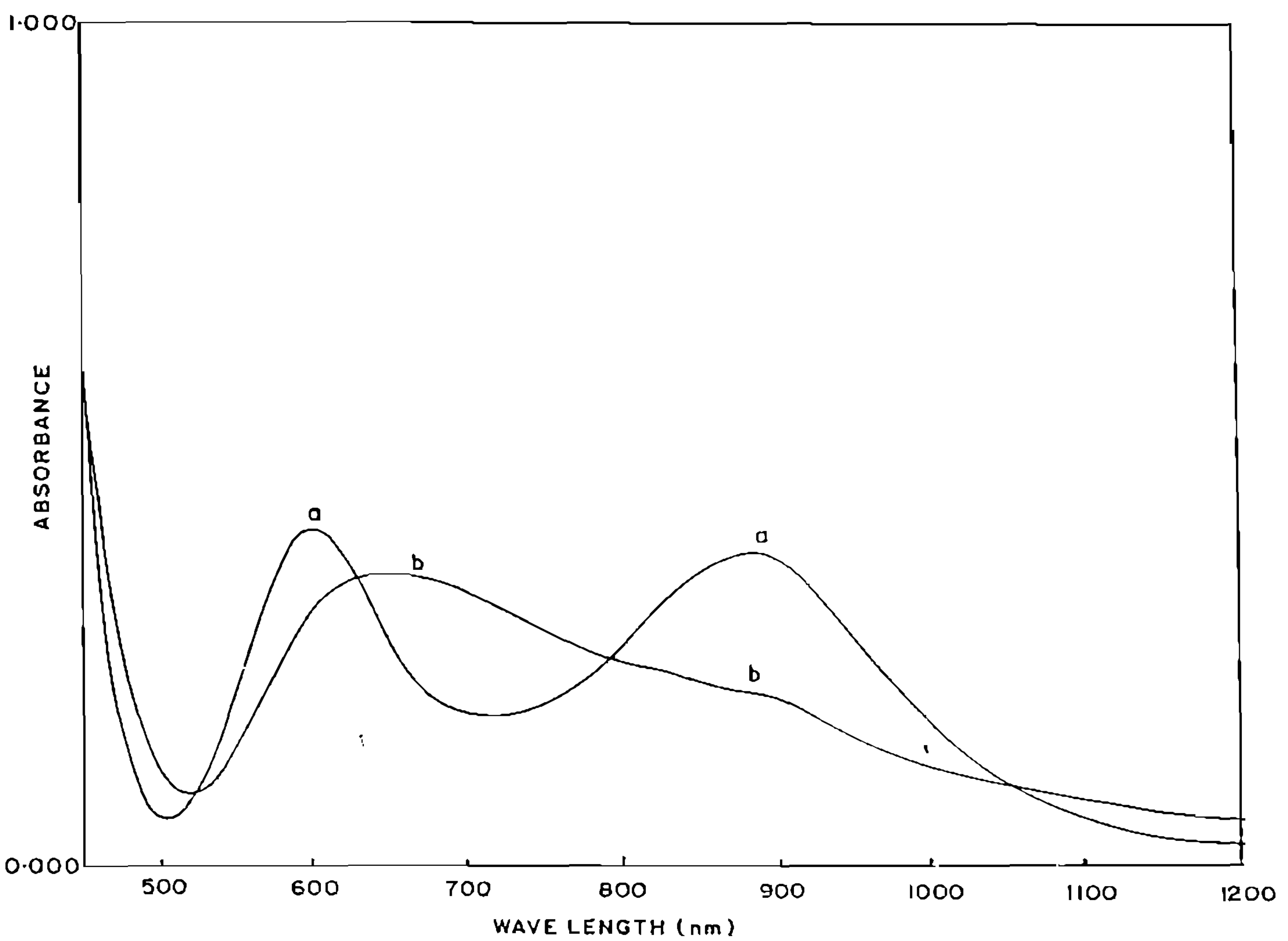


Fig. 6.5 Ligand field spectra of $[Cu(bbdo)]^{2+}$ in aqueous (a) and aqueous SDS (0.010 M) (b) solutions

micelles suggest that the chromophores exist in a microenvironment much less polar than water, exhibiting predominantly hydrophobic interaction with the micelles.

6.3.2 Electrochemistry of Copper(II) Complexes

The cyclic voltammogram of $[Cu(pdto)]^{2+}$ in aqueous 0.1 M $NaClO_4$ solution (Fig. 6.6) reveals the non-Nernstian behaviour of Cu(II)/Cu(I) couple, as may be judged from the limiting peak potential separation (ΔE_p°, ΔE_p value extrapolated to zero scan rate), of 74 mV and the ratio (2.1) of the peak currents (i_{pa}/i_{pc}) compared to the respective values of 59 mV and unity for a one-electron diffusion controlled reversible process. The higher ΔE_p° value is expected of configurational changes accompanying reduction of square-pyramidal $[Cu^{II}(pdto)(ClO_4)]^+$ to tetrahedral $[Cu^I(pdto)]^+$.[21] The high current of the symmetrical anodic peak[22] is typical of adsorption of electrogenerated Cu(I) species. Such adsorption of Cu(I) complexes containing aromatic ligand moieties is common.[23] Interestingly, no such adsorption of Cu(I) species is discerned in aqueous 0.1 M TEABr and the linearity of the i_{pc} *vs* square root of the scan rate plot (passing through the origin) and the values of i_{pa}/i_{pc} (1.1) and ΔE_p° (60 mV) (Fig. 6.7), suggest that the redox tends to become diffusion controlled and reversible. The complex $[Cu(bbdo)]^{2+}$ shows reversible redox behaviour in methanol solution[17] (Chapter 4) but irreversible one in aqueous

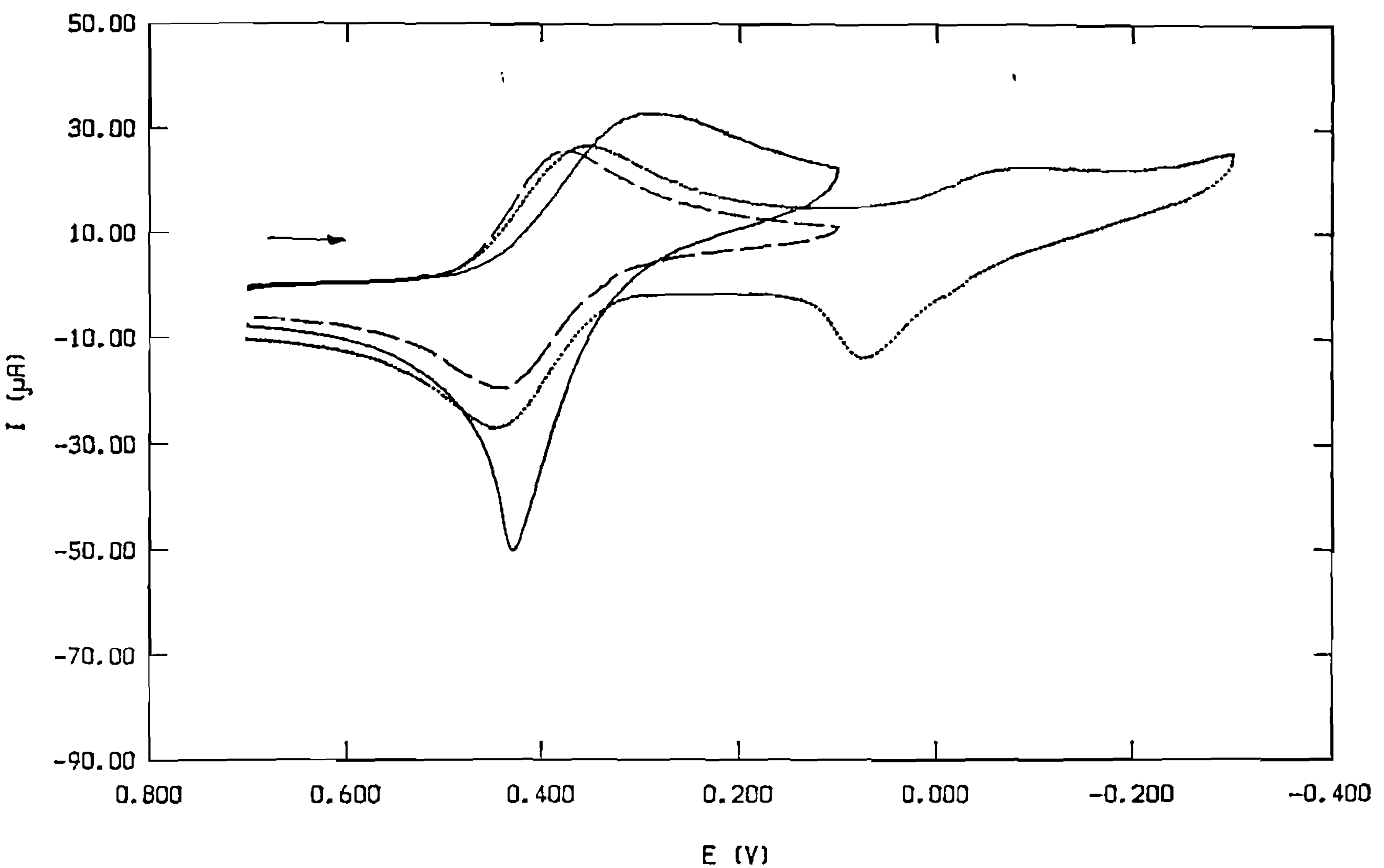


Fig. 6.6 Cyclic voltammograms of $[Cu(pdto)]^{2+}$ (0.001 M) in aqueous solution (0.1 M $NaClO_4$) in the absence (——) and presence of 0.01 M SDS (----) and 0.01 M Triton X-100 (....) at 50 mV/s scan rate

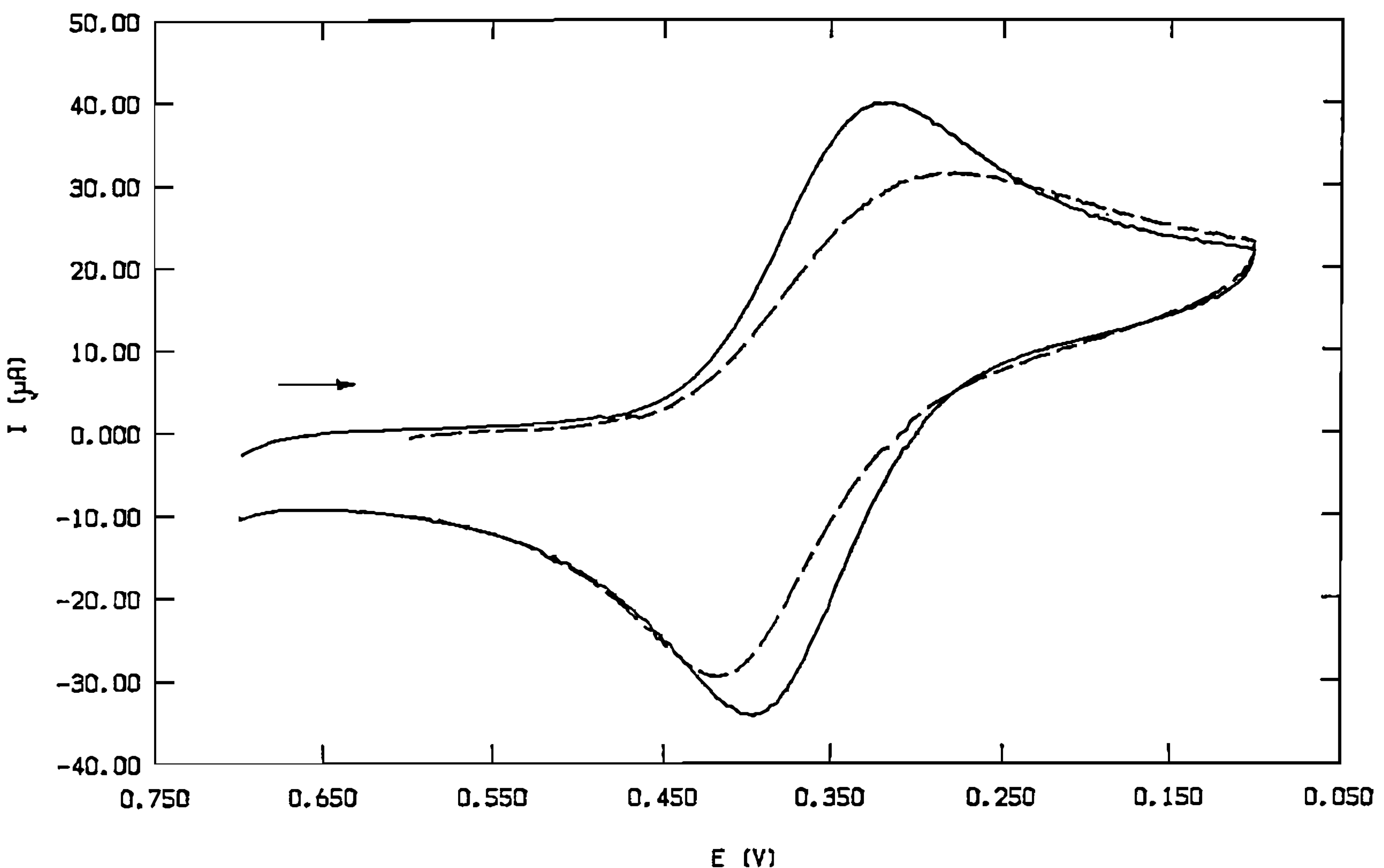


Fig. 6.7 Cyclic voltammograms of $[Cu(pdto)]^{2+}$ (0.001 M) in aqueous solution [0.1 M $(C_2H_5)_4NClO_4$] in the absence (——) and presence (----) of 0.01 M CTAB at 50 mV/s scan rate

solution (0.1 M, $NaClO_4$) (Table 6.2, Fig. 6.8) similar to its pyridine analogue $[Cu(pdto)]^{2+}$. The redox potentials obtained from cyclic voltammetry are consistent with those from differential pulse voltammetry (Fig. 6.9).

The complex $[Cu(pttn)]^{2+}$ shows irreversible redox behaviour (Table 6.2) because of adsorption of Cu(I) species. In contrast, its homologue $[Cu(pttu)]^{2+}$ displays a diffusion controlled and nearly reversible redox (Fig. 6.10) in aqueous solution (Chapter 4), as verified by the constancy of $i_{pc}/\sqrt{\nu}$, low ΔE_p° (67 mV) and i_{pa}/i_{pc} value of unity (Table 6.2), which changes linearly with $\sqrt{\nu}$. The redox potentials of the present complexes follow the trends, $[Cu(pttu)]^{2+}$ > $[Cu(pttn)]^{2+}$; $[Cu(bbdo)]^{2+}$ > $[Cu(pdto)]^{2+}$, illustrating the ability of six-membered chelate rings and bulky bzim[24] to stabilize Cu(I) state (Chapter 5).

6.3.3 Electrochemical Behaviour in SDS Micelles

For all the present complexes the values of both i_{pc} and i_{pa} decrease in SDS micellar solution compared to aqueous isotropic solution. As the SDS concentration is increased there is considerable suppression in the slope of i_{pc} *vs* $\nu^{1/2}$ plot and the diffusion coefficients (D) calculated from these slopes using Randles-Sevciks' equation[26] decreased (Fig. 6.11) compared to those for free complexes. The dramatic difference in electrochemical behaviour in 0.1 M $NaClO_4$ and 0.01 M SDS/0.1 M $NaClO_4$ solutions

Table 6.2 Redox properties[a] of Cu(II) complexes in aqueous solution in the absence and presence of micelles[b] at 50 mV/s scan rate

Complex	Medium[c]	E_{pc} V	E_{pa} V	i_{pc} μA	i_{pa} μA	ΔE_p mV	ΔE_p^0 [d] mV	$E_{1/2}$(V) CV	DPV[e]	i_{pa}/i_{pc}	D x 10^6 cm^2/s	K_{+}/K_{2+}
$[Cu(pdto)]^{2+}$	$NaClO_4$	0.310	0.422	40.9	70.0	112	74	0.366	0.373	2.1	2.7	
	SDS	0.376	0.444	27.8	19.3	68	60	0.410	0.399	1.0	1.6	5.6
	Triton X-100	0.356	0.454	29.7	26.0	98	69	0.405	0.401	1.2	1.4	4.6
	[f]	-0.066	0.074	24.0	22.7	140		0.004	-0.031	1.6		
	TEABr	0.320	0.396	39.7	34.3	76	60	0.358	0.357	1.1	3.2	
	CTAB	0.286	0.416	31.4	29.6	132	66	0.352	0.361	1.4	1.7	0.6
$[Cu(bbdo)]^{2+}$	$NaClO_4$	0.419	0.546	25.0	61.1	127	100	0.483	0.450	2.8	1.2	
	SDS	0.380	0.464	11.0	2.1	84	78	0.422	0.427	0.6	0.2	0.1
	Triton X-100	0.478	0.566	16.4	10.4	88	70	0.522	0.509	1.0	0.6	4.6
	[f]	-0.050	0.084	11.0	0.62	134		0.017	-0.003	0.6		
	TEABr	0.382	0.484	17.6	62.2	102	80	0.433	0.421	3.9	6.1	
	CTAB	0.352	0.464	24.4	20.4	112	67	0.408	0.433	1.4	0.9	0.4
[g]$[Cu(pttn)]^{2+}$	$NaClO_4$	0.294	0.376	54.6	127	82	64	0.335	0.307	2.6	3.0	
	SDS	0.284	0.358	21.6	13.4	74	74	0.321	0.321	1.0	0.5	3.6
	Triton X-100	0.288	0.342	32.0	24.7	54	46	0.315	0.317	1.2	1.0	1.7
[g]$[Cu(pttu)]^{2+}$	$NaClO_4$	0.430	0.510	36.2	30.4	80	67	0.470	0.474	1.1	4.9	
	SDS	0.467	0.540	15.9	12.8	73	–	0.504	0.500	1.1	1.4	0.6
	Triton X-100	0.444	0.525	21.7	17.4	81	63	0.485	0.481	1.1	2.4	0.5

[a] Concentration of $NaClO_4$ and TEABr (tetraethylammonium bromide) = 0.1 M; [b] Concentration of surfactants SDS, CTAB and Triton X-100 = 0.01 M; [c] Supporting electrolyte used is $NaClO_4$ for SDS and Triton X-100 micelles and tetraethylammonium bromide for CTAB micelles; [d] $\Delta E_p^0 = \Delta E_p$ at zero scan rate; [e] Scan rate, 1 mV/s; pulse height, 50 mV; [f] values are for the second reduction observed when the switching potential is -0.3 V; [g] precipitation occurs when CTAB is added.

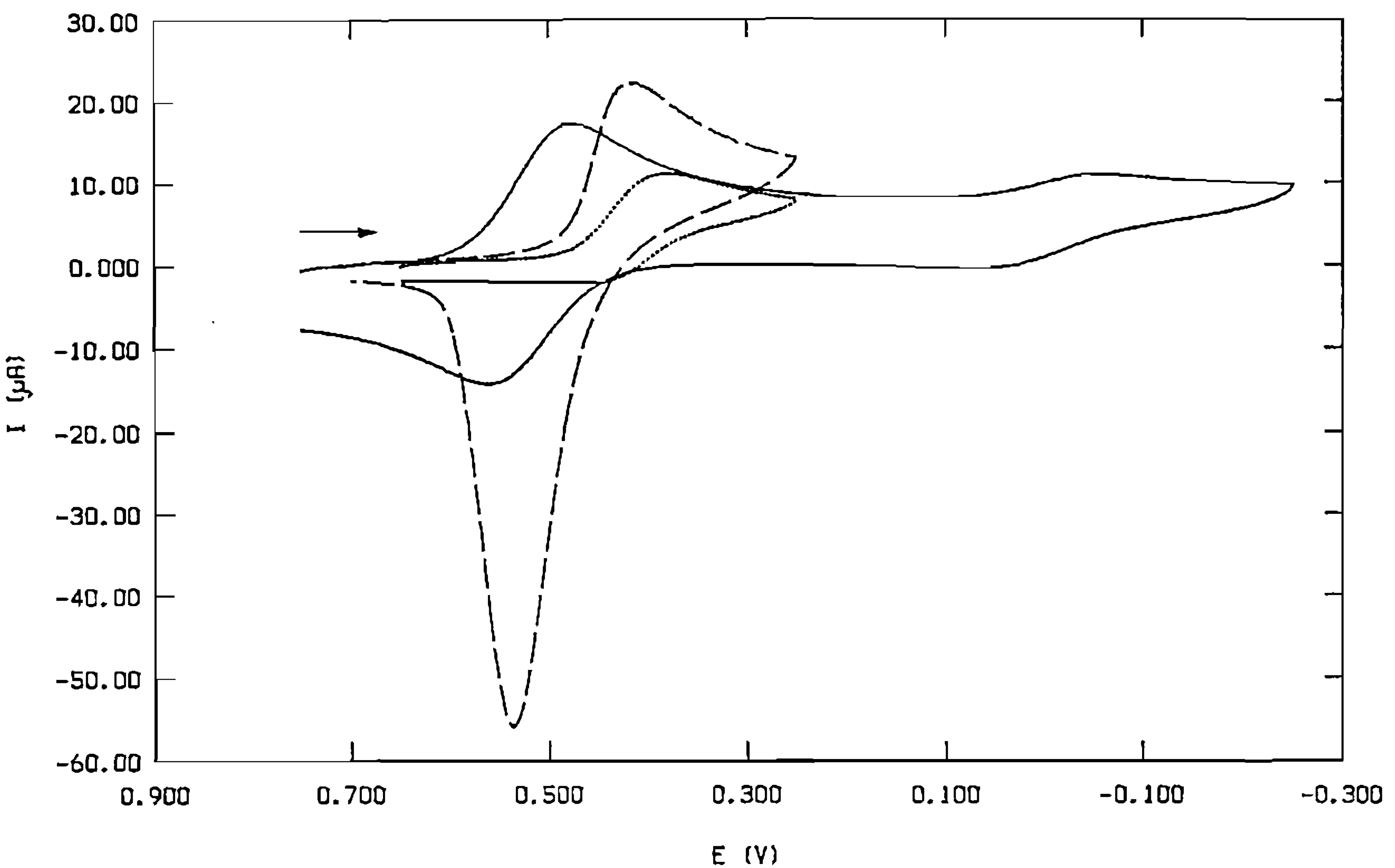


Fig. 6.8 Cyclic voltammograms of $[Cu(bbdo)]^{2+}$ (0.001 M) in aqueous solution (0.1 M $NaClO_4$) in the absence (----) and presence of 0.01 M SDS (....) and 0.01 M Triton X-100 (——) at 50 mV/s scan rate

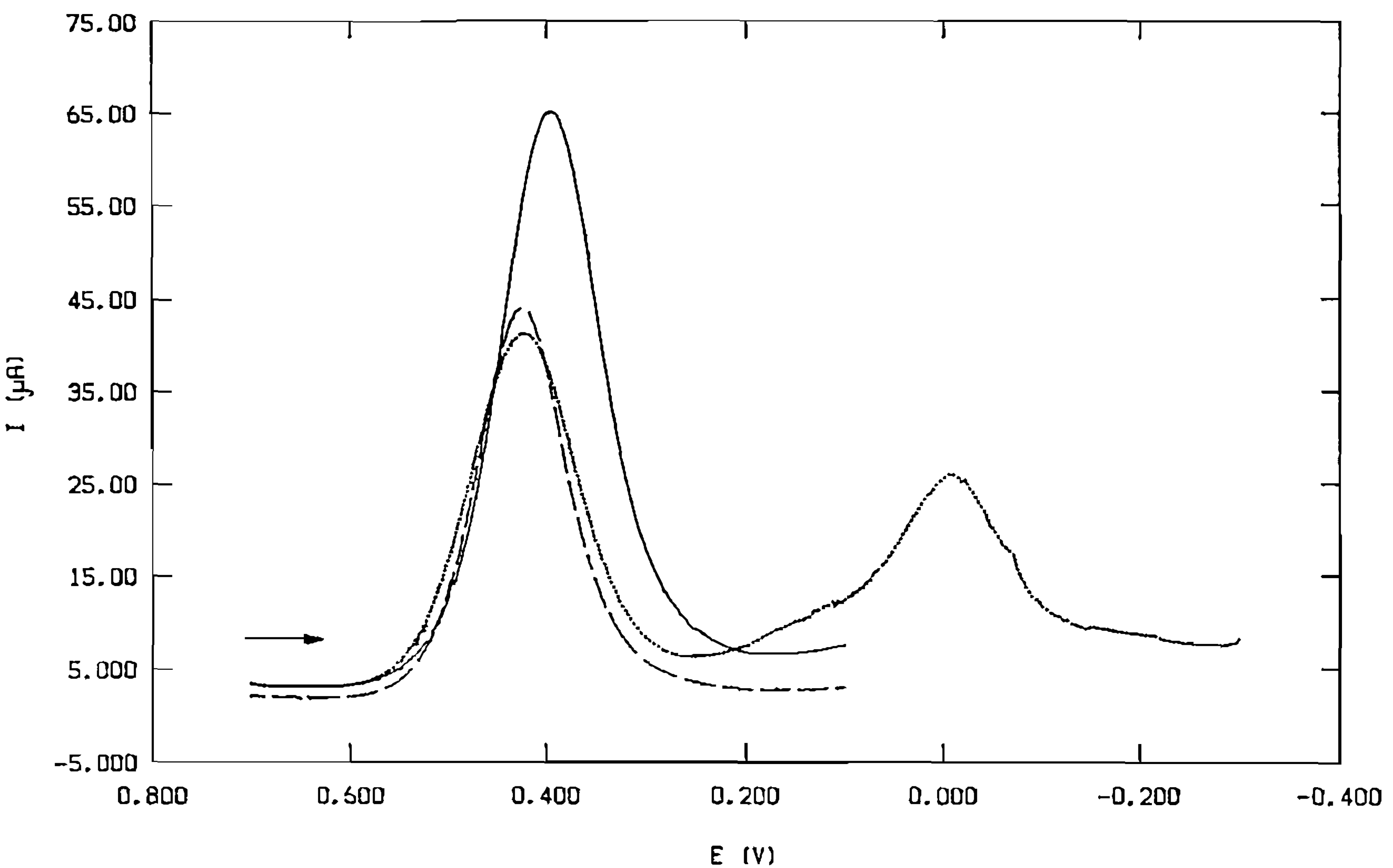


Fig. 6.9 Differential pulse voltammograms of $[Cu(pdto)]^{2+}$ (0.001 M) in aqueous solution (0.1 M $NaClO_4$) in the absence (——) and presence of 0.01 M SDS (----) and 0.01 M Triton X-100 (....) at 1 mV/s scan rate

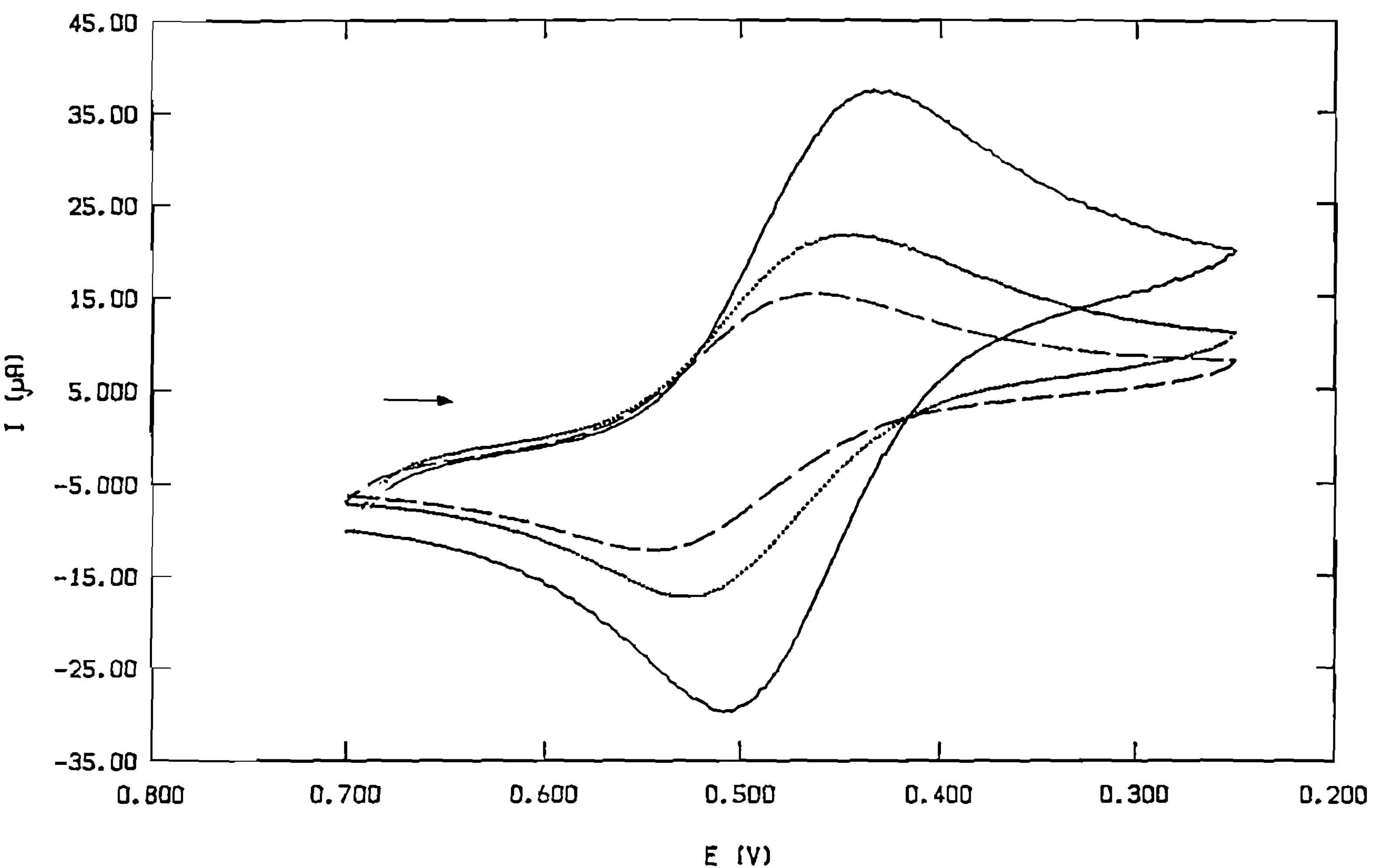


Fig. 6.10 Cyclic voltammograms of $[Cu(pttu)]^{2+}$ (0.001 M) in aqueous solution (0.1 M $NaClO_4$) in the absence (——) and in the presence of 0.01 M SDS (----) and 0.01 M Triton X-100 (....) at 50 mV/s scan rate

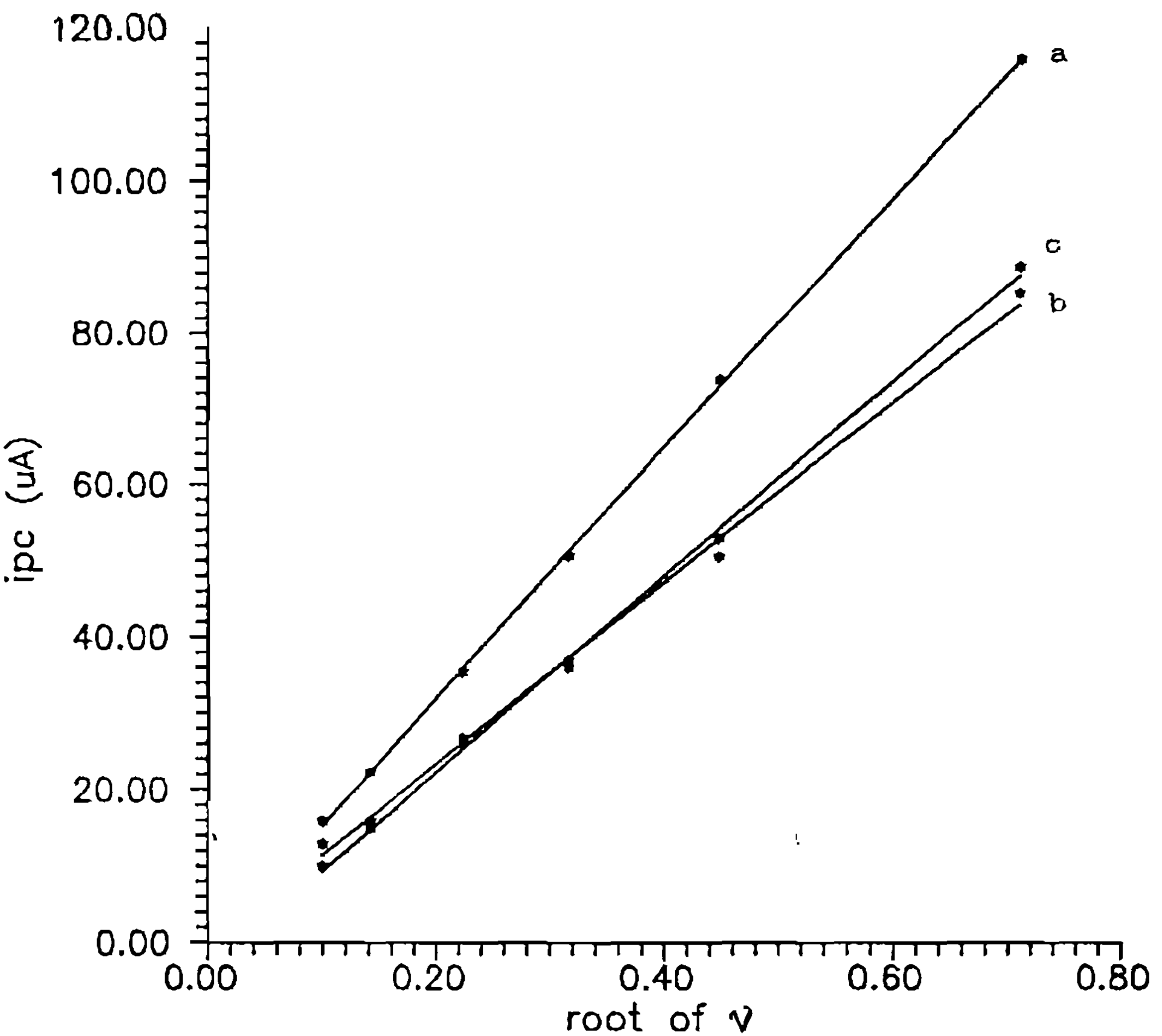


Fig. 6.11 Observed cathodic peak currents *vs* square root of scan rates for $[Cu(pdto)]^{2+}$ in aqueous (a) and in 0.01 M SDS (b) and 0.01 M Triton X-100 (c) micellar solution

indicates that the copper complexes are associated with the micellar environment and that the diffusion of the micelle-solubilized molecule to the electrode surface becomes the rate-determining step of the electrochemical reaction. The increase in effective size of Cu(II) complexes slows down their diffusion and results in lower peak currents and hence diffusion coefficients.[20,26] Analogous behaviour has been reported for methylviologen,[27] $[Os(5\text{-dmbpy})_3]^{2+}$ [28] [5-dmbpy = 5,5′-dimethyl-2,2′-bipyridine] and *trans*-$[ML_2X_2]^+$ [20] [M = Tc, Re; L = dmpe or depe].

For $[Cu(pdto)]^{2+}$ in 0.01 M SDS/0.1 M $NaClO_4$ solution, in contrast to aqueous isotropic solution the ratio of peak currents ($i_{pa}/i_{pc} \approx 1$) which is independent of scan rate, the $\triangle E_p^\circ$ value of 60 mV (Table 6.2) and the linearity of the plot of cathodic (slope, 129.2) and anodic (slope, 84.1) peak currents as defined by the Randles-Sevciks′ equation strongly suggest the attainment of diffusion controlled, almost reversible Cu(II)/Cu(I) redox process (Fig. 6.6); this shows that both forms of redox couple are solubilized and therefore, stabilized in the microenvironment of SDS micelles. The peak currents and peak potentials, when monitored at a constant scan rate and complex concentration, varied systematically on increasing the concentration of SDS (Table 6.3). The plots of $E_{1/2}$ and $\triangle E_p$ *vs* [SDS] show a maximum around 10 mM SDS concentration (Fig. 6.12), which corresponds approximately to the critical micelle concentration (cmc) of SDS (see below). This

Table 6.3 Redox properties of $[Cu(pdto)(ClO_4)](ClO_4)$ complex (0.001 M) in aqueous solution[a] in the presence of SDS micelles with varying concentrations of SDS at 50 mV/s scan rate

[SDS] M	E_{pc} V	E_{pa} V	i_{pc} µA	i_{pa} µA	ΔE_p mV	$E_{1/2}$(V)		i_{pa}/i_{pc}
						CV	DPV	
0.000	0.310	0.422	40.9	70.0	112	0.366	0.373	2.1
0.002	0.342	0.420	38.1	33.5	78	0.381	0.383	1.1
0.004	0.356	0.428	34.0	27.1	72	0.392	0.391	1.1
0.006	0.366	0.434	29.8	21.7	68	0.400	0.394	1.1
0.008	0.368	0.436	28.3	18.5	68	0.402	0.397	1.0
0.010	0.376	0.444	27.8	19.3	68	0.410	0.399	1.0
0.020	0.372	0.450	23.6	16.1	78	0.411	0.395	1.0
0.030	0.362	0.448	19.7	11.5	86	0.405	0.393	0.9
0.040	0.358	0.452	18.2	10.1	94	0.405	0.393	0.9
0.050	0.356	0.458	17.5	9.9	102	0.407	0.394	0.9
0.060	0.340	0.452	17.0	7.0	112	0.396	0.393	0.9

[a]Concentration of $NaClO_4$, 0.1 M; [b]scan rate, 1 mV/s and pulse height, 50 mV

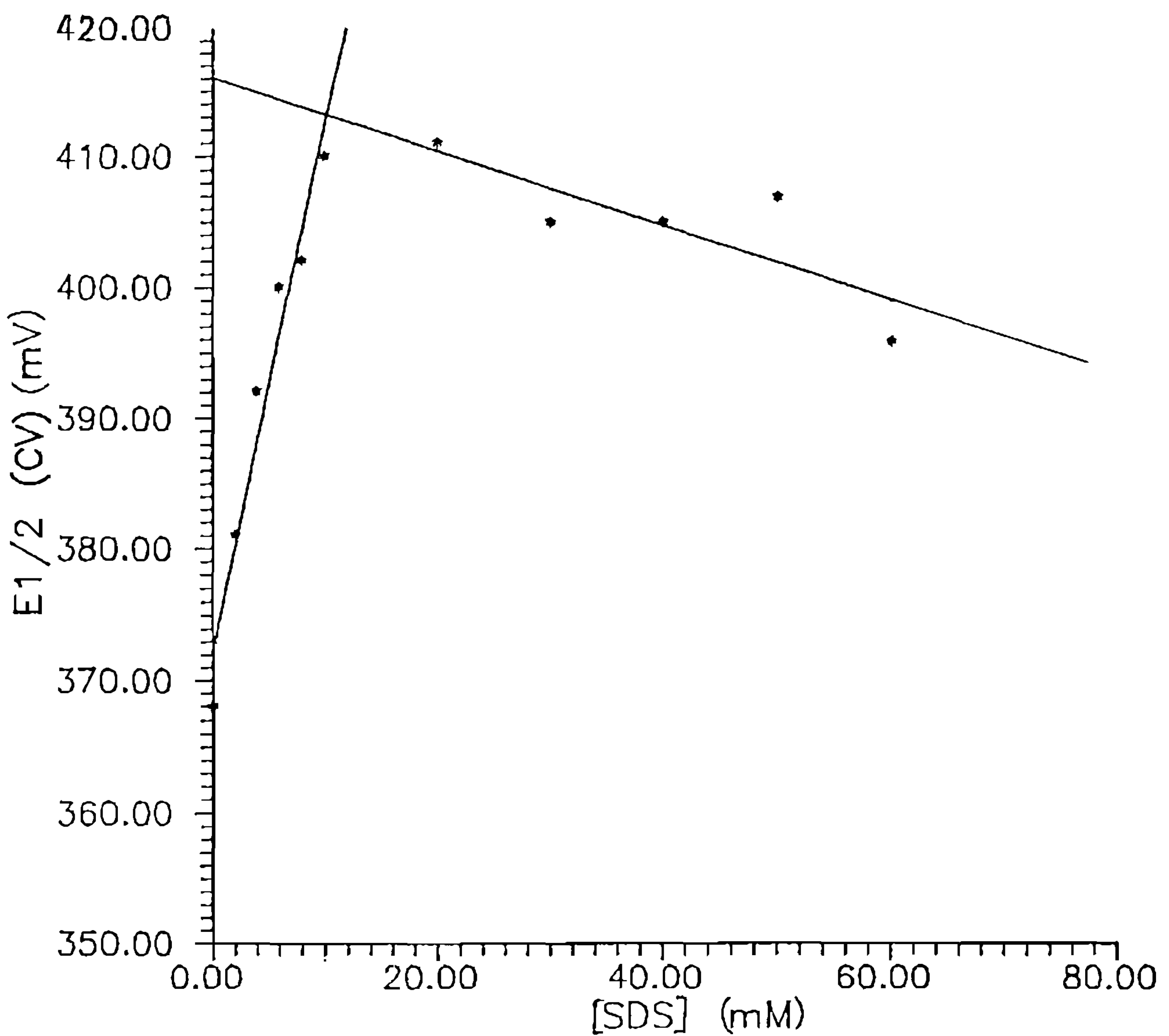


Fig. 6.12 Plot of $E_{1/2}$ values of $[Cu(pdto)]^{2+}$ in aqueous solution *vs* concentration of SDS added

conforms to the Berezin model which considers the surfactant solutions, above cmc, as a two phase system with the redox components partitioned between the aqueous and micellar pseudophases.[29] Further addition of SDS increases the viscosity of the solution,[30] which in turn retards the diffusion of the micelle-bound species and in 70 mM of SDS the redox waves are flattened beyond observation.

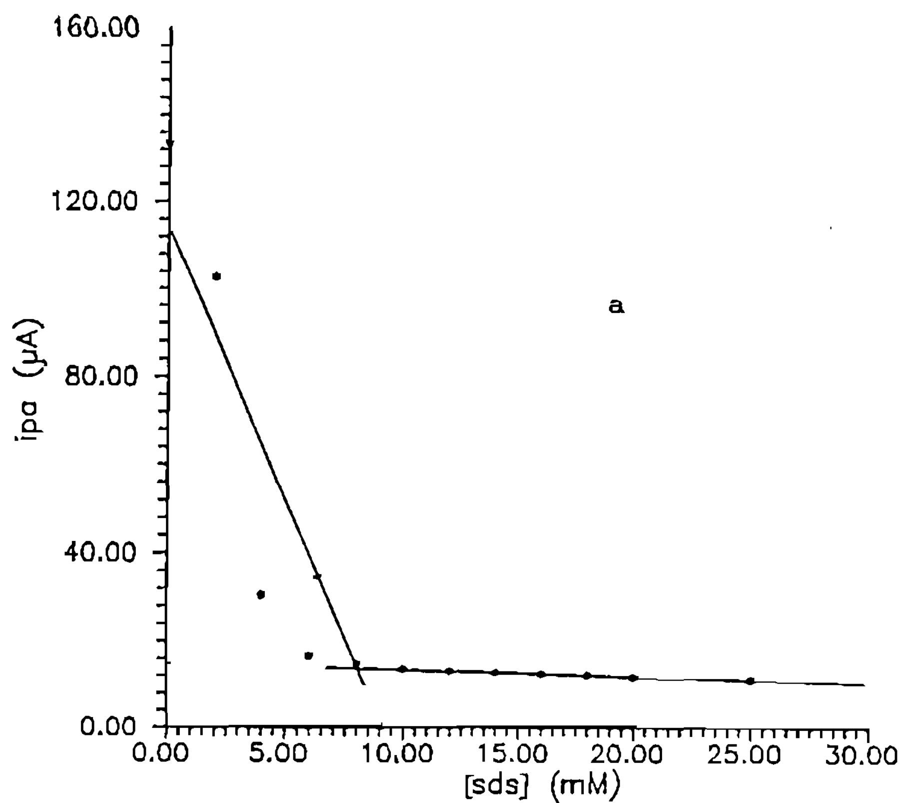
The complex $[Cu(bbdo)]^{2+}$ becomes soluble only when SDS concentration exceeds ≈ 9 mM and its electrochemistry (Fig. 6.8) is similar to its pyridine analogue $[Cu(pdto)]^{2+}$. However, the values of i_{pa}/i_{pc} (0.6) increases with increase in scan rate suggesting that an irreversible chemical reaction and/or a reorientation of the complex in the micellar environment occurs following the electron transfer (EC mechanism);[31] thus the $\triangle E_p^{\circ}$ value (78 mV) is not nearer to the Nernstian value.

When the concentration of SDS is increased, both the cathodic and anodic peak currents decrease up to ≈ 10 mM of SDS beyond which they remain almost constant for both $[Cu(pttn)]^{2+}$ (Table 6.4, Fig. 6.13) and $[Cu(pttu)]^{2+}$ (Table 6.5, Fig. 6.14). In the presence of 0.01 M SDS the peak current ratio and $\triangle E_p^{\circ}$ approach Nernstian values for $[Cu(pttn)]^{2+}$. The shape of the plot of i_{pa}/i_{pc} *vs* square root of scan rate suggests absence of any adsorption of Cu(I) product.[22]

Table 6.4 Redox properties of $[Cu(pttn)](ClO_4)_2$ complex (0.001 M) in aqueous solution[a] in the presence of SDS micelles with varying concentrations of SDS at 50 mV/s scan rate

[SDS] M	E_{pc} V	E_{pa} V	i_{pc} μA	i_{pa} μA	ΔE mV	$E_{1/2}$(V) CV	$E_{1/2}$(V) DPV[b]	i_{pa}/i_{pc}
0.000	0.294	0.376	54.6	127.0	82	0.335	0.307	2.5
0.002	0.280	0.354	47.9	102.5	74	0.317	0.297	2.5
0.004	0.268	0.314	31.7	30.3	79	0.291	0.307	1.4
0.006	0.278	0.350	25.7	16.4	72	0.314	0.314	1.0
0.008	0.280	0.350	23.1	14.6	70	0.315	0.317	1.0
0.010	0.284	0.358	21.8	13.4	74	0.321	0.321	1.0
0.012	0.286	0.358	21.0	13.0	72	0.322	0.319	1.0
0.014	0.290	0.356	20.4	12.6	68	0.323	0.320	1.0
0.016	0.286	0.358	20.2	12.3	72	0.322	0.317	1.0
0.018	0.282	0.360	20.1	12.0	78	0.321	0.317	1.0
0.020	0.284	0.358	20.0	11.6	74	0.321	0.318	1.0
0.025	0.282	0.360	19.9	11.0	78	0.321	0.316	1.0

[a]Concentration of $NaClO_4$, 0.1 M; [b]scan rate, 1 mV/s and pulse height, 50 mV



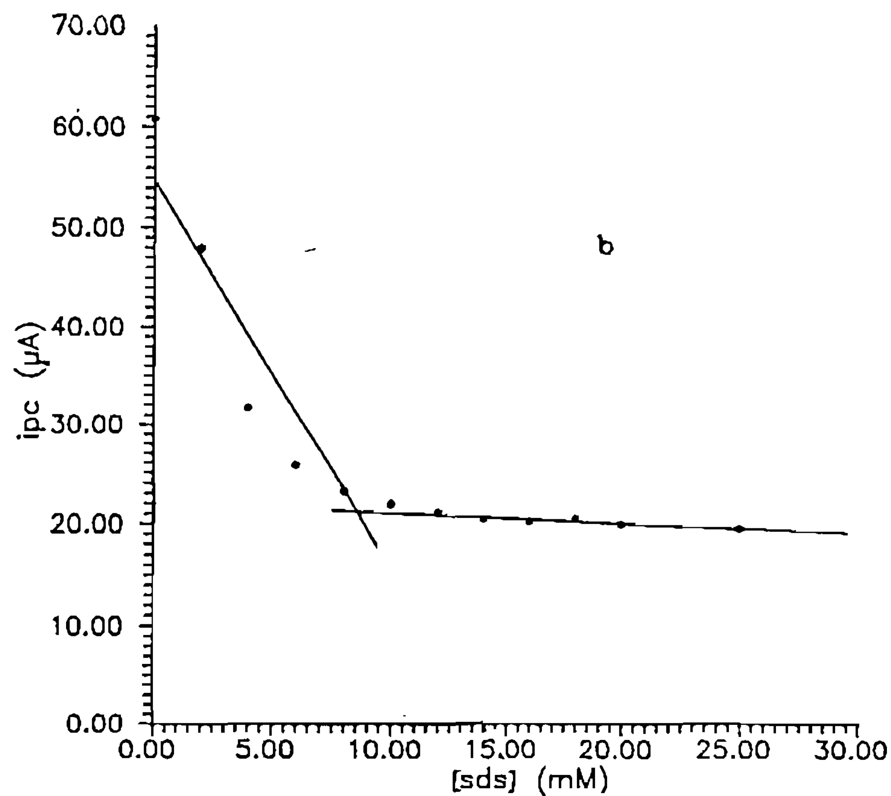
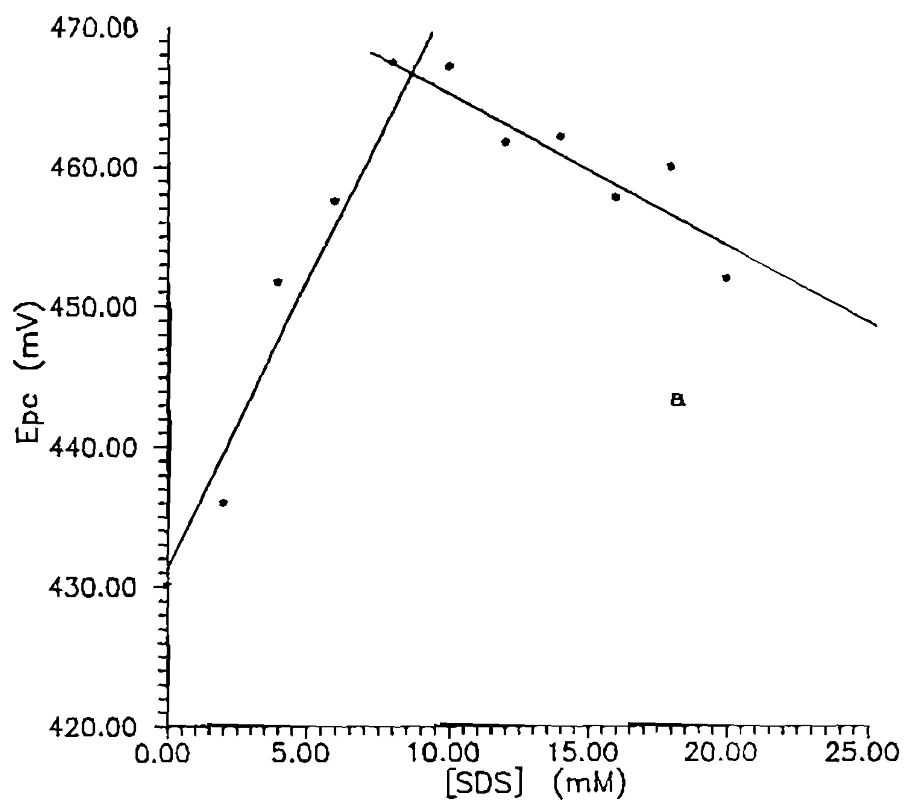


Fig. 6.13 Plot of anodic (a) and cathodic peak current (b) values of $[Cu(pttn)]^{2+}$ in aqueous solution *vs* concentration of SDS added

Table 6.5 Redox properties of $[Cu(pttu)](ClO_4)_2$ complex (0.001 M) in aqueous solution[a] in the presence of SDS micelles with varying concentrations of at SDS 50 mV/s scan rate

[SDS] M	E_{pc} V	E_{pa} V	i_{pc} μA	i_{pa} μA	ΔE mV	$E_{1/2}$(V) CV	$E_{1/2}$(V) DPV[b]	i_{pa}/i_{pc}
0.000	0.430	0.510	36.2	30.4	80	0.470	0.474	1.2
0.002	0.436	0.521	31.2	24.9	85	0.479	0.483	1.1
0.004	0.452	0.531	23.2	17.6	79	0.491	0.493	1.1
0.006	0.458	0.538	18.9	14.7	81	0.498	0.501	1.1
0.008	0.467	0.544	16.4	13.2	77	0.506	0.501	1.2
0.010	0.467	0.540	15.9	12.8	73	0.504	0.500	1.2
0.012	0.462	0.544	14.4	11.7	82	0.503	0.502	1.2
0.014	0.462	0.542	12.9	10.8	80	0.502	0.501	1.2
0.016	0.458	0.542	12.6	10.3	84	0.500	0.499	1.2
0.018	0.460	0.546	12.1	9.7	86	0.503	0.495	1.2
0.020	0.452	0.546	11.3	9.3	94	0.499	0.495	1.2
0.030	0.448	0.548	10.4	8.4	100	0.498	0.487	1.1
0.040	0.437	0.552	10.0	8.0	115	0.494	0.486	1.2
0.050	0.434	0.552	9.6	7.8	118	0.493	0.487	1.2

[a]Concentration of $NaClO_4$, 0.1 M; [b]scan rate, 1 mV/s and pulse height, 50 mV



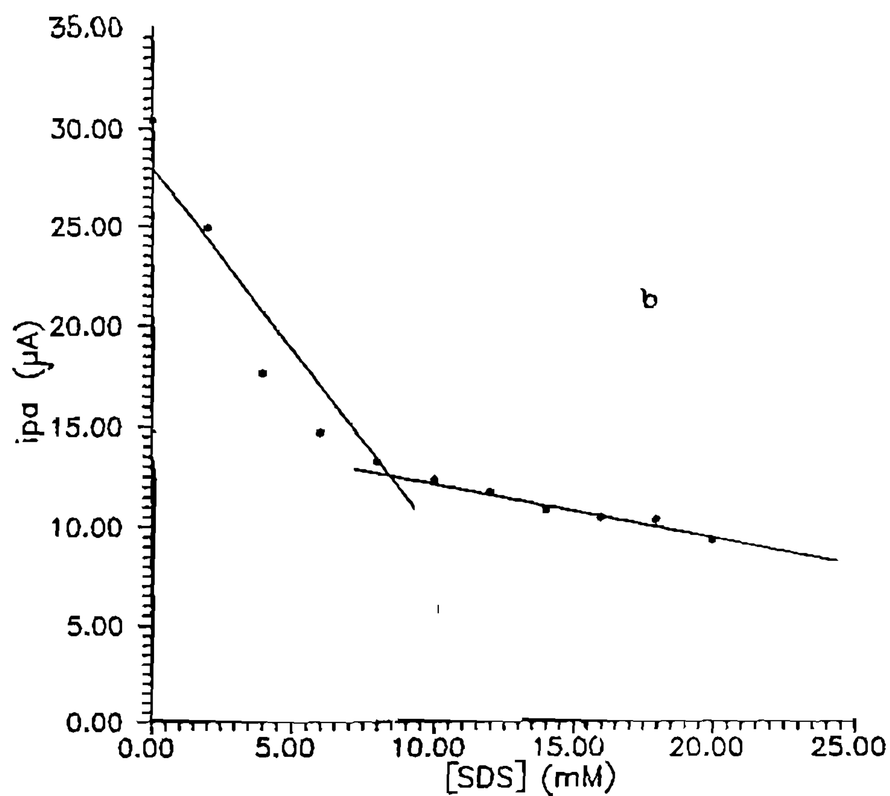


Fig. 6.14 Plot of cathodic peak potential (a) and anodic peak current (b) values of $[Cu(pttu)]^{2+}$ in aqueous solution vs concentration of SDS added

The diffusion coefficients at various concentrations of SDS were analysed using the equation,[32]

$$D_{obs} = [D_f + K_1(S_t - cmc)D_b]/[1 + K_1(S_t - cmc)]$$

where, D_f = diffusion coefficient of the free complex (in the absence of SDS)

D_b = diffusion coefficient of the micellar bound complex

K_1 = association constant per unit of SDS in the micelle

S_t = total molar concentration of added surfactant.

K_1, D_{obs} and cmc values were obtained by a nonlinear parameter optimization of D_{obs}-S_t data, as described in the experimental section (Figs. 6.15, 6.16). The data obtained using this equation are summarized in Table 6.6. The cmc values for SDS in the presence of 0.1 M $NaClO_4$ and 0.001 M $[Cu(N_2S_2)]^{2+}$ or $[Cu(N_2S_3)]^{2+}$ complex are only slightly less than or the same as that (*ca.* 8 mM) reported for SDS in salt free solutions.[33-35] This is interesting because cmc values are generally lowered in the presence of added salts[4] as observed for $[Co(phen)_3]^{3+}$ and $[Co(terpy)_3]^{3+}$ complexes.[32] This may be traced to the higher solubility of the present complexes in aqueous solution.

The value of K_1 obtained for the association of $[Cu(N_2S_3)]^{2+}$ complexes with SDS is much higher than that for $[Cu(pdto)]^{2+}$ (Fig. 6.15); the enhanced hydrophobic nature of $[Cu(N_2S_3)]^{2+}$ complexes, conferred by the additional methylene and thioether groups facilitates their interaction with SDS. $[Cu(pttn)]^{2+}$

Table 6.6 K_1 and cmc values calculated for the Cu(II)/Cu(I) complexes in SDS micelles[a]

Complex	K_1 M^{-1}	cmc mM	$D_f \times 10^6$ cm^2/s	$D_b \times 10^7$ cm^2/s
$[Cu(pdto)]^{2+}$	550 ± 26	8.00	2.69 ± 0.046	5.04 ± 0.009
$[Cu(pttn)]^{2+}$	17150 ± 967	7.95	7.14 ± 0.034	7.42 ± 0.015
$[Cu(pttu)]^{2+}$	1950 ± 143	7.80	2.56 ± 0.041	1.48 ± 0.010
$[Cu(pttu)]^{+}$	2600 ± 106	7.70	1.80 ± 0.027	1.10 ± 0.009

[a] cmc, critical micellar concentration of SDS in the presence of copper complex; D_f, experimental diffusion coefficient of the complex in absence of surfactant; D_b, calculated diffusion coefficient of the micelle bound complex

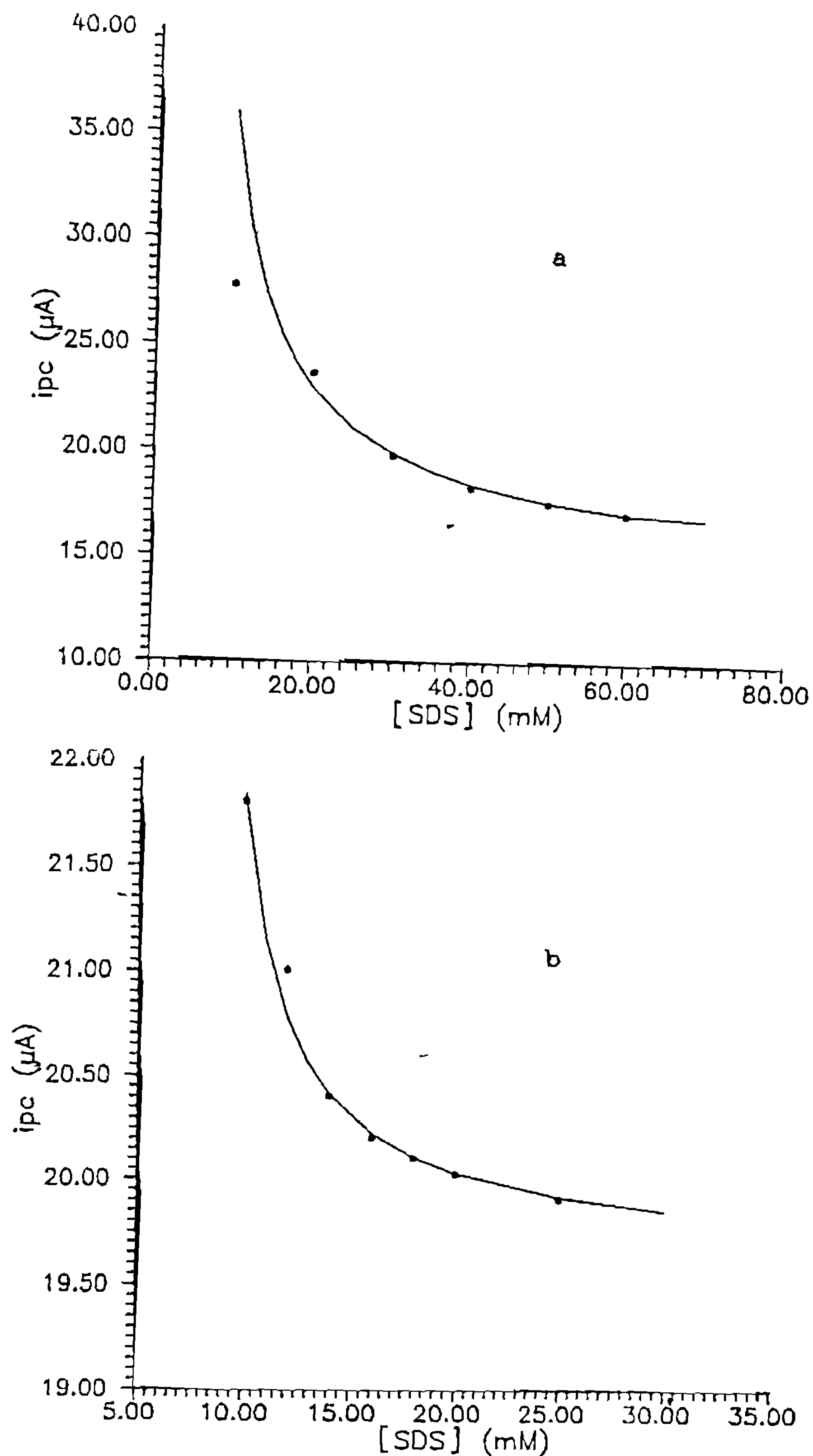
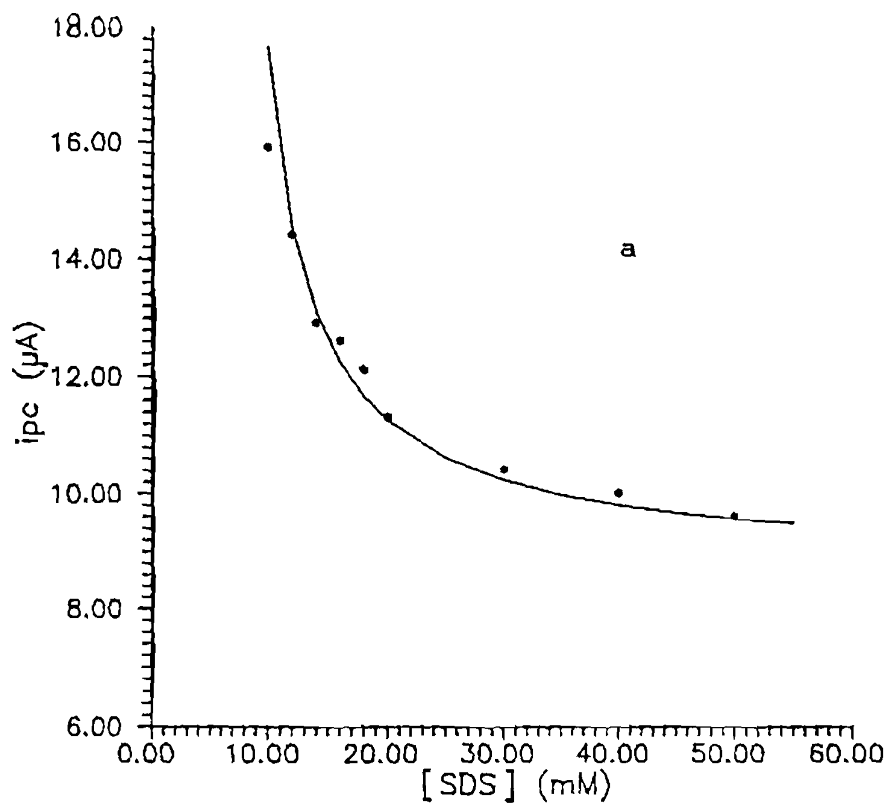


Fig. 6.15 Plot of observed (*) diffusion coefficients of $[Cu(pdto)]^{2+}$ (a), and $[Cu(pttn)]^{2+}$ (b) as a function of SDS concentration. Solid line is the best fit data and the best fit parameters are listed in Table 6.6.



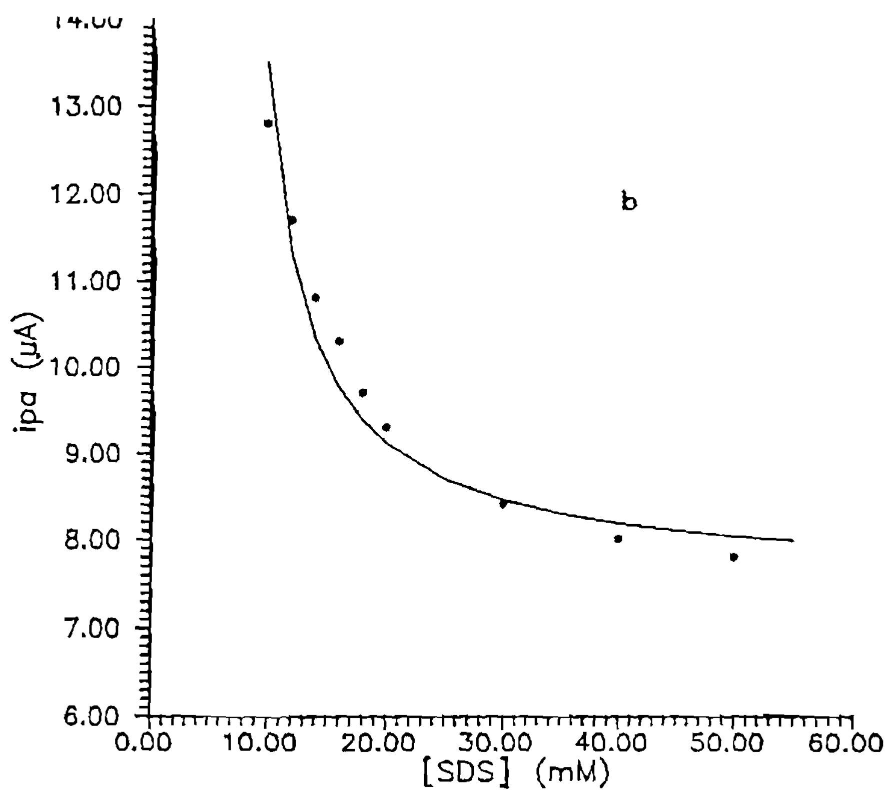


Fig. 6.16 Plot of observed (*) diffusion coefficients of $[Cu(pttu)]^{2+}$ (a) and $[Cu(pttu)]^{+}$ (b) as a function of SDS concentration. Solid line is the best fit data and the best fit parameters are listed in Table 6.6.

exhibits a binding ten-fold stronger than $[Cu(pttu)]^{2+}$, in spite of it possessing decreased hydrophobicity engendered by lesser number of methylene groups; this may be traced to its unique folded and less open geometry, the compactness of which appears to facilitate interaction with SDS.[16] Further, the K_1 value calculated for $[Cu(pttu)]^{+}$ (Fig. 6.16) is larger than that for its oxidised counterpart; the greater hydrophobic solvation of the uncoordinated py moiety in the hydrophobic $[Cu(pttu)]^{+}$ with a tetrahedral structure[17] (Fig. 6.1, Chapter 4), in the micellar interior appears to offset the electrostatic disadvantage of the +1 charge. The K_1 values for the present complexes are much higher than that (550 M^{-1}) determined for tris(phenanthroline) cobalt(III) complex, expected of their open structure and lower hydrophobicity of the ligands.[32,36] Further, they are of the same order as those (1 - 56 x 10^4) for tris-ruthenium(II) complexes of substituted phenanthrolines in Triton X-100 micelles.[37]

6.3.4 Electrochemical Behaviour in 0.1 M TEABr/0.01 M CTAB

In 0.1 M TEABr/0.01 M CTAB solutions the complexes $[Cu(pttn)]^{2+}$ and $[Cu(pttu)]^{2+}$ are insoluble; however, $[Cu(pdto)]^{2+}$ and $[Cu(bbdo)]^{2+}$ are soluble. The values of both the peak currents for $[Cu(pdto)]^{2+}$ are lower and the values of peak current ratio higher (1.4) than those in aqueous 0.1 M $(C_2H_5)_4NBr$ solution (Fig. 6.7); the ΔE_p (ΔE_p°, 68 mV) values are high, revealing an irreversible Cu(II)/Cu(I) couple. The Cu(II)/Cu(I) couple of

$[Cu(bbdo)]^{2+}$ is less reversible, as understood from the higher ΔE_p value (ΔE_p°, 67 mV) and the deviation of i_{pa}/i_{pc} from unity (Table 6.2). For both $[Cu(pdto)]^{2+}$ and $[Cu(bbdo)]^{2+}$ the i_{pa}/i_{pc} and ΔE_p values increase with increase in scan rate, consistent with the involvement of an EC mechanism as for $[Cu(bbdo)]^{2+}$ in SDS micelles. The decrease in peak current which is much less than that in SDS and the reduced solubility in CTAB are typical of the electrostatic repulsion between the solute and the positively charged micelles.

6.3.5 Effect of Triton X-100 Micelles

The redox behaviour in nonionic Triton X-100 surfactant offers some contrasts to those in ionic surfactants. Thus the cyclic voltammograms of $[Cu(pdto)]^{2+}$ (Fig. 6.6) and $[Cu(bbdo)]^{2+}$ (Fig. 6.8) in 5 % Triton X-100 ($\approx$ 0.01 M) exhibit two waves corresponding to Cu(II)/Cu(I) and Cu(I)/Cu(0) couples; the latter is not observed in aqueous isotropic solution. The peak currents and hence D values are suppressed (Table 6.2) for all the Cu(II) complexes, suggesting that the complexes are mainly in the bound form.

For $[Cu(pdto)]^{2+}$ the ΔE_p value decreases (98 mV); the i_{pa}/i_{pc} value is nearer to unity and increases slightly with increase in $\sqrt{\nu}$ (Table 6.2), suggesting no adsorption of Cu(I) species (Fig. 6.6). The second redox process is observed with high

ΔE_p (146 mV) as well as i_{pa}/i_{pc} values indicating the adsorption of electrogenerated metallic copper on the electrode surface.[22] The $E_{1/2}$ value for the Cu(I)/Cu(0) couple is 0.004 V (*vs* SCE) which is very high compared to the reported[15b] value of -0.78 V (*vs* SCE) in acetonitrile, illustrating that hydrophobic interactions stabilize Cu(I) state. A similar redox behaviour is observed for $[Cu(bbdo)]^{2+}$ (Fig. 6.8); however, the i_{pa}/i_{pc} value becomes less than unity for Cu(I)/Cu(0) couple (Table 6.2). $[Cu(pttu)]^{2+}$ also exhibits a quasireversible Cu(II)/Cu(I) redox behaviour (Fig. 6.10) with almost the same values of ΔE_p and i_{pa}/i_{pc} as in aqueous isotropic solution, but no Cu(I) ---> Cu(0) process. Contrastingly, $[Cu(pttn)]^{2+}$ exhibits a redox process with low ΔE_p (54 mV, ΔE_p° = 46 mV) and i_{pa}/i_{pc} (1.2) values, suggesting Cu(II) ---> Cu(0) process and preferential stabilization of the Cu(II) complex by interaction with the non-ionic micelles. The ΔE_p value increases, whereas i_{pa}/i_{pc} value remains constant with increase in scan rate.

6.3.6 Electrochemical Redox Mechanism

The dramatic difference in the spectral and electrochemical properties of Cu(II) complexes in aqueous and aqueous micellar solutions illustrates that the complexes are largely situated within the micellar environment and implies that the redox mechanisms are different and dependent on the nature of the surfactant as well as the Cu(II) complex. The decrease in D values with added surfactants suggest that the micelle-solubilized cations

diffuse to the electrode surface. The absence of adsorption for $[Cu(pdto)]^{2+}$, $[Cu(bbdo)]^{2+}$ and $[Cu(pttn)]^{2+}$ complexes in SDS micellar solution reveals that the electrogenerated Cu(I) species are solubilized and stabilized in micellar environment. It is likely that these species are situated on the micellar surface with much deeper penetration of py/benz moieties into the hydrophobic core. Generally, the configurational changes accompanying Cu(II)/Cu(I) electron transfer are not facile in low molecular weight complexes, compared to blue copper proteins, due presumably to solvent or anion participation in addition to several other factors[38] like adsorption of the reduced species. But in SDS micellar solution both the micelle-solubilized Cu(II) and Cu(I) species appear to have structures ideal for facile electron transfer with minimal structural change leading to the observation of diffusion-controlled, reversible electron transfer. It is interesting to note that $[Cu(bbdo)]^{+}$ undergoes further reaction as discussed already.

We suspect that it is the monopositive $[Cu(pdto)Br]^{+}$ and $[Cu(bbdo)Br]^{+}$ species which are significantly stabilized rather than the corresponding dipositive species in the positively charged stern layer of CTAB micelle. Crystallographic and cyclic voltammetric[39] evidences are available to illustrate the coordination of halide and other such anions to $[Cu(N_2S_2)]^{2+}$ chromophores.[40-43] The $[Cu(pdto)Br]^{+}$ and $[Cu(bbdo)Br]^{+}$ species

solubilized in the hydrophobic core of CTAB micelles has to presumably move to the surface of the electrode against the positively charged micellar surface potential, undergo electron transfer and then return to the hydrophobic environment as seen from the absence of adsorption. Since the reduced species is more hydrophobic than its oxidised counterpart, the reentry is probably faster than the exit process.[32] Interestingly $[Cu(bbdo)]^{+}$ undergoes further reaction as in SDS micelles. The dissociation of coordinated Br^{-} may constitute the structural rearrangement accompanying electron transfer and account for the enhanced irreversibility, compared to aqueous solution. Thus the movement of the complexes to the outer surface of the micelle appears to be a prerequisite for electron transfer.

In Triton X-100 micelles the diffusion of Cu(II) complexes situated in the hydrophobic microenvironment to the electrode surface for reduction and back is relatively facile as there is no opposing surface potential; this is in contrast to the behaviour in CTAB micelles. Thus $[Cu(pttn)]^{2+}$ shows Nernstian redox behaviour in this non-ionic micellar solution; however, the electron transfer is still irreversible for the other three complexes. The non-polar hydrophobic environment provided by these micelles appears unsuitable for stabilizing $[Cu(pdto)]^{+}$ and $[Cu(bbdo)]^{+}$ from further reduction to metallic copper. This confirms the diffusion of electroactive species to the electrode surface for electron

transfer. It is interesting that Cu(I) ---> Cu(0) process for $[Cu(pttu)]^{2+}$ in Triton X-100 and for all the complexes in other micelles is not discernible. We believe that the novel and unique behaviour of $[Cu(pdto)]^{2+}$, $[Cu(bbdo)]^{2+}$ and $[Cu(pttn)]^{2+}$ in Triton X-100 micelles is due to different degrees of stabilization of their Cu(II) and Cu(I) structures by non-Coulombic interactions.

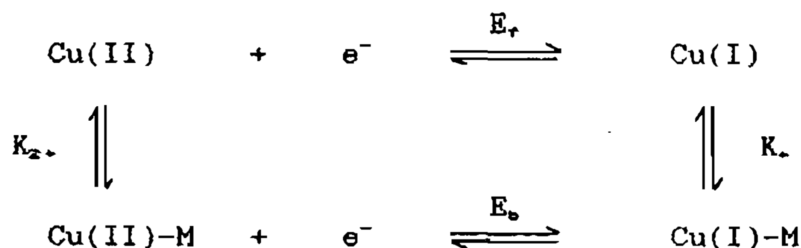
Thus the electrostatic interaction in ionic micelles and dipolar ones in nonionic micelles affect the solubilization and stabilities of the redox species to various degrees and so not only the redox potential and reversibility but also the occurrence of Cu(I) ---> Cu(0) process is dictated by the nature of micellar environment and complex. The `structural reorganisation´ step which may be accompanied by the decomposition of coordinated anion or solvent would account for the decreased reversibility but it is difficult to distinguish these two processes. Thus all stages of redox mechanism are controlled, intriguingly, by the addition of surfactants.

6.3.7 Redox Potentials

The data in Table 6.2 show that the peak potentials are strongly dependent on the nature of the complex and the surfactant used. Alterations of the peak potentials can be expected as a result of preferential interacton between the medium and a member of the redox couple.[26,34] Metal ions are known to bind strongly to

anionic micelles[44] and $[Co(bpy)_3]^{2+}$ [12] and $[MD_2X_2]^{+}$ [20] [M = Tc, Re; D = depe, dmpe; X = Cl^-, Br^-] have been found to be harder to reduce than in water. So the present dipositive copper complexes are also expected to be stabilized by Coulombic interaction with the negatively charged SDS micelles and become harder to reduce. Thus the $E_{1/2}$ values of $[Cu(bbdo)]^{2+}$ and $[Cu(pttn)]^{2+}$ become negative; by contrast, those of $[Cu(pdto)]^{2+}$ and $[Cu(pttu)]^{2+}$ increase, implying that the solubilization and net stabilization of Cu(I) species on the surface of the micelle, with partial hydrophobic interaction substantially offsets the electrostatic interaction and stabilization of the Cu(II) species. Similar positive shifts have been observed for $[Co(phen)_3]^{3+}$ [34] and $[Co(terpy)_3]^{3+}$.[45] The tetrahedral structures[15a,17] (Fig. 6.1) of $[Cu(pdto)]^{+}$ (Fig. 1.10) and $[Cu(pttu)]^{+}$ (Fig. 4.10), the latter with an uncoordinated hydrophobic py moiety, appear to be more hydrophobic than the square-based geometries[15a,17] of the corresponding Cu(II) species. The hydrophobic environment in micelles appears to be less suitable to stabilize presumably tetrahedral $[Cu(bbdo)]^{+}$ and $[Cu(pttn)]^{+}$ species in spite of the strongly hydrophobic bzim and py rings. The compact folded structures of their Cu(II) forms are preferentially stabilized by ionic interaction with anionic SDS micelles; Coulombic solvation energy appears dramatically more important than the hydrophobic interaction. Further, $[Cu(bbdo)]^{2+}$ generated is very unstable, as discussed above.

All the above observations are clearly illustrated by the K_{+}/K_{2+} values (Scheme 6.2, Table 6.2) which are measures of the relative stabilization of the redox components of the Cu(II)/Cu(I) couple in micellar media, with respect to water.



Scheme 6.2

These values are calculated from the shift in $E_{1/2}$ values by assuming reversible binding and using the equation,[44]

$$E_b - E_f = 0.059 \log(K_{+}/K_{2+})$$

where, E_f and E_b are the redox potentials for the free and bound forms respectively and K_{+} and K_{2+} are the equilibrium constants for the binding of Cu(I) and Cu(II) respectively to the micelle (M). The trend in this ratio is consistent with the K_1 values discussed above. Further, this ratio ranges from 0.1 to 5.6, suggesting that the binding of the complexes to micelles is only slightly affected by the complex charge. A similar observation has been made for cobalt(III) tris(phenanthroline) complexes.[32]

In CTAB micelles, both $[Cu(pdto)]^{2+}$ and $[Cu(bbdo)]^{2+}$ exhibit

low values of K_{+}/K_{2+} suggesting that significant solubility stabilization of Cu(II) species (see above) in the hydrophobic core overrides the potentially unfavourable Coulombic interactions. Further, $[Cu(pdto)]^{+}$ rather than $[Cu(bbdo)]^{+}$ is more stabilised over their respective Cu(II) in CTAB micelles, as discussed already.

The nonionic Triton X-100 micelles generate the most interesting electrochemistry. The enhanced ease of reduction of $[Cu(pdto)]^{2+}$, $[Cu(bbdo)]^{2+}$ and $[Cu(pttu)]^{2+}$ observed in this medium may result from solubilization properties of this surfactant, which are dominated by the relatively weak non-Coulombic interactions suitable to stabilize the hydrophobic Cu(I) forms with lower charge. As in SDS micellar solution, $[Cu(pttn)]^{2+}$ is stabilized in this micellar solution also. Thus as the nature of the micelles change from anionic to non-ionic to cationic, their ability to stabilize tetrahedral $[Cu(pdto)]^{+}$ and $[Cu(pttu)]^{+}$ species decreases; while $[Cu(pttn)]^{2+}$ is preferentially stabilized in all the micelles studied, $[Cu(bbdo)]^{+}$ in non-ionic micelles. For a given micelle, the ligand enlargement by incorporating CH_2 and/or thioether donor and the replacement of py by bzim ring lead to a decrease in relative stabilization of Cu(I). Thus the interaction of Cu(II) complexes with micelles depends on their structure as well as the nature of micelles. The stabilization of Cu(I) and hence the $E_{1/2}$ depends on the delicate balance between hydrophobic and electrostatic interactions.

6.4 Conclusions

Significant micellar effects are observed in the redox behaviour of all the present complexes. The stronger association and hence the net solubilization stabilization of most of the present monopositive Cu(I) species in SDS and Triton X-100 micelles, as evident from K_{+}/K_{2+} values, depends primarily on the nature of the ligand as well as the structure of the complexes. This is obviously because hydrophobic interactions involving the coordinated ligands and the micellar interior are more important than electrostatic or dipolar interactions. It has been shown[32] that electrostatic contributions to the micellar binding ranges from *ca.* 5 % for the Co(II) to around 50 % for Co(III) species. A similar variation would be expected for the present Cu(I) and Cu(II) species. For both $[Cu(pdto)]^{2+}$ and $[Cu(bbdo)]^{2+}$ the strong binding of Cu(II) rather than Cu(I) species, to the positively charged CTAB micelles suggest that hydrophobic interactions are more important than Coulombic repulsions. When the hydrophobicity of a complex is increased by substituting py by bzim moiety, the interaction with CTAB micelles is increased. The observation of Cu(I)/Cu(0) redox couple, in addition to Cu(II)/Cu(I) for the CuN_2S_2 chelates in Triton X-100 micelles supports the importance of hydrophobic association for the present systems.

Further, the reversibility of Cu(II)/Cu(I) redox couple of

most of the present copper complexes, in the micellar microenvironments of SDS and Triton X-100 micelles is increased and in some cases the redox potential is raised. This is relevant to the facile electron transfer of blue copper proteins and enzymes in biological environment. This behaviour is in contrast to those observed generally for Cu(II)/Cu(I) couple in non-aqueous solvents and is different from those of Co(II), Tc(III) and Re(III) complexes in micelles;[12,21] the latter complexes do not obviously involve any major structural rearrangement.

The present study reveals that the redox process involves electron transfer to Cu(II) species in aqueous phase, after its exit from micellar subphase. The subsequent rapid reentry of the reduced Cu(I) species into the micellar core is facilitated by its hydrophobic nature. Thus the present work demonstrates the importance of hydrophobic interactions over electrostatic ones in the binding of charged copper complexes to micelles; however, no separation of these contributions to micellar binding is possible. Further, the present study would be expected to pave the way for electrocatalysis by Cu(I) complexes in micellar solutions.

References

(1) Solomon, E. I.; Baldwin, M. J.; Lowery, M. D. *Chem. Rev.* **1992**, *92*, 521.

(2) Addison, A. W.; Rao, T. N.; Sinn, E. *Inorg. Chem.* **1984**, *23*, 1957.

(3) Kitajima, N.; Fujisawa, K.; Moro-oka, Y. *J. Am. Chem. Soc.* **1990**, *112*, 3210; Kitajima, N. *Adv. Inorg. Chem.* **1992**, *39*, 1.

(4) Fendler, J. H.; Fendler, E. J. *Catalysis in Micellar and Macromolecular Systems*; Academic press: New York, 1975.

(5) Fuhrhop, J -H.; Svenson, S.; Boettcher, C.; Rossler, E.; Vieth, H -M. *J. Am. Chem. Soc.* **1990**, *112*, 4307.

(6) a) Franklin, T. C.; Iwunze, M. *J. Electrochem. Soc.* **1980**, *108*, 97; b) Mc. Intyre, G. L.; Blount, H. N. *J. Am. Chem. Soc.* **1979**, *101*, 7720.

(7) Meyer, G.; Nadjo L.; Saveant, J. M. *J. Electroanal. Chem.* **1981**, *119*, 417.

(8) Kirchhoff, J. R.; Deutsch, E.; Heineman, W. R. *Anal. Lett.* **1989**, *22*, 1323.

(9) Fendler, J. H. *Membrane Mimetic Chemistry*; Wiley-Interscience: New York, 1982; Fendler, J. H. *Chem. Rev.* **1987**, *87*, 877.

(10) Yeh, P.; Kuwana, T. *J. Electrochem. Soc.* **1976**, *123*, 1334.

(11) a) Piszkiewicz, D. *J. Am. Chem. Soc.* **1976**, *98*, 3053; b) Broxton, T. J.; Cox, R. A. *Can. J. Chem.* **1993**, *71*, 670.

(12) a)Rusling, J. F.; Kamau, G. N. *J. Electroanal. Chem.* **1985**, *187*, 355; b) Kamau, G. N.; Leipert, T.; Shukla, S. S.; Rusling, J. F. *J. Electroanal. Chem.* **1987**, *233*, 173.

(13) a) Ohsawa, Y.; Aoyagui, S. *J. Electroanal. Chem.* **1982**, *136*, 353; b) Rusling, J. F.; Shi, C-N.; Kumosinki, T. F. *Anal. Chem.* **1988**, *60*, 1260.

(14) Roodt, A.; Sullivan, J. C.; Meisel, D.; Deutsch, E. *Inorg. Chem.* **1991**, *30*, 4545

(15) a) Brubaker, G.; Brown, R.; Yoo, M. K.; Kinsey, R. A.; Kutchan, T. M.; Mottel, E. A. *Inorg. Chem.* **1979**, *18*, 299; b) Sakaguchi, U.; Addison, A. W. *J. Chem. Soc., Dalton Trans.* **1979**, 600; c) Nikles, D. E.; Powers, M. J.; Urbach, F. L. *Inorg. Chem.* **1983**, *22*, 3210.

(16) a) Kanters, R. P. F.; Yu, R.; Addison, A. W. *Inorg. Chim. Acta* **1992**, *196*, 97; b) Adhikary, B.; Lucas, C. R. *Inorg. Chem.* **1994**, *33*, 1376; c) Liu, S.; Lucas, C. R.; Hynes, R. C.; Charland, J. P. *Can. J. Chem.* **1992**, *70*, 1773.

(17) Sivagnanam, U.; Fujisawa, K.; Palaniandavar, M. to be communicated.

(18) Goodwin, H. A.; Lions, F. *J. Am. Chem. Soc.* **1960**, *82*, 5013.

(19) Lindman, B.; Wennerstrom, H. *Top. Curr. Chem.* **1980**, *87*, 1; Menger, F. M. *Acc. Chem. Res.* **1979**, *12*, 111; Dill, K. A.; Koppel, D. E.; Cantor, R. S.; Dill, J. D.; Bendedouch, D.; Chen, S. -H. *Nature (London)* **1984**, *309*, 42.

(20) Kirchoff, J. R.; Heineman, W. R.; Deutsch, E. *Inorg. Chem.* **1988**, *27*, 3608.

(21) Zanello, P. *Comments Inorg. Chem.* **1988**, *8*, 45.

(22) Wopschall, R. H.; Shain, I. *Anal. Chem.* **1967**, *39*, 1514.

(23) Anson, F. C.; Lee, C. W. *Inorg. Chem.* **1984**, *23*, 837.

(24) Sivagnanam, U.; Palaniandavar, M. *J. Chem. Soc., Dalton Trans.* **1994**, 2277; Addison, A. W.; Palaniandavar, M.; Reedijk, J.; van Rijn, J.; Rao, T. N. unpublished work.

(25) Bard, A. J.; Faulkner, L. R. *Electrochemical methods: Fundamental applications*; John Wiley & Sons: New York, 1980; p 218.

(26) Carter, M. T.; Rodriguez, M.; Bard, A. J. *J. Am. Chem. Soc.* **1989**, *111*, 8901.

(27) Kaifer, A. E.; Bard, A. J. *J. Phys. Chem.* **1985**, *89*, 4876.

(28) Oshawa, Y.; Shimazaki, Y.; Aoyagui, S. *J. Electroanal. Chem.* **1980**, *114*, 235.

(29) Berezin, I. V.; Martinek, K.; Yatmimirskii, A. K. *Russ. Chem. Rev. (Engl. Transl.)* **1973**, *42*, 787.

(30) Lindman, B.; Wennerstrom, H. *Top. Curr. Chem.* **1980**, *87*, 1.

(31) Brown, E. R.; Large, R. F. In *Techniques of Chemistry: Physical Methods of Chemistry*; Weissberger, A.; Rossiter, B. W., Eds.; John Wiley & Sons, Inc.: New York, 1971; Chapter VI.

(32) Davies, K.; Hussam, A. *Langmuir* **1993**, *9*, 3270.

(33) Kratohvil, S.; Shinoda, K.; Matijevic, E. *J. Colloid Interface Sci.* **1979**, *72*, 106.

(34) Tarter, H. V.; Lelong, A. L. M. *J. Phys. Chem.* **1955**, *59*, 1185.

(35) Mukerjee, P.; Mysels, K. J. "Critical Micelle Concentration of Aqueous Surfactant Systems"; National Bureau of Standards Report No. NSRDS-NBS 36; U.S. Government Printing Office, Washington, DC, 1971.

(36) Davies, K. M.; Hussam, A.; Rector, B. R., Jr.; Owen, I. M.; King, P. *Inorg. Chem.* **1994**, *33*, 1741.

(37) Dressick, W. J.; Hausenstein, B. L.; Gilbert, T. B.; Demas, J. N.; DeGraff, B. A. *J. Phys. Chem.* **1984**, *88*, 3337.

(38) Bernardo, M. M.; Robandt, P. V.; Schroeder, R. R.; Rorabacher, D. B. *J. Am. Chem. Soc.* **1989**, *111*, 1224.

(39) Cabral, M. F.; De. O. Cabral, J.; van Rijn, J.; Reedijk, J. *Inorg. Chim. Acta* **1984**, *87*, 87.

(40) Addison, A. W.; Rao, T. N.; Reedijk, J.; van Rijn, J.; Verschoor, G. C. *J. Chem. Soc., Dalton Trans.* **1984**, 1349.

(41) Birker, P. J. M. W. L.; Helder, J.; Hankel, G.; Krabs, B.; Reedijk, J. *Inorg. Chem.* **1982**, *21*, 357.

(42) Rietmeijer, F. J.; Birker, P. J. M. W. L.; Gorter, S.; Reedijk, J. *J. Chem. Soc., Dalton Trans.* **1982**, 1191.

(43) Bouwman, E.; Burik, A.; Ten Hove, J. C.; Driessen, W. L.; Reedijk, J. *Inorg. Chim. Acta* **1988**, *150*, 125.

(44) Grieser, F.; Tausch-Treml, R. *J. Am. Chem. Soc.* **1980**, *102*, 7258.

(45) Fernandez, M. S.; Fromherz, P. *J. Phys. Chem.* **1977**, *81*, 1755.

(46) Sivagnanam, U.; Palaniandavar, M. *J. Electroanal. Chem.* **1992**, *341*, 197.

CHAPTER 7

7. A DOLL IN A DOLL SURROUNDED BY DOLLS: NOVEL, SELECTIVE AND COOPERATIVE ASSEMBLY OF CYCLODEXTRINS AROUND [1,8-BIS-(PYRID-2-YL)-3,6-DITHIAOCTANE]COPPER(II)

7.1 Introduction

Cyclodextrins (CDs) are toroidally shaped polysaccharides made up of six (α-CD), seven (β-CD) and eight (τ-CD) D-glucose monomers, joined by α(1-4) bonds.[1] Because of the hydrophobic nature of the inner cavity, they act as hosts for many organic molecules,[2,3] inorganic ions[4-6] and organometallic compounds[7,8] and form inclusion complexes when the guest and the cavity of host are of appropriate size[9] and are the most important and widely studied examples of host molecules. The second sphere coordination of transition metal (platinum and rhodium) complexes bearing hydrophobic ligands, consisting of CDs have been structurally characterized by Alston *et al.*[10-12] in the solid state using X-ray crystallography. In these complexes the hydrophobic ligand penetrates the cavity of the CD *viz* the wider aperture of the receptor associated with the face bearing the secondary hydroxyl groups.

Cyclodextrin is also a well-constructed miniature of an enzyme in the sense that it has a hydrophobic cavity of appropriate

size, sites for introduction of catalytic groups at juxtapositions, and satisfactory water solubility[13] and many enzyme models based on CDs have been reported.[14] The rate and stereochemical pathway of organic reactions are significantly changed by the inclusion complexation of substrates with cyclodextrin. Since the modes of action of such reactions are very similar to those in enzymes or biological receptors, cyclodextrins have been regarded as good models for the biopolymers. Since the structure of CD is well defined, one can observe what is really happening at the action site more unequivocally than in the cases of biopolymers.

It is known that several intermolecular interactions are responsible for CD complexation, acting simultaneously. Several intermolecular interactions have been proposed and discussed as being responsible for the formation of cyclodextrin inclusion complexes in an aqueous solution.[13,15-17] They are hydrophobic interaction, van der Waals interaction, hydrogen bonding, the relief of high energy water from the cyclodextrin-water adduct, together with the formation of a hydrogen bonding network around the O(2), O(3) side of the cyclodextrin macrocycle, upon substrate inclusion.

We have been interested in the elucidation of the novel spectral and electrochemical behaviour of blue copper proteins by constructing models. Since inclusion complex formation of CD, added

in solution or bound to the electrode has been shown to enhance the electrochemical reversibility of several organic guests[18] and since CDs have been studied extensively as models for enzyme active sites,[15,19] we focus our attention on the electrochemical behaviour of Cu(II) complexes designed as models for blue proteins in the presence of CDs. The inclusion phenomenon of bis(pyrid-2-yl-carbinolato)copper(II) by CDs has been investigated[6] but by using EPR and CD spectra. Recently, the effect of α- and β-CDs on the ligand substitution reactions of pentacyano(N-heterocycle)-ferrate(II) complexes has been reported.[20] No study has been made so far on the effect of CDs on the electrochemical behaviour of any metal or its complex species; only the electrochemical oxidation of ferrocene-carboxylic acid in the presence of β-CD has been investigated.[21,22] For the present investigation we have chosen the Type I blue protein model complexes $[Cu(pdto)]^{2+}$ [pdto = 1,8-bis(pyrid-2-yl)-3,6-dithiaoctane],[23] $[Cu(bbdo)]^{2+}$ (bbdo = 1,8-bis(benzimidazol-2-yl)-3,6-dithiaoctane) (Chapter 4),[24] $[Cu(pttn)]^{2+}$ (pttn = 1,9-bis(pyrid-2-yl)-2,5,8-trithianonane)[25] and $[Cu(pttu)]^{2+}$ (pttu = 1,11-bis(pyrid-2-yl)-3,6,9-trithiaundecane) (Chapter 4)[24] with CuN_2S_2 and CuN_2S_3 chromophores (Scheme 6.1, Fig. 7.1). Although a few reports on the inclusion complex formation of metal complexes with CDs are known,[22,26] the complex formation with the CDs, described in the present study is unique and relevant to active transport or concentration of substrates in biological systems.

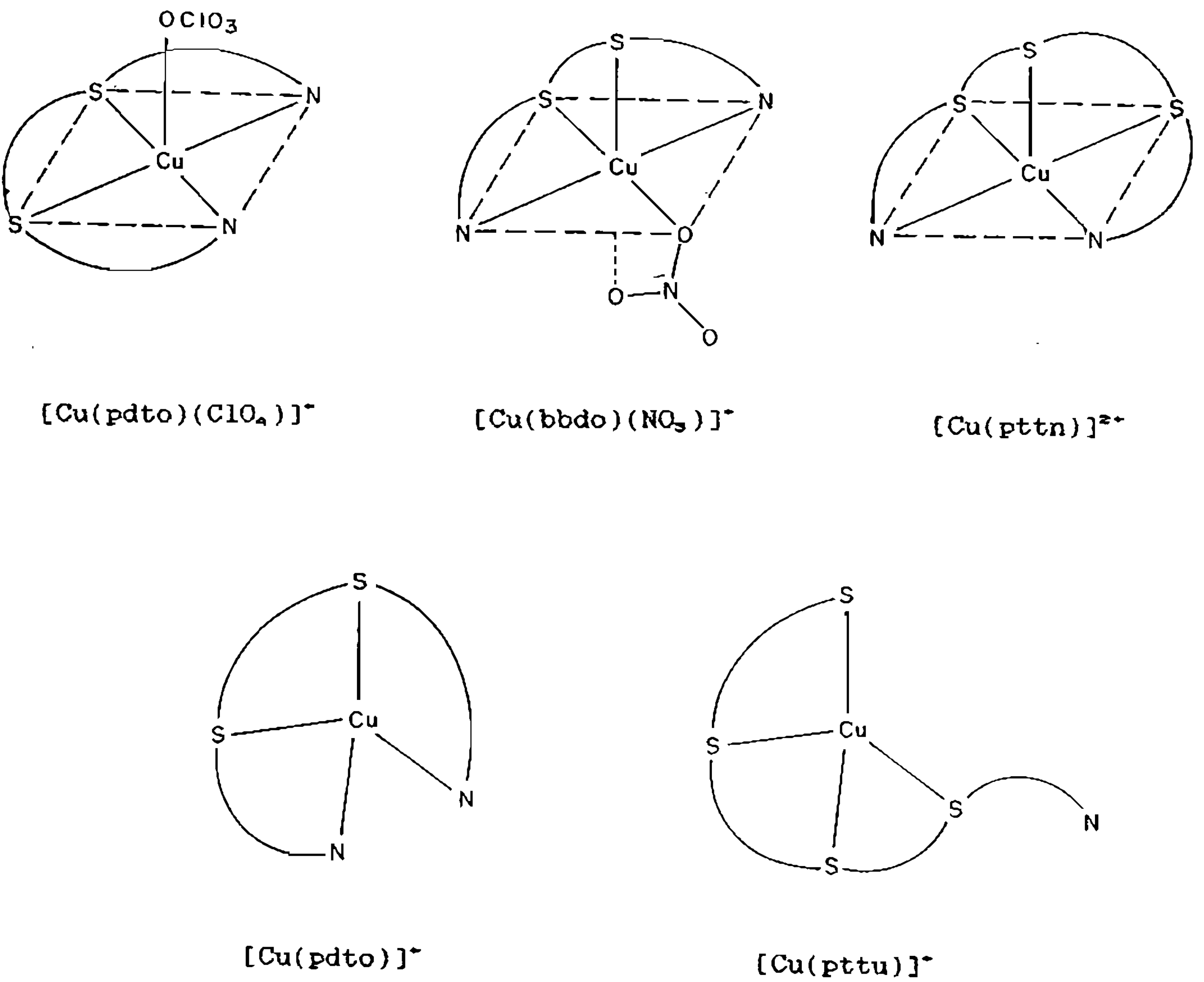


Fig. 7.1 Known structures of Cu(II) and Cu(I) complexes of N_2S_2 and N_2S_3 ligands

7.2 Experimental

7.2.1 Synthesis of Ligands and their Cu(II) Complexes

The ligands pdto, bbdo, pttn and pttu and their $Cu(ClO_4)_2$ complexes were prepared as described in Chapter 6.

7.3 Results and Discussion

7.3.1 Electronic and EPR Spectra

All the present Cu(II) complexes exhibit one (16.7 kK) or two (16.7 - 11.2 kK) intense ligand field (16.4 kK) (Fig. 7.2) and a highly intense S(σ) ---> Cu(II) charge transfer bands (29.3 - 28.1 kK) (Fig. 7.3).[24,26,27] For almost all the complexes there is a small but significant reduction or enhancement in molar absorptivities of both these bands, on the addition of excess (0.010 M) α-, β- and τ-CDs in aqueous solution (Table 7.1); however, there is no change in position of the bands (Figs 7.2 - 7.4) as observed in acetonitrile solution (Chapter 6), suggesting that the binding of CDs to the complex is not sufficiently strong to affect the primary coordination sphere. This is supported by the frozen solution EPR spectral study of the complexes in the presence of excess CDs (2 % aqueous solution), which shows no change in either $g_{||}$ or $A_{||}$ value.

7.3.2 Electrochemical Behaviour of the Complexes

The cyclic voltammogram of $[Cu(pdto)]^{2+}$ in aqueous solution

Table 7.1 Electronic spectral data for copper(II) complexes[a] in the presence of excess[b] cyclodextrins

complex	Medium	LF band[c]	CT band[c]
$[Cu(pdto)]^{2+}$	H_2O	16.8 (494)	28.6 (3212)
	MeCN	16.9 (743)	28.0 (4664)
	α-CD	16.8 (408)	28.6 (2900)
	β-CD	16.8 (619)	28.6 (1798)
	τ-CD	16.8 (426)	28.6 (2795)
$[Cu(bbdo)]^{2+}$	H_2O	16.7 (168) 11.4 (189)	29.3 (3764) 24.7 (1417)
	MeCN	16.9 (220) 11.6 (210)	28.7 (2810)
	α-CD	16.7 (172) 11.3 (189)	29.3 (1991) 24.7 (684)
	β-CD	16.7 (173) 11.3 (192)	29.3 (2070) 24.7 (682)
	τ-CD	16.7 (187) 11.4 (186)	29.3 (2002) 24.7 (639)
$[Cu(pttn)]^{2+}$	H_2O	16.7 (411) 11.2 (179)	28.1 (3589)
	MeCN	16.7 (450) 11.2 (190)	27.7 (4760)
	α-CD	16.7 (392) 11.2 (168)	28.3 (3104)
	β-CD	16.7 (375) 11.2 (160)	28.3 (3417)
	τ-CD	16.8 (384) 11.2 (165)	28.3 (3403)

$[Cu(pttu)]^{2+}$	H_2O	16.7 (296)	26.4 (1909)
	MeCN	16.3 (490) 11.1 (100)	26.1 (3280)
	α-CD	16.7 (196)	26.4 (1579)
	β-CD	16.6 (517)	28.4 (2015)
	τ-CD	16.8 (356)	28.4 (2080)

[a] Concentration of the complex, 0.001 - 0.0015 M; [b] concentration of α-CD, 0.010 M; β-CD, 0.010 M; τ-CD, 0.010 M; [c] $\bar{\nu}_{max}$ values in kK and ε in M^{-1} cm^{-1} in parentheses

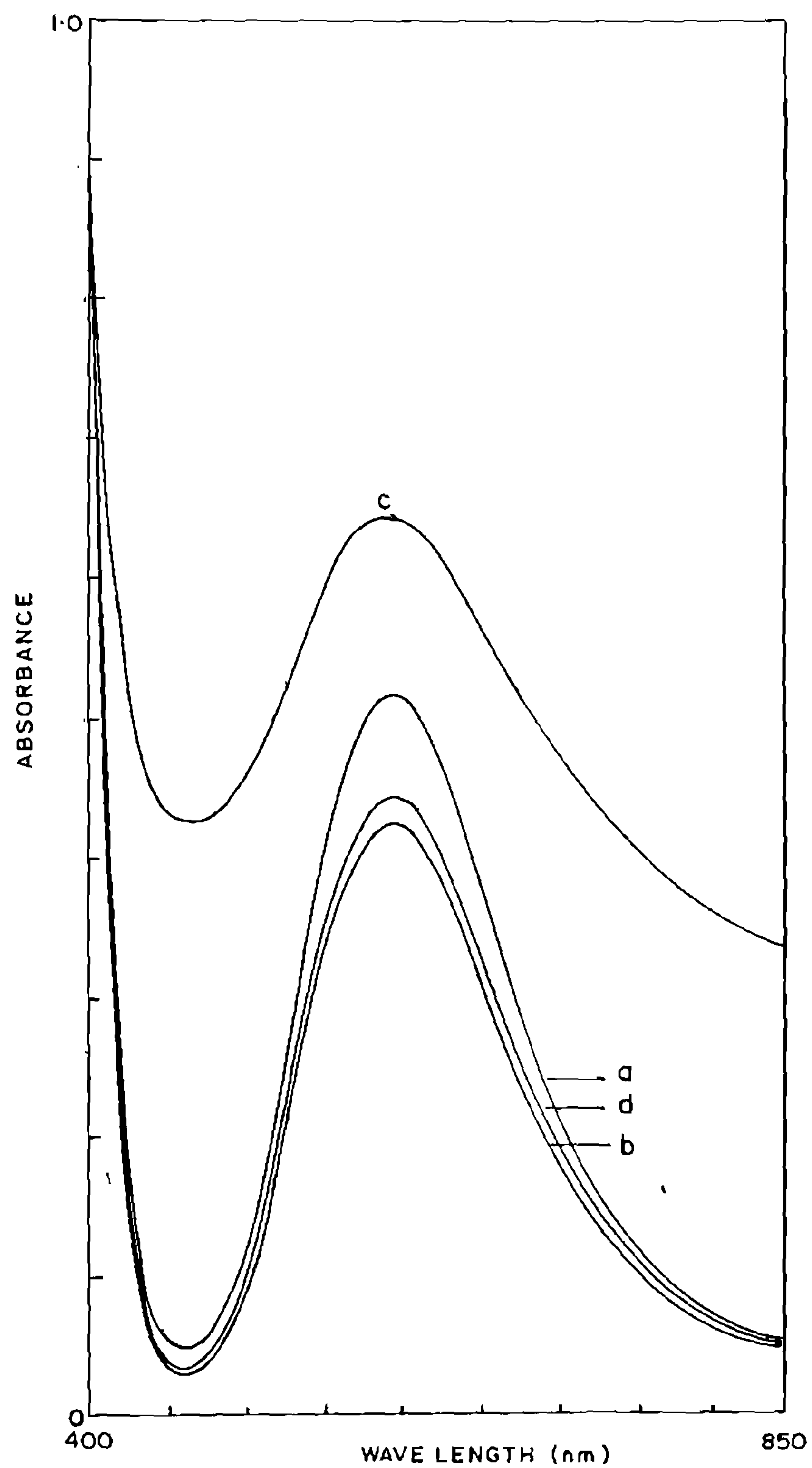


Fig. 7.2 Ligand field spectra of $[Cu(pdto)]^{2+}$ in aqueous (a) and aqueous α-CD (0.010 M) (b), β-CD (0.010 M) (c) and τ-CD (0.010 M) (d) solutions

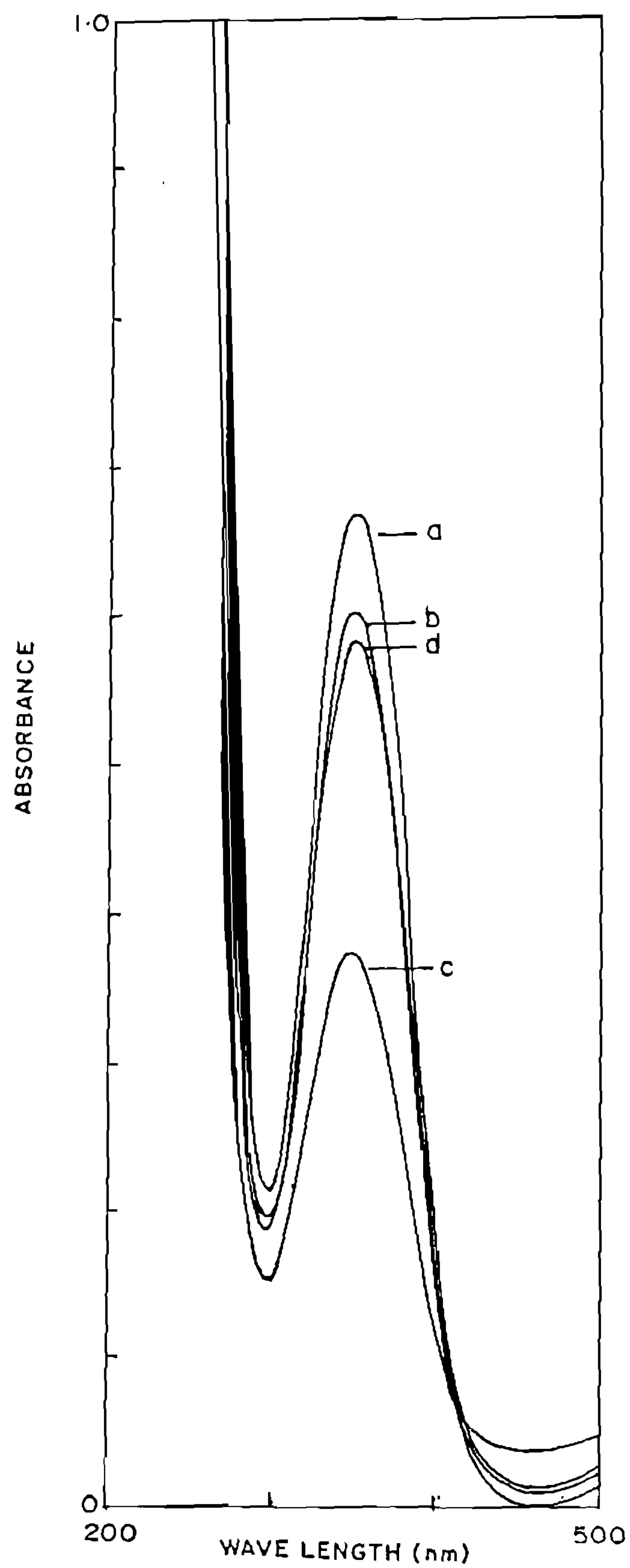


Fig. 7.3 Charge transfer spectra of $[Cu(pdto)]^{2+}$ in aqueous (a) and aqueous α-CD (0.010 M) (b), β-CD (0.010 M) (c) and τ-CD (0.010 M) (d) solutions

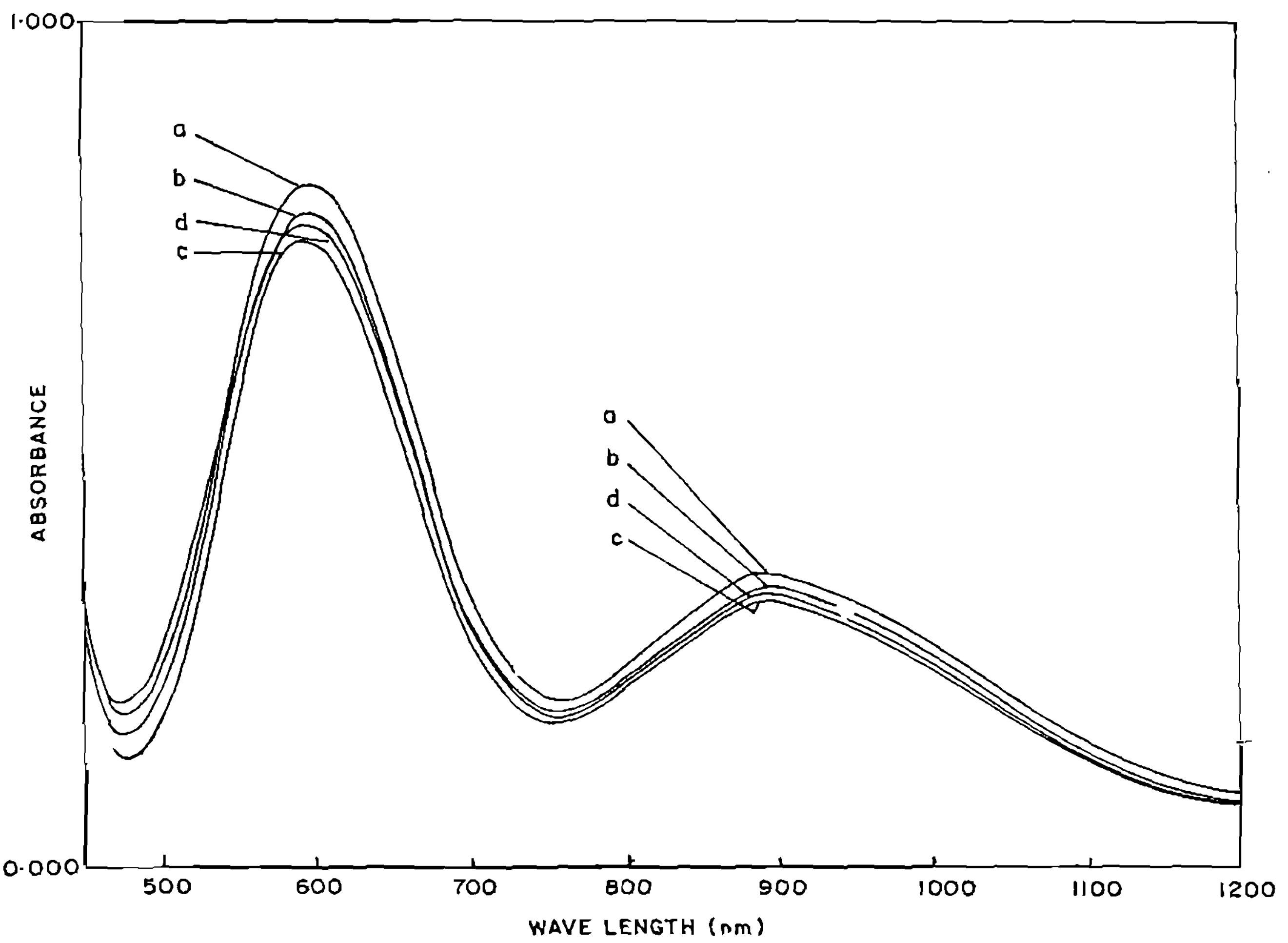


Fig. 7.4 Ligand field spectra of $[Cu(pttn)]^{2+}$ in the aqueous (a) and aqueous α-CD (0.010 M) (b), β-CD (0.010 M) (c) and γ-CD (0.010 M) (d) solutions

on a glassy carbon electrode (GC) at 50 mV/s shows that the Cu(II)/Cu(I) couple is irreversible (Fig. 7.5), as evident from the very high values of ΔE_p and peak current ratio (i_{pa}/i_{pc}) (Table 7.2). The symmetrical anodic peak with high current is obviously due to adsorption of Cu(I) product formed on reduction. A copper(I) complex containing aromatic rings has been observed to be adsorbed on the surface of GC electrode.[28] The weak adsorption of the product $[Cu(pdto)]^+$ is revealed by the shape of i_{pa}/i_{pc} *vs* $\sqrt{\nu}$ plot (Fig. 7.6).[29] The redox of $[Cu(pdto)]^{2+}$ is irreversible (ΔE_p, 126 mV) on a platinum sphere electrode also; however, the i_{pa}/i_{pc} value is nearer to unity suggesting no adsorption of Cu(I) species on the electrode. Electrochemical irreversibility of copper chelates with flexible ligands is generally attributed to the configurational change accompanying electron transfer reaction.[30] Thus the entirely different X-ray structures[23] of $[Cu(pdto)(ClO_4)]^+$ (square pyramidal) and $[Cu(pdto)]^+$ (tetrahedral) complexes (Fig. 7.1) explain the observed irreversibility of the Cu(II)/Cu(I) couple. The bzim analogue of the pdto complex, $[Cu(bbdo)]^{2+}$ also shows irreversible redox behaviour (ΔE_p, 214 mV; i_{pa}/i_{pc}, 3.2) (Fig. 7.7) in aqueous 0.01 M $NaClO_4$ solution, again due to adsorption of the product of reduction.

The complex $[Cu(pttn)]^{2+}$ shows irreversible redox behaviour (Fig. 7.8) with high i_{pa}/i_{pc} and ΔE_p (80 mV) values because of

Table 7.2 Redox properties of Cu(II) complexes (0.001 M) in aqueous solution (0.1 M $NaClO_4$) in the presence of cyclodextrins[a] on a glassy carbon electrode at 50 mV/s scan rate

Complex	CD	E_{pc} mV	E_{pa} mV	i_{pc} μA	i_{pa} μA	ΔE_p mV	$E_{1/2}$ (V) CV	$E_{1/2}$ (V) DPV[b]	i_{pa}/i_{pc}	D X 10^6 cm^2/s	K_1/K_{2+}
$[Cu(pdto)]^{2+}$	0	0.304	0.430	40.0	79.4	126	0.367	0.369	2.3	2.82	
	α-CD	0.296	0.418	34.3	33.1	122	0.357	0.367	1.4	2.23	0.68
	β-CD	0.318	0.424	33.9	29.8	106	0.371	0.371	1.2	2.23	0.52
	τ-CD	0.286	0.442	33.8	30.5	156	0.364	0.375	1.3	1.97	0.63
$[Cu(bbdo)]^{2+}$	0	0.428	0.552	23.8	58.2	124	0.490	0.457	2.8	1.29	
	α-CD	0.394	0.551	13.7	45.5	157	0.473	0.449	3.8	0.29	0.86
	β-CD	0.412	0.530	18.6	59.9	118	0.471	0.443	3.6	0.77	0.48
	τ-CD	0.400	0.520	14.7	39.9	120	0.460	0.433	3.1	0.40	0.36
$[Cu(pttn)]^{2+}$	0	0.268	0.372	54.6	131	84	0.330	0.303	2.9	5.12	
	α-CD	0.280	0.364	50.6	92.6	84	0.322	0.294	2.2	4.79	0.89
	β-CD	0.276	0.362	49.8	106	86	0.319	0.297	2.5	4.47	0.65
	τ-CD	0.272	0.358	43.8	83.8	86	0.315	0.295	2.3	3.24	0.56
$[Cu(pttu)]^{2+}$	0	0.434	0.512	38.9	31.8	78	0.473	0.475	1.1	1.20	
	α-CD	0.428	0.512	36.0	28.0	84	0.470	0.471	1.1	2.02	0.96
	β-CD	0.436	0.522	29.9	24.0	86	0.479	0.477	1.1	1.40	1.26
	τ-CD	0.458	0.542	28.6	24.7	84	0.500	0.504	1.1	2.02	3.10

[a] Concentration of α-, β- and τ-CDs, 0.005 M; [b] scan rate, 1 mV/s and pulse height, 50 mV.

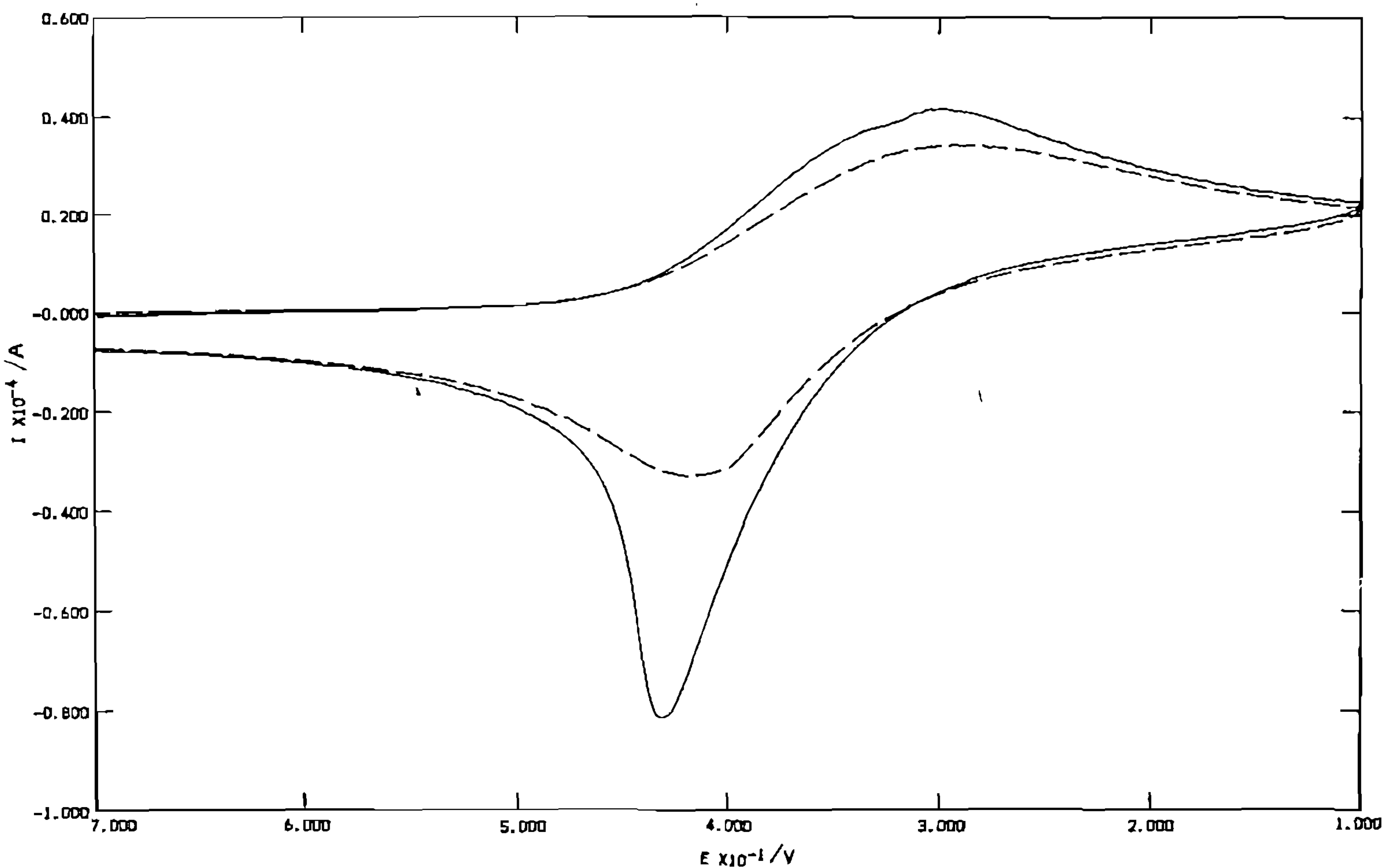


Fig. 7.5 Cyclic voltammograms of $[Cu(pdto)]^{2+}$ (0.001 M) in aqueous solution (0.1 M $NaClO_4$) in the absence (——) and presence of 0.010 M β-CD (----)

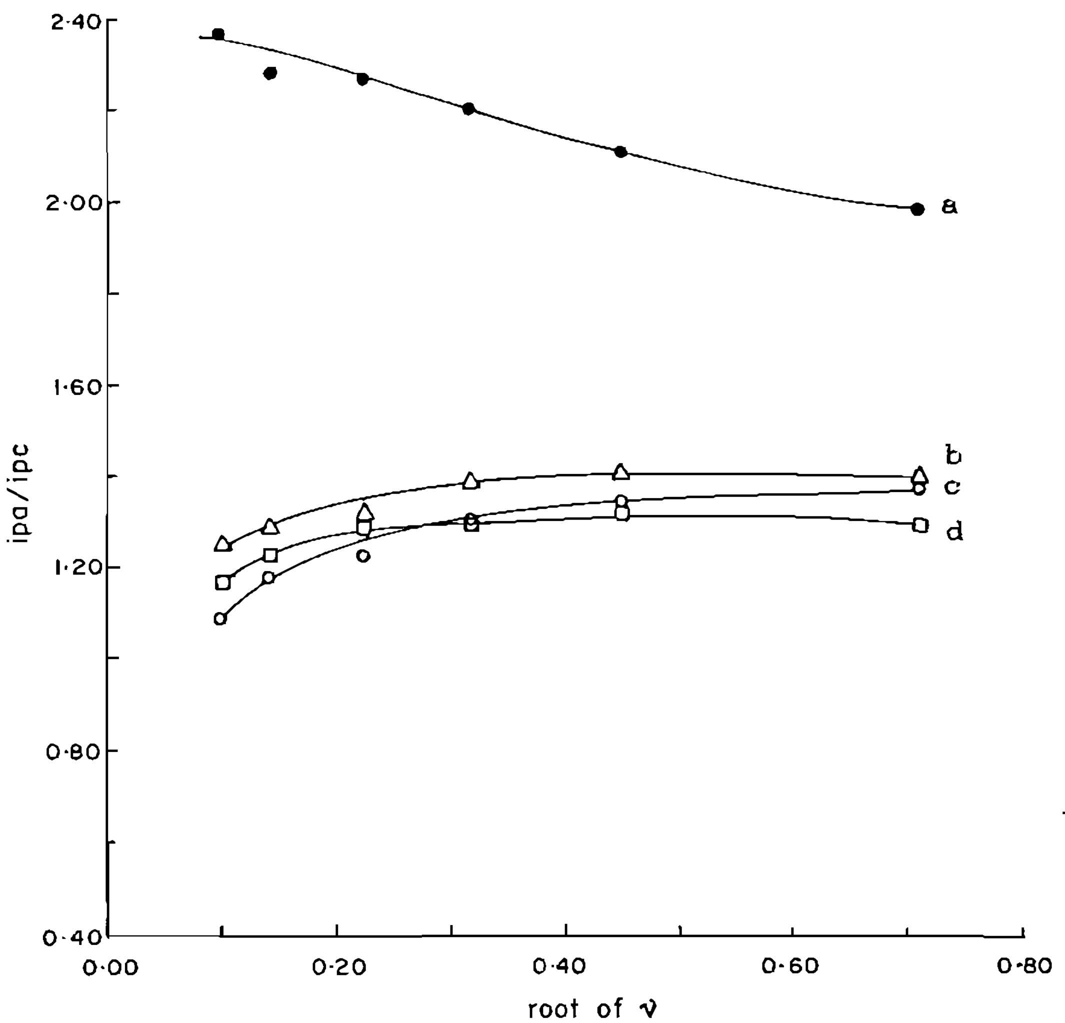


Fig. 7.6 Plot of i_{pa}/i_{pc} *vs* square root of the scan rate for $[Cu(pdto)]^{2+}$ in the absence (a) and presence of α-CD (b), β-CD (c) and τ-CD (d) solutions

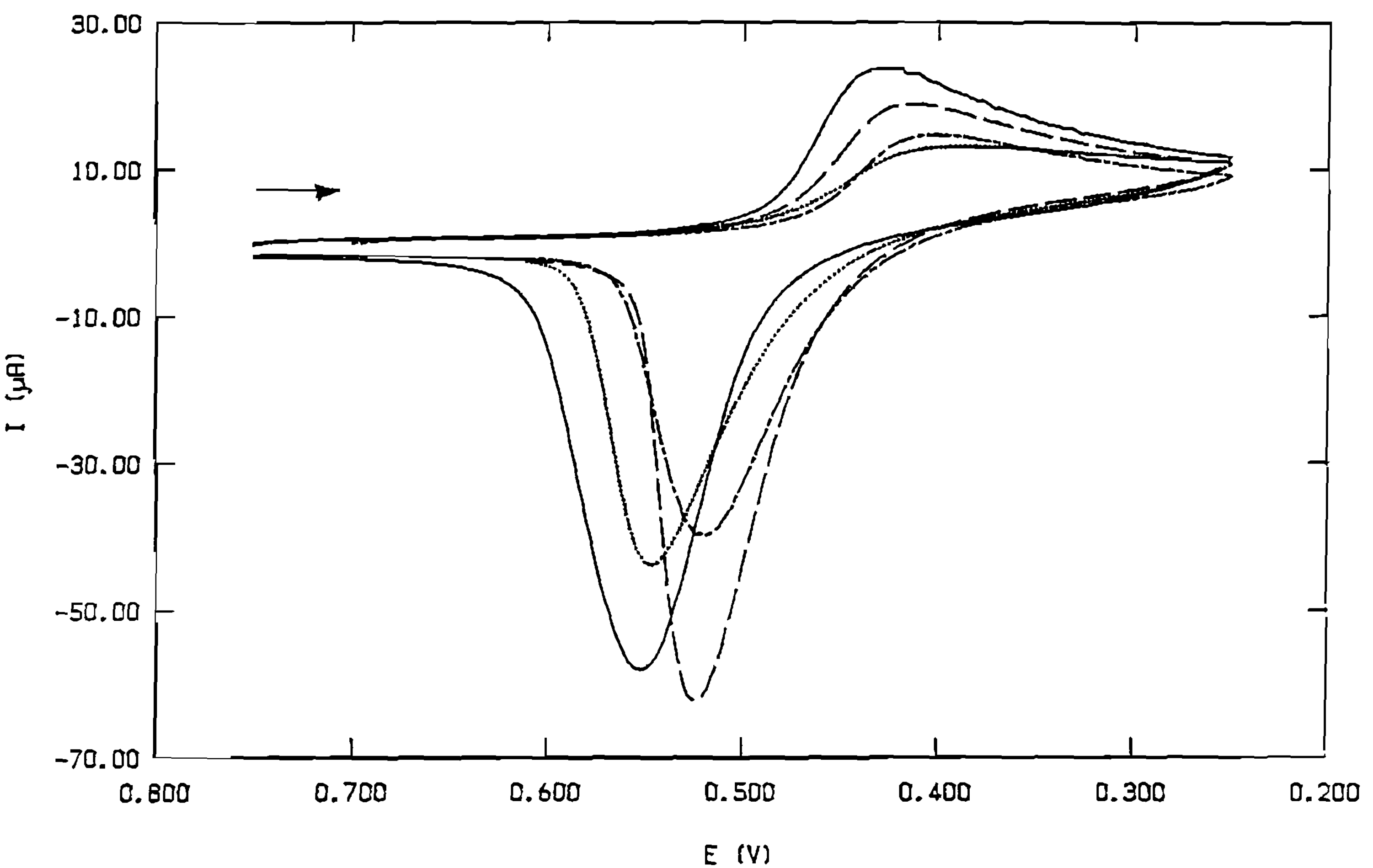


Fig. 7.7 Cyclic voltammograms of $[Cu(bbdo)]^{2+}$ (0.001 M) in aqueous solution (0.1 M $NaClO_4$) in the absence (———) and presence of 0.01 M α-CD (....), β-CD (0.01 M) (----) and τ-CD (0.01 M) (-----) at 50 mV/s scan rate

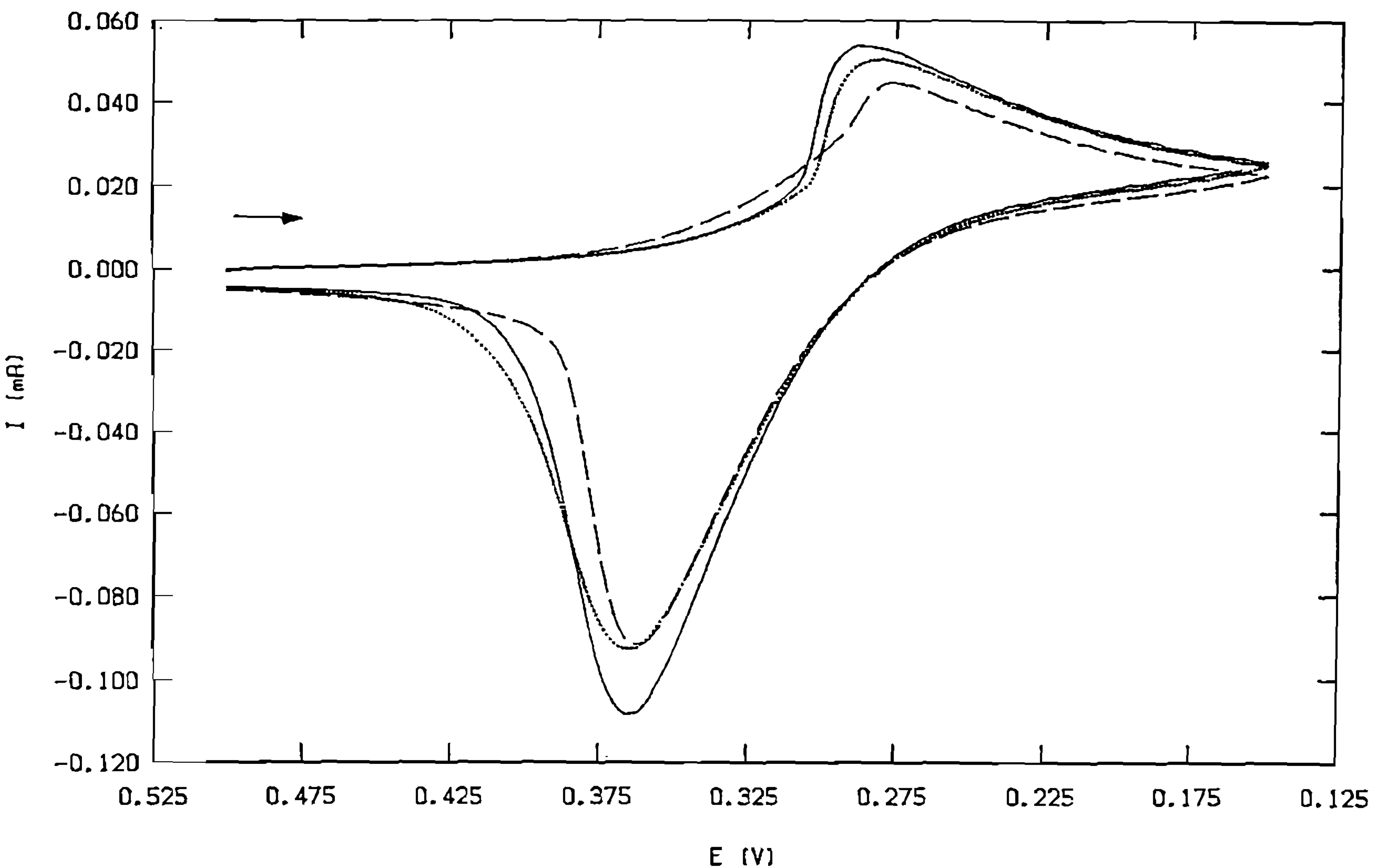


Fig. 7.8 Cyclic voltammograms of $[Cu(pttn)]^{2+}$ (0.001 M) in aqueous solution (0.1 M $NaClO_4$) in the absence (———) and in the presence of 0.01 M α-CD (....) and 0.01 M γ-CD (----) at 50 mV/s scan rate

adsorption of Cu(I) species. In contrast, its homologue $[Cu(pttu)]^{2+}$ displays a nearly reversible redox behaviour (Fig. 7.9) in aqueous solution, as verified by the constancy of $i_{pc}/\sqrt{\nu}$, low ΔE_p value and i_{pa}/i_{pc} value of unity (Table 7.2).

7.3.3 Electrochemical Behaviour of Dithioether Complexes in the Presence of CDs

The incremental addition of α-, β- and γ-CDs to $[Cu(pdto)]^{2+}$ in aqueous solution diminishes the anodic peak current considerably and there is substantial cathodic shift in the anodic peak potential. But the changes in current and potential of the cathodic peak are comparatively small. Thus on the addition of α- and β-CDs the Cu(II)/Cu(I) redox becomes diffusion controlled and reversible, as inferred from the linear i_{pc} vs $\sqrt{\nu}$ plot passing through the origin (Fig. 7.10), the decrease in ΔE_p and the approach of i_{pa}/i_{pc} values towards unity (Table 7.2).

When the concentration of CDs is increased, the values of both anodic and cathodic peak currents decrease up to a certain concentration and then remains constant suggesting completion of adduct formation of the copper complex with CDs (Table 7.2). All the plots of i_{pa}, E_{pa} and ΔE_p *vs* CD concentration show inflexion points at approximately five for α-, four for β- and three for γ-CD (Fig. 7.11 a-c), which correspond to completion of adduct formation of $[Cu(pdto)]^{2+}$ with CDs and a doll in a doll in a

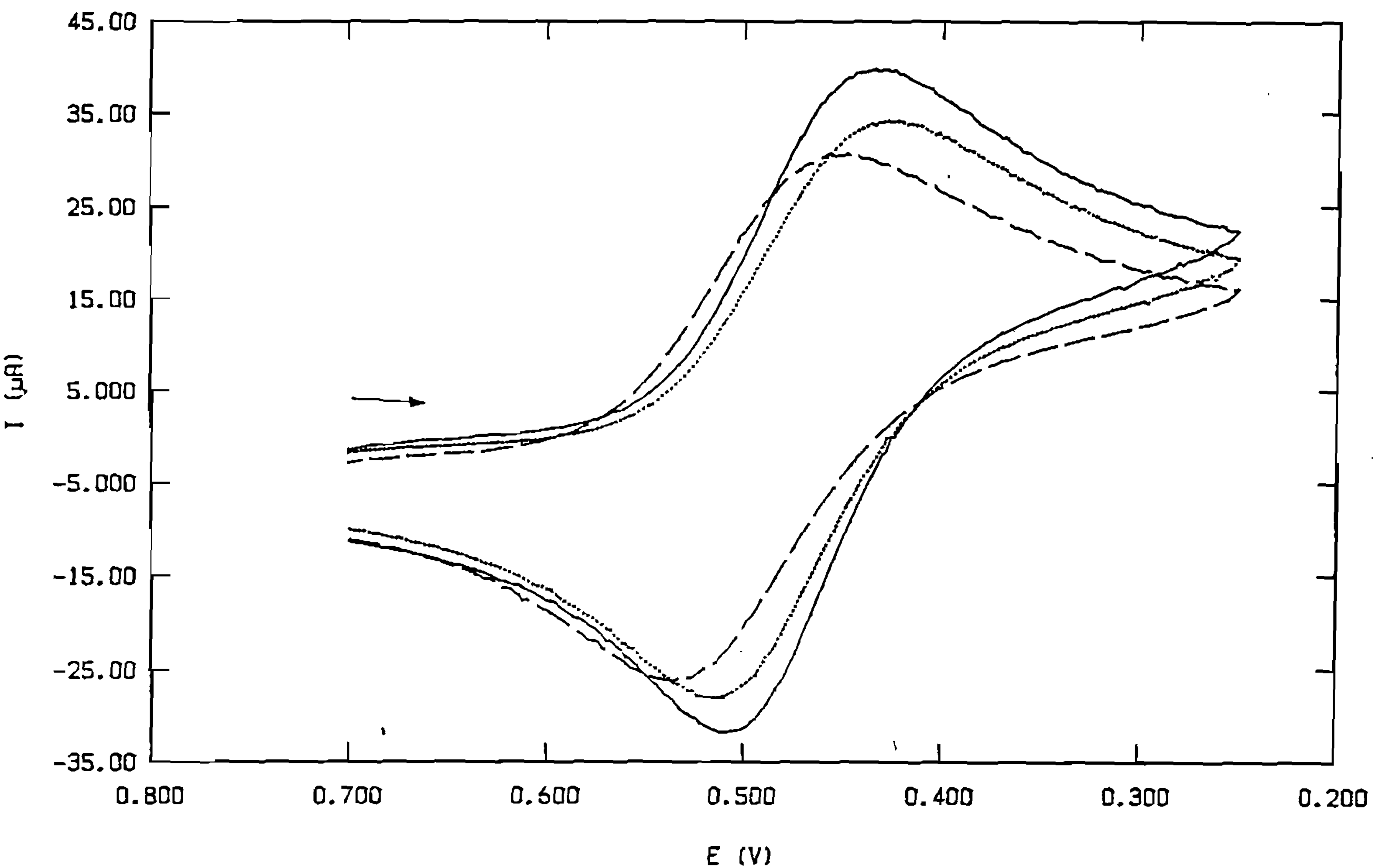


Fig. 7.9 Cyclic voltammograms of $[Cu(pttu)]^{2+}$ (0.001 M) in aqueous solution (0.1 M $NaClO_4$) in the absence (——) and in the presence of 0.01 M α-CD (....) and 0.01 M τ-CD (----) at 50 mV/s scan rate

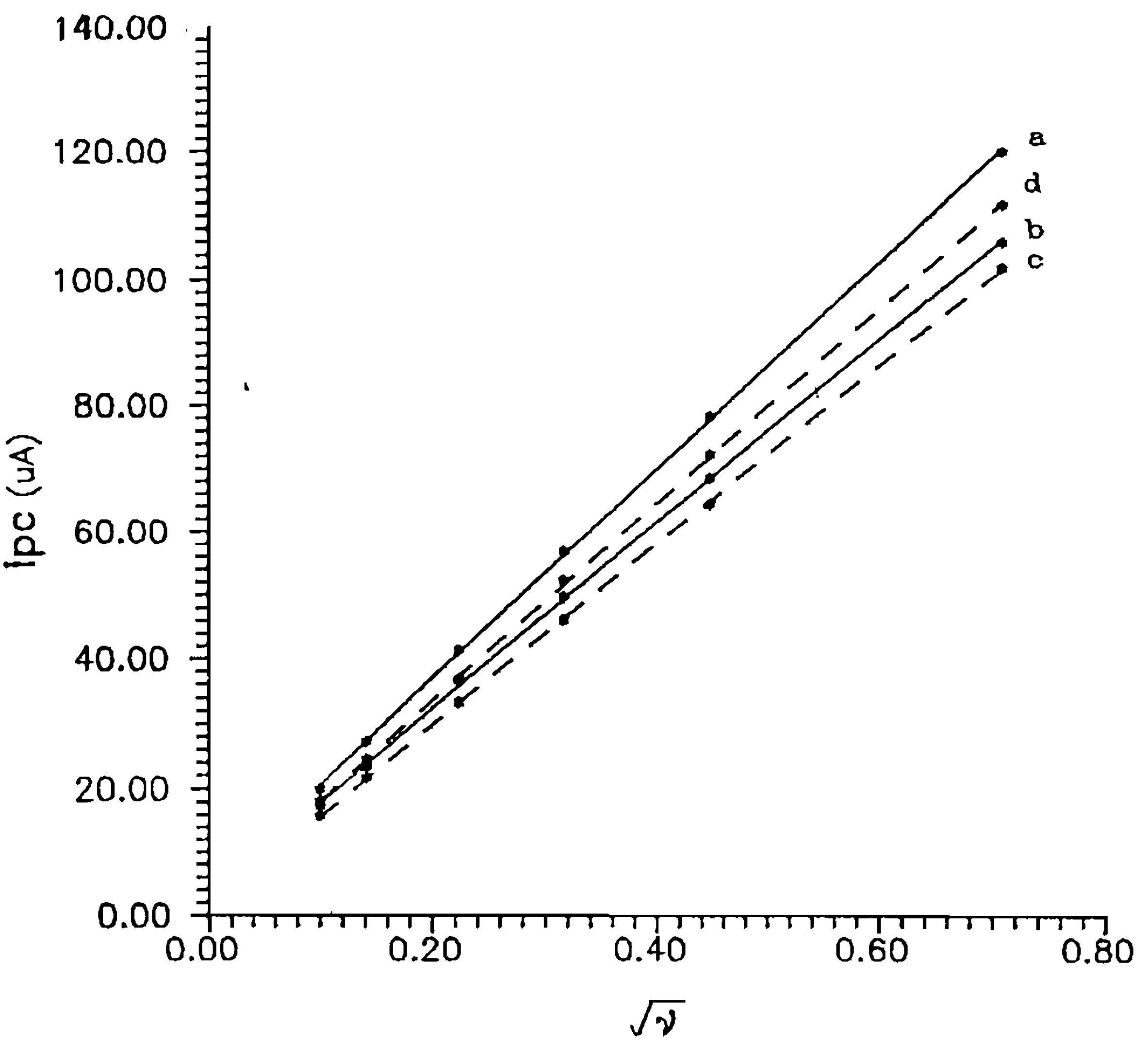


Fig. 7.10 Plot of i_{pc} values *vs* square root of the scan rate for $[Cu(pdto)]^{2+}$ (0.001 M) in the absence (a) and in the presence of α-CD (b), β-CD (c) and τ-CD (d)

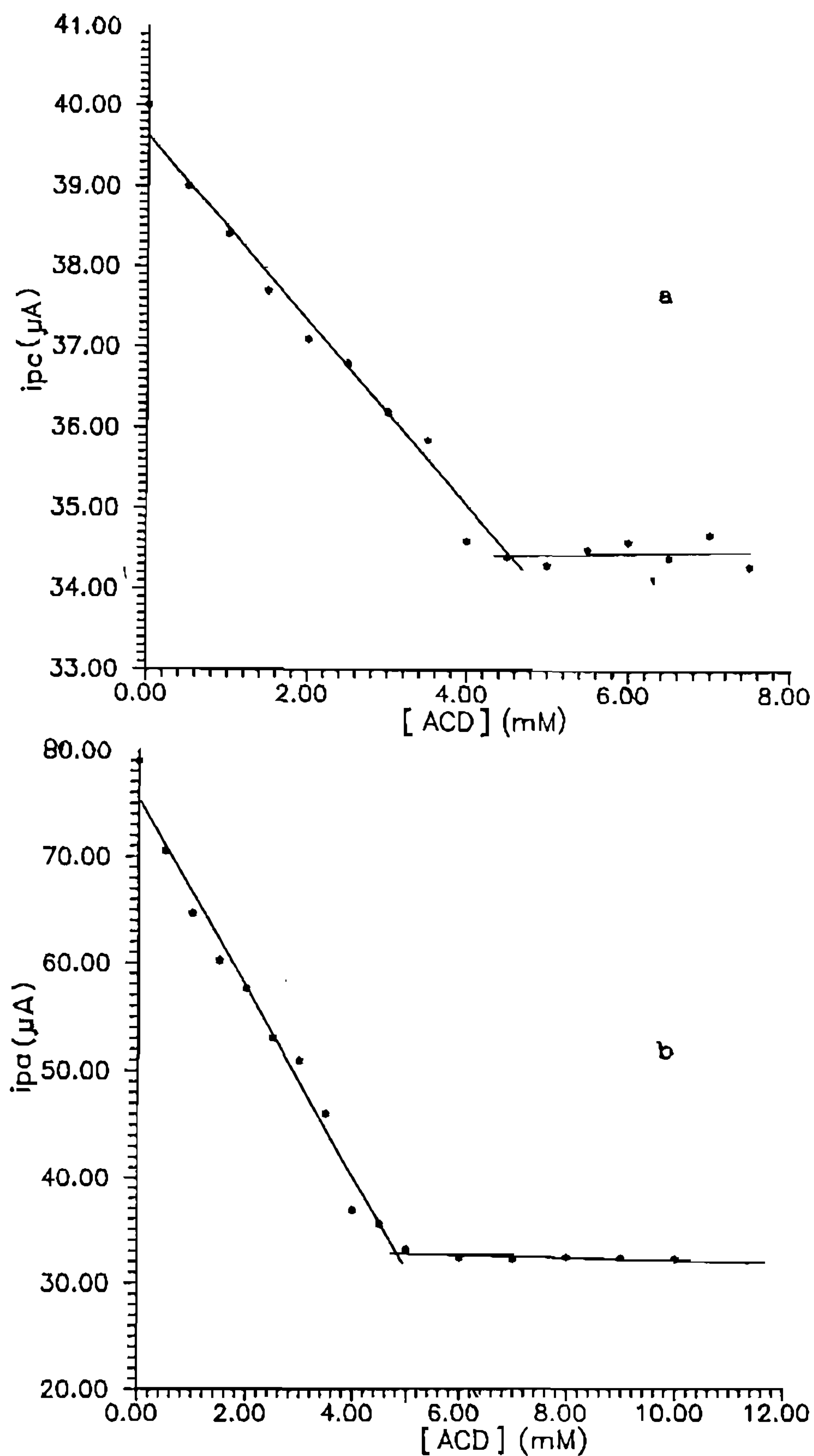
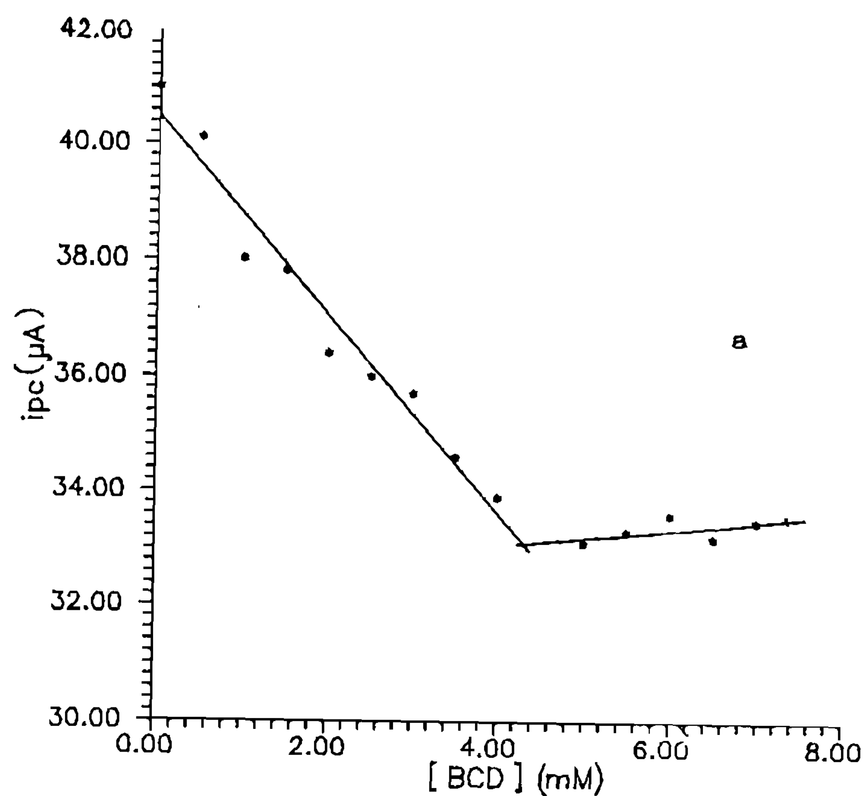


Fig. 7.11a Plot of observed cathodic (a) and anodic (b) peak current values of $[Cu(pdto)]^{2+}$ from CV *vs* concentration of α-CD added



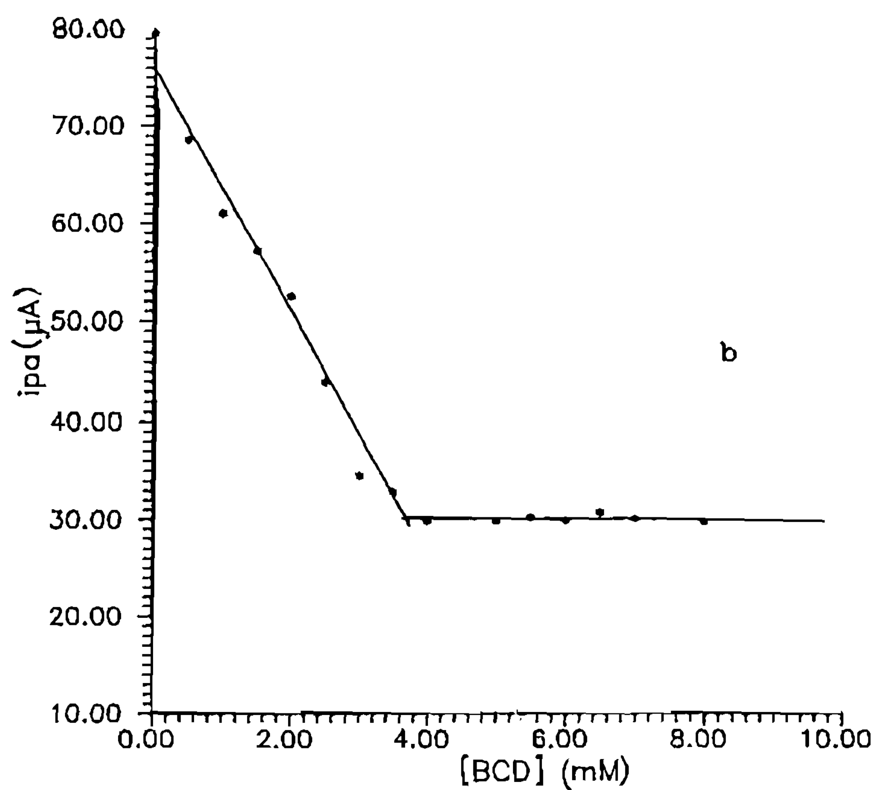


Fig. 7.11b Plot of observed cathodic (a) and anodic (b) peak current values of $[Cu(pdto)]^{2+}$ from CV *vs* concentration of β-CD added

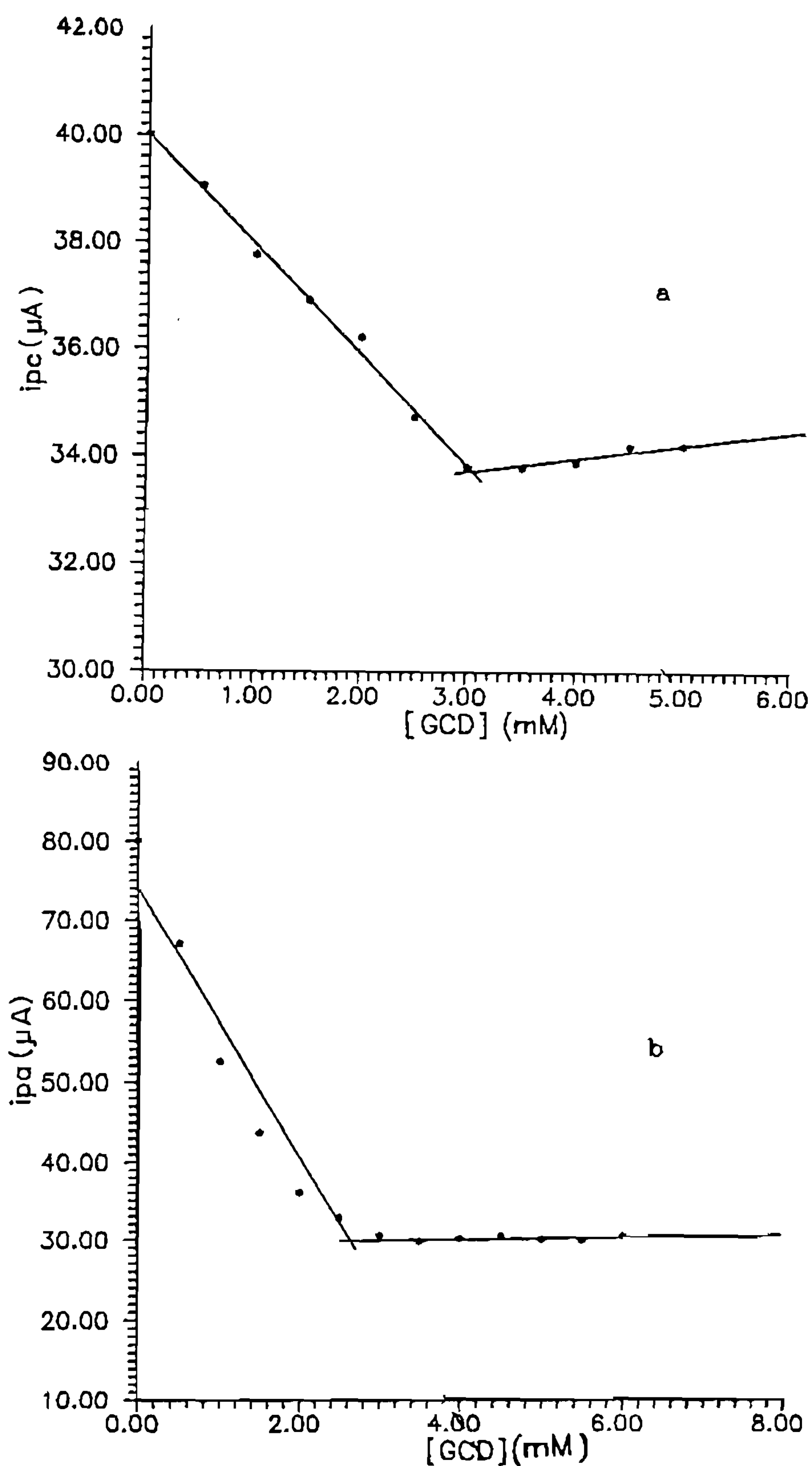


Fig. 7.11c Plot of observed cathodic (a) and anodic (b) peak current values of $[Cu(pdto)]^{2+}$ from CV *vs* concentration of τ-CD added

doll arrangement. The limiting concentrations of CDs, at which inflexions are observed, depends interestingly upon the size or number of D-glucose monomers in the CD molecule. The observation of such saturation points has often been proved difficult or impossible.[21] However, Yokoi has used EPR spectroscopy to observe the inclusion of one and two molecules of bis(2-pyridylcarbinolato)copper(II) with α- and τ-CDs respectively.[4] Harada *et al.*[24] have reported that ferrocene needs two molecules of α-CD and one molecule of τ-CD to form inclusion complexes. But no such regular array of CDs around even organic substrates has been noticed previously. However, it has been already shown that the modified or substituted β-CD forms aggregates, specifically with 4-nitrophenol and not with other substrates.[22] In the Cu(II)/Cu(I) redox potential range, the coverage of the electrode by CD molecules is greater[31] (or their orientation is adequate to form a more compact layer) which can also reduce the peak current value. Thus the peak current ratio in the presence of α-, β- and τ-CDs increases only slightly with increase in scan rate suggesting that the Cu(II) species is very slightly adsorbed on the surface of the electrode;[29] this is in contrast to the CD-free solutions where Cu(I) species is weakly adsorbed. If the prevention of adsorption has led to the observed reversibility, then the presence of D-glucose should also lead to such a reversibility; but no such reversibility is observed even at higher concentrations of

D-glucose. So it is clear that it is only adduct formation which renders the redox behaviour diffusion-controlled and reversible. We have shown that inclusion complex formation of MV^{2+} by β-CD is an effective and selective method to reduce adsorption and hence to confer reversibility on the electroactive species.[18] Similar inclusion phenomenon is not obviously involved for $[Cu(pdto)]^{2+}$, as the sizes of the CD cavities are much smaller than that of the complex.

Water molecules enclosed within the uncomplexed CD cavity cannot have a full complement of hydrogen bonds owing to interference from the glucopyranose ring of CD, so that they are enthalpy-rich.[32] The expulsion of these enthalpy-rich molecules into bulk water upon substrate inclusion results in a negative enthalpy change, together with a negative entropy change. This explanation was supported by an X-ray crystallographic study of β-CD dodecahydrate,[33] which showed that 6.5 water molecules within the cavity are disordered over 8 sites and display extensive thermal motion. Second sphere coordination of transition metal complexes bearing hydrophobic ligands by cyclodextrins have been characterized structurally in the solid state by X-ray crystallography.[10-12] In these adducts, the hydrophobic ligand of the complex penetrates the cavity of the CD *via* the wider aperture of the receptor associated with the face bearing the secondary

hydroxy groups. However, the X-ray crystal structure of the 1:1 adduct formed by the platinum complex with β-CD has shown that the PMe_3 ligand of the complex is inserted into and bound to the narrow primary hydroxy-group-bearing face of the β-CD torus; the complex lies within a severely disordered surface which could be forming a lid on the wider secondary hydroxy-group-bearing face of the β-CD torus.[11] So the interaction of the present complex with CDs may involve expulsion of a few water molecules on the partial inclusion of py or bzim ring into the primary or secondary hydroxy-group-bearing face of CDs; there may be also simple interactions of hydrogen bonding residues of ligands, like -NH- group with hydroxyl groups of the CDs.

The addition of β-CD shifts E_{pc} to a slightly more positive potential rendering Cu(II) to be easily reduced; in contrast, the presence of other CDs make the reduction relatively difficult. The differential pulse voltammograms (Fig. 7.12) observed show that the peak potential is not much affected by the addition of CDs; however, the peak current decreases but slightly, consistent with CV meaeurements.

From the slope of i_{pc} *vs* $\sqrt{\nu}$ plot, the values of diffusion coefficient (D) were calculated using Randles Sevcik's equation.[34] In the presence of α-, β- and γ-CDs the slope is suppressed and thus there is always a decrease in D values (Table 7.2) indicating

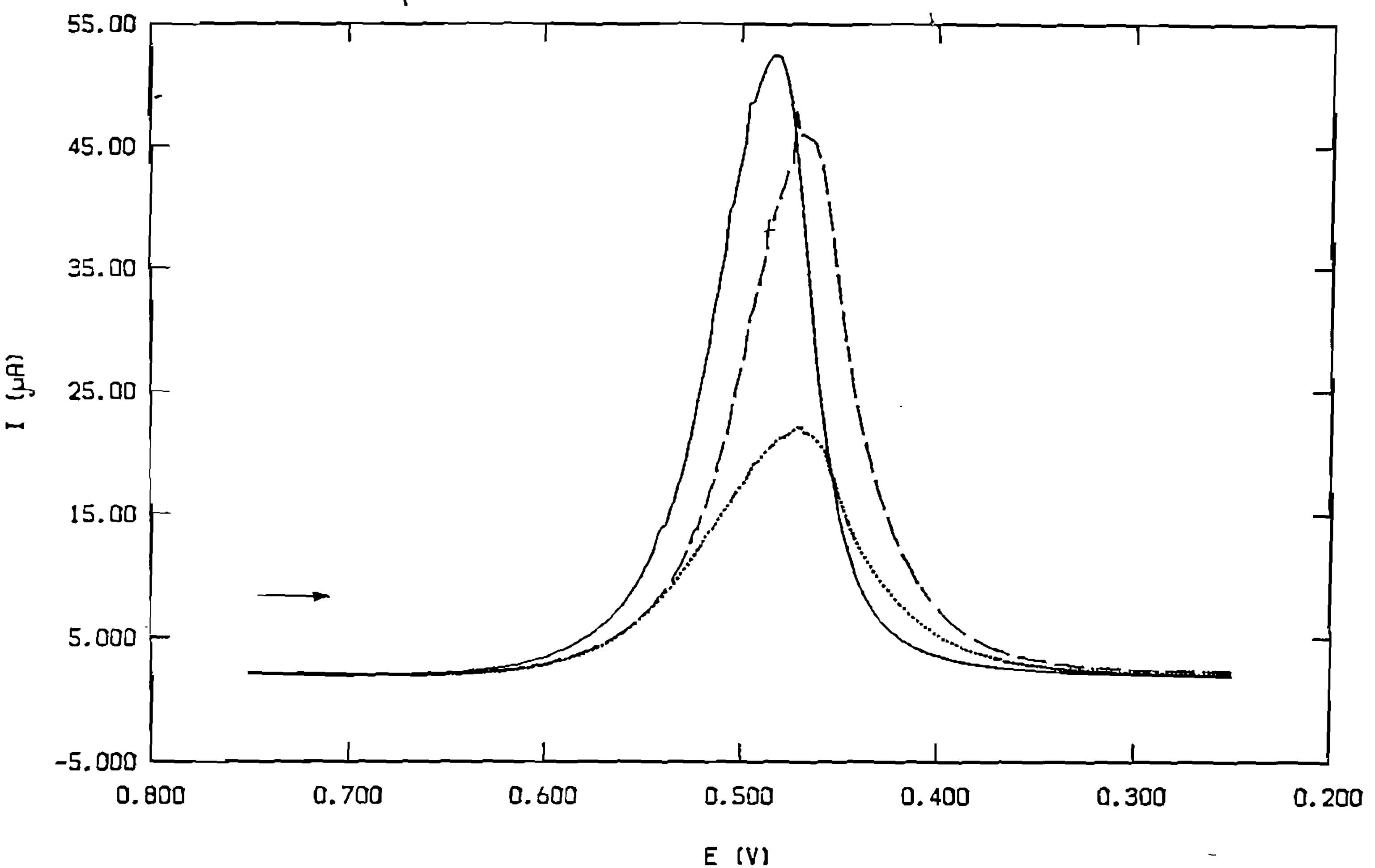


Fig. 7.12 Differential pulse voltammograms of $[Cu(bbdo)]^{2+}$ (0.001 M) in aqueous solution (0.1 M $NaClO_4$) in the absence (——) and presence of 0.01 M β-CD (----) and 0.01 M α-CD (....) at 1 mV/s scan rate

that the Cu(II) complex diffuses slowly to the electrode mainly in a form bound to the CDs. The diffusion coefficients of the CD-bound complexes (D_c) calculated from the i_{pc} values at the limiting concentration of CDs are collected in Table 7.2 and are also typical[35] of one electron transfer.

The association constant K_a for $Cu(pdto)^{2+}$ with all the three CDs has been calculated using the diffusion coefficient of the free complex (D_f) and the observed diffusion coefficients (D_{obs}) at various concentrations of CDs using the relation,[34]

$$D_{obs} = \{(D_f - D_{obs})/K_a[CD]\} + D_c$$

The value of K_a is obtained from the slope (Fig. 7.13) and the value of D_c, the diffusion coefficient of the CD-bound complex, from the intercept of the linear plot of D_{obs} *vs* $(D_f - D_{obs})/[CD]$. The K_a values thus calculated suggest that the stability of $[Cu(pdto)]^{2+}$-CD adducts varies in the order β-CD (414 M^{-1}) > α-CD (288 M^{-1}) > γ-CD (172 M^{-1}). For several organic substrates β-CD has been shown to exhibit selective inclusion complex formation. For the present complex also, though the mechanism of interaction is different, selectivity seems to have been achieved to certain extent.

The uncomplexed β-CD includes a larger number of high energy water molecules than the uncomplexed α-CD.[33,37] If the major part of the binding energy is derived from the relief of high energy

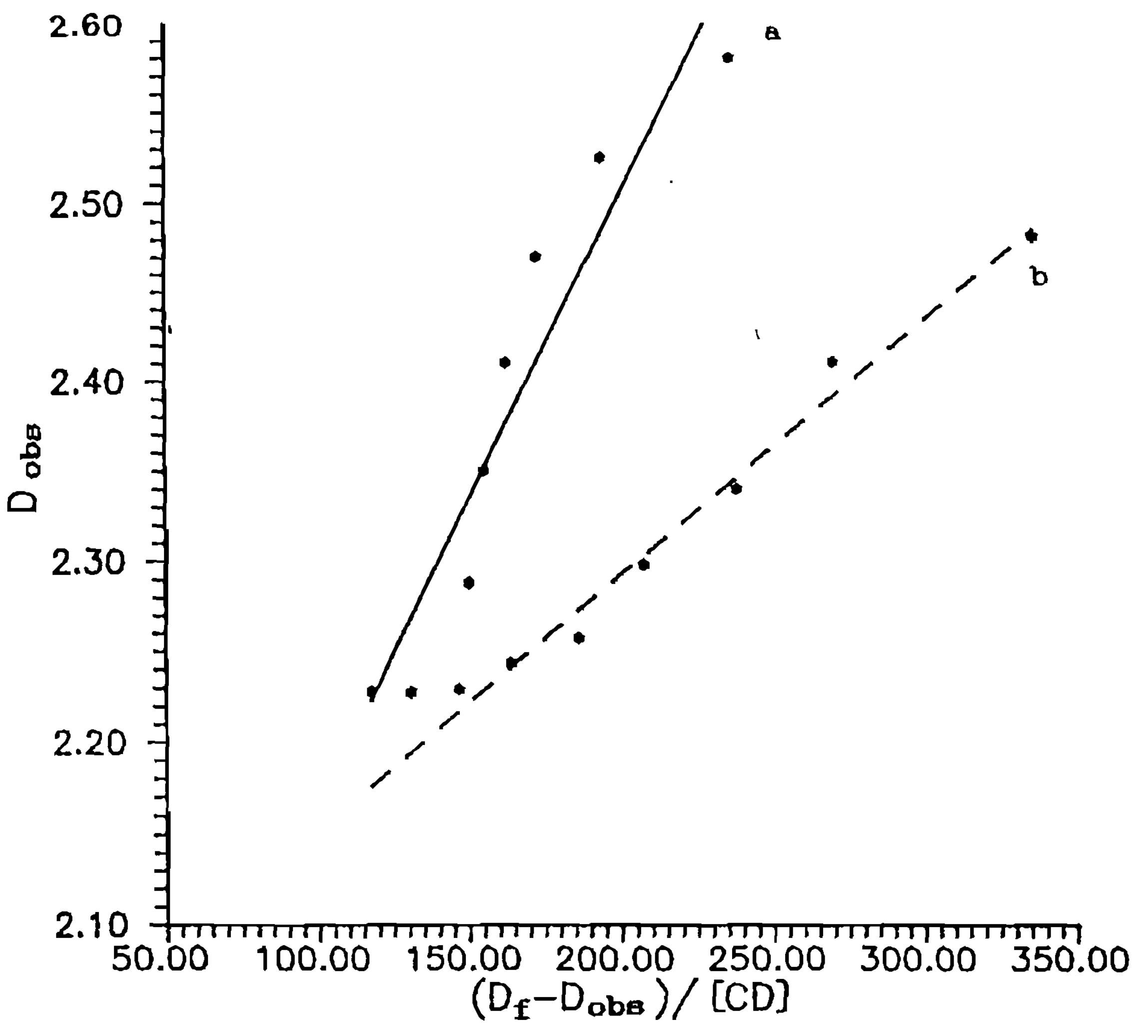


Fig. 7.13 Plot of D_{obs} *vs* $(D_f - D_{obs})/[CD]$ for $Cu(pdto)^{2+}$ in the presence of α-CD (a) and β-CD (b)

water, β-CD should give more negative enthalpy of complexation than α-CD. This presumption illustrates the higher association constant observed for the interaction of β-CD. In contrast, the values of ΔH° and ΔS° for the formation of β-CD inclusion complexes with *p*-nitrophenol,[38] *p*-nitrophenylglycosides,[38] and *m*- and *p*-disubstituted benzenes[39] are considerably less negative than those of the corresponding α-CD complexes.

The anodic and cathodic peak currents of $[Cu(bbdo)]^{2+}$, the benzimidazole analogue of $[Cu(pdto)]^{2+}$, decrease and the peak current ratio slightly increases when the concentration of α-, β- (i_{pa} slightly increased) and γ-CDs is increased; however, no inflexions are observed. The ΔE_p value decreases slightly for all the three CDs; the redox potential also decreases by about 20 mV for all the three CDs, suggesting that the Cu(II) species is not stabilized in CD solutions.

7.3.4 Electrochemical Behaviour of Trithioether Complexes in the Presence of CDs

Addition of α-CD in steps to aqueous $[Cu(pttn)]^{2+}$ solution does not alter much Cu(II)/Cu(I) redox process (Fig. 7.8). The values of ΔE_p and $E_{1/2}$ remain the same; however, the peak currents decrease but without any change in i_{pa}/i_{pc} values. Addition of β-CD decreases both the peak currents (slightly) and the peak current ratio (2.9 to 2.3), suggesting that adsorption of Cu(I)

species formed on reduction is prevented to some extent but not fully. Both the peak potentials and the $\triangle E_p$ value remain unchanged; however, the $E_{1/2}$ decreases slightly (0.330 to 0.319 V). On the addition of γ-CD the decrease in i_{pa} (43 μA) is much greater than that in i_{pc} (13 μA) and the i_{pa}/i_{pc} value decreases (2.6 to 2.0). Both the peak potentials decrease by about 20 mV indicating (Fig. 7.8) that both Cu(II) and Cu(I) species are equally destabilized by interaction with γ-CD and the $E_{1/2}$ value decreases only slightly; however, $\triangle E_p$ value remains almost unaltered.

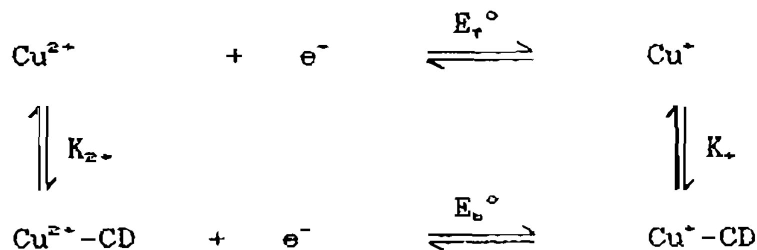
Addition of α-CD does not change the redox properties ($\triangle E_p$, $E_{1/2}$ and i_{pa}/i_{pc}) of $[Cu(pttu)]^{2+}$; however, both the peak currents decrease slightly (3 μA) (Fig. 7.9). Addition of β-CD to this complex increases the anodic peak potentials slightly (10 mV) (Fig. 7.9), which results in an increase in both $\triangle E_p$ and $E_{1/2}$ (0.473 to 0.479 V) values. There is also a considerable reduction in both peak current values but the peak current ratio remains the same (1.1). But incremental addition of γ-CD to this complex increases both the cathodic and anodic peak potentials, leading to an increase in the $E_{1/2}$ value (0.471 to 0.500 V); however, the $\triangle E_p$ does not change appreciably. There is also a considerable reduction in both the peak current values but i_{pa}/i_{pc} remains the same (1.1).

Further, the interesting changes in electrochemical properties observed for $[Cu(pdto)]^{2+}$ were not observed for the other Cu(II) complexes, suggesting that the interaction of the

former with CDs is selective. This may be because no dissociation of metal-ligand coordinate bond but stereochemical rearrangement from four-coordinate square-planar geometry to four-coordinate tetrahedral geometry occurs on electron transfer; the dissociation of a M-L bond would amount to breaking up and reforming of the assembly of CDs around the redox active species. On the other hand, the electron transfer to a five-coordinate $[Cu(pttu)]^{2+}$ complex would lead to formation of four-coordinate $[Cu(pttu)]^{+}$ in which one of the $Cu-N_{py}$ bond is dissociated (Chapter 4) (Fig. 4.10).

7.3.5 Changes in Redox Potentials

From the shifts in redox potentials on the addition of CDs, the ratio of formation constants (K_{+}/K_{2+}) were calculated assuming a reversible electrode reaction and reversible binding of Cu(II) and Cu(I) species to CDs (Scheme 7.1) and using the general



Scheme 7.1

formula,[18]

$$E_b^\circ - E_f^\circ = 0.059 \log(K_{+}/K_{2+})$$

where E_b° and E_f° are the formal potentials of the redox couple (+2/+1) in the bound and free forms respectively and K_{2+} and K_{+} are the equilibrium constants for the binding of CD to Cu(II) and Cu(I) respectively. The formation and dissociation of the adducts are expected to be fast enough to maintain an equilibrium on the time scale of the CV experiment. The values of K_{+}/K_{2+} (Table 7.2) illustrates that Cu(II) rather than Cu(I) forms of all the complexes interact strongly with all the CDs; however, the value is greater than unity for $[Cu(pttu)]^{2+}$ in β- and τ-CDs and almost unity in α-CD suggesting that the interaction of Cu(I) rather than Cu(II) form with the CDs is stronger.

7.3.6 Is the Binding of CDs Cooperative ?

Allosteric regulation of binding and catalysis is a common feature in the regulation of enzymes by molecular effectors. When the affinity of an enzyme for a substrate increases with increasing effector concentration, the allostery is termed positive cooperativity, and the transition from the inactive to the active state of the protein is the allosteric transition. Positive cooperativity in the binding of inorganic guests to synthetic hosts has been observed in dicoronands linked by a biphenyl,[40] gable porphyrins,[41] porphyrin dimers,[42] and crystalline heme models.[43]

It has been reported also in micelle-catalysed reactions.[44] Titrations of $[Cu(pdto)]^{2+}$ against CDs led to sigmoidal rather than hyperbolic curves. Replotting of the titration data according to Hill equation,[22,44a]

$$\ln[Y/(1-Y)] = h \ln[X] - \ln K_D$$

where, X = concentration of cyclodextrin added,

Y = ratio of the observed change in the value of i_{pa} or i_{pc} of the complex, on adding the CD to the maximum change in the respective electrochemical property

h = the hill coefficient.

K_D = overall dissociation constant (= K_A^{-1})

gave linear graphs (Fig. 7.14) where the slope is defined as the Hill coefficient (h), which is construed as an index of cooperativity. Non-cooperative systems exhibit $h \approx 1.0$, positively cooperative systems $h > 1.0$ and negatively cooperative systems $h < 1.0$. As a point of reference, hemoglobin has $h = 2.8$, while myoglobin has $h = 1.0$ towards binding of oxygen.

For the binding of $[Cu(pdto)]^{2+}$ to CD molecules, the h values calculated using i_{pc} and i_{pa} values are collected in Table 7.3. For all the three CDs, the value of h is found to be greater than unity (1.8 to 2.3). Hill coefficients greater than unity are the experimental hallmark of positive cooperativity,[22] in which

Table 7.3 Hill coefficients (h) and the K_a values* using i_{pa} and i_{pc} values for the interaction of $[Cu(pdto)]^{2+}$ with CDs

parameter used	α-CD		β-CD		γ-CD	
	h	$K_a (M^{-1})$	h	$K_a (M^{-1})$	h	$K_a (M^{-1})$
i_{pa}	2.09	3680	1.87	4730	1.44	900
i_{pc}	1.47	1450	1.25	2130	1.49	920

* K_a values are 1/[intercept] and h values are the slopes of the plots of ln [Y/(1-Y)] *vs* ln [X] (Fig. 7.14)

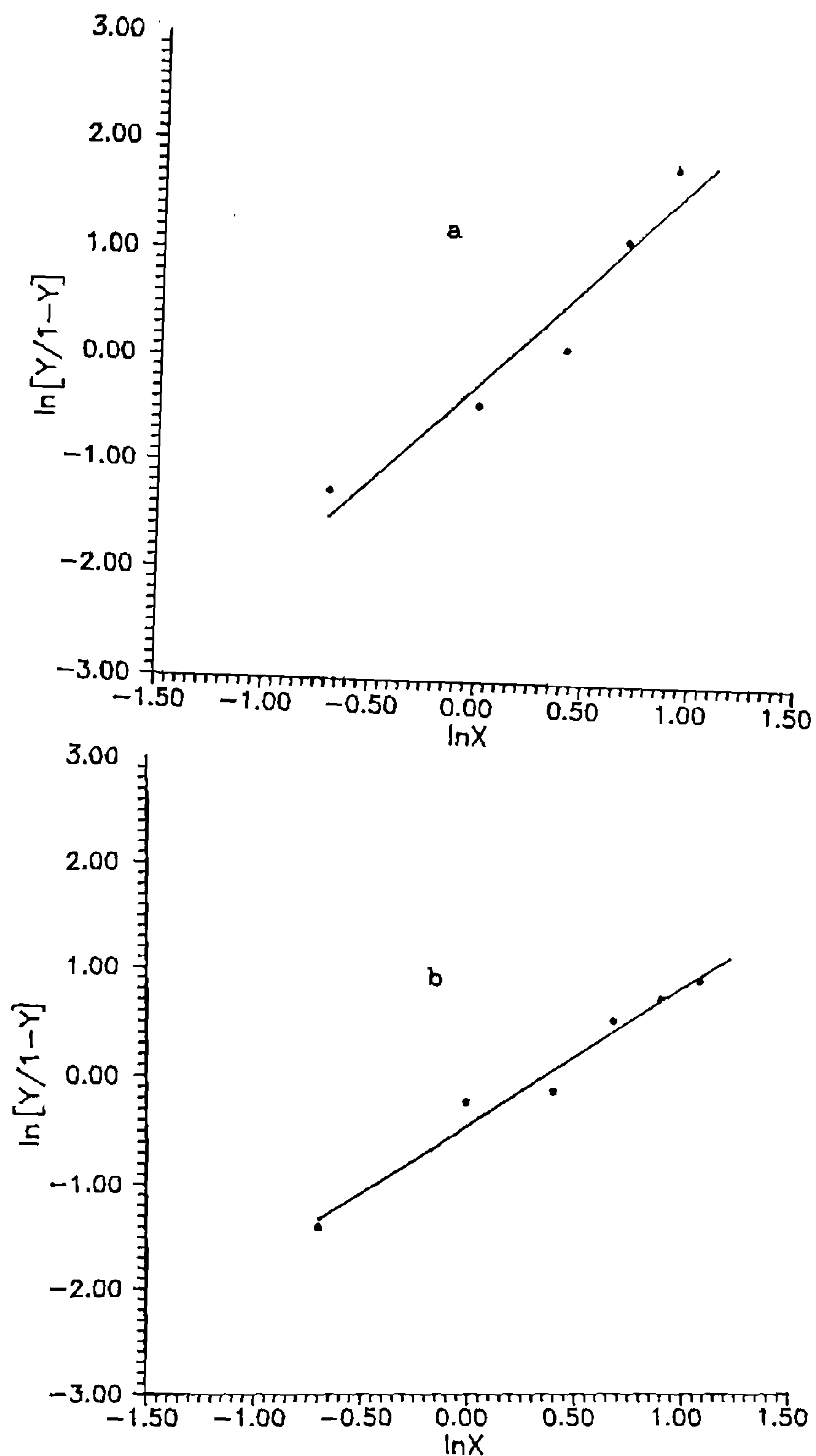


Fig. 7.14 Plot of ln [Y/1-Y] *vs* lnX using cathodic peak current (a) and anodic peak current values of $[Cu(pdto)]^{2+}$ in the presence of β-CD.

initial binding events render subsequent binding events more favorable. Thus the present study shows that the binding of CDs to $[Cu(pdto)]^{2+}$ is cooperative. The analysis of i_{pa} and i_{pc} gave values of K_a ($1/K_D$) which are in the same order of magnitude as that calculated earlier and the trend in K_a for different CDs is also the same.

7.4 Conclusions

The present voltammetric study reveals that the Cu(II)/Cu(I) redox couple of $[Cu(pdto)]^{2+}$ becomes free from adsorption effects so as to enhance its reversibility in the presence of five, four and three mM of α-CD, β-CD and τ-CD respectively. These limiting concentrations decrease with increase in the size of the CD molecule, which is consistent with the formation of arrays of CDs around the copper(II) complex. However, in other Cu(II) complexes no significant changes in redox properties has been observed in the presence of CDs.

The CDs have been reported to be effective hosts for many molecules by inclusion complex formation but the present assembly of CDs around the redox active species can be regarded as a new and multifunctional model for the biological systems of molecular recognition.[32]

The self-assembly of the CD molecules to form functional aggregates like micelles illustrate the principle of cooperativity

in enzymes. The positive cooperativity observed for the binding of all the three CDs with $[Cu(pdto)]^{2+}$ implies the stimulation of the interaction of additional substrate molecules by interaction of the first molecule with the enzyme.[22]

The present study reveals that the binding of Cu(II) species with β-CD is stronger than that with α- or τ-CD and that the binding of CDs to $[Cu(pdto)]^{2+}$ tends to be very selective.

References

(1) Ohashi, M.; Kasatani, K.; Shinohara H.; Sato, H. *J. Am. Chem. Soc.* **1990**, *112*, 5824.

(2) Munoz de La Pena, A.; Ndou, T. T.; Zung, J. B.; Greene, K. L.; Live D. H.; Warner, I. M. *J. Am. Chem. Soc.* **1991**, *114*, 1572.

(3) Komiyama, M.; Bender, M. L. *J. Am. Chem. Soc.* **1978**, *100*, 2259; Eftink, M. R.; Andy, M. L.; Bystrom, K.; Perlmutter, H. D.; Kristol, D. *J. Am. Chem. Soc.* **1989**, *111*, 6765; Paleper, R.; Reinsborough, V. C. *Aust. J. Chem.* **1990**, *43*, 2119.

(4) Sanemasa, I.; Fujiki M.; Deguchi, T. *Bull. Chem. Soc. Jpn.* **1988**, *61*, 2663.

(5) Goledzinowski, M. *J. Electroanal. Chem.* **1989**, *267*, 171.

(6) Yokoi, H.; Satoh, M.; Iwaizumi, M. *J. Am. Chem. Soc.* **1991**, *113*, 1530.

(7) Alston, D. R.; Ashton, P. R.; Lilley, T. H.; Stoddart, J. F.; Zarzycki, R. *Carbohydrate Res.* **1989**, *192*, 259.

(8) Trainor, G. L.; Breslow, R. *J. Am. Chem. Soc.* **1981**, *103*, 154.

(9) Harada, A.; Takahashi, S. *J. Chem. Soc., Chem. Commun.* **1986**, 1229.

(10) Alston, D. R.; Slawin, A. M. Z.; Stoddart, J. F.; Williams, D. J. *Angew. Chem. Int. Ed. Engl.* **1985**, *97*, 771.

(11) Alston, D. R.; Slawin, A. M. Z.; Stoddart, J. F.; Williams, D. J. *Angew. Chem. Int. Ed. Engl.* **1985**, *24*, 786.

(12) Alston, D. R.; Slawin, A. M. Z.; Stoddart, J. F.; Williams, D. J. *J. Chem. Soc., Chem. Commun.* **1985**, 1602.

(13) Bender, M. L.; Komiyama, M. *Cyclodextrin Chemistry*; Springer-Verlog: New York, 1978; pp. 14-16.

(14) Krechl, J.; Castulik, P. *Chemica Scripta* **1989**, *29*, 173 and refs cited therein.

(15) Tabushi, I. *Acc. Chem. Res.* **1982**, *15*, 66.

(16) Saenger, W. *Angew. Chem. Int. Ed. Engl.* **1980**, *19*, 344.

(17) Griffiths, D. W.; Bender, M. L. *Adv. Catal.* **1973**, *23*, 209.

(18) Sivagnanam, U.; Palaniandavar, M. *J. Electroanal. Chem.* **1992**, *341*, 197.

(19) Tabushi, I.; Shimizu, N.; Sugimoto, T.; Shiozuka, M.; Yamamura, K. *J. Am. Chem. Soc.* **1977**, *99*, 7100.

(20) a) Shortreed, M. E.; Wylie, R. S.; Macartney, D. H. *Inorg. Chem.* **1993**, *32*, 1824; b) Wylie, R. S.; Macartney, D. H. *Inorg. Chem.* **1993**, *32*, 1830.

(21) Matsue, T.; Evans, D. H.; Osa, T.; Kobayashi, N. *J. Am. Chem. Soc.* **1985**, *107*, 3411.

(22) Peter, R. C.; Salek, J. S.; Sikorski, C. T.; Kumaravel, S. G.; Lin, F-T. *J. Am. Chem. Soc.* **1990**, *112*, 3860.

(23) Brubaker, G. R.; Brown, J. N.; Yoo, M. K.; Kinsey, R. A.; Kutchan, T. M.; Mottel, E. A. *Inorg. Chem.* **1979**, *18*, 299.

(24) a) Addison, A. W.; Palaniandavar, M.; Reedijk, J.; van Rijn, J.; Rao, T. N. unpublished work. b) Sivagnanam, U.; Fujisawa, K.; Palaniandavar, M. to be communicated.

(25) Kanters, R. P. F.; Yu, R.; Addison, A. W. *Inorg. Chim. Acta* **1992**, *196*, 97; Adhikary, B; Lucas, C. R.; *Inorg. Chem.* **1994**, *33*, 1376; Liu, S.; Lucas, C. R.; Hynes, R. C.; Charland, J. P. *Can. J. Chem.* **1992**, *70*, 1773.

(26) Harada, A; Takahashi, S. *J. Chem. Soc., Chem. Commun.* **1984**, 645.

(27) Sakaguchi, U.; Addison, A. W. *J. Chem. Soc., Dalton Trans.* **1979**, 600; Nikles, D. E.; Powers M. J.; Urbach, F. L. *Inorg. Chem.* **1983**, *22*, 3210.

(28) Anson, F. C.; Lee, C. W. *Inorg. Chem.* **1984**, *23*, 837.

(29) Wopschall, R. H.; Shain, I. *Anal. Chem.* **1967**, *39*, 1514.

(30) Zanello, P. *Comments Inorg. Chem.* **1988**, *8*, 45.

(31) Goledzinowski, M. *J. Electroanal. Chem.* **1989**, *267*, 171.

(32) Matsui, Y.; Nishioka, T.; Fujita, T. In *Topics in Current Chemistry: Quantitative Structure-Reactivity Analysis of the Inclusion Mechanism by Cyclodextrins*; Boschke, F. L., Ed.; Springer-Verlag: New York, 1985; p 62.

(33) Lindner, K.; Saenger, W. *Carbohydr. Res.* **1982**, *99*, 103.

(34) Bard, A. J.; Faulkner, L. R. *Electrochemical methods: Fundamental applications*; John Wiley & Sons: New York, 1980; p 218.

(35) Sivagnanam, U.; Palaniandavar, M. *J. Chem. Soc., Dalton Trans.* **1994**, 2277.

(36) Taraszewska, R. J.; Piasecki, A. K. *J. Electroanal. Chem.* **1987**, *226*, 137.

(37) Bergeron, R. J.; Meely, M. P. *Bioorg. Chem.* **1976**, *5*, 197.

(38) Harata, K. *Bioorg. Chem.* **1980**, *9*, 530.

(39) Harata, K. *ibid.* **1981**, *10*, 225.

(40) Rebek, J. Jr.; Marshall, L. *J. Am. Chem. Soc.* **1983**, *105*, 6668; Rebek, J., Jr. *Acc. Chem. Res.* **1984**, *17*, 258; Rebek, J., Jr.; Costello, T.; Marshall, L.; Wattley, R.; Gadwood, R. C.; Onan, K. *J. Am. Chem. Soc.* 1985, *107*, 7481.

(41) Tabushi, I.; Kugimiya, S. *J. Am. Chem. Soc.* **1986**, *108*, 6926; Tabushi, I.; Kugimiya, S.; Sasaki, T. *J. Am. Chem. Soc.* **1985**, *107*, 5159; Tabushi, I.; Sasaki, T. *J. Am. Chem. Soc.* **1983**, *105*, 2901.

(42) Traylor, T. G.; Mitchell, M. J.; Ciccone, J. P.; Nelson, S. *J. Am. Chem. Soc.* **1982**, *104*, 4986.

(43) Collman, J. P.; Brauman, J. I.; Rose, E.; Suslick, K. S. *Proc. Natl. Acad. Sci. U.S.A.* **1978**, *75*, 1052.

(44) a) Piszkiewicz, D. *J. Am. Chem. Soc.* **1977**, *99*, 1550; b) Piszkiewicz, D. *J. Am. Chem. Soc.* **1976**, *98*, 3053.

SUMMARY

This thesis describes the synthesis and study of Cu(II) complexes of certain multidentate ligands with varying number of thioether donors and chelate ring sizes. The complexes have been characterized using various spectral and electrochemical techniques and the results may lead to a better understanding of the importance of thioether sulfur coordination in the copper site of cuproproteins. In addition, the electrochemistry of these model complexes in aqueous solutions of various cyclodextrins and surfactants have been investigated.

Chapter 1 contains an introduction to various types, structure and functions of copper proteins. A few important and relevant model compounds designed earlier for the proteins have been reviewed briefly. A brief account of cyclodextrins and surfactants chemistry and enzyme models based on them are included in this chapter. The scope of the present work is also presented.

In Chapter 2 are described the origin of the chemicals used, the purification of solvents and supporting electrolytes and the spectral methods and electrochemical techniques employed in the present investigation.

Chapter 3 describes the synthesis of the ligands, HOCO-$(CH_2)_m$-SCH_2CH_2S-$(CH_2)_n$-SCH_2CH_2S-$(CH_2)_m$-COOH, where m = 1, n = 3 (L3); m = 2, n = 3 (L4) m = 1, n = 2 (L5); m = 2, n = 2 (L6) and HOCO-CH_2-$(S\text{-}CH_2CH_2)_4$-S-CH_2-COOH (L7) and their characterization using various spectral techniques. The 1:1 copper(II) perchlorate complexes of these ligands have been generated in solution and their spectral and electrochemical behaviour investigated. The electronic spectra of all the Cu(II) complexes exhibit a ligand field band in the range 15.0 - 16.5 kK, and an intense absorption band around 26.0 kK originating from S(σ) ---> Cu(II) CT transition. Very high Cu(II)/Cu(I) redox potentials are exhibited by these complexes. The complexes with propionic acid moieties possess redox potentials higher than those with acetic acid moieties; this may be ascribed to the distortion induced by the bulkiness of the propionic acid group. An increase in the number of sulfur atoms from four to five increases the redox potential appreciably.

In Chapter 4 are described the synthesis of Cu(II) complexes of the linear quadridentate ligand, 1,8-bis(benzimidazol-2-yl)-3,6-dithiaoctane (bbdo) and the linear quinquidentate ligand, 1,11-bis(pyrid-2-yl)-3,6,9-trithiaundecane (pttu) with N_2S_2 and N_2S_3 donor sets respectively. The ligand bbdo forms complexes of the type $Cu(bbdo)X_2$ ($X = ClO_4^-$, NO_3^-). The nitrate $[Cu(bbdo)(NO_3)]NO_3$ crystallizes in the monoclinic space group $P2_1/a$ with

a = 15.990(7), b = 13.706(4), c = 10.972(4) Å and β = 93.90(3)° and Z = 4. The structure was solved by heavy-atom Patterson methods, expanded using Fourier techniques and refined by the least squares technique to R = 0.079 for 1138 observed reflections with $I > 2.0\ \sigma(I)$. The coordination geometry around copper(II) is best described as severely distorted octahedral with both the benzimidazole nitrogens [Cu-N, 1.99(1) and 1.93(1) Å], a thioether sulfur atom [Cu-S(2), 2.443(6) Å] and one oxygen atom of the nitrate ion [Cu-O(11), 2.06(6) Å] constituting the equatorial plane and the second sulfur [Cu-S(1), 2.533(6) Å] and one more oxygen from the coordinated nitrate anion [Cu-O(12), 2.727(6) Å] occupying the axial positions. The ligand field and EPR spectra are consistent with trigonal bipyramidal geometry in the solid state, whereas in solution two ligand field bands (11.2 and 16.7 kK) and an axial EPR spectra were observed suggesting a $d_{x^2-y^2}$ ground state. The preliminary structure of Cu(I) complex of pttu ligand shows a tetrahedral geometry around copper. The ligand field and EPR spectra of $[Cu(pttu)](ClO_4)_2$ reveal a square-based geometry and an interesting solvent-dependent chemistry. All the $[CuN_2S_2]^{2+}$ and $[CuN_2S_3]^{2+}$ complexes exhibit an intense S(σ) ---> Cu(II) CT band around 29.2 kK and a high Cu(II)/Cu(I) redox potential. The effect of ligand enlargement on structure and properties of these complexes are discussed in comparison to those known already.

In Chapter 5 are dealt with the synthesis of the linear

quadridentate $R-(CH_2)_m-SCH_2CH_2S-(CH_2)_n-SCH_2CH_2S-(CH_2)_m-R$, where m = 1, n = 2 (L1); m = 1, n = 3 (L2); m = 2, n = 2 (L3); m = 2, n = 3 (L4) and the pentadentate $R-CH_2-(S-CH_2CH_2)_4-S-CH_2-R$ (L5) (R = benzimidazol-2-yl) ligands and the 1:1 copper(II) perchlorate complexes of these ligands. Some of the quadridentate compounds also formed complexes of the type $CuLX_2$ (X = Cl^-, NO_3^- or BF_4^-). All the complexes exhibit an absorption band around 30.0 kK originating from a S(σ) ---> Cu(II) CT transition. In solution the ClO_4^- and BF_4^- salts of $[Cu(L1)]^{2+}$ exhibit only one ligand-field band (14.8 kK) while the other complexes show two bands (≈ 11.0, 15.0 - 16.0 kK). The polycrystalline EPR spectra of the former complexes are axial while those of the other complexes are rhombic. The cryogenic solution EPR spectra of the former complexes differ from those of the other complexes by exhibiting comparatively low $g_{\parallel}$ values and well resolved nitrogen superhyperfine structures. All these spectral features suggest a unique 'folded' geometry for the $[Cu(L1)]^{2+}$ complex.

Among the tetrathioether complexes, the Cu(II) ---> Cu(I) redox potential increases with increase in the number of six-membered chelate rings, implying an increase in preference for the copper(I) over the copper(II) state. For copper(II) complexes of bis(benzimidazolyl)thioether ligands with all-five-membered chelate rings the potential increases with increase in the number of thioether donors.

Voltammetric studies of biomimetic Cu(II) complexes of bis(pyrid-2-yl) di- and trithia and bis(benzimidazol-2-yl) dithia ligands in aqueous sodium dodecylsulphate (SDS, anionic), cetyltrimethylammonium bromide (CTAB, cationic) and Triton X-100 [α-[*p*-(1,1,3,3-tetramethylbutyl)phenyl]-ω-hydroxypolyoxyethylene(9.5), nonionic] micellar solutions carried out on glassy carbon electrode were presented in Chapter 6. The electronic spectral properties of Cu(II) complexes in micellar solutions are consistent with their incorporation in various types of hydrophobic microenvironments.

For most of the complexes, the adsorption of Cu(I) species observed in aqueous solution is absent and the reversibility of Cu(II)/Cu(I) couple is increased in SDS and Triton X-100 micellar solutions. From the dependence of i_{pc} values on SDS concentration, the micellar binding constant K_1 has been estimated. Compared to aqueous isotropic solutions, the $E_{1/2}$ values in micellar solutions either decrease or increase depending upon the nature of the surfactant and the hydrophobicity as well as the structure of the complexes. The ratio of equilibrium binding constants K_{+}/K_{2+} of Cu(I) and Cu(II) species does not follow the same trend in SDS, CTAB and Triton X-100 solutions indicating that the interaction of the cationic complexes depend on a delicate balance between hydrophobic and electrostatic interactions. Interestingly, for complexes with CuN_2S_2 chromophore Cu(I)/Cu(0) couple is also observed in Triton X-100 micelles.

In Chapter 7 are discussed the redox of Cu(II) perchlorate complexes of certain N_2S_2 and N_2S_3 chelates, reported as Type I blue copper protein models in the presence of α-, β- and γ-CD in aqueous solution. The addition of CDs to the complexes cause substantial decreases in peak currents rather than in peak potentials. The i_{pa} rather than i_{pc} or ΔE_p or $E_{1/2}$ value is very sensitive to the variation in the concentration of CDs. The reversibility of the Cu(II)/Cu(I) couple of $[Cu(pdto)]^{2+}$ is enhanced, as shown by the decrease in ΔE_p and that of i_{pa}/i_{pc} towards unity. The plots of i_{pa}, i_{pc}, E_{pa} and ΔE_p *vs* the number of moles of the CDs show sharp inflections, interestingly, at five, four and three moles of α-, β- and γ-CDs respectively, the number of CDs in the array being dictated by the size of the CD. There occurs the formation of novel and regular arrays of CDs around the complex, rather than the usual inclusion complex formation by CDs and also illustrates the prevention of adsorption of $[Cu(pdto)]^{+}$ on the glassy carbon electrode. For the other complexes the changes in redox properties in the presence of CDs is not as regular and significant as in $[Cu(pdto)]^{2+}$. The plots of changes in i_{pa} and i_{pc} *vs* the concentration of CDs give the value of Hill's coefficient greater than unity (1.8 - 2.3), which is the hallmark of positive cooperativity. The values of K_1/K_{21} and K_a for complex formation with CDs have been determined and discussed. Significant reduction or enhancement in ϵ_{max} values have been observed both for the ligand field and charge transfer bands in the presence of all the three CDs.